Co-ordinate excitation control and governing of turbo-generators.

Hazell, Philip Antony

Award date:
1982

Awarding institution:
University of Bath

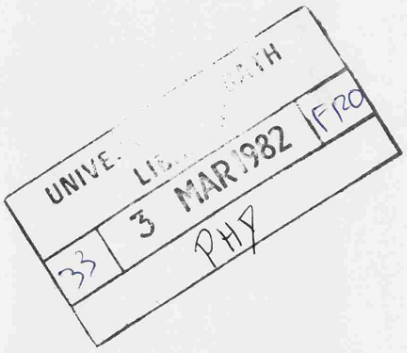
UNIVE
LIB
3 MAR 1982
F20
33
PHY

CO-ORDINATE EXCITATION CONTROL AND GOVERNING OF TURBO-GENERATORS

submitted by Philip Antony Hazell B.Sc.(Hons.)

for the degree of Ph.D.

of the University of Bath

1981

P.A.Hazell

Bath, August 1981

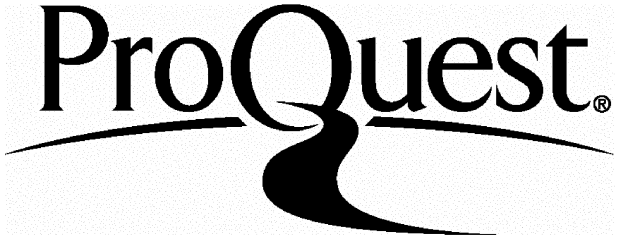

SUMMARY

This dissertation is concerned with the improvement of the transient response of turbo-generator sets following a severe system disturbance. The improvement in response is obtained by the application of a single additional system state into the relevant controllers. The system state used is that of rotor acceleration. Theoretical studies are carried out to obtain the feedback gains required for single machine co-ordinate control of excitation and governing. The study is then extended to a multi-machine system.

The control laws obtained from the theoretical studies are applied in the laboratory to micromachine systems. A method of obtaining a rotor acceleration feedback control signal is developed and applied to these laboratory micromachine systems. The acceleration transducer forms an essential part of a dedicated microprocessor data acquisition system, which, apart from the functions of data collection and processing, performs a real time simulation of the governor turbine model. The output of this simulation is then used to control the micromachine prime mover torque. An essential feature of the microprocessor system is the determination of control laws for both the governing and excitations systems during transient conditions.

ACKNOWLEDGEMENTS

The work presented in this thesis was carried out under the supervision of Mr. A.R. Daniels, Senior Lecturer in the School of Electrical Engineering, University of Bath, England. The author wishes to express his gratitude to Mr. Daniels for his constant interest, encouragement and guidance.

The author is grateful to Professor K.V. Diprose, Dr. B.A. White and Mr. V.S. Gott for their valuable advice and helpful discussions. Thanks should also be extended to past and present post-graduate students of the School of Electrical Engineering, University of Bath, for their practical help and theoretical discussions. Financial support from the Science Research Council and the University of Bath is gratefully acknowledged.

The author is indebted to Professor F.J. Eastham, for the facilities provided by the University. The practical help given by the Royal Naval Engineering College Manadon, is gratefully appreciated.

TABLE OF CONTENTS

LIST OF PRINCIPAL SYMBOLS

The principal symbols used in this thesis are listed as follows. Symbols which do not appear in the list will be defined in the text as they are introduced.

v_d, v_q	= stator voltages in d and q axes respectively
V_{fd}	= field voltage
V_f	= field voltage referred to the armature circuit
i_d, i_q	= stator currents in d and q axes respectively
i_{fd}, i_{1d}, i_{1q}	= currents in field, and d and q axis damper windings respectively
R_a	= stator resistance in d and q axis windings
r_{fd}, r_{1d}, r_{1q}	= resistances in field and d and q axis damper windings respectively
Ψ_d, Ψ_q	= stator flux linkages in d and q axes respectively
Ψ_{fd}, Ψ_{1d}, Ψ_{1q}	= flux linkages in field and d and q axis damper windings respectively
x_{ffd}, x_{11d}, x_{11q}	= total reactances of field and d and q axis damper windings respectively
x_{ad}, x_{aq}	= mutual reactances between any pair of d axis windings and between the q axis windings respectively

x_d, x_q = synchronous reactances in d and q axes respectively

x_d' = d axis transient reactance

x_d'', x_q'' = d and q axis subtransient reactances respectively

e_q' = q axis voltage behind transient impedance

e_d'', e_q'' = d and q axis voltage behind subtransient impedances respectively

T_{do}', T_d' = d axis transient open and short circuit time constants respectively (sec.)

T_{do}'', T_d'' = d axis subtransient open and short circuit time constants respectively (sec.)

T_{qo}'', T_q'' = q axis subtransient open and short circuit time constants respectively (sec.)

T_{qo}', T_q' = q axis transient open and short circuit time constants respectively (sec.)

P_e = electrical terminal power

T_e = air gap torque

T_m = mechanical torque

K_d = damping factor

H = inertia constant (kWs/kVA)

M = $H/\pi f_o$

ω_o, f_o = rated frequency (rad/s and Hz respectively

ω = instantaneous angular velocity of rotor (rad/s)

γ = rotor slip speed (rad/s)

δ = rotor angle (rad)

V_b, V_t = voltages at infinite busbar and machine terminals respectively

R_t, X_t = transfer resistance and reactance respectively

R_l, X_l = transmission line resistance and reactance respectively

R_x, X_x = generator transformer resistance and reactance respectively

p = differential operator d/dt

s = Laplace operator

t = time (sec.)

K_i = state feedback gains i=1,2,...,n

V_r = reference to excitation regulator

V_i = state feedback signal to excitation system

V_s = derivative feedback signal of AVR

T_{mo} = torque reference to governing system

T_i = state feedback signal to governing system

Δ = prefix to denote a deviation about the initial operating point

T = superscript to denote transpose of a matrix or vector

$\dot{}$ = superscript to denote differentiation w.r.t. time t

o = subscript to denote steady state value

r = subscript to denote reference

The constants T and K with appropriate subscripts denote control system time constants and gains.

CHAPTER 1 INTRODUCTION

1.1 The Evolution of Modern Generating Plant

The evolution of modern power generating plant is an interesting and varied subject. The stimuli for development during the early phases was primarily a demand for higher outputs combined with an increasing requirement for improvement in efficiency. However, latterly, additional pressures are being brought to bear, particularly on environmental grounds, placing restrictions on where power stations may be placed and the amount of overhead transmission lines available. These pressures tend to favour large thermally efficient plant with the minimum of interconnection with the rest of the system.

In 1888[1] C.A. Parsons used a steam turbine as the prime mover, in the first high speed a.c. generator system. The generator was a dynamo fitted with slip rings. The rotating armature as originally used by Parsons was soon discarded, since it was found impractical to remove the high level of electrical power using slip rings. Instead, the rotating field and stationary armature configuration was taken up. By 1912 the basic form of the turbogenerator had been established with the construction of a 25MW set by C.A. Parsons. Since that time the increasing unit output has been largely achieved as a result of refinements in engineering techniques and materials, rather than by fundamental design changes. Heat extraction techniques in particular,

have played a large part in the increase in electrical output of generating units. Hydrogen cooling of the rotor appeared in the early 1950's and later stator cooling using water. Improved insulation techniques, coupled with stator cooling has allowed significant increases in unit output.

These trends in turboalternator design have lead to increases in unit output, without increasing the rotating mass at the same rate, accompanied by a reduction in the short circuit ratio. Both of these features are detrimental to stability. A lower short circuit ratio reduces the capability to transmit power for a given field current. The lower values of inertia constant H indicate that less mechanical power is required to increase the load angle under transient conditions.

1.2 The Stability Problem

It is desirable that a system of synchronous machines should remain in synchronism following a disturbance to the system. The machine system is an interconnected set of components with dynamic properties, and the stability of the system is dependent on these dynamics. For stability, oscillations resulting from a disturbance must die away, leaving the machines again in synchronism. A power system is never in a true steady state since there is always some form of disturbance applied, ranging from the multiplicity of small domestic and industrial load changes during the day, to major load and line switching activities. A pseudo steady state

stability requirement for a system can be defined such that it remains stable during the normal load fluctuations. Dynamic stability is then the ability to withstand significant load changes and line switchings. A further form of stability is described as transient stability, that is, the ability of the system, or local generators connected to a large system, to withstand a severe transient. Typically, a 3-phase short circuit close to the generator transformer high voltage terminals, is taken as a standard system transient in theoretical work. The 3-phase fault is taken as standard in preference to single phase to ground or phase to phase faults, which, even though more common are less severe in the stability context.

When a 3-phase short circuit is applied close to the generator transformer high voltage terminals, the voltage at that point collapses and prevents electrical power flow from the generator to the rest of the system. During the fault the power balance between mechanical input power and electrical output power is disturbed. The excess input power must be dissipated, either in increased electrical losses, or, used to increase the angular momentum of the rotating mass. During the transient period, the high values of current cause excessive losses which result in a retarding force which is evident as angular back swing[2]. The magnitude of the initial back swing is small and is generally neglected. Neglecting the back swing, the excess input power is absorbed as additional kenetic energy in the

rotating mass, thus increasing the angular velocity of the machine and in turn increasing the angle of the machine emf relative to the system. When the short circuit is removed, power transfer is resumed, at a level dependent on the new load angle, machine emf and system voltage. The machine will generally return to synchronism if the excess kenetic energy can be transferred to the system as electrical power. This leads to the definition of first swing transient stability which may be regarded as a measure of the likelihood of the machine not pole slipping on the first rotor swing.

First swing stability provides a reasonable means of comparing the stability of power systems. Common techniques available to obtain a measure of transient stability are pre-post fault impedance curves and critical fault clearance times[3]. First swing stability does not, however, give any regard to the operation of the machine if it survives the first swing. For a comparison of what happens after initial swing, or for subsequent stability, it is necessary to define some form of performance criterion which would generally be a function of terminal voltage and load angle. Naturally, such a criterion should regard early damping out of oscillations as important.

First swing stability is affected most by the physical limitations of the generating set. Taking the case of excitation control systems, it is the ceiling voltage available for field forcing which is of importance. The large terminal voltage error is sufficient to drive the system to its limits.

Looking at governing systems the standard 4% droop characteristic does not offer much improvement since the speed deviations are not large enough to cause large changes in the ouput torque. Under these circumstances, it is readily seen that, if the governing side is to play more of a role in first swing stability, then the governor system must include some form of additional signals.

For subsequent stability, however, the performance of the system is not so much limited by the physical restraints of the plant, but by the nature of the controls applied to them.

1.3 Effect of Plant Items on Stability

It has been shown by many authors that fast acting, high ceiling voltage, exciters are beneficial in the increase of transient stability margins. During the fault the terminal voltage error is sufficient to raise the exciter to maximum demand, which maximises both dissipation during the fault and power transfer after the fault. However, simple terminal voltage feedback, though superior to constant excitation, is not very effective in damping out subsequent oscillations[4]. The general reason is that the field voltage remains high for too long, resulting in excessive power transfer and an over shoot in load angle recovery. Supplementary signals can be used to provide more control over the field voltage resulting in better damping without degredation of terminal voltage response.

Assuming a standard 4% droop governing system, bearing in mind the small speed deviation present during faults, there is little change in turbine output over the fault duration in contrast with the dramatic changes in main exciter field voltage associated with A.V.R. action. However, modern fast acting electro-hydraulic governing systems are capable of swift control action which can significantly reduce power output during a fault, improving first swing stability, and also improving subsequent damping provided a suitable control strategy is employed. This thesis is concerned with the improvement of turbogenerator transient stability by the use of additional feedback into both the governor and exciter.

1.4 Stabilizing Signals and Control

The application of effective stabilizing signals is dependent on two factors. Firstly, the control signals must be available for feedback purposes. Secondly, the plant to which feedback signals are applied, must be capable of responding to those control signals. To provide a useful contribution, a stabilizing signal must either describe, or embody one of the states of the system. Practical stabilizing signals include shaft speed[5], terminal power[6,7] and frequency deviation[8].

Historically the advent of fast acting high ceiling excitation systems[9], capable of a significant influence on the generator field voltage allowed the first effective

controls. The prime mover, being very much slower in response, was often assumed to deliver constant torque, and as such, played no control role during transients.

Several methods by which control schemes may be derived, have been used by various authors[10,11,12]. Most early work used linearized system models. Optimal control methods have been applied[13], but techniques using the solution of the matrix riccatti equation produce controls requiring access to all system states. Such controls are not easily applied in practice. Suboptimal controls have been derived by using nonlinear methods[14] and reduced numbers of system states[15,16,17].

When considering a stabilizer using a reduced set of system states, those states which have a beneficial effect must be chosen. It is reasonable to assume that, in a system utilizing all states for feedback purposes, some of those states will be dominent in control. The states that play little contribution to the overall response can be eliminated from the control with little penalty. If the mechanical states of a system are considered (load angle, rotor speed and acceleration) then differing contributions will be made by each of these when used as feedback control signals. These effects have been discussed by several authors[18,19].

Load angle has been shown to be the least useful signal[18], being sensitive to parameter and gain variations. Deviation of machine speed from synchronous speed has an

improved tolerance to parameter changes. The best signal in this group is rotor acceleration[19]. It has the most inherent phase advance and as such, can provide timely influence on the system. Acceleration is, however, difficult to measure and various methods have been tried to overcome this problem. Transient electrical power ΔP_e is an acceptable substitute for acceleration while no control, is exercised on the prime mover torque[18]. If, however, the torque changes significantly, ΔP_e is no longer an indication of accelerating power and its usefulness is reduced. This has been shown by Lu[17] in theoretical co-ordinate excitation and governing control studies for the single machine system.

With the introduction of the electro-hydraulic governor, it became possible to produce significant changes in mechanical power input under transient conditions. This has prompted the introduction of various control schemes, from the open loop fast valving[20] to co-ordinate controls using both linear[21,22] and nonlinear methods[23]. Most literature deals with theoretical studies but some practical results have been reported[24,25].

Some techniques used to develop co-ordinate controls on single machine systems are also applicable to multi-machine systems. The inverse Nyquist technique is particularly common in this area with controls generated for single machine systems[26] and multi-machine systems[27]. An attraction of this technique is that interaction between machines can be reduced by using cross coupled feedback terms. The inverse

Nyquist approach is, however, based on linear theory and multi-variable controllers so obtained may well assume excessive control effort, quite beyond the capability of the actual plant. When limitations are present on control variables the effectiveness of the control is reduced, both in terms of individual machine response and interaction[28]. A reduction in effectiveness is similarly obtained if cross coupling terms are lost.

The approach used in this study, for both the single machine co-ordinate control and the multi-machine control, is based on nonlinear system equations and function minimization techniques, to obtain suboptimal controls. In all studies the additional stabilizing signal is restricted to acceleration of the machine in question. A suitable transducer for determining acceleration has been developed for a micromachine system allowing practical implementation of the controls developed.

CHAPTER 2 OPTIMAL CONTROL AND SYSTEM THEORY

2.1 Optimal Control

The purpose of Optimal Control theory is to obtain a control function which, when applied to the system under investigation, causes the system to behave in some optimum manner. The control function may be either a time sequence or continuous and what is taken as an optimum response for the system is to some extent arbitrary. Optimality of the control system is generally measured by a performance index I, usually taken as the time integral over a specified interval of some function of the system giving information about the error between desired operation and actual operation. It is often necessary to include some form of cost function in the performance index to ensure that the control effort is restricted to practical limits.

In order to obtain an optimal control function from all the possible control functions, it is necessary to know precisely the structure of the system, the values of the parameters and also the initial state of the system. If any of these are only approximately known then only approximate controls can be found, producing so called suboptimal control. It is generally not possible to produce an analytic solution for the required optimal or suboptimal control and solutions have to be based on a set of necessary, rather than sufficient, conditions for optimality.

Some methods by which the optimal control problem has been tackled, using the calculus of variation, Pontryagin minimum principle and dynamic programming are discussed in this section.

For the dynamic system represented by

$$\dot{x} = f(x,u,t) \qquad 2.1$$

Where x is the state n vector and u is the control m vector the performance index may be given as

$$I = \int_{t_o}^{t_f} L(x,u,t)\ dt \qquad 2.2$$

where L , the objective function, provides the performance criterion for the system. The requirement is to obtain the conditions to be satisfied by the vector x(t) and u(t) for the interval $t_o \leq t \leq t_f$ which minimizes the performance index I. However this function minimization problem is constrained by the requirements of the state equation 2.1 . Variational calculus can be used to convert the problem to an unconstrained function minimization by the use of Lagrange multipliers which create a new performance measure L' such that

$$L'(\dot{x},x,u,\lambda(t),t) \triangleq L(x,u,t) + \lambda^T(t)\{f(x,u,t)-\dot{x}\} \qquad 2.3$$

where $\lambda(t)$ is the vector of Lagrange multipliers. To minimize the performance index, the following necessary conditions must be satisfied[29].

$$\frac{\partial L'}{\partial u} = 0 \qquad \text{(Control Equation)} \qquad 2.4$$

$$\frac{\partial L'}{\partial \lambda} = 0 \qquad \text{(State Equation)} \qquad 2.5$$

$$\frac{\partial L'}{\partial x} - \frac{d}{dt}\frac{\partial L'}{\partial \dot{x}} = 0 \qquad \text{(Euler-Lagrange Equation)} \qquad 2.6$$

$$\left[\tilde{x}^T \frac{\partial L'}{\partial \dot{x}}\right]_{t_o}^{t_f} = 0 \qquad \text{(Transversality Condition)} \qquad 2.7$$

where $\tilde{x}$ is an arbitrary n vector defined over the closed interval $[t_o, t_f]$. This formulation using equations 2.4-2.7 creates a two point boundary value problem, (TPBVP), with conditions set at both initial and final points, which in general requires iterative techniques to obtain a solution. It is not convenient when constraints must be placed on the control variables and also requires that the state equations have continuous first partial derivatives with respect to the control variables.

It is possible to relax the requirements for continuous partial derivatives of the state equation with respect to the control variables and unconstrained control, by means of Pontryagins formulation in terms of the Hamiltonian together with Pontryagins minimum principle.

The Hamiltonian Function

$$H(x,\lambda(t),u,t) \triangleq L(x,u,t) + \lambda^T f(x,u,t) \qquad 2.8$$

gives rise to the following necessary conditions to minimize

the performance index.

$$\frac{\partial H}{\partial u} = 0 \qquad \text{(Control Equation)} \qquad 2.9$$

$$\frac{\partial H}{\partial \lambda} - \dot{x} = 0 \qquad \text{(State Equation)} \qquad 2.10$$

$$\frac{\partial H}{\partial x} + \dot{\lambda} = 0 \qquad \text{(Adjoint Equation)} \qquad 2.11$$

$$\left[- \tilde{x}^T \lambda \right]_{t_o}^{t_f} = 0 \qquad \text{(Transversality Condition)} \qquad 2.12$$

The Pontryagin minimum principle states that, for the optimal trajectory, the Hamiltonian takes its minimum value H*, given by

$$H^* = \inf_{u(t)} H(x, \lambda(t), u, t) \qquad 2.13$$

where u(t) is a member of the set of admissable controls and inf (infimum) denotes greatest lower bound.

Dynamic programming may be used, defining a minimum performance function by

$$E(x,t) \triangleq \min_{u(t)} \int_{t_o}^{t_f} L(x,u,\sigma)\, d\sigma \qquad 2.14$$

where L is the performance measure and u is a member of the set of admissible controls. The necessary conditions that the optimal control must satisfy is Bellmans Equation

$$-\frac{\partial E}{\partial t}(x,t) = \min_{u(t)} \; L(x,u,t) + f^T(x,u,t) \frac{\partial E}{\partial x}(x,t) \qquad 2.15$$

which implies the following equation be satisfied.

$$-\frac{\partial E}{\partial t} = L(x,u,t) + f^T(x,u,t) \frac{\partial E}{\partial x}(x,t) \qquad 2.16$$

and

$$\frac{\partial L}{\partial u}(x,u,t) + \frac{\partial f}{\partial u}\frac{\partial E}{\partial x}(x,t) = 0 \qquad 2.17$$

The solution of equation 2.16 the Hamiltonian-Jacobi Equation is the minimum performance function E(x,t). With E(x,t) known solution of equation 2.14 gives the optimal control.

There is no general solution at present available for the Bellman partial differential equation 2.15. The Hamiltonian-Jacobi differential equation 2.16 can be solved for the so called linear regulator case, corresponding to a linear system with a quadratic performance measure. The result obtained corresponds to that obtained by the solution of the matrix Riccati equation.

Consider the linear regulator system described by

$$\dot{x} = Ax + Bu \qquad x(t_o) = x_o \qquad 2.18$$

requiring an optimal control u over the closed interval $[t_o, t_f]$, which minimizes the quadratic performance index I:

$$I = \int_{t_o}^{t_f} x^T Q_1 x + u^T Q_2 u \, dt + x^T(t_f) Q_3 x(t_f) \qquad 2.19$$

where Q_1 and Q_3 are n×n positive semi-definite symmetric matrices and Q_2 is an m×m positive definite symmetric matrix, n is the dimension of the state matrix and m is the dimension of the control vector u.

By Pontryagins equation the Hamiltonian function for the extremum condition is

$$H = x^T Q_1 x + u^T Q_2 u + \lambda^T (Ax + Bu) \qquad 2.20$$

also,

$$\dot{x} = Ax + Bu \quad x(t_o) = x_o \qquad \text{(State Equation)} \qquad 2.21$$

$$\dot{\lambda} = -2Q_1 x - A^T \lambda \qquad \text{(Adjoint Equation)} \qquad 2.22$$

$$\lambda(t_f) = 2Q_3 x(t_f) \qquad \text{(Transversality Equation)} \qquad 2.23$$

$$\frac{\partial H}{\partial u} = B^T \lambda + 2Q_2 u = 0 \qquad \text{(Control Equation)} \qquad 2.24$$

giving the optimal control as

$$u^* = -Q_2^{-1} B^T \lambda / 2 \qquad 2.25$$

Substituting equation 2.25 into the state equation 2.18

$$\dot{x} = Ax - BQ_2^{-1} B^T \lambda / 2 \quad x(t_o) = x_o \qquad 2.26$$

If λ takes the form

$$\lambda(t) = 2P(t)x(t) \qquad 2.27$$

then, on differentiation of equation 2.27

$$\dot{\lambda} = 2\dot{P}x + 2P\dot{x} \qquad 2.28$$

When equations 2.22,2.23 and 2.26 are substituted into equation 2,28 it follows that

$$2(\dot{P} + PA + A^T P - PBQ_2^{-1} B^T P + Q_1)x = 0 \qquad 2.29$$

Equation 2.29 holds for all x only if the coefficient matrix of x is identically zero, which implies that P should satisfy

$$\dot{P} = PBQ_2^{-1} B^T P - PA - A^T P - Q_1 \qquad 2.30$$

from equations 2.27 and 2.23 the boundary condition is

$$P(t_f) = Q_3 \qquad 2.31$$

Q_3 is symmetric therefore so is $P(t)$. Equation 2.30 is the matrix Riccati equation. The optimal control is given by

$$u^* = - Q_2^{-1} B^T P x \qquad 2.32$$

Solution of equation 2.30 provides the symetric matrix P, which may be used in the equation 2.32 to provide the gain matrix for the state feedback. For a time invariant system, with the control interval extended to infinity, $\dot{P} = 0$ and the matrix Riccati equation becomes

$$PA + A^T P + Q_1 - PBQ_2^{-1} B^T P = 0 \qquad 2.33$$

where A and B are constant matrices.

This form of control uses linear feedback of all the states. In practical systems it is unlikely that all the states will be available in a form suitable to implement such a control scheme.

2.2 System Modelling

Modelling of dynamic systems is performed by representing the physical processes by the sets of differential and algebraic equations. The equations relate the behaviour of internal states and output states to input stimuli as a function of time. Formulation of the equations representing the system is generally based on energy storage and transfer

mechanisms within the system. This results in sets of integro-differential equations which are amenable to state space representation. When modelling a physical system, it is seldom necessary and generally impossible to produce an exact mathematical description of a physical system. The reasons for this are that, when determining the mathematical model for the system a finite set of equations is chosen which are necessarily an incomplete description of the nature of the system.

The order of a model may be reduced for one or more reasons. Computation time tends to increase dramatically as the number of variables rise and so it is usual to trim the order down to a level which produces acceptable results without incurring unnecessary expense. Also, the higher the order, it is often more difficult to obtain accurate parameter values. For this reason it is not always necessarily the case that a more complex representation produces a more accurate simulation.

In general, when a physical system is represented by a mathematical model, the model used is different to some degree. Conversely if a physical realization is attempted of a mathematical dynamic system, the resulting system is not identical to that intended. These differences are often due to neglecting, or not accurately representing non-linearities and also by the use of lumped parameters, to represent distributed parameters.

Mathematically, a physical system may be regarded as

$$F_o(\dot{x},x,P_o,t) = 0 \qquad 2.34$$

where F_o is an operator defining the structure of the system, which may or may not be linear, P_o is the parameter vector and x is the state vector. A mathematical model representing the system could be

$$F(\dot{x},x,P,t) = 0 \qquad 2.35$$

where F and P have analogous definitions to F_o and P_o. A condition for 2.35 to represent 2.34 to a sufficient degree is that F be in the neighbourhood of F_o in the operator space and similarly P should be in the neighbourhood of P_o in the parameter space. There should be no discontinuities in these regions if slight changes in any element are not to produce dramatic changes in the overall system response.

To put the various inaccuracies into perspective it is necessary to study the sensitivity of the system to each type of error[30]. System sensitivity is a measure of the change in behaviour of a dynamic system as a result of changes in the structure or parameters of the system. In this context the term dynamic system applies equally well to both physical systems and mathematical models. It can be seen that stability of a system is a special case of a more general sensitivity theory.

2.3 System Equations

The model used for simulation purposes is shown diagrammatically in Fig. 2.1. The machine data used is representative of typical 500MW turbogenerator sets, and the transmission system is based on Pembroke power station as described in Chapter 3.

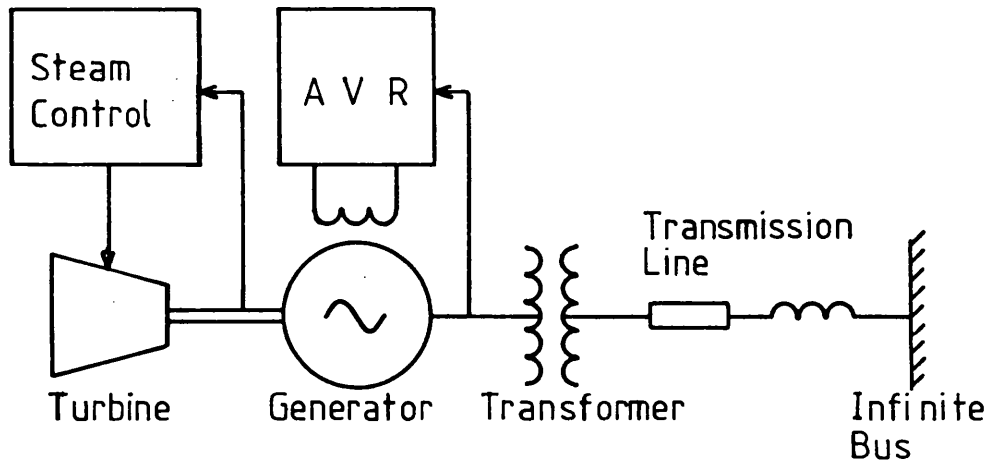

Fig. 2.1 System Model

2.3.1 The Synchronous Machine

The synchronous generator model is based on the Park's 2-axis equations for an idealized synchronous machine. The Park's equations are obtained by transforming the original stator phase variables into components on the pole and interpole axes[31,32,33,34], the Direct and Quadrature axes respectively. In this investigation, balanced conditions are

assumed, allowing the simplification that no zero sequence quantities need be considered. The windings of the idealized machine are shown in Fig. 2.2. The current paths in the rotor on the direct and quadrature axes, together with any deliberate damping windings, are represented by a single closed coil on each axis.

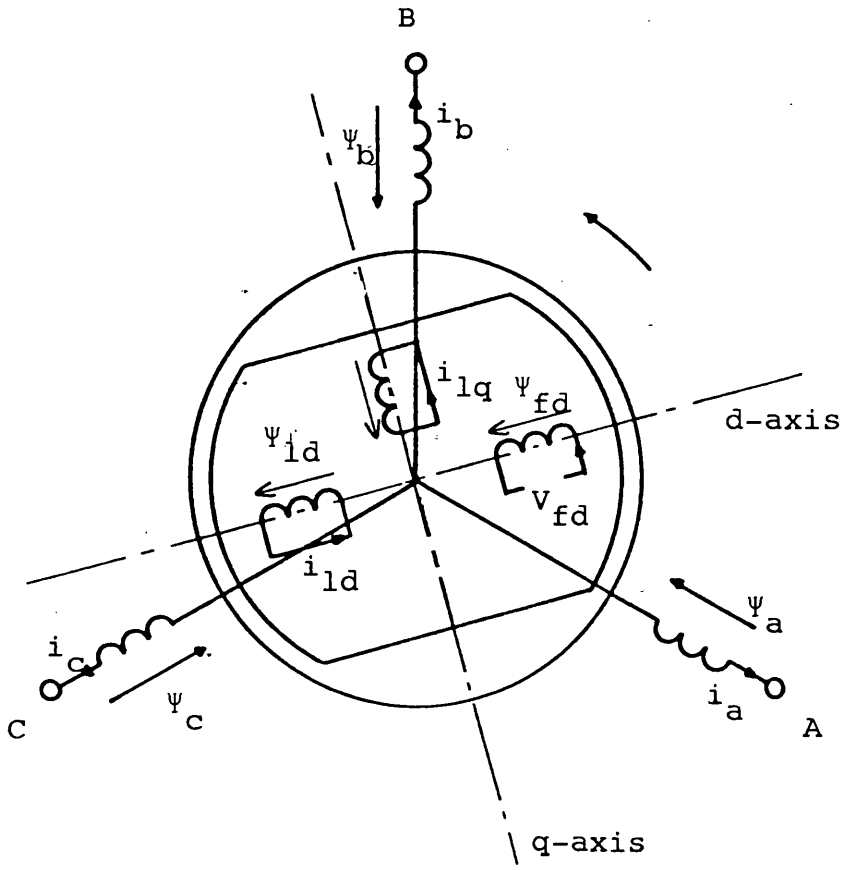

Fig. 2.2 Idealized Machine Windings

To obtain the equations for the idealized machine the following assumptions are applied.

1) A current in any winding produces an mmf wave, which is sinusoidally distributed around the air gap.

2) Hysteresis effects are neglected.

3) There is no interaction between direct and quadrature axes. That is a component of mmf acting along the direct axis, is assumed to produce a sinusoidally distributed flux wave in the direct axis only. Similarly quadrature mmf produces a sinusoidally distributed flux wave in the quadrature axis.

The flux linkage equations in the direct and quadrature axes and the generated voltage equations can be obtained from Fig. 2.2, in which the algebraic signs correspond to generator action.

Flux linkage equations:

$$\Psi_{fd} = x_{ffd} i_{fd} - x_{ad} i_d + x_{ad} i_{1d} \qquad 2.36$$

$$\Psi_d = x_{ad} i_{fd} - x_d i_d + x_{ad} i_{1d} \qquad 2.37$$

$$\Psi_{1d} = x_{ad} i_{fd} - x_{ad} i_d + x_{11d} i_{1d} \qquad 2.38$$

$$\Psi_q = -x_q i_q + x_{aq} i_{1q} \qquad 2.39$$

$$\Psi_{1q} = -x_{aq} i_q + x_{11q} i_{1q} \qquad 2.40$$

Voltage equations:

$$v_{fd} = p\Psi_{fd}/\omega_o + r_{fd} i_{fd} \qquad 2.41$$

$$v_d = p\Psi_d/\omega_o - \omega\Psi_q/\omega_o - r_a i_d \quad 2.42$$

$$0 = p\Psi_{1d}/\omega_o + r_{1d} i_{1d} \quad 2.43$$

$$v_q = p\Psi_q/\omega_o + \omega\Psi_d/\omega_o - r_a i_q \quad 2.44$$

$$0 = p\Psi_{1q}/\omega_o + r_{1q} i_{1q} \quad 2.45$$

Air gap torque equation:

$$T_e = \Psi_d i_q - \Psi_q i_d \quad 2.46$$

For this and subsequent models the equation of motion of the rotor is given by:

$$Mp^2\delta = T_m - T_e - K_d p\delta/\omega_o \quad 2.47$$

and the machine terminal voltage is given by:

$$V_t = \sqrt{(v_q^2 + v_d^2)} \quad 2.48$$

Saturation may be modelled by making the machine reactances a function of the flux levels in the iron circuits[34]. However, saturation effects have been neglected, since it has been shown[35], that saturation has little effect on transient stability. In the swing equation[36] the damping coefficient K_d is assumed constant. Values for K_d may be estimated[37,38], but the value is never known precisely due to turbine damping and the lack of precision in other machine parameters.

Equations 2.36-2.48 provide a seventh order representation that takes account of the decay of stator flux linkages, which give rise to power frequency oscillation in the machine

axis voltages and currents. It also predicts the initial braking torque which gives a rotor backswing observed on site tests at the inception of the fault[2]. The equations can be rewritten in operational form by eliminating rotor currents.

$$pe_d'' = \{(x_q - x_q'')i_q - e_d''\}/T_{qo}'' \qquad 2.49$$

$$pe_q' = \{V_f - (x_d - x_d'')i_d - e_q''\}/T_{do}' \qquad 2.50$$

$$pe_q'' = \{e_q' - (x_d' - x_d'')i_d - e_q'' - \left[T_1(e_q'' - x_d''i_d) + T_2x_di_d - T_{kd}V_f\right]/T_{do}'\}/T_{do}'' \qquad 2.51$$

$$v_d = p(e_q'' - x_d''i_d)/\omega_o + \omega(e_d'' + x_q''i_q)/\omega_o - r_ai_d \qquad 2.52$$

$$v_q = p(-e_d'' - x_q''i_q)/\omega_o + \omega(e_q'' - x_d''i_d)/\omega_o - r_ai_q \qquad 2.53$$

To reduce computation time it is possible to reduce the order of the representation. By neglecting the decay of stator flux linkages, machine speed variation and the less significant terms, the fifth order representation is obtained.

$$pe_d'' = \{(x_q - x_q'')i_q - e_d''\}/T_{qo}'' \qquad 2.54$$

$$pe_q' = \{V_f - (x_d - x_d')i_d - e_q'\}/T_{do}' \qquad 2.55$$

$$pe_q'' = \{e_q' - (x_d' - x_d'')i_d - e_q''\}/T_{do}'' \qquad 2.56$$

$$e_d'' = v_d + r_ai_d - x_q''i_q \qquad 2.57$$

$$e_q'' = v_q + r_ai_q + x_d''i_d \qquad 2.58$$

$$T_e = e_d"i_d + e_q"i_q - (x_d" - x_q")i_d i_q \qquad 2.59$$

The elimination of power frequency terms associated with the stator flux decrement allows an increase in integration step length, which is useful if a large number of optimization runs are required. If a further reduction in order is required then the third order system, obtained by neglecting damper windings, may be used.

$$pe_q' = \{V_f - (x_d - x_d')i_d - e_q'\}/T_{do}' \qquad 2.60$$

$$0 = v_d + r_a i_d - x_q i_q \qquad 2.61$$

$$e_q' = v_q + r_a i_q + x_d' i_d \qquad 2.62$$

$$T_e = e_q' i_q - (x_d' - x_q) i_d i_q \qquad 2.63$$

2.3.2 Transmission System

To make simulation of the transmission system tractable the following assumptions are made.

1) The transformer magnetising and line charging currents are negligible.

2) The transformer and transmission line can be represented by lumped series resistance and inductance.

Park's transformation on the 3-phase equations for the transmission system yields the following equations in the d-q axes of the generator.

$$v_d = V_b \sin\delta + X_t p i_d/\omega_o + R_t i_d - \omega X_t i_q/\omega_o \qquad 2.64$$

$$v_q = V_b\cos\delta + X_t p i_q/\omega_o + R_t i_q + \omega X_t i_d/\omega_o \qquad 2.65$$

2.3.3 Excitation System

The generator excitation system adopted for this study is shown in Fig. 2.3, capable of representing most systems, by appropriate choice of parameters. The actual parameters used reflect a thyristor system which enables bipolor field forcing.

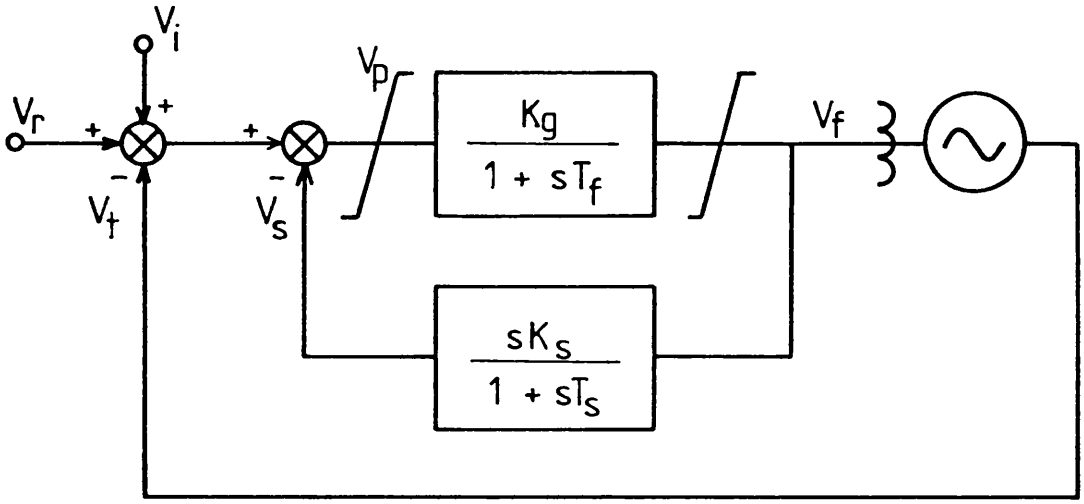

Fig. 2.3 Excitation System Representation

The following assumptions are made in creating the excitation system model.

1) The parameters do not change during transient conditions.

2) Saturation may be represented by simple voltage limits.

3) The thyristor converter characteristics are linear.

4) The terminal voltage transducer is linear and introduces no delays.

It is also assumed that there is no reactive power limiting

circuitry in operation. State feedback V_i is applied at the terminal voltage and reference summing junction and is therefore subject to the A.V.R. dynamics.

2.3.4 The Governor and Turbine

The prime mover system consists of three major elements, the boiler, the governor and the turbine. The time constants associated with the boiler systems are very long compared with the transient disturbances considered on the system. For the present investigation the boiler can be considered as an infinite steam source, that is, one which delivers steam at a constant temperature and pressure. It is thus analogous to the infinite bus of the electrical system.

Governors have, traditionally been devices for speed regulation[39]. The mechanical flyball device attributed to James Watt has been the basis of governing systems from the earliest turbo-generating sets, right up until the mid twentieth century. The success of the Watt-type system has been founded on proven reliability and the ability to allow parallel operation of many machines with acceptable load sharing. The small displacements caused by speed changes are used to direct hydraulic servos to position the governing values.

However, as the demands made on generating systems have risen and unit sizes increased the short comings of the Watt-type mechanical governing system have become apparent. Deadband

is always a problem in such mechanical systems and the more recent governing systems try to eliminate the deadband in the early stages, by the use of electrical speed transducers[40]. Usually the transducer is of the inductive pickup type, monitoring a multi-tooth gear on the turbine shaft, or a multi-pole permanent magnet tacho-generator may be used. The speed error is obtained by comparison of the actual speed with a suitable reference, the error signal is used as an input to the hydraulic servo system. The so called electro-hydraulic (EH) governing system provides an ideal vehicle for implementation of additional controls to obtain improved system response. The electrical nature of the signal stages allows a simplified interface for digital control. The Watt-type principle used in the mechanical-hydraulic (MH) governor survives though, as part of the overspeed safety trip system.

Throttle valve control of steam flow, through the turbine system is the primary means by which the rate of conversion from energy held in the steam, to mechanical energy, is performed. As mentioned earlier, the boiler time constants are large and power control by means of adjustment of boiler set points will not be considered in this study. In early turbines consisting of a single stage, or two stages with a short interconnection, the action of the throttle or governing valve had effectively a direct control on the power output. However, as unit outputs increased and high efficiencies were required, the thermodynamics of the steam cycle dictated increased steam temperature and pressures. The high pressure (HP) stage was the result. Greater overall efficiency is

obtained if, after passing through the HP stage the steam is returned to the boiler, prior to expanding through the intermediate pressure (IP) and low pressure (LP) turbine stages. The effect of the reheater[41] is to introduce a long time constant into the system as a result of the long pipe work and the boiler tubing.

The type of turbine used in this investigation is a three stage axial flow system with reheater. Super heated steam is fed from the boiler through emergency stop valves and governing valves to the HP stage. After the HP stage the steam is returned to the boiler to boost the thermal energy of the steam before it is delivered to the IP and LP turbine stages. The LP stage exhausts under vacuum into the condenser where the steam condenses by heat exchange with the cooling water. The condensate is then fed to the boiler feed pumps to continue the cycle. Generally the energy conversion in the HP cylinder is 25 to 30% of the total machine output, the large storage capacity of the reheat system dictates that a second set of emergency stop valves are placed before the IP turbine stage. Also, a set of intercept valves are located prior to the IP stage. If governing is limited to the valves before the HP stage, the maximum control effort in the short term is 25 to 30% of full load due to the reheater delay. Clearly any form of control which is required to make a contribution in the short term must control the intercept valves as well as the HP valves. It is assumed therefore that governing action is applied equally to both the HP and IP valves, and that, as a result, all three

cylinders can be assumed to be amalgamated into a single cylinder with a single control input.

2.3.5 Derivation of Governor-Turbine Model

The block diagram of Fig. 2.4, shows a detailed nonlinear representation of an electro-hydraulic governor-turbine system, based on data published by HAM[40]. Since this study is not directly involved with the thermodynamic behaviour of the turbine system, the additional networks used on the intercept valve control for thermodynamic reasons, have been omitted so that both the HP and IP valves are assumed to be driven together by the same signal. Also, the effect of reheater steam storage is such that over the transient periods of interest the intercept values are assumed to be fed with steam at constant temperature and pressure.

By linearization and reduction, an equivalent transfer function which represents the dynamic behaviour of the system of Fig. 2.4, can be obtained. The transfer function so obtained is 8th order. The linearized system response to a step input is shown in Fig. 2.5, in blue ink and can be seen to be very similar in form to a damped second order system. A further manufactures model[42] subject to similar assumptions regarding steam conditions and valve control has been reduced and an equivalent transfer function of the 4th order obtained. The step response is in red ink in Fig. 2.5. For comparison, the step response of a single lag with time constant 0.25s is shown in green ink.

For parameter values refer to Appendix 1

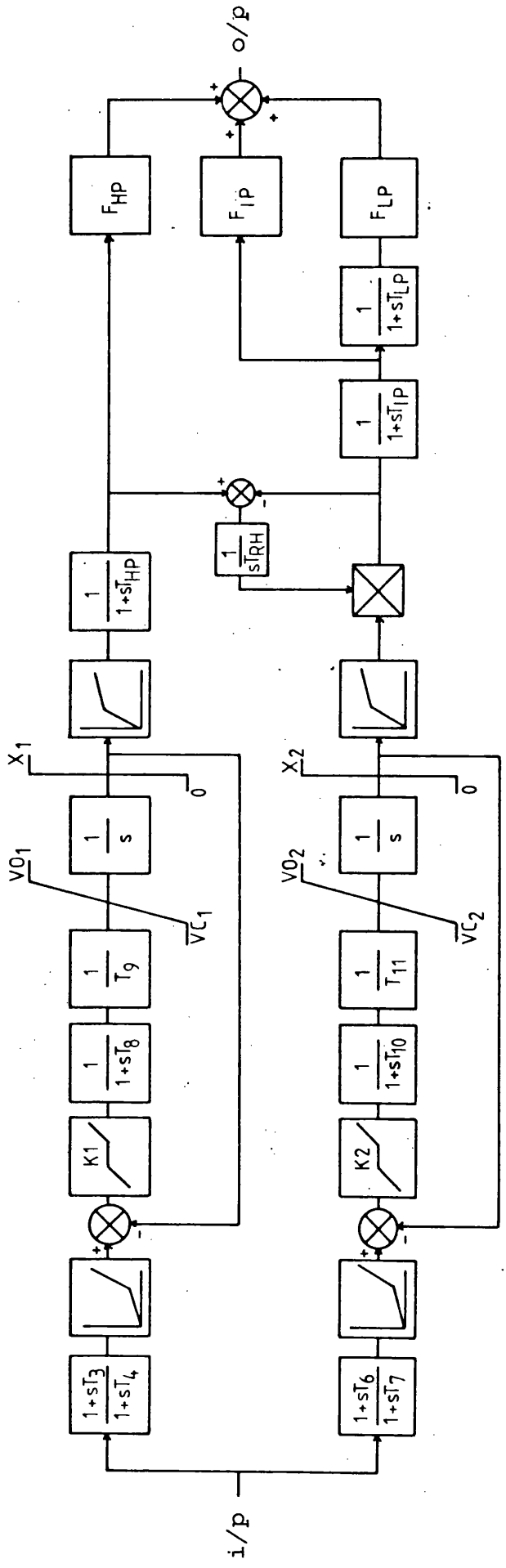

Fig. 2.4. Detailed Nonlinear Governor Turbine Model

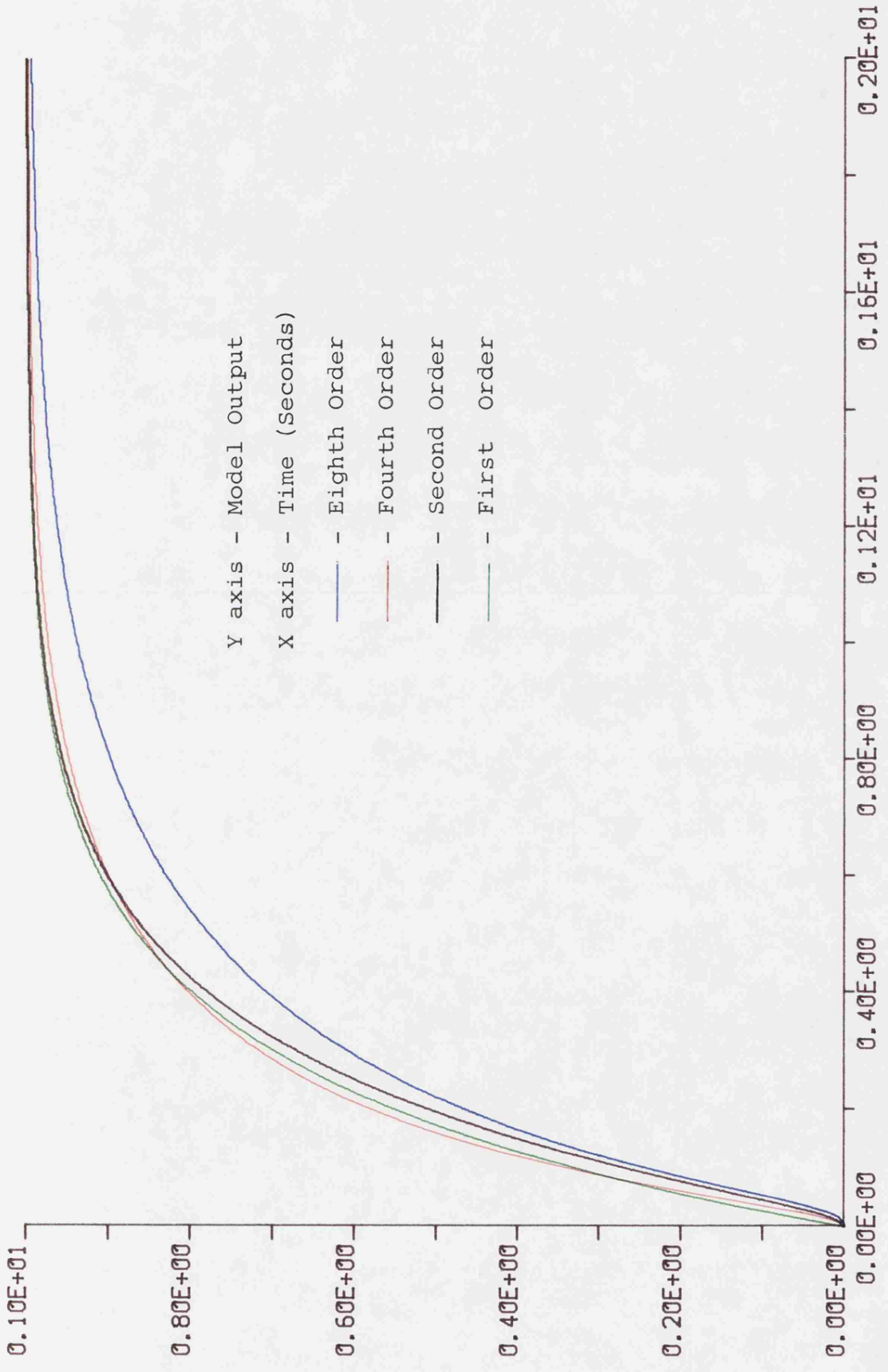

Fig. 2.5 Governor Turbine Model Step Responses

Both of the models discussed above are used to represent systems similar to those of the Pembroke machines. These linearized models are valid for small disturbances. However, the form of fault and the nature of the additional controls applied in this investigation result in control demands which are large and change rapidly. It is therefore necessary to use a model which takes into account, not only the absolute position limits of the steam valves, but also their velocity limits. The absolute velocity limits are generally lower for opening the steam valves compared with the closing rates due to the spring assistance in the latter case.

The model adopted may be represented as in Fig. 2.6, where the following assumptions apply.

1) Both superheater and reheater outputs are infinite steam sources, that is they supply steam at constant temperature and pressure.
2) Both HP and IP steam valves travel in unison and are subject to the same constraints.
3) Turbine power is a linear function of valve displacement over the operating range.
4) Turbine efficiency is constant over the small speed range considered.
5) All steam passes through the complete system.
6) Instrumentation transducers have negligible dynamics.

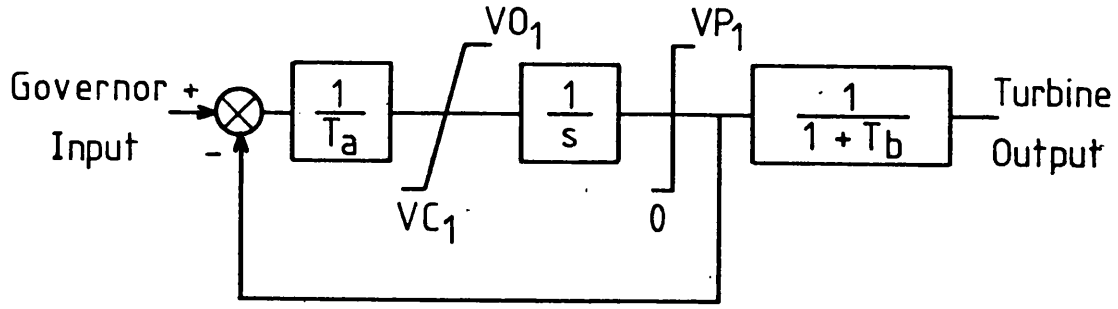

Fig. 2.6 Governor and Turbine Representation

A step response for the model of Fig. 2.6, with the rate limits neglected is given in Fig. 2.5, in black ink. Even though it does not fit either of the previous curves precisely it is clearly representative of the type of system under consideration. A single lag representation, the green curve of Fig. 2.5, is insufficient because it would not afford an acceptable placement of the valve velocity and position limits.

CHAPTER 3 THE MICROMACHINE SYSTEM

3.1 Introduction

For micro-alternator studies to be of value, it is necessary that the model system, of which it is a part, is based on a section of the real supply network. In the U.K., Pembroke Power Station lends itself to this type of study. Situated on the South West coast of Wales, it is a large thermal station based on four 500MW sets powered by three stage axial flow turbines operating at 3000 rpm. The generator terminal voltage is 22kV, which is stepped up by an on line tap change transformer to the transmission voltage of 400kV. The power transmission from the station is via two double circuit 400kV lines. The line pairs connect to the 400kV grid system at different points, but the line lengths are similar and little accuracy is lost if all four lines are assumed to be equal in length at 110km. The 400kV substations used for termination can be assumed to represent an infinite bus for theoretical purposes.

Thus Pembroke Power Station and its associated transmission system approximate the turbo-generator, transmission line and infinite bus system of Fig. 3.1,, so often used in theoretical studies. The micro-alternator system, based on Pembroke, has been described elsewhere[43], but the essential parts are described here for completeness.

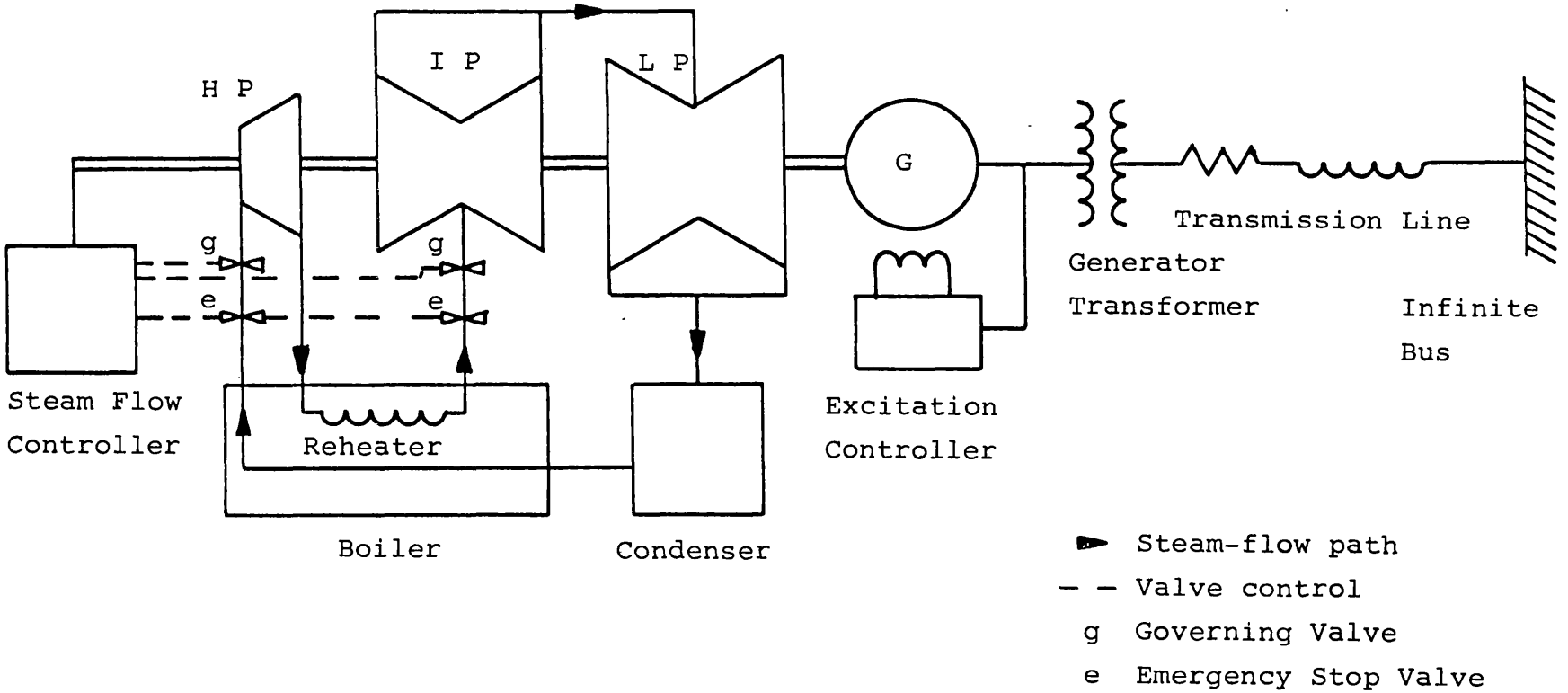

Fig 3.1 Turbogenerator, Transmission Line and Infinite Bus System

3.2 Micro-alternator and the Per Unit System

The four generators of the Pembroke system can be assumed to be identical and the four line circuits can also be assumed to be identical. This allows the simplification that for either a single machine single line to a base of its own MVA, or the whole station using all lines to a base of the gross MVA of the site, the per unit values are the same. Table 3.1 shows the per unit values for a single machine, together with the generator transformer and line values. A homegeneous system of per unit values is obtained by using the total station MVA as a base and referring all values to it by the use of standard formulae and Table 3.2 shows the resulting per unit values.

If the model system is to behave in the same way as the real system under dynamic conditions, the per unit quantities of each must be the same. In order to obtain an acceptable correlation, a specially designed micromachine as described by Hammons and Parsons[44] must be used. When defining the micromachine per unit system, it is necessary to choose the base values of system voltamperes (VA) and voltage so that the resulting per unit values reflect those of the real system. Two important parameters for correct dynamic operation are the direct access synchronous reactance x_d and the inertia constant H. The inertia constant is defined as

$$H = \frac{K_e}{S} \qquad 3.1$$

where K_e is the kenetic energy of the rotating machine at synchronous speed and S is the system base VA.
The inertia constant for the Pembroke system obtained from Table 3.2(a) is 4.44pu. Experimental data[43] gives the value of K_e to be 15.3kJ and manipulation of equation 3.1 gives S=3.45kVA for the micromachine system. The d-axis synchronous reactance x_d is given by

$$x_d = \frac{\bar{x}_d \, S}{V_{ao}^{\,2}} \qquad 3.2$$

where $\bar{x}_d$ is the absolute unsaturated direct axis synchronous reactance and V_{ao} is the base voltage. Hence substitution of

$$V_{ao} = \sqrt{\frac{\bar{x}_d \, S}{x_d}} \qquad 3.3$$

known values of parameters in equation 3.3 gives the base value of voltage to be 206V for the micromachine system. Base values for current and impedance may be derived using the following equations.

$$I_{ao} = \frac{S}{V_{ao}\sqrt{3}} = 9.65A \qquad 3.4$$

$$Z_{ao} = \frac{V_{ao}^{\,2}}{S} = 12.3\Omega \qquad 3.5$$

The per unit parameters of the micromachine are given in Table 3.3 which shows, that by careful selection of the per

unit base values, most of the per unit reactance parameters are either equal or close to the real system. However, the time constants do not show such good correlation, particularly the values of T'_{do} and T'_{d} the direct axis open and transient time constants. This is due to design limitations inherent in the micromachine. Even though the nominal rating of the micro-alternator is 3kVA and the housing is for 30kVA machine, there is still insufficient cross section in the windings to reduce the resistances to the required per unit values. The armature resistance values are improved by the use of deep slots and the oversize housing, but it is not possible to add much copper to the field winding without detriment to the magnetic properties. Table 3.3 shows that the values of x_d and x'_d are close to the required values and equation 3.6 shows that, if

$$x_d' = \frac{T_d'}{T_{do}'} x_d \qquad 3.6$$

then the ratio between T'_d and T'_{do} is correct. In order to change the magnitude of the time constant without changing their ratio, a so called time constant regulator is used in the field circuit. This regulator is considered in a later section but, in essence, the use of a high gain amplifier with feedback makes it possible to reduce the effective resistance of the field circuit, thereby varying the time constants.

3.3 Transmission Network

The transmission network consists of a simulation of the

generator transformer, the transmission lines and infinite bus. The model departs in some ways from the real system but these points are covered in the relevant sections.

3.3.1 Infinite Bus

Although the voltage and power levels for the model are within standard laboratory supply capabilities, the regulation of this type of supply is generally poor when it services a wide range of laboratories. The theoretical concept of an infinite bus is that of a zero impedance voltage source at the system frequency. Many laboratory supplies have too high an impedance which makes them vulnerable to distortion from local loading. To overcome the problem, a dedicated 330kVA 10.75kV/311V distribution transformer is connected to the University 6.6kV distribution network. The measured impedance referred to the model kVA is 0.0015pu when supplying approximately 5pu current. The bus transformer therefore only contributes 1.4% to the line impedance. This justifies its approximation to an infinite bus.

3.3.2 Transmission Line Model

In order to simulate the transmission line system a number of assumptions need to be made. It has already been stated that all four lines are assumed to be the same length. It is further assumed that the line impedances are symmetrical so that each may be represented using isolated single phase

networks of cascaded π elements. Four π sections are used to represent the distributed nature of the line impedance. The single line representation is given in Fig. 3.2. Table 3.4 gives the required and actual values used. The transmission line simulation does not accurately reflect unbalanced faults but this is not considered a limitation in view of the standard 3 phase symmetrical fault used throughout the theoretical and practical studies.

3.3.3 Generator Transformer Model

In power systems, it is economic to transmit power in bulk using very high voltages to keep I^2R losses to a minimum. It is not feasible to generate directly at these high voltages, so some means of increasing the generator terminal voltage is required. The generator transformer has two tasks in real systems. Firstly, it is used to step up the generated voltage to transmission levels. The second task is to enable the generator terminal voltage to be kept within tight limits for local loads while at the same time giving some adjustment of reactive power supplied to the grid system. The second function is performed by allowing on line tap changing which varies the effective turns ratio between primary and secondary windings. The two functions of the generator transformer have been separated in the model system. Since the generating and transmission voltages are at the same level, it is, therefore, not feasible to model the tap changing facility local to the micro-alternator. However, a 50kVA,

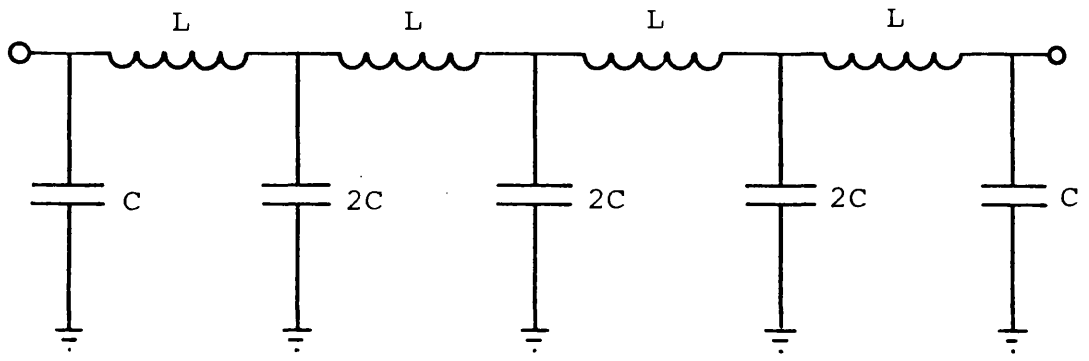

Fig. 3.2 Single Phase Transmission Line Model

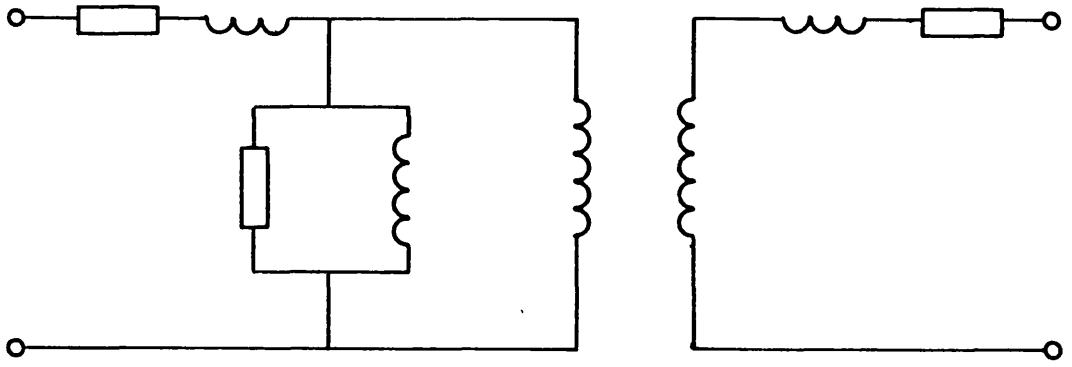

Fig. 3.3(a) Single Phase Transformer Equivalent Circuit

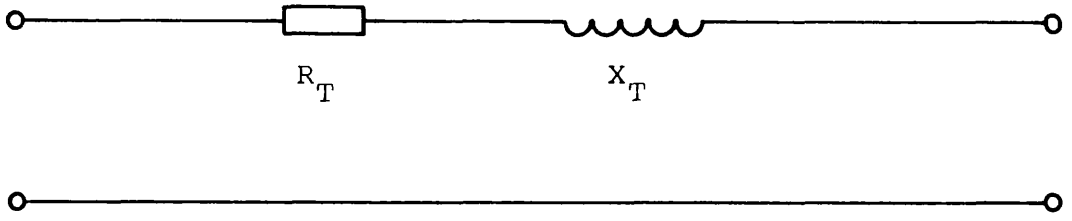

Fig. 3.3(b) Transformer Model Realization

415V auto transformer, normally used for distribution voltage trimming, is directly connected to the infinite bus. The motorised on load tap change of the auto transformer is used to regulate the infinite bus voltage between +4% and -9%. Thus in the model, control over reactive power is performed by changing the infinite bus voltage rather than the line voltage local to the generator. The error involved in this is small.

Single phase equivalent circuits are used to represent the generator transformer windings. The standard equivalent circuit of Fig. 3.3(a) is simplified by the unity turns ratio and by neglecting the magnetization losses, to that of Fig. 3.3(b) which is accurately realizable in terms of reactance but not resistance. Table 3.5 summarizes the corresponding per unit parameters.

3.3.4 Fault Throwing Equipment

The analytical studies use a 3 phase short circuit at the generator transformer high voltage terminals as a standard fault for comparison purposes. Computer simulation software can easily arrange for consistent fault initiation and removal. It is imperitive that physical tests taken on the micromachine system are similarly controlled, otherwise comparisons between physical and analytical results are meaningless.

To maintain close control over the fault initiation and fault duration, back to back thyristors are used in preference to mechanical relays. Fig. 3.4 shows the overall system. Consistent fault inception is obtained by triggering from a zero voltage crossing of one of the infinite bus lines. Fault duration is controlled by a variable duration mono stable which is used to gate the thyristor firing pulses. Use of thyristors allows faithful representation of circuit breakers that do not chop the current, since current remains flowing until a natural current zero.

3.4 Micro-alternator Excitation System

3.4.1 Field Power Circuits and Time Constant Regulator

A common feature of all excitation control systems is a high amplification factor from signal to power levels. The micromachine system uses a linear d.c. coupled transistor amplifier. The amplifier is a commercial unit rated at 60V, 12A, and 300W, which is adequate for the field system. The overall response of the power amplifier is such that dynamics may be modelled using standard operational amplifier techniques without the need of compensation for power stage dynamics.

It is well known that the micromachine direct axis transient time constant T'_{do} is not representative of a large machine. To compensate for this, a time constant regulator developed by Martin[43] is used. It can be shown that, by the use of a

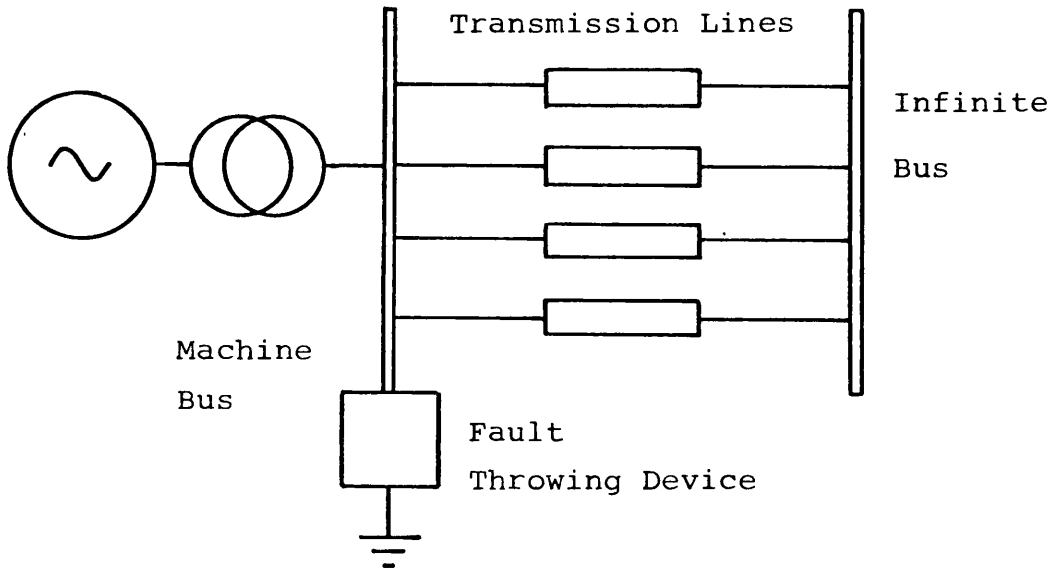

Fig. 3.4 Fault Throwing System

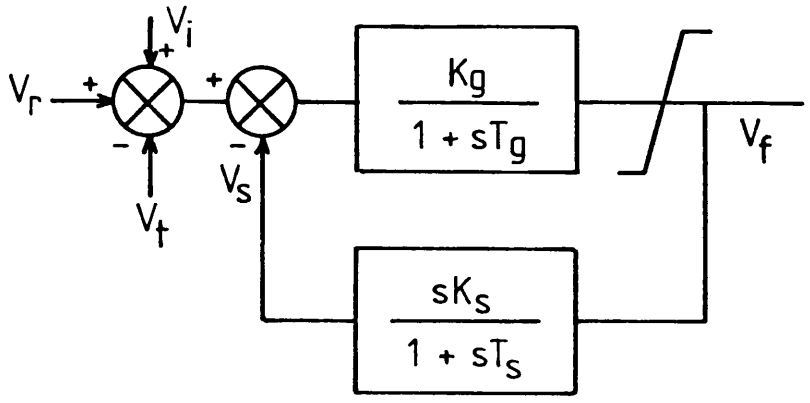

Fig. 3.5 Basic Automatic Voltage Regulator

high gain amplifier and feedback techniques, the effective time constant of a circuit is determined by the feedback transfer function H(s). For the micromachine, a shadow winding is present, tightly coupled to the main field winding, which may be used to obtain a signal for all induced voltages in the field. An external shunt resistor provides signals proportional to currents in the field. Using suitable gains H(s) and hence the micromachine time constants can be made to correspond to the parameters of the Pembroke Machines.

3.4.2 Automatic Voltage Regulator Simulation

The steady state terminal voltage error specified for standard generating equipment for the Central Electricity Generating Board is limited to ±0.5%. To maintain this accuracy, a forward gain of 200 or more is required. This high value of gain necessitates the use of stabilizing feedback. Fig. 3.5 shows the basic AVR transfer function. This is a simplified model which neglects the dynamics of both the terminal voltage transducer and the initial stages of amplification. The model is based on a modern thyristor excitation system capable of field voltage reversal with the limits on field voltage set at ±6.87pu. The realization of the limit system is such that, in either limiting condition, the input is clipped. This method gives a hard knee to the characteristic and also prevents saturation of the gain elements. Fig. 3.6 shows the complete model AVR which also contains a so called low gain input which was found necessary when analogue state feedback was used. The low gain input

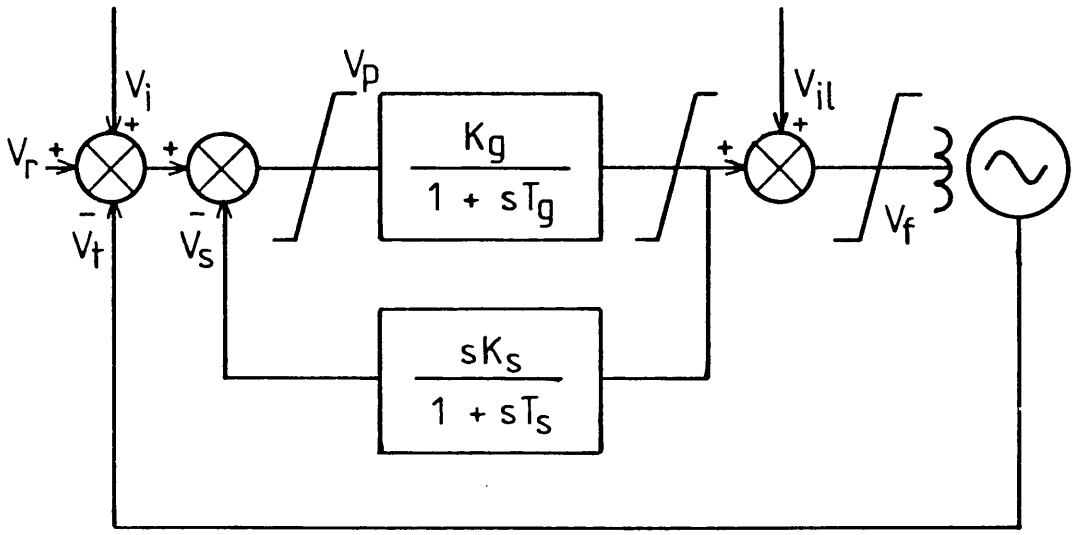

Fig. 3.6 Complete Model Automatic Voltage Regulator

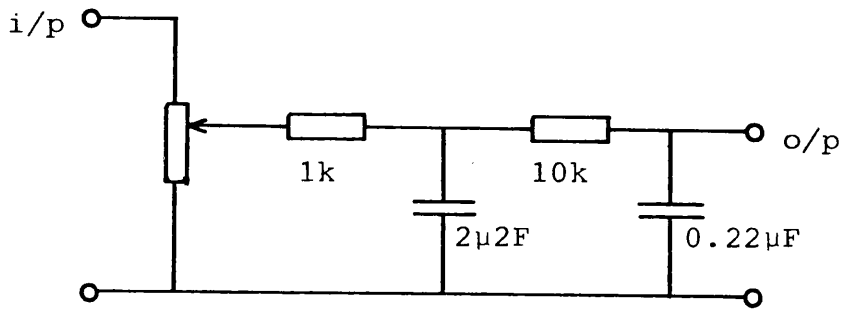

Fig. 3.7 V_t Filter Ciruit

corresponds to feeding directly into the main field winding and as such is not available on a large generator.

3.4.3 Terminal Voltage Transducer

The micromachine terminal voltage is obtained by means of three single phase transformers which both isolate and bring the voltage levels down to electronic levels. When the terminal voltage signal is full wave rectified an inherent 300Hz ripple is present. The simple filter shown in Fig. 3.7 is used to reduce the ripple without seriously degrading the transient response of the transducer. The remnant 300Hz injected into the AVR is eliminated by the system dynamics.

Two transducers are required, one for normal instrumentation purposes, the other for the AVR electronics. Due to the very high forward gain of the AVR model it is essential to reduce spurious input signals. It has been found most effective to perform the summation of reference voltage and terminal voltage feedback directly using a dedicated floating V_t signal. In this way ground reference problems are removed and the input offset error of the operational amplifier is seen merely as part of the reference voltage.

3.5 Analogue Measurement of States

3.5.1 Load Angle

For a synchronous machine with a conventionally wound rotor

it is possible to define load angle as the angle between the phasor corresponding to the infinite bus voltage and the phasor corresponding to the emf generated in the machine armature windings from flux set up by the field current. The field flux is fixed spatially with respect to the rotor. At the floating condition, when no energy transfer takes place, the phasors are in line and the load angle is zero. Under these conditions the terminal voltage phasor is also in line, and so may be taken as a reference if the machine is run on open circuit. If an a.c. tachogenerator, with the same number of poles as the micromachine, driven by the micromachine shaft is aligned so that its output voltage is in phase with the terminal voltage on open circuit, the phase difference between the tacho voltage and infinite bus voltage is a measure of load angle. By forming square waves from the sinusoidal voltages and taking suitable logical combinations, load angle information is available as a mark space signal. Before this signal is of any value as a control signal heavy filtering must be applied.

3.5.2 Transient Velocity

Transient velocity was obtained by differentiating the output of the load angle transducer. As the original signal was a filtered mark space signal, a pure differentiation would tend only to reconstitute the original signal. In order to avoid this, a limited frequency response was used in the differentiator with a 100Hz notch filter used to suppress the predominent noise.

3.6 The Prime Mover

The prime mover in the model system is a separately excited d.c. machine. The field winding is supplied by a constant current source so that the output torque is directly proportional to the armature current. The armature current source was originally a single phase fully controlled thyristor bridge circuit[43] but even closed loop control of such a system did not give a very good frequency response. Additional inductance in the armature circuit was used in an attempt to maintain continuous conduction. This had the benefit of more linear gain in the thyristor control system and a smoother current wave form. The inherent problem with the thyristor bridge, that of uncontrollability after the thyristor has been fired, aggravates the control problem and results in a system of limited frequency response.

While governor control was assumed to play no part in the transient behaviour of the systems, the thyristor bridge constant current source was acceptable. However, when studies include governor action it is clear that the quality of the armature current control must be such that the armature current follows the dynamics of the system being modelled and should not be conditioned by the response of the current control system. Ideally, the armature current should be derived from a linear power amplifier. The power levels required are of the order of 32 amperes at 160 volts for the full load condition on the micromachine and this would require an unacceptable level of power dissipation

over the full operating range if a fully linear system was used. A compromise solution has been adopted. A slit width chopper circuit, using a Darlington configuration with a high power transistor operating in the switching mode, is used to maintain the mean armature current at the desired value.

In the slit width modulator, the current control is such that the actual value of current lies between two bounds, one above, the other below the required mean current value. The bounds are used as switching functions for the transistor to either apply the supply voltage to the armature or remove the supply so that the current flows in a free wheel diode. The chopping frequency is dependent on the load characteristics and the slit width. Torque variations caused by the excursions of armature current about the mean value are effectively smoothed by the inertia of the micromachine. Further information regarding the operation of the slit width modulator is given in Appendix A2.

	Base MVA	588
	Machine rating MW	500
x_{ad}	Direct axis mutual reactance	2.59pu
x_{aq}	Quadrature axis mutual reactance	2.52pu
x_{ld}	Direct axis armature leakage reactance	0.21pu
x_{lq}	Quadrature axis armature leakage reactance	0.20pu
x_{lfd}	Field leakage reactance	0.162pu
x_{lkd}	Direct axis damper leakage reactance	0.0204pu
x_{lkq}	Quadrature axis damper leakage reactance	.0204pu
r_a	Armature resistance	0.00310pu
r_{fd}	Field resistance	0.00120pu
r_{kd}	Direct axis damper resistance	0.0174pu
r_{kq}	Quadrature axis damper resistance	0.0070pu
H	Inertia constant	4.4pu
SCR	Short circuit ratio	0.4pu

Table 3.1(a) Per Unit Parameters for a Single Pembroke Machine

Base MVA	600
Resistance	0.005pu
Reactance	0.160pu
Tapping range %	+2, -16

Table 3.1(b) Pembroke Generator Transformer Parameters

	Base MVA	100
	Resistance	0.00135pu
	Reactance	0.0185pu
	Susceptance	0.735pu

Table 3.1(c) Pembroke Single Circuit Line Parameters

	Base MVA	2352
x_d	Direct axis synchronous reactance	2.8pu
x_q	Quadrature axis synchronous reactance	2.72pu
x_d'	Direct axis transient reactance	0.362pu
x_d''	Direct axis subtransient reactance	0.230pu
x_q''	Quadrature axis subtransient reactance	0.220pu
T_{do}'	Direct axis transient open circuit time constant	7.3s
T_d'	Direct axis transient short circuit time constant	0.945s
T_{do}''	Direct axis subtransient open circuit time constant	0.0314s
T_d''	Direct axis subtransient short circuit time constant	0.020s
T_{qo}''	Quadrature axis subtransient open circiut time constant	0.116s
T_q''	Quadrature axis subtransient short circuit time constant	0.00936s
H	Inertia constant	4.4pu
SCR	Short circuit ratio	0.4pu

Table 3.2(a) Normalized Generator Parameters

	Base MVA	2352
R_T	Resistance	0.00490pu
X_T	Reactance	0.157pu
	Tapping range %	+2, -16

Table 3.2(b) Normalized Generator Transformer Parameters

	Base MVA	2352
R_t	Resistance	0.007940pu
X_t	Reactance	0.109pu
B_t	Susceptance	0.125pu

Table 3.2(c) Normalized Total Line Parameters

	Micromachine				Pembroke	
Base Rating	3.45kVA				2352MVA	
r_a	0.0970	Ω	0.00790	pu	0.00310	pu
x_d	34.5	Ω	2.8	pu	2.8	pu
x_q	33.5	Ω	2.72	pu	2.72	pu
x_d'	4.44	Ω	0.361	pu	0.362	pu
x_d''	2.22	Ω	0.180	pu	0.230	pu
x_q''	3.76	Ω	0.306	pu	0.220	pu
T_{do}'	0.398	s	0.398	s	7.3	s
T_d'	0.0514	s	0.0514	s	0.945	s
T_{do}''	0.0280	s	0.0280	s	0.0314	s
T_d''	0.0140	s	0.0140	s	0.020	s
T_{qo}''	0.0792	s	0.0792	s	0.116	s
T_q''	0.0089	s	0.0089	s	0.00926	s
Ke	15.3	kJ				
H			4.4	pu	4.4	pu
SCR			0.416	pu	0.400	pu

Table 3.3 Micromachine and Pembroke Per Unit Parameters

	Required		Actual	
Resistance	0.0318pu	0.391Ω	0.0318pu	0.391Ω
Inductance	0.436pu	16.0mH	0.410pu	16.0mH
Capacitance	0.0313pu	8.08μF	0.0310pu	8.00μF

Table 3.4 Single Circuit Model Line Parameters

	Required		Actual	
Resistance	0.0049pu	0.0603Ω	0.0130	0.16Ω
Inductance	0.157pu	6.15mH	0.157pu	6.15mH

Table 3.5 Model Generator Transformer Parameters

CHAPTER 4 EVOLUTION OF THE DIGITAL SYSTEM

4.1 Introduction

The use of a micromachine system in an effective manner for the investigation of synchronous generator stability makes it necessary to perform the following functions. Data collection from the system to generate control signals, application of the controls to the system and then collection of data showing the effect on performance of the applied controls.

The micromachine system at Bath has been in existence since 1968. The original system[43], had purely analogue control and instrumentation. Attempts to implement state feedback in the excitation system failed mainly because of noise problems in the selected states. The theoretical studies on which the controls were based used the deviation from steady state values of the control states as feedback signals. Constant adjustment of the d.c. level, backing off circuits was necessary to prevent drift problems. The state deviation is often small compared with the steady state level and the signal value may only be of the order of noise present. This was particularly evident with the transient velocity signal[45]. The best analogue method of deriving transient velocity was found by taking the derivative of the load angle, even though the raw load angle signal was in a mark space form which required heavy filtering before analogue differentiation was possible.

Only when the first digital system was introduced[45] was it possible to implement successful state feedback controls. This original digital system employed an Intel I8080 as the central processor. There were no support devices easily available, at the time when the system was developed, for interrupt priority handling or extended arithmetic operations. An in-house peripheral interrupt priority card was developed which gave a means of ordering interrupts in a daisy chain but did not implement any means of setting at which level interrupts could be accepted. Thus only the software interrupt enable, disable, instructions could be used to regulate interrupt service activity.

The poor arithmetic capability of the I8080 was a limitation, which was overcome by only performing the essential arithmetic operations in the I8080. In particular, no divide operations were performed because they would have to be software routines, and as such, very time consuming. Multiplication suffered from similar timing constraints, since the operation would be performed by software. Only a small number of multiplications were performed per control cycle, and these were based on highly optimized routines. To compute control laws in the I8080 would have required general purpose routines to cope with varying coefficients, so the PDP 11 was used to perform calculations on the data presented to it by the I8080, the results being transferred back to the I8080 for output as a control function. Even though support devices were becoming available for the I8080 cpu which could cope with interrupt priority problems and

help with the arithmetic limitations, it was considered that the system would still be held back by the short comings of the basic I8080 instruction set and word size. A more powerful microprocessor was obviously needed. The TMS 9900 microprocessor was becoming available and being a 16 bit word device with unsigned multiply and divide as part of the instruction set, it would go a long way toward solving the arithmetic limitations experienced. The TMS 9900 also has 15 levels of maskable interrupt which together with the context switch allows efficient response to external events.

This chapter describes the major elements of the present digital system. Frequent reference is made to the original Intel I8080 based system designed by Burrows[45], to show the course of evolution. The overall system is shown in Fig. 4.1 throughout this Chapter reference is made to the overall supervising computer as the PDP 11. In this particular application a PDP 11/34 is used but any compatible machine can be used.

4.2 Interface Requirements Between PDP 11 and TMS 9900 Processors

In the research application of the system, it is necessary to be able to efficiently develop software for both the PDP 11 and the TMS 9900 microprocessor. It is also necessary to be able to perform bidirectional data transfers between the two machines.

The PDP 11 system is ideally suited for program development

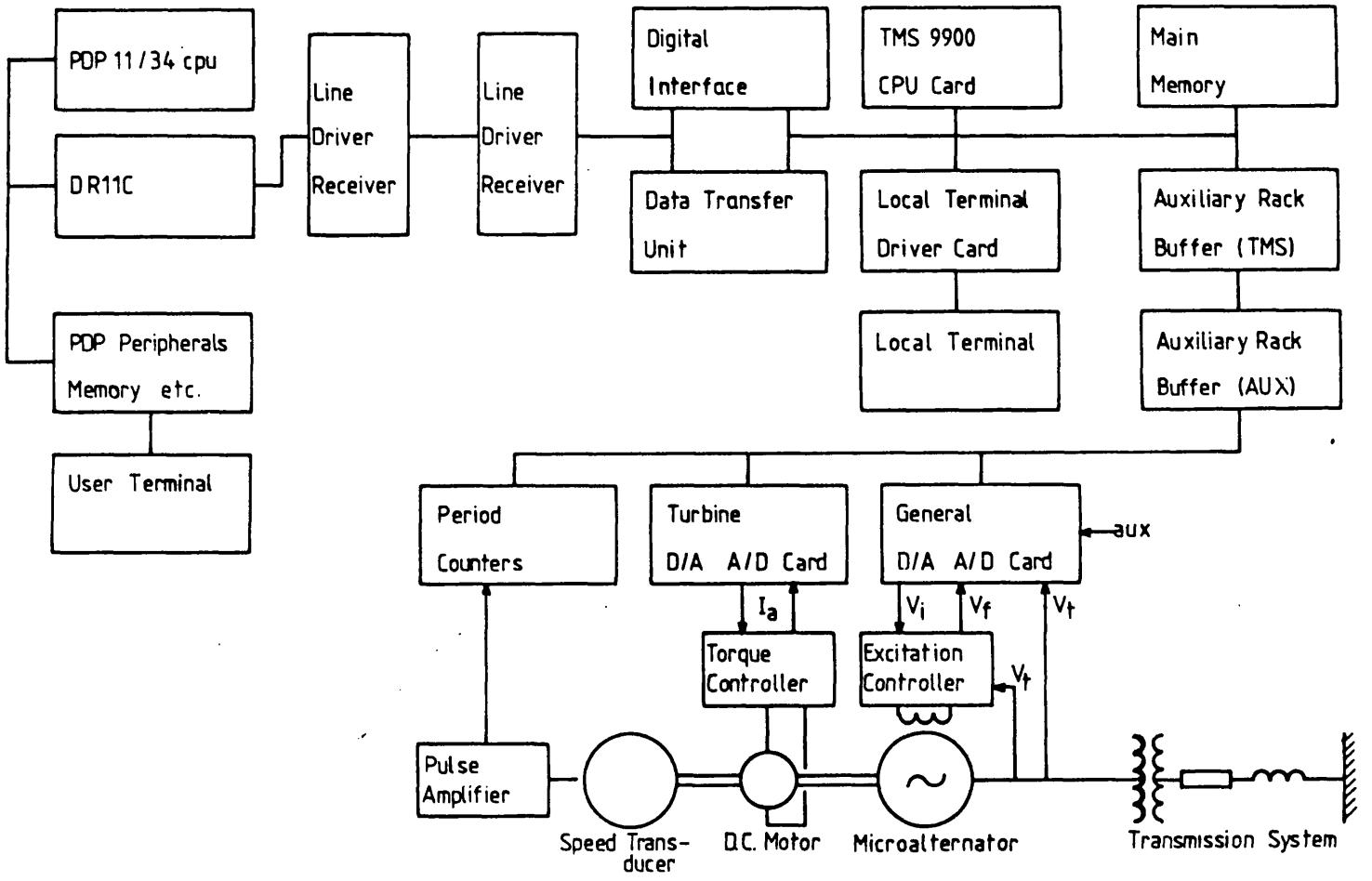

Fig. 4.1 Minicomputer, Microprocessor and Micro-alternator System

by virtue of its large disc storage capacity, terminal facilities and utility programs. In-house PDP 11 software for microprocessor development originally developed for the I8080 system has been changed to support the TMS 9900 and extensively improved.

The philosophy of the interface system is to implement the following functions.

1) Down line loading of microprocessor programs from the PDP 11.

2) Full software debug using the PDP 11 to supervise operation of the program within the microprocessor.

3) Bidirectional data transfer between the PDP 11 and the microprocessor under program control.

A single card providing all the required functions was not considered practical so the interface function was split into two logically independant cards. One card contains the data transfer logic, while the other contains the down line loading and debug circuits. For convenience the cards are termed the Data Transfer Unit (DTU) and the Digital Interface (I/F).

4.2.1 Physical Connection Between the Microprocessor System and the PDP 11.

The PDP 11 series of computers can support external devices by means of the Digital Equipment Corporation DR11C module. This has three memory mapped registers, a control and status

register, an output register and an input register. Both the input and the output registers are 16 bit parallel units. The control and status register allows for two interrupt signals from the external device with independant enables and two program controllable output bits[46]. These features allow a system to be developed which satisfies the interface specification.

Both the PDP 11 and TMS 9900 are 16 bit machines and so, under operational conditions, it is sensible to allow data transfers using the full 16 data bits. Taking this approach, it is necessary to have some means of differentiating between data transactions with the DTU and transactions with the I/F. The DR11C control and status register bits CSR00 and CSR01 provide a means of making the distinction. Table 4.1 shows the data modes used.

CSR01	CSR00	Data Mode
0	0	DTU Data
0	1	Not Used
1	0	I/F Data
1	1	I/F Control

Table 4.1

The PDP 11 computer and the microprocessor systems are housed in separate rooms. Communication between the digital systems uses a parallel data link consisting of twenty twisted pair

current loops for each direction. A connection schedule is provided in Appendix A3.

4.2.2 Digital Interface Functions

The I8080 - PDP 11 interface used a single step mode for program debug. At each memory access information was available to the user which gives the current address and the type of access. A pseudo breakpoint facility was used which single stepped the I8080 program under PDP 11 control until an instruction acquisition at an address in the breakpoint table was found. The breakpoint feature was useful for debug but the effective processor speed was slow, making it unsuitable for any attempt at running even small sections of code which interfaced with external events in real time. The TMS 9900 interface has been designed to allow program execution at full processor speed in the breakpoint mode. By use of an extended operation trap instruction[47], at the required address, control is passed to a short routine which triggers the interface hardware to gain control of the microprocessor. A single step mode of operation is also provided using a similar technique, but in this case the external operation instruction is jammed on to the data bus replacing the normal instruction at each new instruction acquisition. The use of the external operation context switch for debug routines is a powerful feature, since the entire working environment of the program code under debug is available. That is, the work space pointer, program counter and processor status are all immediately available for inspection as

registers within the extended operation work space. With the exception of only three registers internal to the cpu all registers are resident in main memory and standard memory location manipulation can be performed on them giving great flexibility.

The down line loading of the microprocessor memory on the I8080 system was geared towards speed, with an automatic address increment, or decrement facility. Operational experience with this showed that, since program loading is infrequent, very little time is saved, at the expense of increased circuit complexity. A major element in the TMS 9900 interface philosophy is to make the interface hardware as simple as possible commensurate with fulfilling its requirements, and if necessary increasing the PDP 11 processor effort to compensate. The down line loading feature follows this approach, requiring several PDP 11 operations to fill and check a microprocessor memory location. At each stage it is possible to check that the correct address is present on the address bus and that the data is correctly written. When the next location is loaded the entire operation is repeated. The somewhat pedestrian approach is barely noticed in practice.

Full descriptions of the I/F are provided in Appendix A3 for both software operation, from the PDP 11 point view, and hardware. Fig. 4.2 shows the major elements of the I/F in block diagram form.

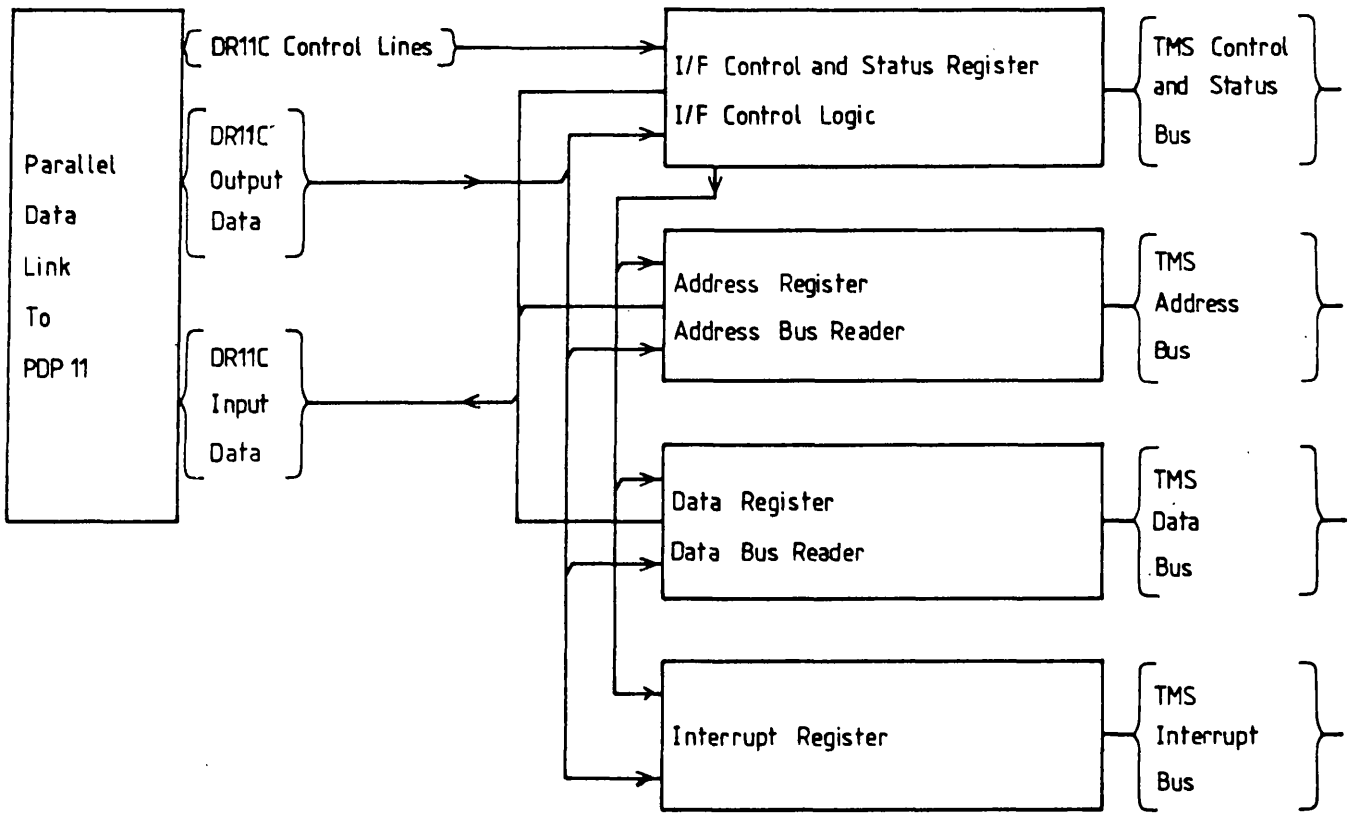

Fig.- 4.2 Digital Interface Block Diagram

4.2.3 Data Transfer Unit

The Data Transfer Unit (DTU) has been developed to allow fast data transfer between the TMS 9900 microprocessor and the PDP 11, Fig. 4.3 gives a block diagram of the system. Transfers are made in word wide parallel fashion. The DTU has been specifically designed for use with the Digital Equipment Corporation DR11C. By using parallel interface the data rate is limited in practice solely by the response of the software at each end.

Software controlling transfers may be based either on a simple flag testing of the handshake bits for a simple system, or may use the full interrupt structure of both processors. The DR11C in the PDP 11 is fitted at the standard hardware interrupt level[46], and is run in accordance with the appropriate operating system software constraints for the interrupt service software priority levels. The microprocessor interrupts are fully software programmable for interrupt levels between 1 (the highest) to 15 (the lowest), separate interrupt requests are available on both machines for input and output. A complete guide to the DTU operation is given in Appendix A3 for both software and hardware functions.

4.3 The Digital System Transducers

The TMS 9900 system interfaces with the micromachine hardware by a set of memory mapped registers which are used as input output devices. The TMS 9900 communications register unit,

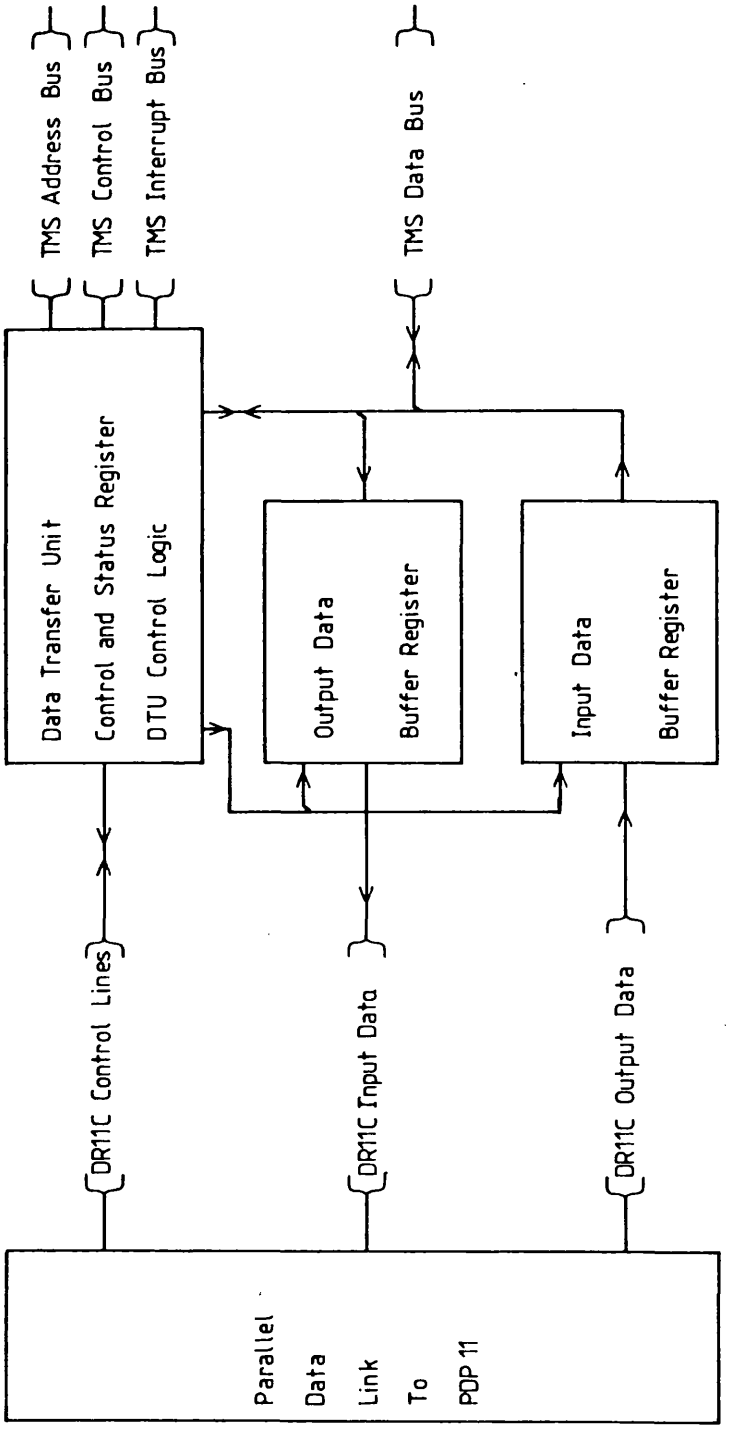

Fig. 4.3 Data Transfer Unit Block Diagram

CRU, is not used for any real time data acquisition because in general, complete word transfers are required. The memory map technique is faster and more convenient. The following sections give only a cursory view of the electronic hardware, more detail is available in the appropriate section of the Appendix.

4.3.1 Auxiliary Rack

To avoid undue loading of the main TMS 9900 system busses, and also to provide a simple means of performing input output to device registers, a dedicated input output block, has been set aside in the TMS 9900 memory map. The block is nominally 64 words in length, and is accessible through a buffer card on the main system bus. The buffer card function is to provide initial block decode of the locations and bus buffering. Of the 64 memory locations available, the first 16 are local to the buffer card, but space limitations permit only 4 words to be decoded. These locations are used as control registers for devices requiring interrupts to be placed on the TMS 9900 system interrupt bus. The remaining 48 locations are available in the auxiliary rack. Communication between the TMS 9900 system buffer card and devices in the auxiliary rack is controlled by a second buffer card in the auxiliary rack.

4.3.2 Analogue to Digital and Digital to Analogue Ports

The measurement of analogue quantities is performed using 12 bit successive approximation analogue to digital converters.

The conversion process is initiated under software control by setting an appropriate start bit in the control and status register. Conversion time is 25μs and so no facility to interrupt the processor on completion is provided, but the status of each converter is available as a bit in the control and status register.

For instrumentation purposes, the micromachine terminal voltage, as derived from a simple three phase full wave rectifier and filter circuit, is converted to digital form. Also the prime mover current is measured using a filtered version of the shunt feedback voltage to the transistor controller. The micromachine exciter field voltage is also measured as a standard parameter. A further analogue to digital converter is always available for measurement of miscellaneous quantities.

Two digital to analogue channels are used. The first is for a current demand input to the prime mover armature current controller. The second is used to provide the transient state feedback signal into the excitation control system.

4.3.3 Speed Measurement System

As mentioned earlier, transient velocity measurement for the micromachine system has been difficult. To overcome the problems associated with the existing tachogenerator a shaft mounted digital transducer was used[45]. The device consisted of a disc with a single slot which passed two transmissive

infra-red source and detector assemblies as shown in Fig. 4.4.

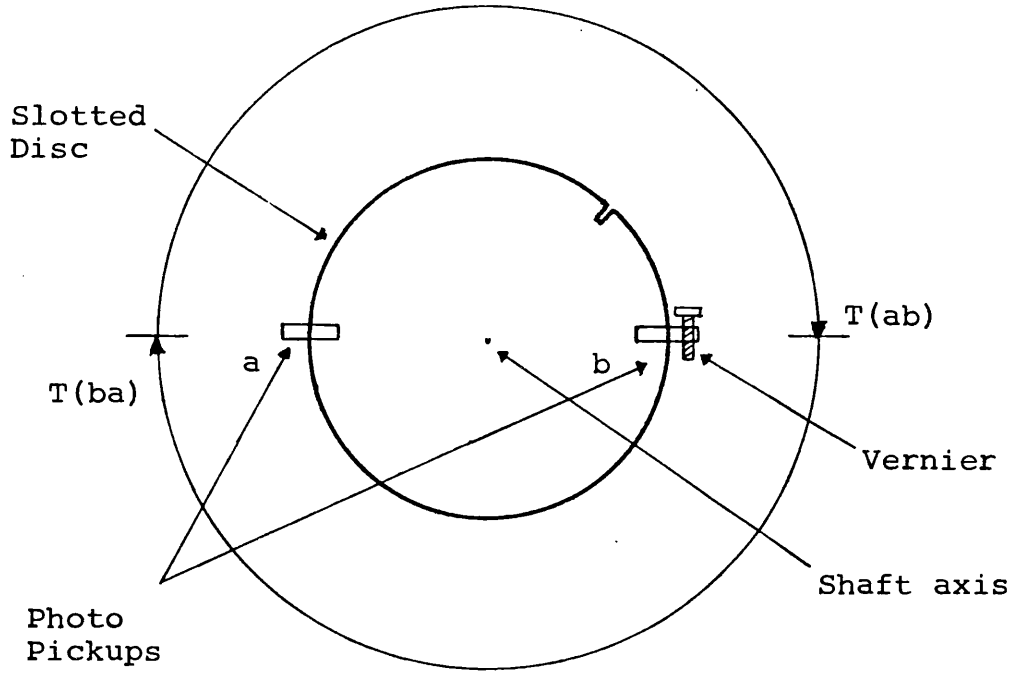

Fig. 4.4 Original Slotted Disc Transducer

The time interval between the slot passing photo device (a) and then passing photo device (b) was measured as T(ab)μs. Similarly the period from device (b) to device (a) was measured as T(ba)μs. Thus for the four pole machine operating at synchronous speed T(ab) = T(ba) = 20000μs.

The maximum speed change expected is of the order of 2% so it is reasonable to use changes in period as being proportional to changes in speed. Thus the transducer arrangement of Fig. 4.4 can be used to obtain an indication of transient

velocity. To avoid introduction of an offset between period values T(ab) and T(ba), it was necessary to include a vernier adjustment for the position of photo device (b). Even after calibration, it was difficult to maintain T(ab) close to T(ba) for steady state operation. To overcome this problem a simple filter arrangement was introduced of the form

$$P'_n = \frac{(P'_{n-1} + P_n)}{2} \qquad 4.1$$

where P'_n is the averaged period at sample instant n and P_n is the present sample value of period as measured by T(ab) or T(ba).

The rotor transducer also afforded a measure of load angle when used in conjunction with the phase of the infinite bus. By measuring the time interval between the passing of a photo device and a positive going zero crossing of the infinite bus voltage, a measure of rotor position relative to the infinite bus is obtained. Subtracting the no load, floating count from the present count gives a measure of load angle. Here, as in the change on speed measurements it is possible to minimize errors due to variation in systems speed by additional computation. However since speed changes are small the error level is only of the order of 2%, and no correction factor was applied in the I8080 system.

A theoretical study[18] has shown that the rotor acceleration is a very desirable state for feedback purposes. It is also

perhaps the most difficult state to obtain. It has been shown that the single slotted disc system can produce transient velocity signals far more acceptable for feedback purposes than have previously been possible with tacho-generator systems[25]. However, due to the mismatch between alternate period counts, attempts to use a first difference technique to obtain acceleration have failed. When the averaging process was performed acceptable speed values were obtained but these too produced unacceptable acceleration curves. The effect of the averaging was to introduce a low pass filter into the system, creating a further delay on top of the inherent delay caused by the method of period sampling to obtain the speed. The original device could therefore produce speed data at 20ms intervals which was based on a binary weighted average of the present transducer data and all the preceeding data.

It was clear that if an acceleration signal was to be obtained from differences in speed measurements, an even more accurate means of deriving speed was required. The results obtained so far from analogue transducers were disappointing and after consideration of the improvement made by the first digital transducer, it was decided to look closely at the error modes for the first system and to try to overcome them.

The photo assembly mounting arrangement was fabricated using standard angle iron bolted to micromachine and bed plate. It was not certain that this micromachine shaft axis remained fixed relative to the photo devices during faults, either due

to the shaft moving on its bearings or due to vibration of the photo device supports. Also, the photo detector employed had a large aperture and could have been subjected to reflections of the infra-red beams interfering with the precise threshhold at which the electronics determined the passing of a slot.

The problems could not be solved effectively using the existing transducer so a new design was developed. The overriding requirement is to measure the period of a machine revolution accurately. This requires two factors, a stable time reference and an accurate means of defining the limits of a machine revolution. The time reference has never been considered a problem since the microprocessor systems used have always had crystal controlled clocks. Experience with the two photo pickup system has shown that the attempt to split the mechanical shaft revolution into two halves, equivalent to the electrical cycles of the four pole machine, is nullified due to the required averaging process.

4.3.3.1 Second Generation Speed Transducers

If the same photo device is used to both start and stop the period count, the mechanical alignment problem is removed. Adopting this technique also gives the added advantage that mechanical vibration effects of rotational speed are reduced, since the measurements are always made at the same point. The misalignment of the photo device relative to the micro-alternator shaft axis is minimized by running the photo device

support on a bearing mounted on the shaft, Fig. 4.5 shows the general arrangement of the first, second generation transducer and Fig. 4.6 shows the second. By running the machine system as its own lathe and turning the machine shaft in situ prior to mounting the transducer, the minimum of vibration is imparted to the mounting system. By these techniques, it is possible to maintain the photo device fixed with respect to the machine shaft.

A further feature of the second generation transducers is the small aperture used to restrict the infra-red light input to the photo detector. The aperture is 0.1mm and at synchronous speed the rotating slot travels at approximately 0.0125mm per μs so that, the transit time for the leading edge is, of the order of 8μs. The narrow aperture is close to the photo detector and thus reduces to a minimum any spurious reflections, enabling the detection circuit to operate on a well defined slope with an effective rise time of 8μs determined by the mechanical arrangement.

The rotating section of the first, second generation transducer contains a single slot milled in the rim of the cupped disc. A cupped disc is used to increase the rigidity of the rotating element. As the single slot passes a fixed aperture, infra-red light is allowed to pass from the diode source to the photo transistor detector. The rising edge of the photo current in the sensor is used in the detector electronics to fire a monostable of short pulse duration. The pulse is subsequently used to start and stop counters measuring the

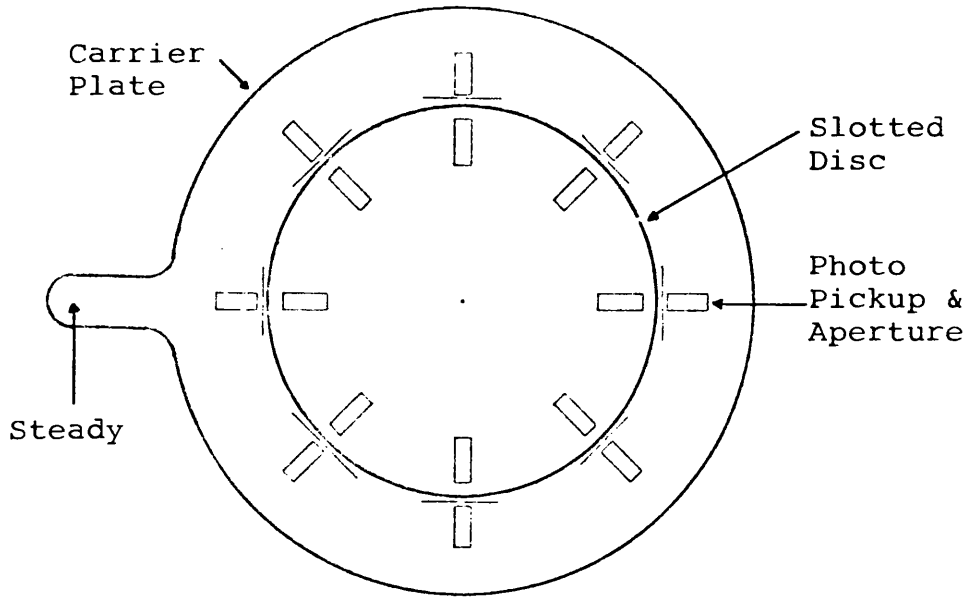

Fig. 4.5 Eight Pickup Single Slot Transducer

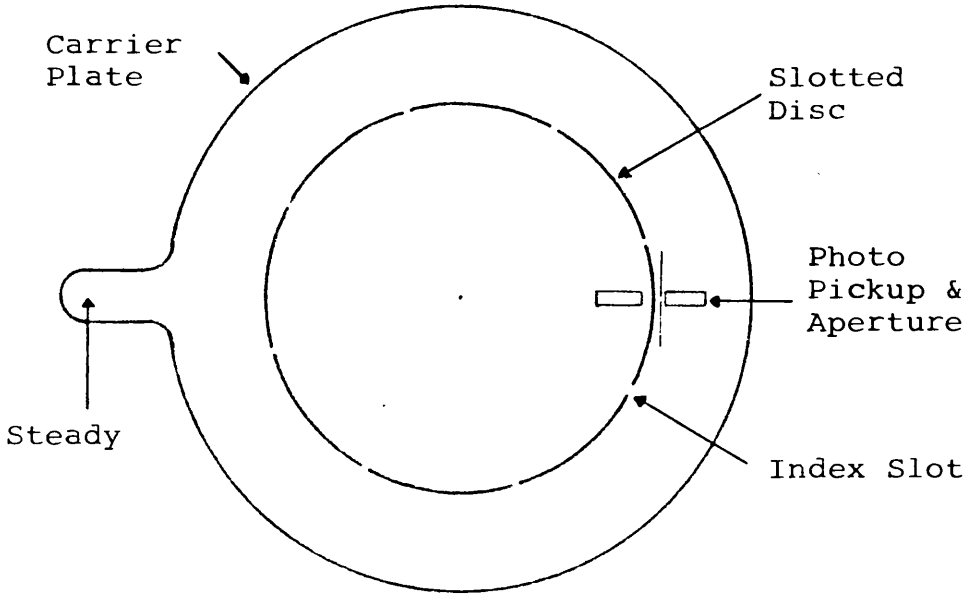

Fig. 4.6 Single Pickup Eight Slot Transducer

elapse time between pulses. To reduce the delay time between samples a total of eight transmissive photo assemblies are used, equally spaced around the stationary carrier plate. The period timing is maintained at 1μs quantization, this enables a whole 40ms period to be represented in a 16 bit word which affords simple manipulation by the TMS 9900 microprocessor. Also at 1μs quantization, the electronics can fix a slot crossing to within 0.0125mm, which is probably more precise than the mechanical system warrants. Using these techniques it was found that a small amount of axial preload on the bearing was required before consistent data was obtained in the steady state. Even in steady state operation the values obtained from the transducer for system period varied but when consideration is given to the fact that the period is being measured to 0.0025% it is natural that the transducer should show up the small fluctuations which are always present.

The manner in which the period data is made available is shown in Fig. 4.7. Each photo pickup on the carrier plate effectively produces a pulse Q_n , n = 1,2,3,... at approximately 40ms intervals, as in Fig. 4.7(a). The vertical arrows indicate the pulses and the sloping line represents the period count in μs being built up between pulses. The pulse Q_n triggers the following sequence in its associated period counter circuits. Counting ceases and when the data is stable it is clocked into a buffer register, the counter chain is then reset and counting resumes. This sequence takes a fixed time, of the order of 1μs, and has no detrimental

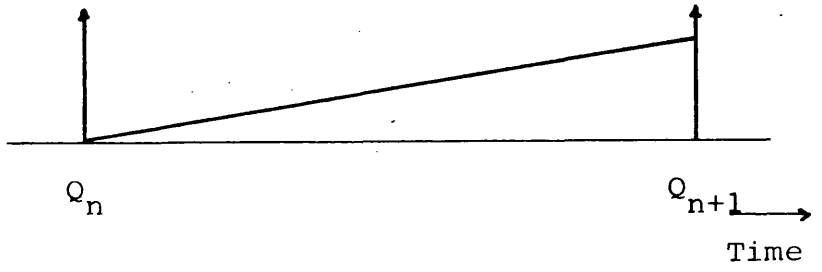

Fig.4.7(a) Period Counter Operation

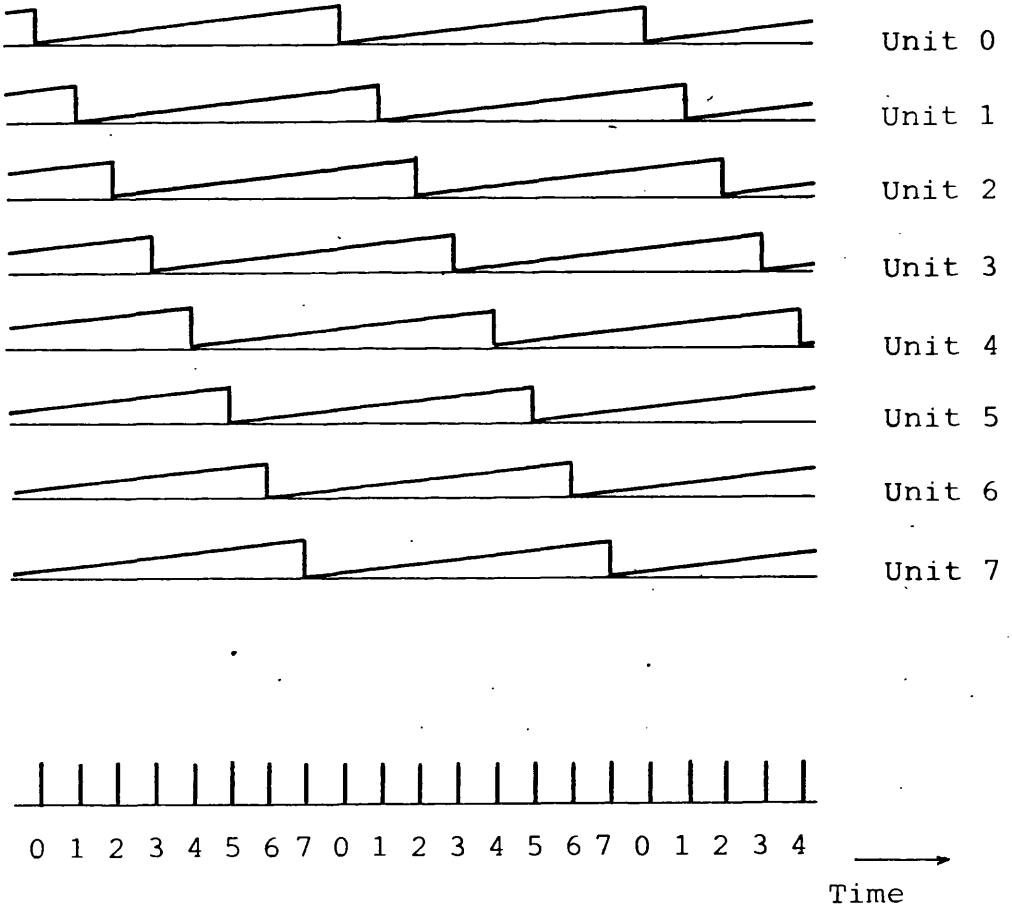

Fig.4.7(b) Period Data Availability

effect on the system accuracy. Thus for each pickup-counter set, period data is updated every 40ms. Fig. 4.7(b) expands the single pickup-counter concept to the eight pickups which are evenly distributed around the stationary carrier plate. The upper section shows how the data for each pickup is built up and the lower section shows the manner in which the data becomes available to the microprocessor.

The transducer of Fig. 4.5 using a single rotating slot and eight stationary photo pickups was found to give acceptable acceleration information but its fabrication was time consuming. Ways of reducing the manufacturing effort were sought, resulting in the second, second generation speed transducer given in Fig. 4.6. The system uses a single stationary photo pickup with a rotating cupped disc containing eight slots evenly placed around the periphery. This provides essentially the same configuration as the former system but with the fixed and rotating parts conceptually transposed. In this construction only one small aperture need be fabricated and the eight rotating slots can be conveniently milled accurately without undue effort.

The output of the photo pickup is shown for one shaft revolution in Fig. 4.8, where the duration of the pulses are exaggerated for clarity. The rising edge of each pulse is used in conjunction with a simple counter system to produce a series of Q pulses in a form identical with the former transducer. One of the slots has its trailing edge displaced thus producing the larger index pulse in Fig. 4.8.

The index slot is used by the control electronics of the simple counter to ensure that there is a fixed relationship between the Q pulses and the mechanical shaft position, when running in the vicinity of synchronous speed.

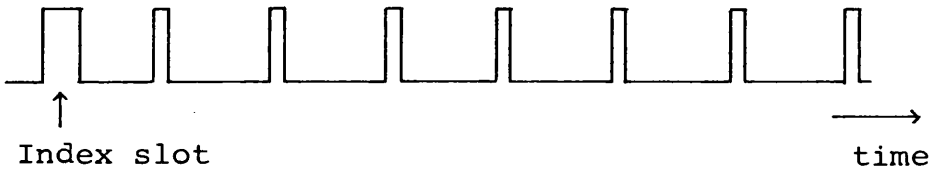

Fig. 4.8 Photo Pickup Output for Eight Slot Transducer

4.3.3.2 Quantitative Angular Velocity and Acceleration

Taking the period of one complete rotation of the four pole machine shaft as the basis for speed measurement has two main features. New data is only available at the end of a sample period, and the period information can only give the mean angular velocity over the sample interval (40ms).

The discrete nature of the data is not a problem since subsequent processing is performed using digital techniques which inherently is a discrete time process. The effect of sampling over a complete revolution is to introduce a time delay into the system. The mean speed is assumed to be valid at the mid point of the sample and is thus delayed by 20ms. The time delay is a necessary penalty paid for obtaining an accurate speed estimate.

During the standard 3 phase faults applied to the system the

micromachine dynamics produce rotor oscillations superimposed on the synchronous speed. Equation 4.2 shows the transient speed in an idealized form

$$\omega = \omega_s + \omega_d \cos(2\pi ft) \qquad 4.2$$

and the first derivative of equation 4.2 with respect to time gives

$$\frac{\delta\omega}{\delta t} = -\omega_d \, 2\pi f \sin(2\pi ft) \qquad 4.3$$

For simplicity a 2 pole machine is assumed, giving the synchronous speed ω_s as 100π rad s^{-1}; maximum speed deviation ω_d = 2 rad s^{-1} and frequency of oscillation f = 1.25Hz.

The maximum expected rate of change of ω with time is obtained from equation 4.3 when the sine term is unity. Taking the maximum value of equation 4.3 and creating a difference equation for small time intervals, equation 4.4 is obtained in the form,

$$\Delta\omega = \omega_d \, 2\pi f \, \Delta t \qquad 4.4$$

Substitution of numbers in equation 4.4 produces a maximum change in ω over a sample interval of 0.628 rad s^{-1}, which is 0.2% of the nominal speed. In view of the small rate of change in ω it is reasonable to use the sampling method to obtain ω. The time delay of 20ms on a frequency of 1.25Hz produces a phase shift of 9 degrees.

The machine speed at sample time n can be derived from equation 4.5 in which the additional factor k has value 2 and is inserted to compensate for the fact that the micromachine is a four pole machine.

$$\omega_n = k \frac{2\pi}{T_n} \qquad 4.5$$

In any control scheme using state feedback which requires $\Delta p\delta$ as a parameter, $\Delta\omega$ may be used. However, it is more convenient to perform manipulations directly on the period quantities rather than first converting the readings to speeds. The small changes in speed superimposed on the mean are not lost during arithmetic process since only difference operations are performed. In this way a compromise is obtained between processor effort and accuracy. By failing to obtain the reciprocal values an error of below 1% is introduced in the final value for ω.

The acceleration of the system can be obtained from a simple first difference of speed values over a small time interval as in the following equation

$$p^2\delta \simeq \frac{\Delta\omega}{\Delta T} \simeq \frac{\omega_n - \omega_{n-1}}{\Delta T} \qquad 4.6$$

The cupped disc transducers provide period data as a slot passes a photo pickup. Period information becomes available as shown in Fig. 4.7 at 5ms intervals. The data is in the form of a count of micro seconds for the last complete

revolution. The notation C_{mn} will be used to label each count, where m is the counter unit number m = 0,1,...,7 and n is the sample number n = 1,2,3,... . The value T in equation 4.5 is therefore $C_{mn}\ 10^{-6}$s. Substituting in equation 4.6 and rearranging gives

$$\frac{\Delta\omega}{\Delta T} = \frac{k2\pi}{\Delta T\ 10^{-6}} \left\{ \frac{1}{C_{mn}^*} - \frac{1}{C_{mn}} \right\} \qquad 4.7$$

in which C_{mn}^* denotes the count available ΔT after C_{mn}. Equation 4.7 can be further rearranged to give

$$\frac{\Delta\omega}{\Delta T} = \frac{k2\pi}{\Delta T\ 10^{-6}} \left\{ \frac{C_{mn} - C_{mn}^*}{C_{mn}^* \cdot C_{mn}} \right\} \qquad 4.8$$

The product term $C_{mn}^*\ C_{mn}$ in the denominator of equation 4.8 produces a value of the order of $1.6\ 10^9$. In view of the small speed changes, little error is introduced by assuming $C_{mn}^*\ C_{mn}$ as a constant and absorbing all the constant terms of equation 4.8 into a single value such that

$$\frac{\Delta\omega}{\Delta T} = \frac{\kappa}{\Delta T} \left(C_{mn} - C_{mn}^* \right) \qquad 4.9$$

where κ has the value $7.95\ 10^{-4}$ rad s^{-1}. It has been shown by Lu[17] that the suboptimal feedback systems developed are tolerant of magnitude error in the acceleration signal, so that the small errors introduced by the above assumptions are

insignificant.

Having period data available every 5ms, it is possible to compute an estimate for acceleration at that rate. It is also possible to trade phase shift for noise improvement by making ΔT larger and computing $p^2\delta$ using multiples of 5ms for ΔT. The smoothest practical signals are obtained by differencing C_{mn+1} and C_{mn} which produces a time delay of 60ms and a phase shift of 27 degrees. The minimum phase shift obtainable is 11.25 degrees using C_{m+1n} and C_{mn}. The phase shifts quoted are based purely on the sampling delay. Even though the phase shift is significant, it is not normally necessary to include any additional filtering and so no additional phase shift is inserted.

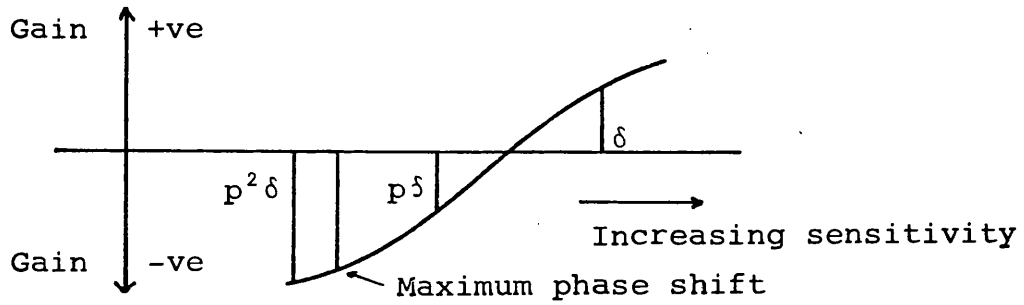

Fig. 4.9 Feedback Sensitivity Trend

Fig. 4.9 shows the general trend observed in the theoretical studies of Lu[17] and Lee[16]. The optimum feedback gain for load angle δ is positive and the resulting controller is sensitive to parameter changes. Transient velocity feedback

$p\delta$ improves upon this, the optimum gain is negative and the control is less sensitive to parameter changes. The best single feedback state with regard to system sensitivity and resulting performance uses $p^2\delta$. However, it is very difficult to measure $p^2\delta$ without introducing phase shift into the signal. The maximum phase shift introduced, assuming equation 4.2 with the values stated, is shown in Fig. 4.9. Clearly, even though the slotted transducer does not produce instantaneous values for $p^2\delta$, the information gained is valuable in a control sense.

4.3.3.3 Acceleration Signals from the Second Generation Speed Transducers

For these tests a three phase short circuit fault of 220ms duration is applied to each machine, running at full load with constant torque input and constant excitation. The acceleration curves obtained from the original second generation speed transducer are given in Fig. 4.10, the second transducer results are given in Fig. 4.11. In each case three acceleration curves are given corresponding to calculating the signal using equation 4.9 with sample spacing times ΔT of 5ms, 10ms and 40ms, the phase difference between the data sets is just discernable. The curves are those which would be obtained using the standard data capture programs which store data with a 20ms sample interval

In both systems taking the period difference over the minimum time, as one would expect, produces the noisiest signals.

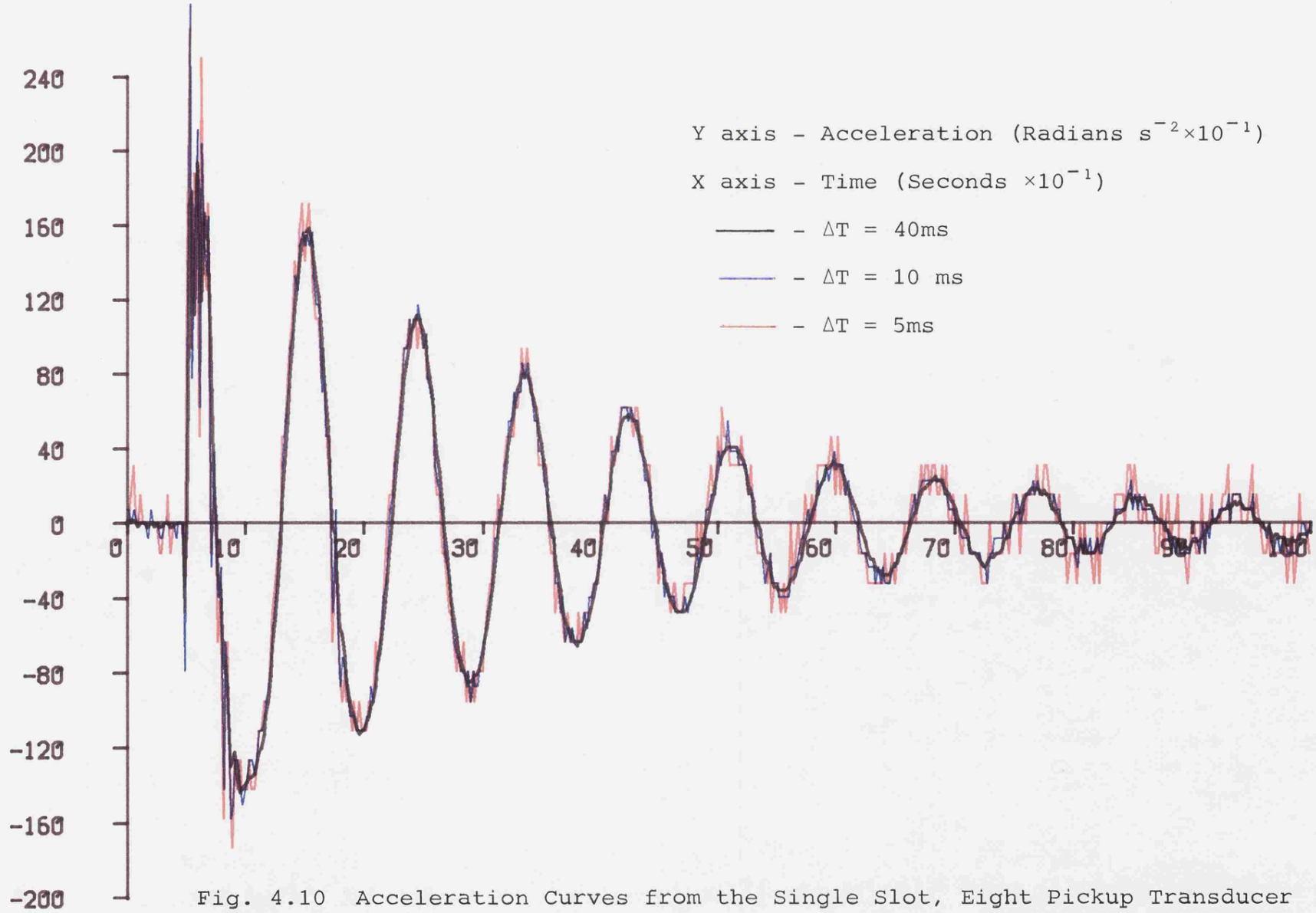

Fig. 4.10 Acceleration Curves from the Single Slot, Eight Pickup Transducer

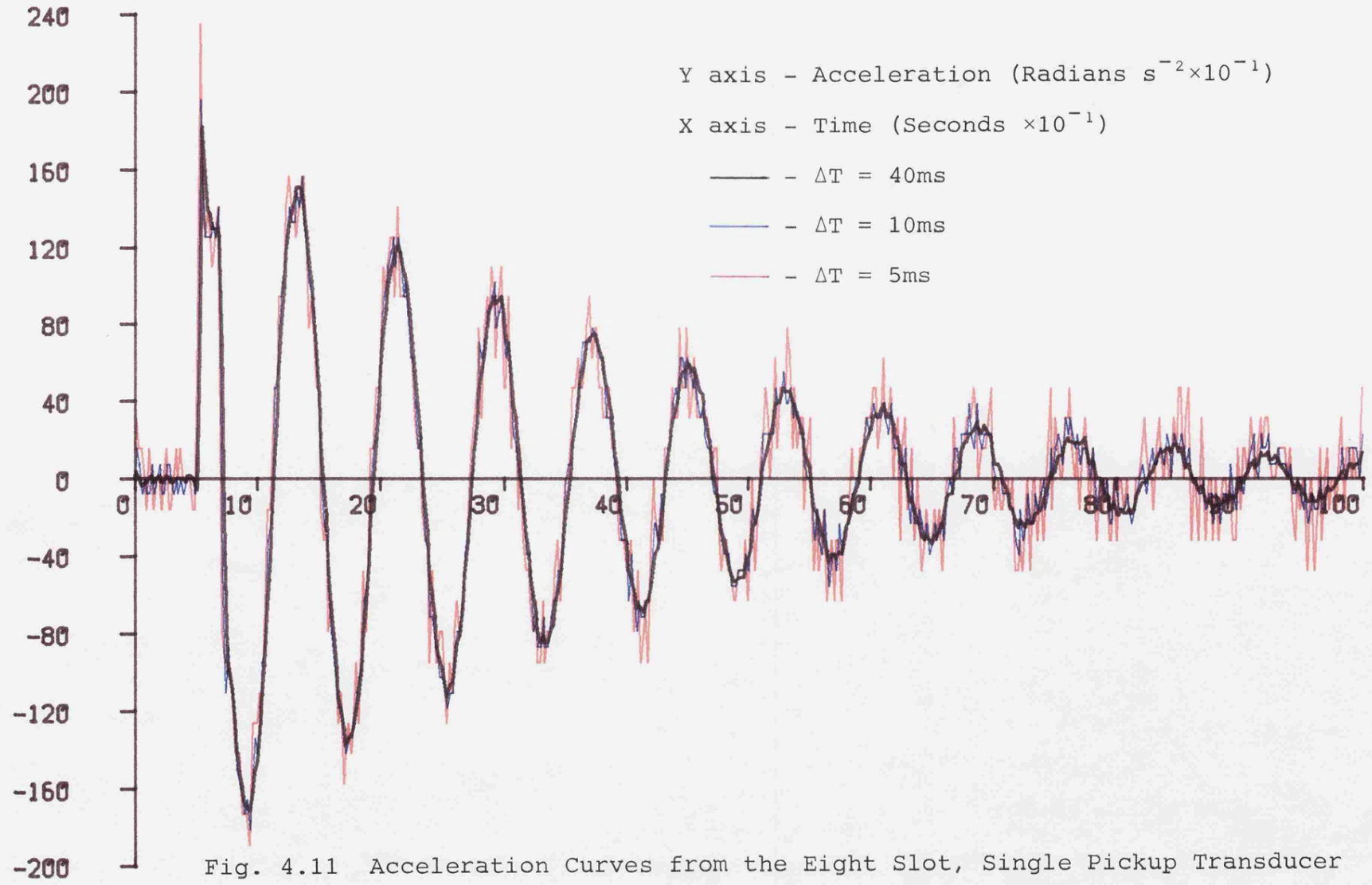

Fig. 4.11 Acceleration Curves from the Eight Slot, Single Pickup Transducer

This problem is associated with quantization in the period data and as such becomes apparent as one returns to steady state, by which time the most useful transient control action should be over, allowing the additional feedback signal to be removed. If however the control is retained the noise injected is of high frequency, with an average value corresponding to that required. These high frequency components are generally absorbed in the larger time constants within the system.

The overall form of the output from both transducers is the same. The later transducer curves of Fig. 4.11 appear to contain a little more noise than the first, second generation transducer. This is most likely due to manufacturing tolerances in the support bearing and a less effective axial preload system. One interesting feature apparent in Fig. 4.10 but not Fig. 4.11, is a high frequency ringing effect on the early part of the response curve. Fig. 4.12 gives an expanded view of the ringing phenomenon, in this case the data is not taken from the original data set, but from a specially collected set with points plotted at 5ms intervals. It is clear that the fault has excited some part of the system with a frequency of approximately 16Hz. Both transducers use similar steady mechanisms and both should behave similarly to differences in speed between the fixed and rotating components. The ringing phenomenon is not fully understood but may be associated with different mechanical couplings used between the micro-alternators and prime movers. However in the control sense the area under the acceleration curve is the important factor

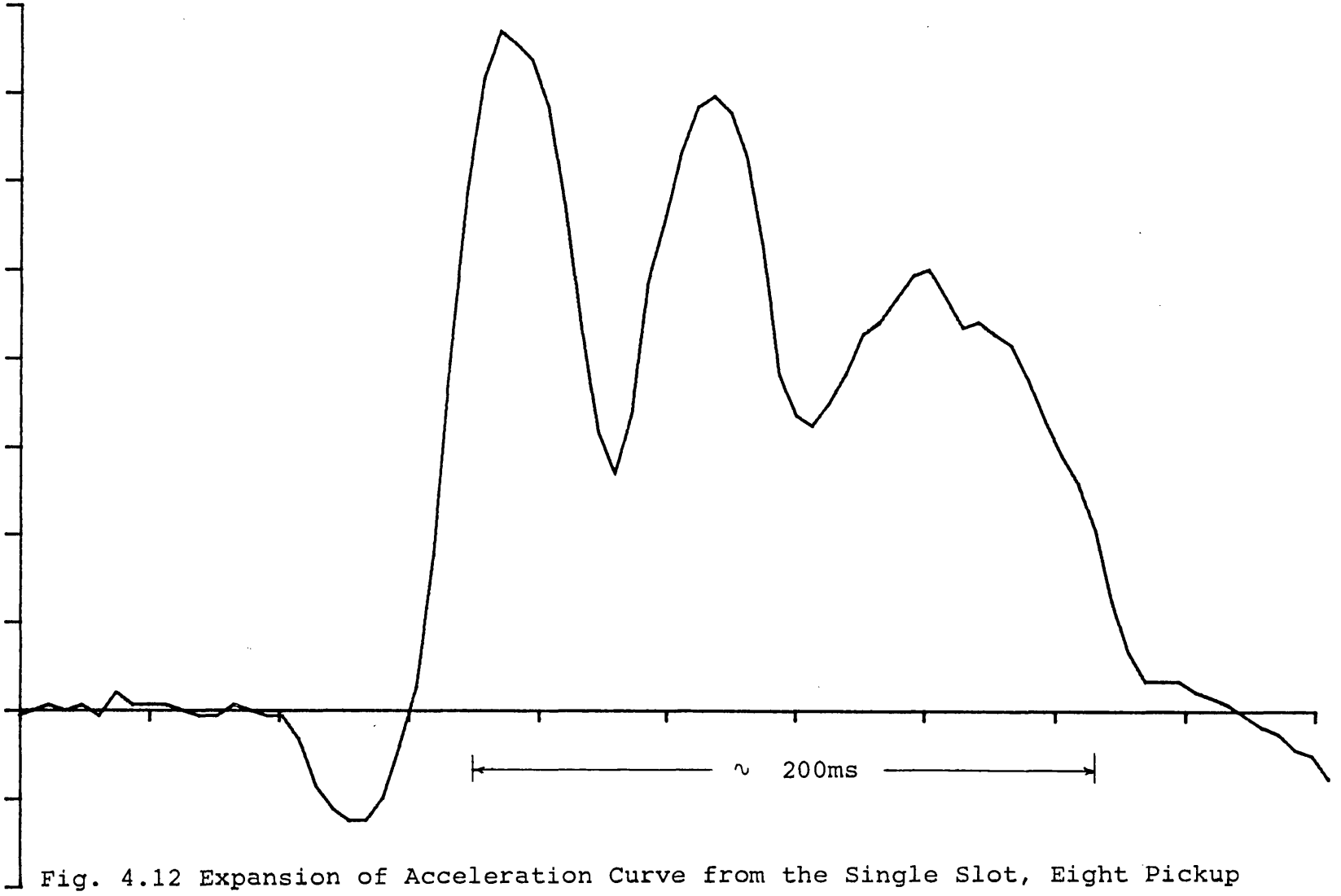

Fig. 4.12 Expansion of Acceleration Curve from the Single Slot, Eight Pickup Transducer Showing the Initial Oscillations.

and this is not unduly affected by the high frequency components.

4.3.3.4 Derivation of Load Angle from the Cupped Disc Transducers

The cupped disc transducers produce a pulse of 500ns duration from eight sources positioned 90 electrical degrees apart or 5ms apart in time at synchronous speed. Fig. 4.13 shows pulses from one of these sources represented as arrows on the time axis, together with an arbitrary phase voltage of the infinite bus drawn to the same time scale. The fixed relation between the generator electrical axis and the shaft provides a means of measuring load angle by taking the time interval

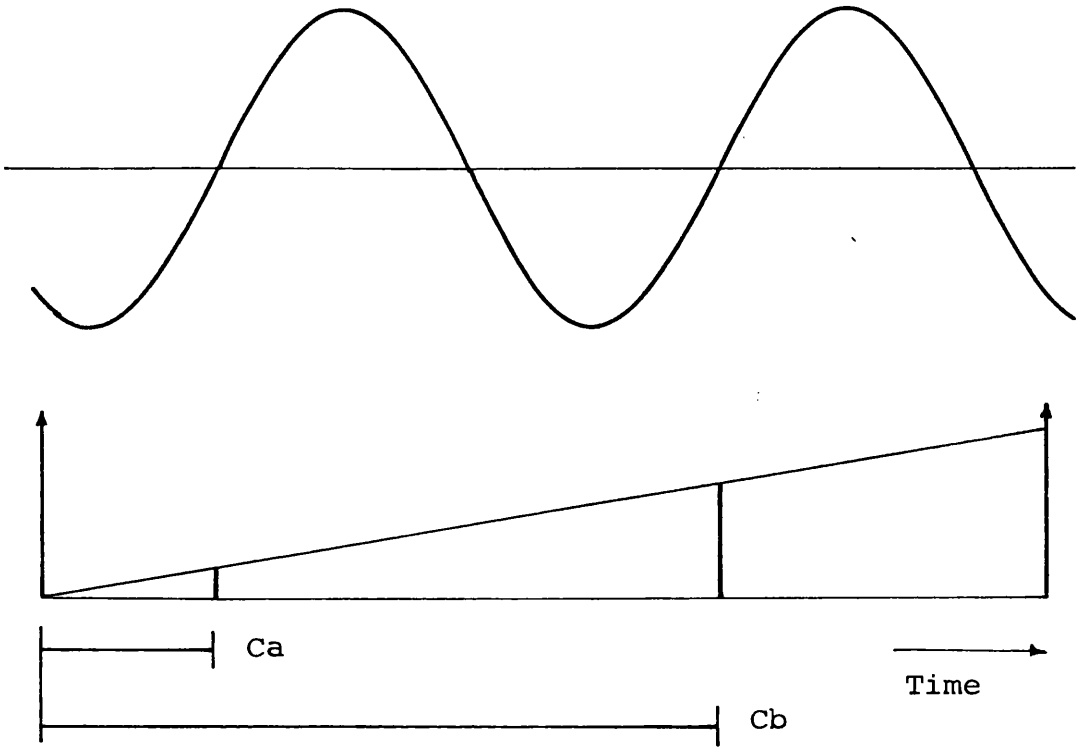

Fig. 4.13 Load Angle Measurement

between a slot pulse and positive going zero crossings of the infinite bus voltage. This may be performed by taking micro-second counts Ca and Cb of Fig. 4.13. Under steady state floating conditions, values Cao and Cbo may be obtained corresponding to zero load angle. Load angles within the normal operating ranges can then be calculated by applying the following equation.

$$\delta = (Ca - Cao) \frac{4\pi}{C_{mn}} \qquad 4.10$$

The data Cb can be processed in a similar manner.

4.3.3.5 Wide Range Speed Transducer

The cupped disc speed transducers are primarily designed for accurate speed measurement about synchronous speed. However, at lower speeds, the counter circuits, used to determine the period of a shaft revolution overflow. This makes the output unsuitable for speed determination from standstill to synchronous speed. To overcome this limitation, a wide range transducer has been developed which is capable of estimating speed over the full operating range. The implementation is a simple tracking A/D converter following the transformed and rectified output of an a.c. tachogenerator, driven by the micromachine shaft. The accuracy of the transducer is limited to approximately 5% of the full speed value, but it is adequate for determination of when the cupped disc transducer output is valid.

CHAPTER 5 SYSTEM SOFTWARE

5.1 Introduction

This chapter describes the software used in the micromachine control system and the interaction between the PDP 11 mini-computer and the TMS 9900 microprocessor. The overall software philosophy is to provide adequate control of the micromachine at all times and also to enable the exchange of information between the PDP 11 and the TMS 9900.

5.2 The Software Environment

In all digital computer systems it is found that some activities are required more frequently than others. Prime examples of this are input output (i/o) operations which involve movement of information between the program environment and other system elements. A typical program would read data from a disc based file, operate on the data, and then write a further file to the disc containing the results of the operation. In activities such as this, the programmer is not concerned with the actual way in which the data is obtained from, or written to the storage medium and his only requirement is that information should be available regarding the success or otherwise of any particular transaction. A further useful option is to have the choice between either allowing program execution to continue in parallel with the i/o or wait pending the i/o completion. With the former choice, some form of i/o completion routine is required which may either

propagate the transfer or perform some simple flag setting operation.

Input-output operations are generally handled by the computer operating system, rather than by hand programming by the user, and the programmer is encouraged to write programs in a device independent fashion so that the actual data structure associated with the physical device is irrelevant to the user and the source or destination of data is an easily changeable parameter.

The operating system used on the PDP 11 is the Digital Equipment Corporation's RSX 11-M, a "Real time Multi-programming System" designed for a fast and efficient response to real time events. The processor activity is directed to the highest priority job able to run. In some ways, the use of RSX 11-M is a compromise solution in that for the fastest real time work a single user, dedicated, system should be used in which certain liberties may be allowed to increase execution speed at the expense of the systems integrity. However, in the process of program development only a very small amount of time is actually spent using the full potential of a computer in real time work, so it is sensible to use a multi-user system to provide maximum utilization of the machine. The RSX 11-M operating system is ideal in this respect, since, once the programs are developed, the running priority can be raised to the highest level, which will then effectively lock out lower priority jobs.

It is possible to use the PDP 11 at its maximum speed for interrupt service, but at the expense of the operating system integrity. It is not thought worth sacrificing the operating system facility just to increase speed. Comparative tests have been carried out to look at the visible difference in interrupt response between RSX 11-M and RT 11 a single user "real time" system. When running equivalent software the RSX 11-M response, as expected, was slower but the difference was not excessive. A penalty for using fully compatible software is that even with the data collection program running in the PDP 11 at maximum priority, there can be no guarantee that processing will always be completed within a single data collection period. Fig. 5.1, shows the PDP 11 utilization over a typical cycle.

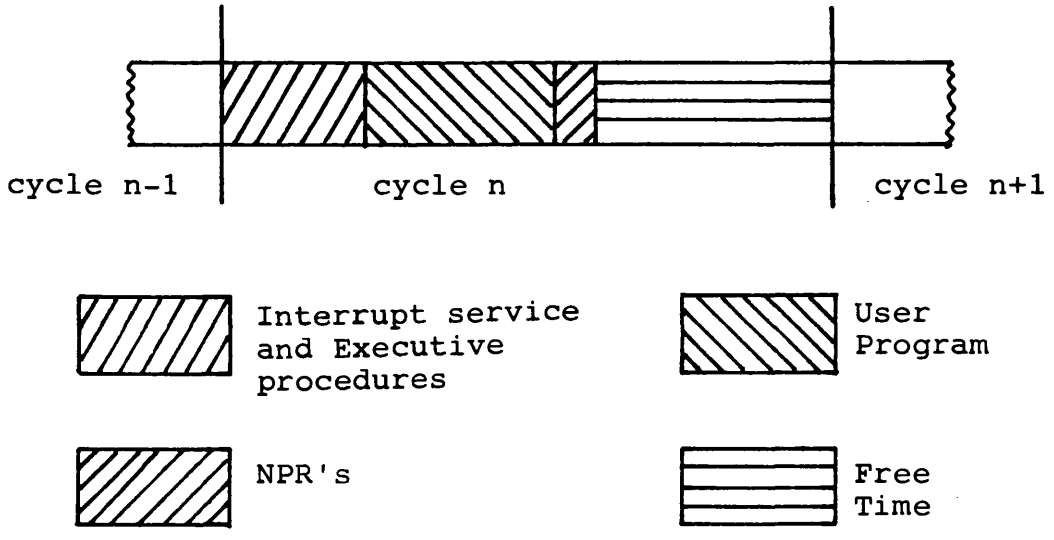

Fig. 5.1 PDP 11 utilization over a typical collection cycle

The processes of Fig. 5.1 are, of course, normally interspersed, but for clarity, each type of process has been amalgamated. Under normal operating conditions there is free processor time which is used by the executive to run lower priority tasks. However, if the lower priority jobs are i/o intensive or there is excessive check-pointing, the system may become less responsive to the priority task. This is partly due to additional executive activity handling the i/o. A significant single factor is disc drive activity, which performs non processor requests (NPR)[48]. These request use of the unibus to perform transfers between memory and the disc drive and are not affected by processor priority. When check-pointing, it is possible for these activities to take up to 20% of unibus time. As a result of these activities, it may not be possible to complete all processing for the data collection routine in a single cycle. In order to provide some lee-way, such that, what could be free time in subsequent cycles, can be used to catch up on lost processing time, it is important that the microprocessor software is tolerant of these time slips.

Since all the necessary control functions are implemented within the TMS 9900 microprocessor, and the PDP 11 is used primarily as a data logger and intelligent terminal, it is unnecessary to maintain continuous communication between the microprocessor and the PDP 11. The software developed for the microprocessor allows for both recoverable time slips in communications caused by moderate extensions in transfer cycle time and total gaps in the data record, which occur if

PDP 11 activity is so great that normal time slip contingency fails to remove the backlog. The communication between the TMS 9900 and PDP 11 is handled in the microprocessor by specially developed software which forms the foundations upon which all the TMS 9900 programs are based.

5.3 Data Transfer

To enable programmed data transfers between the PDP 11 and TMS 9900 using the full RSX 11-M operating system, it is necessary to supply a software interface between the RSX 11-M executive and the physical device. In this case the TMS 9900 microprocessor is accessed by means of in-house hardware connected to the PDP 11 by a DR11C[46] modual. The specialized software is termed a device handler and has several entry points, some are used by the RSX 11-M executive to initiate or abort transfers, while others provide the direct interrupt entry points used when a hardware interrupt is taken.

Data transfers between the PDP 11 and TMS 9900 are performed in parallel sixteen bit words and the protocol adopted is simple. The first word of any data transfer is an identifier, which is followed by a word count. Data then follows until the end of transmission when a check sum is transmitted. The check sum is the 2's complement of the sum of all preceeding words, including the identifier and word count for the particular transfer. Even though the protocol is simple and does not provide any intrinsic method of error correction, it does provide two safety factors. Firstly all transfers

must have the identifier as the first value and secondly, the check sum must be correct. Additionally, the expected word count is compared with the actual one input when transferring data from the TMS 9900 to the PDP 11. In practice the latter is found to be a useful check on software rather than hardware. In general, a hardware malfunction would be detected by either an incorrect identifier or check sum. Use of a simple check sum technique will catch nearly all credible errors, but it is not impossible for multiple errors to have a self cancelling effect. However, the check sum is a sixteen bit word and therefore has 2^{16} possible values, it is very unlikely that errors will cancel.

5.4 TMS 9900 System Software

As indicated earlier, digital computer programs often require special routines or facilities which are frequently used, but the programmer is not interested in the precise mechanism by which they are performed. Data transfer between the PDP 11 and the TMS 9900 is just such an activity. It would be possible to include the necessary code to perform the i/o operations in each program written for the TMS 9900, but this would be inconvenient and time consuming. Instead a specialized set of software has been developed which provide the i/o functions. The interface between the user program and the system software is the extended operation instruction (XOP)[47] which performs a context switch into the system software, it also allows direct passing of a parameter. The parameter is a pointer to a table detailing the required function. By adopting a

structured table driven approach to the i/o operation it is possible to implement a powerful i/o processing system. One of the advantages of predefining a table driven structure is that much of the processing may be performed by common code, with only device dependant elements being coded separately. The table driven nature also allows simple queuing of i/o transactions. The two main data structures are the Device Block (DB) shown in Fig. 5.2 and the Function Block (FB) of Fig. 5.3. The device block contains all necessary parameters and pointers to start and propagate i/o related to a specific device. It is maintained solely by the system and separate device blocks exist for PDP 11 input and output. The function block (FB) is generated by the user and acts as an information link between the systems software and the user. When queuing an i/o function the address of the function block is transferred to the systems software as the parameter of the extended operation.

The flow chart of Fig. 5.4 details the process of queuing an i/o request. If the request is valid, a pointer to the function block (FB), Fig. 5.3, is inserted in the device block (DB) queue for the appropriate device, Fig. 5.2. If the device block queue is empty prior to the insertion, then the transfer initialization code is entered immediately and the relevant hardware set up, otherwise the element is just queued pending availability of the hardware. Return is made to the user program with the carry bit clear, if the request element was queued successfully. On error detection the carry bit is set and further information regarding the nature

Offset	Element
0	Unit ID
2	Total number of current Q elements
4	Pointer to next free Q slot
6	Maximum number of Q elements
10	Initialization routine WP
12	Initialization routine PC
14	Current Q element pointer
16	Next Q element pointer
	Space reserved

Fig 5.2 Device Block Definition

Offset	Element
0	Function code
2	Subfunction code
4	Error return
6	Buffer address
10	Word count
12	Completion routine WP
14	Completion routine PC
16	Error routine WP
20	Error routine PC

Fig 5.3 Function Block Definition

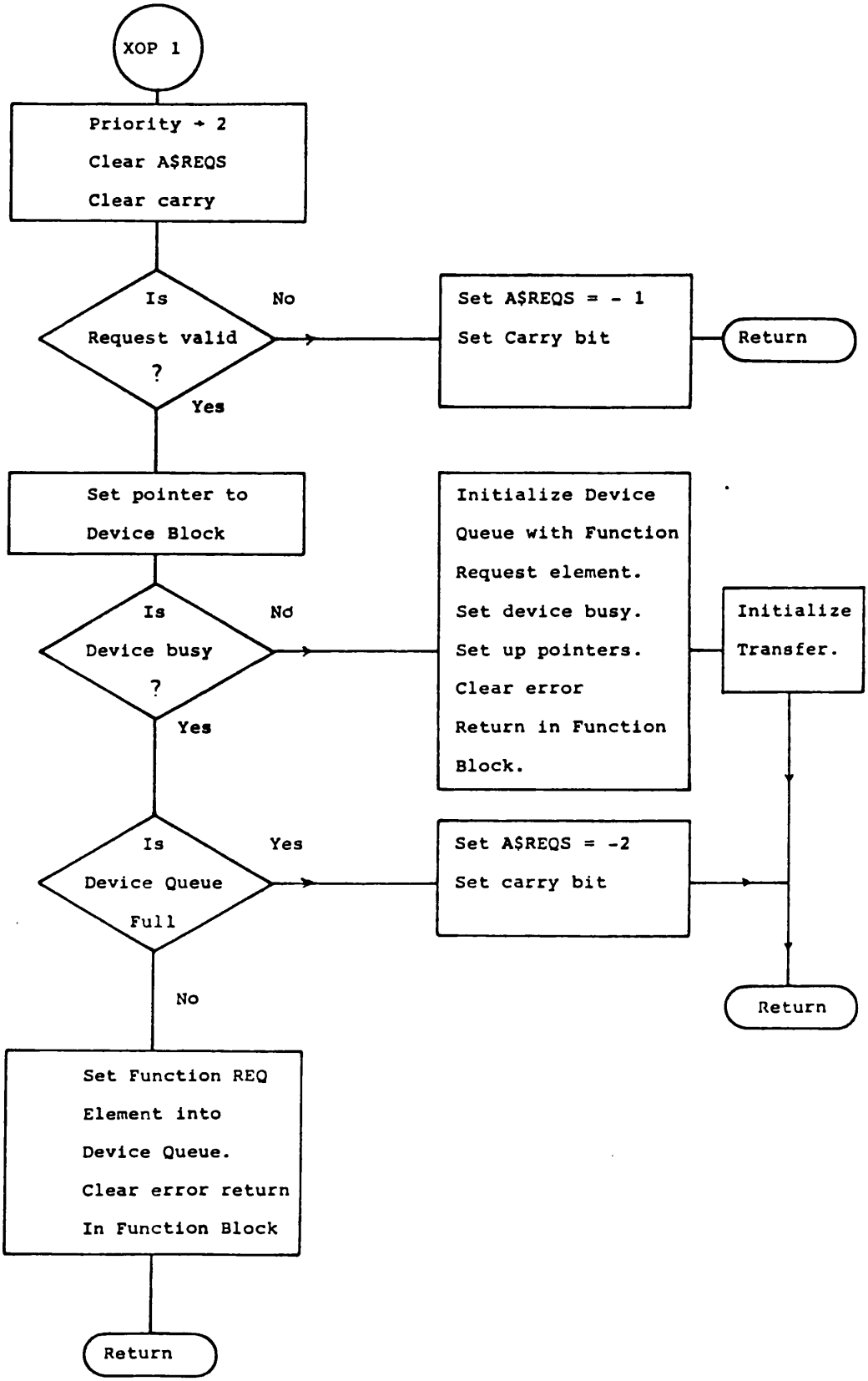

Fig. 5.4 Queuing an i/o Request Flow Chart

of the failure is available in location A$REQS as below.

A$REQS	
0	Successful queuing
-1	Illegal function request
-2	No room in device queue

Assuming successful queuing, the i/o now continues under interrupt until completion. By this means, parallel processing may be obtained allowing program code execution to continue while the i/o propagates under interrupt, transparent to the user. If necessary the user program can be suspended until completion of the i/o, by use of XOP 2 with the transferred parameter equal to the address of the function block for which the program is waiting. By convention, return is made from XOP 2 with the carry bit set if the transfer fails.

When an i/o transaction terminates either as a result of an error condition or successful completion, the interrupt service routine branches to common completion code, flow charted in Fig. 5.5. If an error condition exists and the user has specified an error handling routine in the function block, the error routine is entered. The function block is then tested for a completion routine supplied by the user. If present it is called, otherwise the completion code continues to dequeue the current queue element and, if necessary, ripples the remaining queue elements and initiates the next transfer. The status of the transfer is returned in the function block

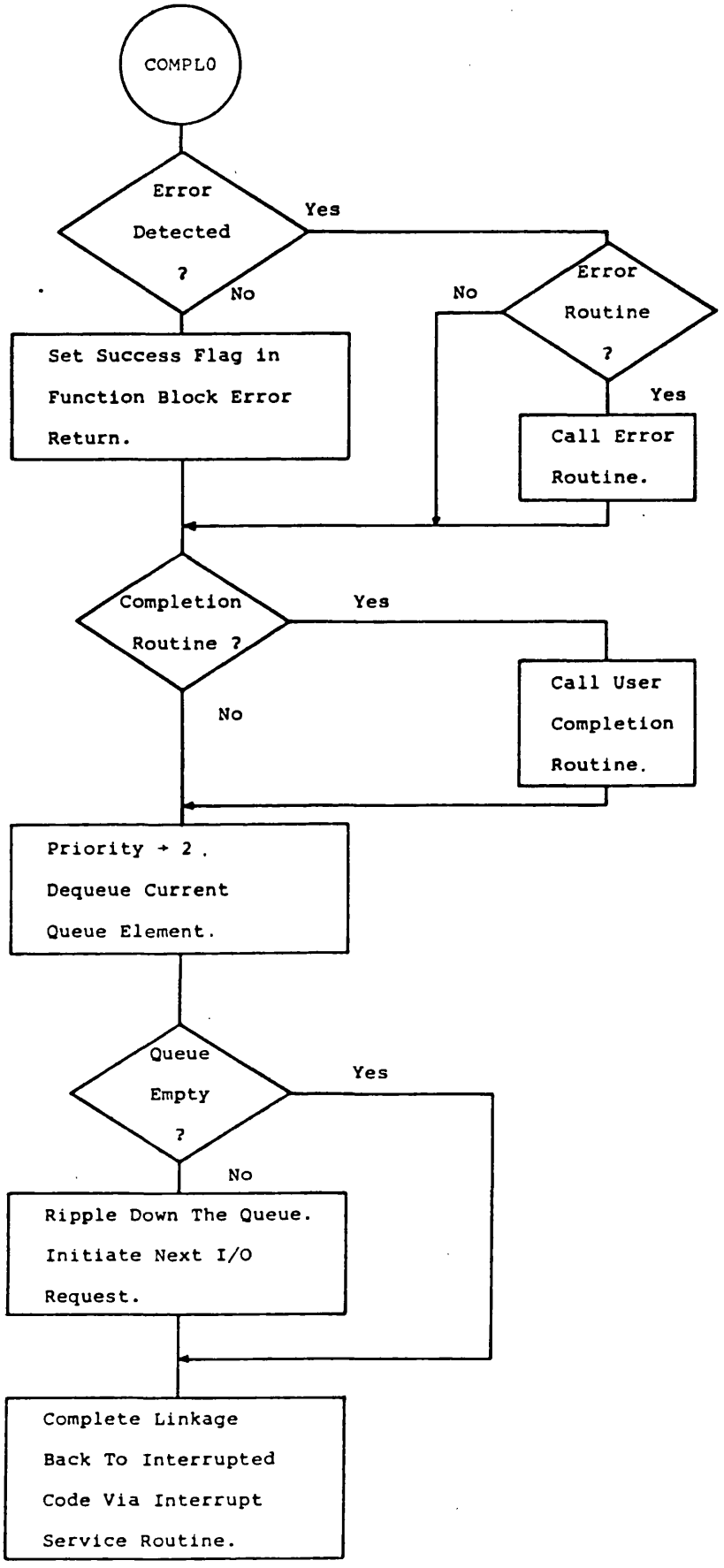

Fig. 5.5 Common i/o Completion Code Flow Chart

error return word, as below.

FB error return

+1	Success
0	Transfer still in progress
-1	Hardware error
-2	Identifier error

It can be seen that the i/o transfer system enables two distinct points at which errors may be found. The first is at the initial queuing stage prior to any physical transaction, which is always determined at a fixed point in the operation of the program. This error may be due to incorrect programming or a queue overflow condition, which can be handled as necessary, by contingency software. The second error detection phase is generally asynchronous with the user program, since it is caused by activation of the interrupt service routine. For this reason, the capability of an error handling routine has been included to allow immediate user action if necessary. For similar reasons, the optional completion routine is made available so that the user has a means of activating a short subroutine at the instant i/o completes. This may be a simple flag manipulation routine or may be used to re-enter the queue manager to propagate a set of transfers.

Further miscellaneous system routines developed to make user programming easier are available. A general software initialization routine, extended operation three, is used to clear all possible interrupt sources, and is also used to initialize

the local terminal. Extended operation six provides a null job for the processor, which is performed when the processor is not involved with any interrupt servicing. The null job is used to generate a distinctive pattern on the processor data bus display lights. At first sight, this may appear trivial, but it gives a simple means of roughly assessing the overall free time on the system. Extended operation seven is used as an error trap handler and its function is to provide a single routine which can be used to log soft errors or perform a controlled shut down in the event of a fatal error.

5.5 PDP 11 Running Software

The role of the PDP 11, when running in the data collection mode is purely as an intelligent front end terminal handler and data logging device. The software used for a single machine system is shown in flow chart Fig. 5.6. Essentially, the PDP 11 acts as an interface between the user and the microprocessor system to input control parameters and commands which are then interpreted and relevant data is sent to the TMS 9900 system.

Normally data would be transferred continuously from the microprocessor and most information obtained is of no interest. Only that data immediately prior to and during a transient disturbance is needed. To enable storage of the conditions prior to the transient, a rolling stack technique is employed, which updates the last data record and ripples down previous

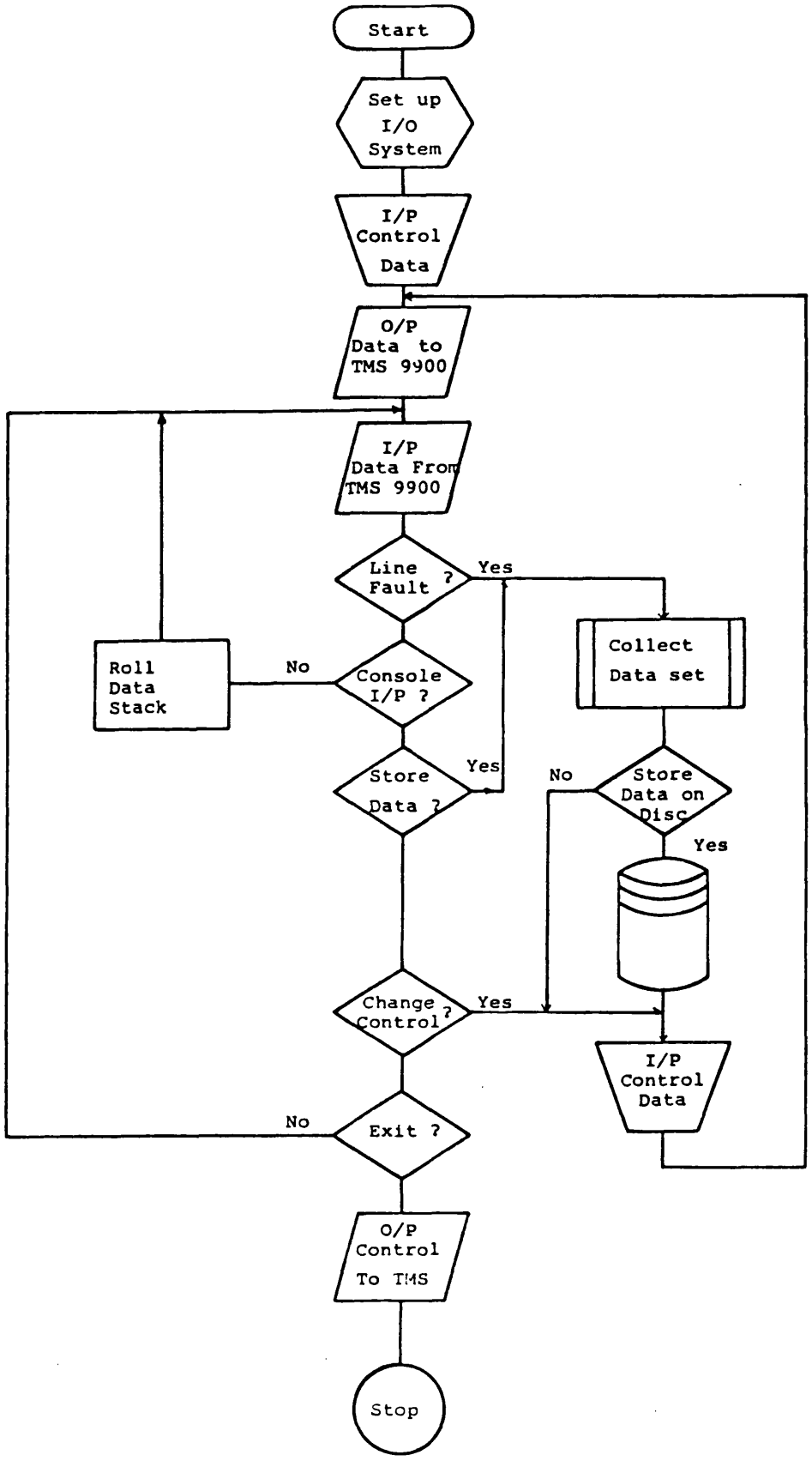

Fig. 5.6 PDP 11 Running Software Flow Chart

data discarding the oldest data record. Data collection can be triggered either by a line fault flag sent from the microprocessor or by a simple terminal command. When a full data set is obtained, the PDP 11 instructs the microprocessor to discontinue data transmission. The data set can then be stored in a file for subsequent examination. The control parameters can then be changed if required prior to returning to the data collection mode.

5.6 TMS 9900 Running Software

The TMS 9900 software used for control, data collection and transfer, relies heavily on the system software described above. The control program has two modes of operation. At first the start up, or main program is entered as flow charted in Fig. 5.7. This is used to initialize all necessary data for the control software. The main program terminates with a call into the null job XOP 6, with all subsequent processing carried out under interrupt.

The most important interrupt is the shaft velocity transducer which provides an interrupt every 5ms at synchronous speed. Since shaft velocity changes are small under all normal operating conditions, including transients, the 5ms separation of shaft interrupts form a suitable basis for directing system operation. Fig. 5.8 shows a simplified flow chart for the speed transducer interrupt service routine. By adopting this means of distributing activity, data transfer to the PDP 11 is initialized every 20ms and the governor model is calculated

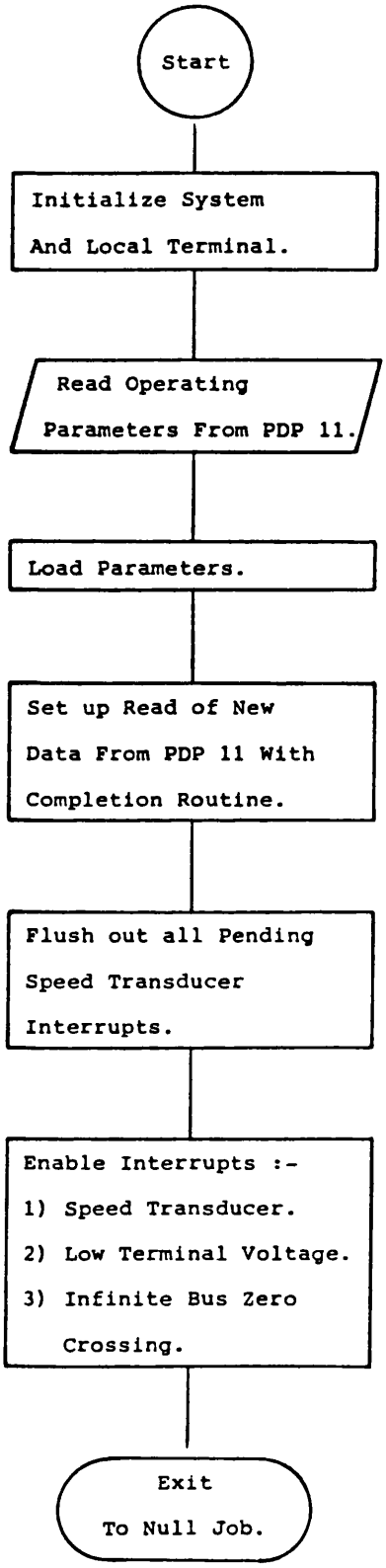

Fig. 5.7 TMS 9900 Initialization Program Flow Chart

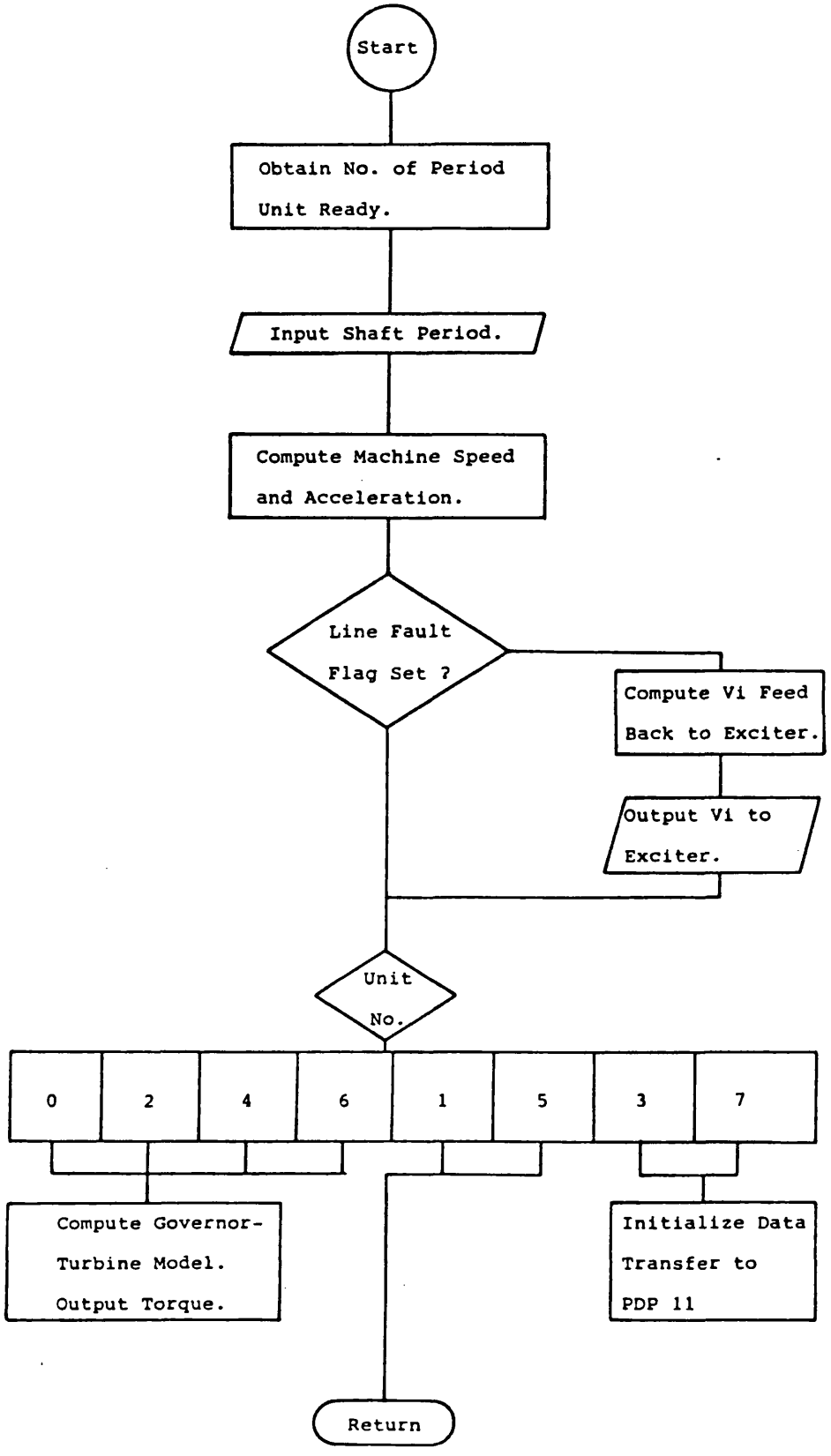

Fig. 5.8 Speed Transducer Interrupt Service Routine

every 10ms to update the torque input to the micromachine system. The speed information is available and the acceleration is calculated at the beginning of each interrupt cycle to be available for control purposes. A typical time sequence over a micromachine shaft revolution is shown in Fig. 5.9, where the arrows indicate the instant at which the interrupt is taken.

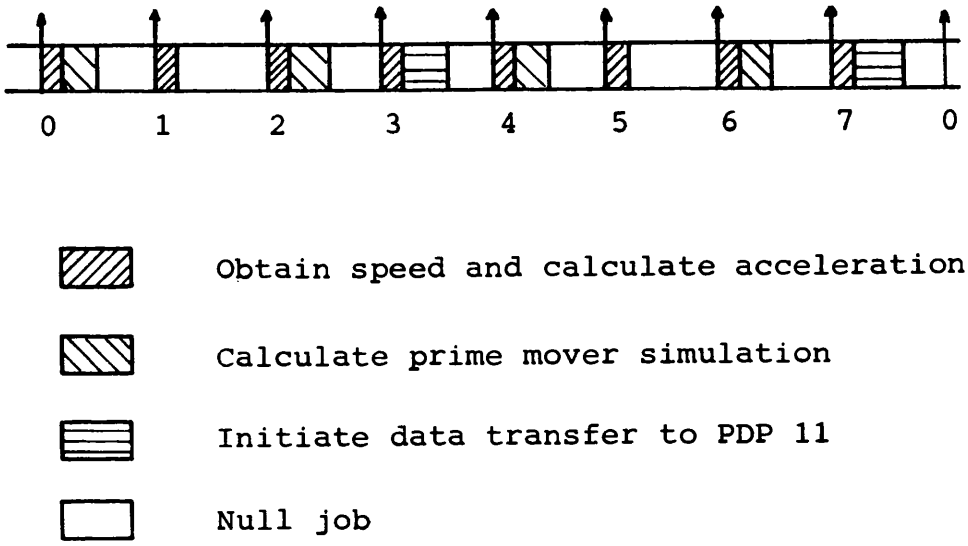

Fig 5.9 TMS 9900 Utilization Over a Shaft Revolution

Additionally, the infinite bus interrupt on a positive going zero crossing, is used to obtain load angle data, and a low terminal voltage interrupt is used to set a line fault flag which initiates a control and data storage sequence.

CHAPTER 6 CO-ORDINATE CONTROL OF A SINGLE MACHINE SYSTEM

6.1 Introduction

This chapter investigates, for the single machine, transmission line and infinite bus system, the use of co-ordinate control of both excitation and governing, using a single additional feedback signal in both control loops. This work is directly based on the work of Lu[17]. Theoretical studies[18,49,50] have shown that significant improvement in transient stability can be obtained by suboptimal controls applied to the excitation of turbo-generators. These results hold for either constant torque input, or conventionally governed systems, where the effect of governor action is slight. However, in modern turbo-generator plant, the electro hydraulic governor is now common place. The control advantages of these units over their mechanical hydraulic forerunners indicates that they have a significant role to play in system stability. The speed of response and ability to control the steam valves by injection of electrical auxiliary signals has led to the technique known as fast valving[51,20]. The technique addresses the problem of energy imbalance during the fault, by attempting to remove mechanical input power. Generally, on detection of a fault condition a valve control sequence is entered which demands rapid closure, after a predetermined time interval the valve is reopened at a slower rate. In this form, fast valving is essentially, an open loop control. The effect of the procedure is to reduce the net accelerating power, which in turn reduces the first rotor swing. In the simple implementation of fast

valving, there is no co-ordination between the excitation control and the governing system. Clearly, a superior overall response would be expected if integration of the excitation and governing systems into a single co-ordinate controller could be achieved.

In practice there are limitations on the manner in which controls maybe applied to the turbine system[40], primarily associated with the intercept valve sequencing, needed to obtain thermodynamic efficiency. It has been shown[51,52] that an attractive form of fast valving control, in terms of steam flow through the boiler, turbine system, is to apply control only to the intercept valves. This will produce approximately 70% of the possible control effort with the advantage of minimizing disruption to the boiler control system, since the large volume of the reheater acts as a reservoir for the incoming steam. This form of control, acting only on part of the system may be modelled in a manner analogous to that used by Concordia[41], for the effects of the reheater. However, the model described in Chapter 2 is utilized, in which control is assumed over both HP and IP valves.

Various authors have applied optimal control theory to the design of excitation controllers and governing systems of synchronous generators[10,11,13,53,54]. Generally these studies use a linearized model of the power system about a particular operating point[13,53,54]. Early work[13,53]formed optimal controls with respect to a quadratic performance index by solution of the matrix Riccati equation, resulting in feedback of all

system states. This type of feedback is not easily implemented since not all states are directly measurable. Suboptimal controls based on a linearized model, but using only feedback of measurable output variables, have been obtained through solution of the Liapunov matrix equation[54]. Open loop controls have also been considered[10]. Most of the literature deals with theoretical studies, but experimental work has been reported [21,22,24,55,56].

The optimal and suboptimal controls obtained by the above methods produce optimum performance for small disturbances, such as those encountered with small changes in set point, or system load. However these controls may not remain optimum for large disturbances. This is because the controls are based on small variations around the operating point and for optimum or suboptimum performance under large disturbances, the control should be based on the original non-linear model,of the system. The open loop control technique is mathematically sound for precisely known systems, but is difficult to apply in practice. Open loop controls are in general sensitive to both system operating conditions and parameters, so that the optimum control obtained for one set of conditions is very unlikely to produce optimum results at any other operating point.

6.2 Application of Suboptimal Control Theory to the Single Machine System

Optimal control theory requires that, for the optimum response

of a system, it is necessary to feedback all system states. However, it may not be practical or even possible to measure all states. Under such conditions a number of possibilities are available. It may be possible to use the data which is available, as inputs to a predictor algorithm which provides an estimate of the remaining states. Alternatively feedback can be confined to only those states which are measurable, thus producing a suboptimal controller. In the majority of practical systems, it is found that the system response is more sensitive to some states than others and in this case little benefit will be gained from feeding back the entire set states.

It has been shown by previous authors that quite acceptable suboptimal control may be obtained by feedback of a reduced number of system states. By assuming the form of the state feedback, the problem of determining the best system gains, can be transformed from the more restricted optimal control problem to one of parameter optimization by function minimization of the objective function. The function minimization technique allows a more straight forward handling of practical constraints on the system variables.

Recent interest in PID controllers[57] for governor systems, using proportional, integral and derivative of speed, has shown improvements over the conventional governing systems using the standard droop characteristic. It has been shown[19] that the acceleration feedback is more effective in the steam flow control than the rotor angle and speed. Acceleration only feedback control[58] has been shown to provide comparable

suboptimal control to that of PID control. Lu[17] has shown that in systems with single variable suboptimal control applied to the exciter only, three states are acceptable, $p^2\delta$ the rotor acceleration, ΔP_e the transient electrical power and Δi_d the change in direct axis current. Although ΔP_e or Δi_d feedback had given similar responses to acceleration feedback in the excitation only system, they were found to be less ameanable to co-ordination with acceleration feedback in the steam control, in the co-ordinated control study. In view of these results, this study is restricted to the additional state feedback of acceleration into both the excitation and steam flow controls. A further incentive for the use of acceleration feedback is that there is no steady state level, so that no special steps are necessary to remove offsets by means of wash out filters and the like.

6.3 Single Machine System for Co-ordinate Control

6.3.1 The System

The single machine system used in this investigation is given in block diagram form in Fig. 6.1. The system components are those derived in Chapter 2 and the synchronous machine is represented by the 7th order model. The excitation and governor-turbine systems are represented using second order models, which are adequate for representing the pertinent characteristics of the system. The exciter is output limited and the governor-turbine simulation has both velocity and position limits placed on the governing valves. There is

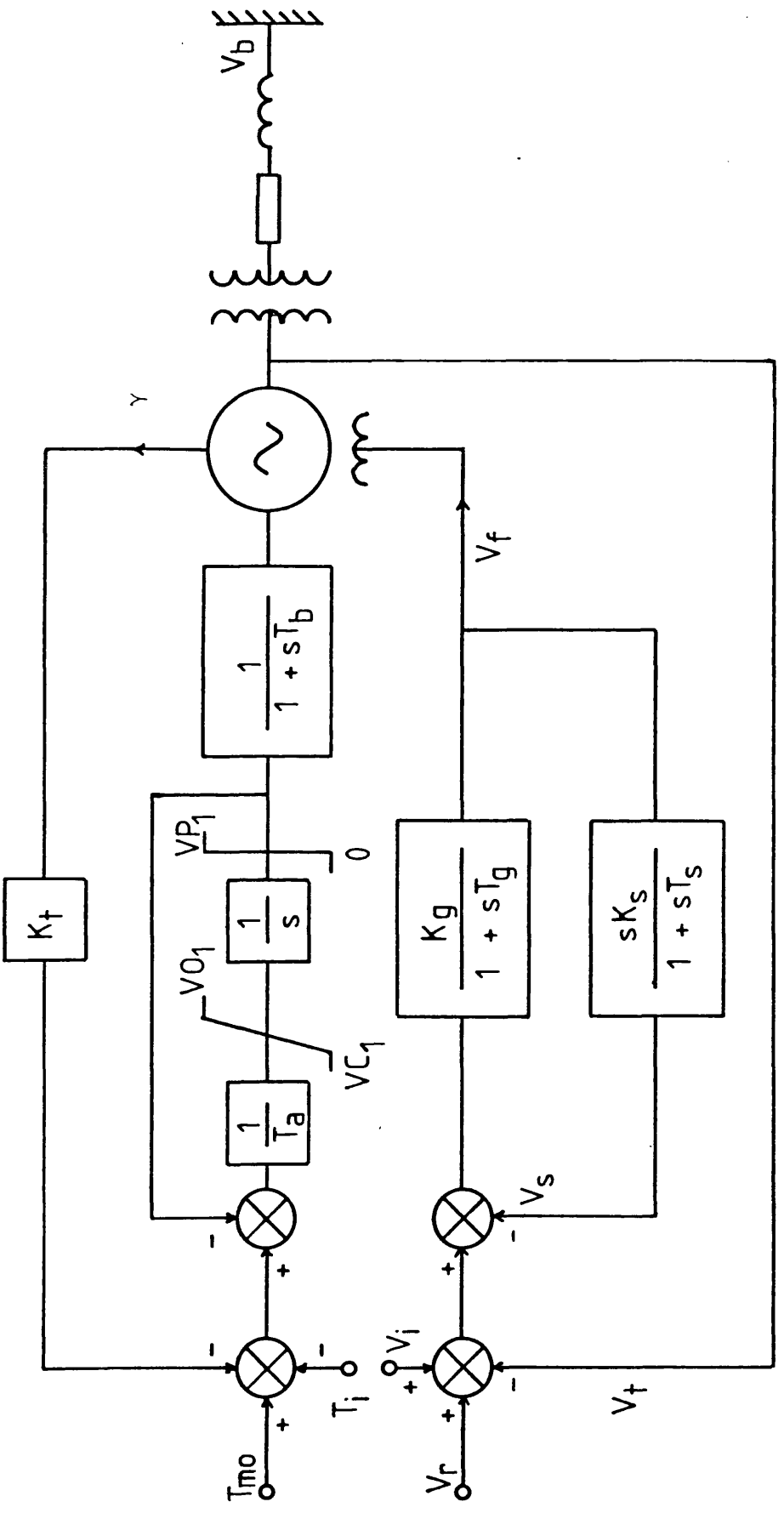

Fig. 6.1 Single Machine System Block Diagram

provision for additional state feedback controls to be applied to both excitation and governing systems via inputs V_i and T_i respectively.

6.3.2 Transient Response Optimization

The system response is to be optimized by the non-linear optimization procedure, using linear state feedback. The excitation system state feedback is a linear function of a single state, thus

$$V_i = K_1 \Delta X_1 \qquad 6.1$$

Similarly the governing system extra state feedback is given by

$$T_i = K_2 \Delta X_2 \qquad 6.2$$

where ΔX is the deviation of the feedback state from its steady state valve and K_1 and K_2 are the optimizing parameters. In this case the rotor acceleration $p^2\delta$ is used for both X_1 and X_2 . Since there is no acceleration in the steady state the value of $p^2\delta$ can be used directly.

6.3.3 Choice of Objective Function

The performance index I , the final value of the objective function is the interface between the system designers requirements and the mathematics which perform the minimization process. The designers task is to provide a suitable formulation of the objective function so that minimization of the performance index ensures the required system response.

The performance index originally used by Lu was of the form

$$I = \int_0^t \left(A1 \ \Delta V_t^2 + \frac{A2}{0.1 + t} \Delta\delta^2 \right) dt \qquad 6.3$$

which had been found satisfactory for excitation only control. When applied to the co-ordinate control, the inverse time factor heavily weighted the first swing at the expense of making the subsequent response sluggish. This behaviour was not apparent in the excitation only controller since terminal voltage error will always raise the field voltage to the limit during the fault, swamping any state feedback. As the terminal voltage recovers, the state feedback can then act to improve the response. With co-ordinate control, it is possible to effect the first swing by control means and so both first and subsequent oscillation must be more evenly balanced as contributors to the performance index. The performance index was therefore changed to

$$I = \int_0^t \left(A1 \ \Delta V_t^2 + \Delta\delta^2 \right) \left(1 + A2 \ t \right) dt \qquad 6.4$$

Early damping of the system is ensured by the time factor which penalizes deviations which take a long time to die away. During the fault, for any given system, there is practically nothing that can be done to limit the terminal voltage deviation and so the ΔV_t^2 term imparts a value comprising a constant plus a term dependent on subsequent voltage recovery. Limitation of the first rotor swing is automatically ensured by the square term $\Delta\delta^2$ which penalizes large excursions. The art of the design process is to choose the weighting factors

A1 and A2 to obtain the best compromise between first swing stability, terminal voltage recovery and subsequent damping. In all the following results the values of A1 and A2 are fixed at 0.1 and 70.0 respectively.

6.3.4 The Single Machine Co-ordinate control Optimization Program

The crux of the program is a NAG library routine, for multi-variable function minimization, based on the Quasi-Newton method of Gill and Murray[59]. At each point, the performance index is evaluated, together with its sensitivity with respect to the gains. A systematic sequence of searches is performed, using sensitivity information to provide the direction of search and polynomial interpolation is used to estimate the minimum in the search direction.

The optimization program flow chart is given in Fig. 6.2. Linear searches are continued until either the convergence criteria are met or reduction of the performance index is not achieved. A local search is then performed to ensure that the point reached is not a saddle point. If a saddle point is detected, the linear searches are continued. When the local minimum is found, the process is terminated and the responses plotted.

The non-linear nature of the system indicates that there would be multiple local minimum, while the precise location found would depend on the acceptance criteria and the initial

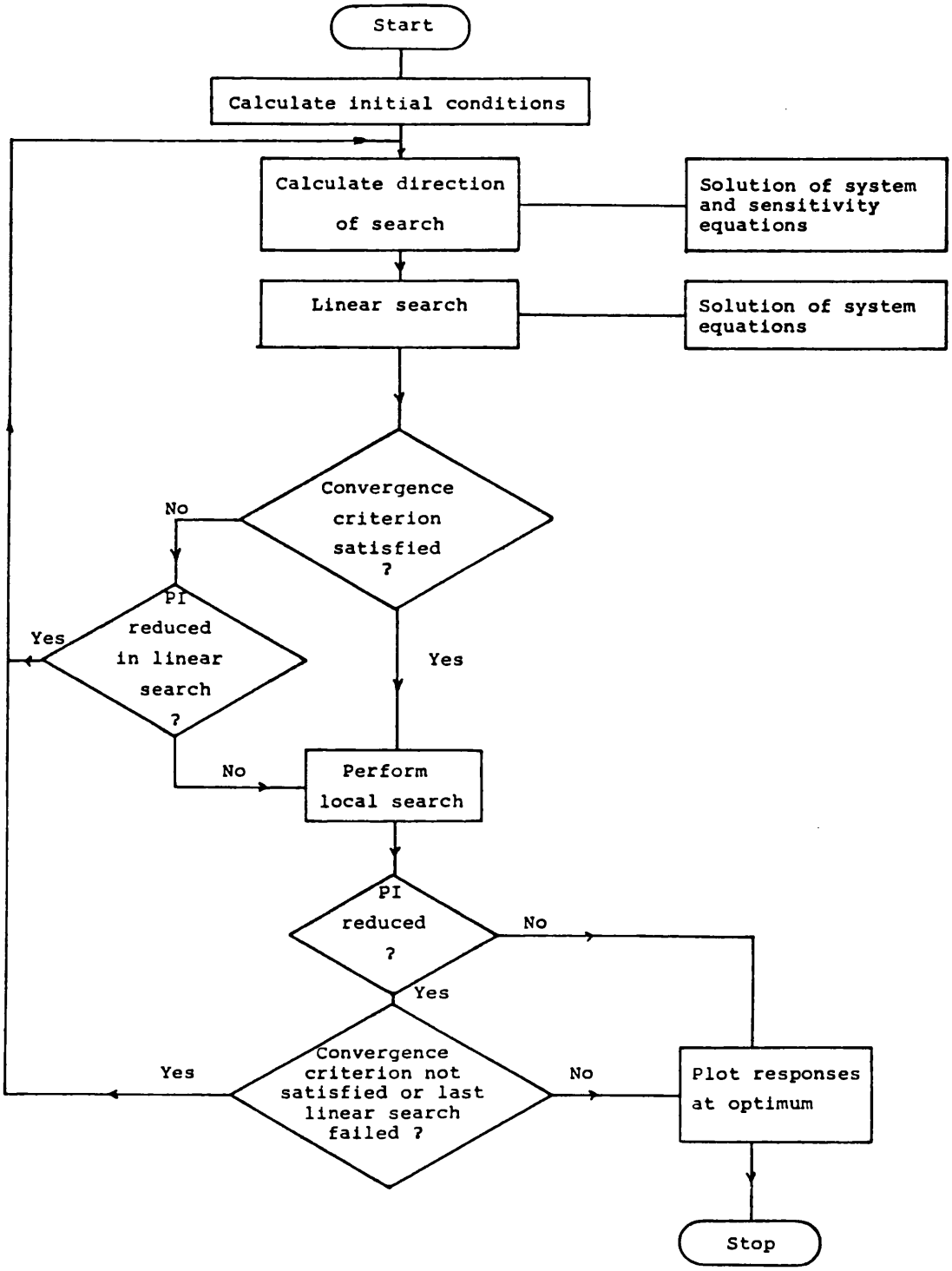

Fig. 6.2 Optimization Program Flow Chart

estimate of the minimum given to the routine. A practical view has been used to select the final feedback gains, bearing in mind the multiplicity of uncertainties within the system and the practical accuracy to which the feedback state can be measured.

6.3.5 System and Sensitivity Equations

The sensitivity equations are derived by differentiating the system equations with respect to the feedback gain constants. The system equations are

$$pe_d'' = \{(x_q - x_q'')i_q - e_d''\}/T_{qo}'' \qquad 6.5$$

$$pe_q' = \{V_f - (x_d - x_d'')i_d - e_q''\}/T_{do}'' \qquad 6.6$$

$$pe_q'' = \{e_q' - (x_d' - x_d'')i_d - e_q'' - (T_1(e_q'' - x_d''i_d) + T_2 x_d i_d - T_{kd}V_f)/T_{do}'\}/T_{do}'' \qquad 6.7$$

$$p\delta = \gamma \qquad 6.8$$

$$p\gamma = (T_m - T_e - K_{dd}\gamma)/M \qquad 6.9$$

$$pV_f = \{(V_r - V_t + V_i - V_s)K_g - V_f\}/T_g \qquad 6.10$$

$$pV_s = (K_s pV_f - V_s)/T_s \qquad 6.11$$

$$pI = (\Delta V_t^2 + A1\Delta\delta^2)(1 + A2t) \qquad 6.12$$

$$pi_d = \{pe_q'' - \omega_o(V_b \sin\delta + (R_t + R_a)i_d) + \omega(e_d'' + (x_q'' + X_t)i_q)\}/(X_t + x_d'') \qquad 6.13$$

$$pi_q = \{-pe_d" + \omega(e_q" - (X_t + x_d")i_d) - \omega_o(V_b\cos\delta + (R_t + R_a)i_q)\}/(X_t + x_q") \quad 6.14$$

$$py = (T_{mo} - T_i - K_t\gamma - y)/T_a \quad 6.15$$

$$pT_m = (y - T_m)/T_b \quad 6.16$$

with auxiliary equations

$$V_i = K1\Delta X_1 \quad 6.17$$

$$T_e = e_d"i_d + e_q"i_q - (x_d"-x_q")i_di_q \quad 6.18$$

$$\omega = \omega_o + \gamma \quad 6.19$$

$$v_d = V_b\sin\delta + X_tpi_d/\omega_o + R_ti_d - \omega X_ti_q/\omega_o \quad 6.20$$

$$v_q = V_b\cos\delta + X_tpi_q/\omega_o + R_ti_q + \omega X_ti_d/\omega_o \quad 6.21$$

$$V_t = \sqrt{(v_d^2 + v_q^2)} \quad 6.22$$

$$T_i = K2\Delta X_2 \quad 6.23$$

where $K_{dd} = K_d/\omega_o$.

The sensitivity equations with respect to the feedback gain constants K1 and K2 are therefore

$$p\left(\frac{\partial e_d"}{\partial K}\right) = \{(x_q-x_q")\frac{\partial i_q}{\partial K} - \frac{\partial e_d"}{\partial K}\}/T_{qo}" \quad 6.24$$

$$p\left(\frac{\partial e_q'}{\partial K}\right) = \frac{\partial V_f}{\partial K} - (x_d-x_d")\frac{\partial i_d}{\partial K} - \frac{\partial e_q"}{\partial K})/T_{do}' \quad 6.25$$

$$p\left(\frac{\partial e_q"}{\partial K}\right) = \{\frac{\partial e_q'}{\partial K} - (x_d'-x_d")\frac{\partial i_d}{\partial K} - \frac{\partial e_q"}{\partial K} - (T_1(\frac{\partial e_q"}{\partial K} - x_d"\frac{\partial i_d}{\partial K}) + T_2x_d\frac{\partial i_d}{\partial K} - T_{kd}\frac{\partial V_f}{\partial K})/T_{do}'\}/T_{do}" \quad 6.26$$

$$p\left(\frac{\partial \delta}{\partial K}\right) = \frac{\partial \gamma}{\partial K} \qquad 6.27$$

$$p\left(\frac{\partial \gamma}{\partial K}\right) = \left(\frac{\partial T_m}{\partial K} - \frac{\partial T_e}{\partial K} - K_{dd}\frac{\partial \gamma}{\partial K}\right)/M \qquad 6.28$$

$$p\left(\frac{\partial V_f}{\partial K}\right) = \left\{\left(-\frac{\partial V_t}{\partial K} + \frac{\partial V_i}{\partial K} - \frac{\partial V_s}{\partial K}\right)K_g - \frac{\partial V_f}{\partial K}\right\}/T_g \qquad 6.29$$

$$p\left(\frac{\partial V_s}{\partial K}\right) = \left(K_s p\left(\frac{\partial V_f}{\partial K}\right) - \frac{\partial V_s}{\partial K}\right)/T_s \qquad 6.30$$

$$p\left(\frac{\partial I}{\partial K}\right) = 2.0\left(\Delta V_t \frac{\partial V_t}{\partial K} + A1\Delta\delta\frac{\partial \delta}{\partial K}\right)(1 + A2t) \qquad 6.31$$

$$\begin{aligned} p\left(\frac{\partial i_d}{\partial K}\right) = \{ & p\left(\frac{\partial e_q''}{\partial K}\right) - \omega_o\left(V_b\cos\delta\frac{\partial \delta}{\partial K} + (R_t + R_a)\frac{\partial i_d}{\partial K}\right) \\ & + \omega\left(\frac{\partial e_d''}{\partial K} + (x_q'' + X_t)\frac{\partial i_q}{\partial K}\right) \\ & + \left(e_d'' + (X_t + x_q'')i_q\right)\frac{\partial \omega}{\partial K}\}/(X_t + x_d'') \end{aligned} \qquad 6.32$$

$$\begin{aligned} p\left(\frac{\partial i_q}{\partial K}\right) = \{ & -p\left(\frac{\partial e_d''}{\partial K}\right) - \omega_o\left(-V_b\sin\delta\frac{\partial \delta}{\partial K} + (R_t + R_a)\frac{\partial i_q}{\partial K}\right) \\ & + \omega\left(\frac{\partial e_q''}{\partial K} - (X_t + x_d'')\frac{\partial i_d}{\partial K}\right) + \left(e_q'' - (X_t + x_d'')\right)\frac{\partial \omega}{\partial K}\}/(X_t + x_q'') \end{aligned} \qquad 6.33$$

$$p\left(\frac{\partial y}{\partial K}\right) = \left(-\frac{\partial T_i}{\partial K} - K_t\frac{\partial \gamma}{\partial K} - \frac{\partial y}{\partial K}\right)/T_a \qquad 6.34$$

$$p\left(\frac{\partial T_m}{\partial K}\right) = \left(\frac{\partial y}{\partial K} - \frac{\partial T_m}{\partial K}\right)/T_b \qquad 6.35$$

where $K = K_1, K_2$ in turn.

The auxiliary sensitivity equations are described by

$$\frac{\partial V_i}{\partial K_1} = K_1\frac{\partial X_1}{\partial K_1} + \Delta X_1 \qquad 6.36$$

$$\frac{\partial V_i}{\partial K_2} = K_1 \frac{\partial X_1}{\partial K_2} \qquad 6.37$$

$$\frac{\partial T_e}{\partial K} = \frac{\partial e_d''}{\partial K} i_d + \frac{\partial i_d}{\partial K} e_d'' + \frac{\partial e_q''}{\partial K} i_q + \frac{\partial i_q}{\partial K} e_q''$$

$$- (x_d'' - x_q'')(i_d \frac{\partial i_q}{\partial K} + i_q \frac{\partial i_d}{\partial K}) \qquad 6.38$$

$$\frac{\partial \omega}{\partial K} = \frac{\partial \gamma}{\partial K} \qquad 6.39$$

$$\frac{\partial V_t}{\partial K} = (v_d \frac{\partial v_d}{\partial K} + v_q \frac{\partial v_q}{\partial K})/V_t$$

$$= (v_d (V_b \cos\delta \frac{\partial \delta}{\partial k} + X_t p(\frac{\partial i_d}{\partial K})/\omega_o + R_t \frac{\partial i_d}{\partial K} - \omega X_t \frac{\partial i_q}{\partial K}/\omega_o$$

$$- X_t i_q \frac{\partial \omega}{\partial K}/\omega_o) + v_q (-V_b \sin\delta \frac{\partial \delta}{\partial K} + X_t p(\frac{\partial i_q}{\partial K})/\omega_o$$

$$+ R_t \frac{\partial i_q}{\partial K} + X_t \frac{\partial i_d}{\partial K}/\omega_o + X_t i_d \frac{\partial \omega}{\partial K}/\omega_o))/V_t \qquad 6.40$$

$$\frac{\partial T_i}{\partial K_1} = K_2 \frac{\partial X_2}{\partial K_1} \qquad 6.41$$

$$\frac{\partial T_i}{\partial K_2} = K_2 \frac{\partial X_2}{\partial K_2} + X_2 \qquad 6.42$$

where $K = K_1, K_2$ in turn.

6.4 Theoretical Optimization Results

The input parameters used for the optimization program are those for the micromachine. Fault duration, governor valve rate limits and exciter stabilizer time constants are variables entered for each run. From the series of optimization studies

performed only representative results will be reproduced and discussed. Table 6.1 summarizes the controls and resultant performance indices.

6.4.1 Discussion of Results for 220ms Fault Duration

Fig. 6.3(a) shows the dramatic improvement in load angle response possible by co-ordinate control. Curve A0 will be taken as a standard curve. It represents the basic machine system with an automatic voltage regulator and fast governor, and is characterized by the large undershoot and oscillations which die away slowly. For comparative purposes, a constant torque prime mover and automatic voltage regulator system is given in curve A1. In this case, the initial rotor swing is greater, as expected, but the rotor oscillations are more damped. The co-ordinate control of curve A2 has a greatly reduced first swing and a very small undershoot which persists for approximately 1.5 seconds. Comparison of the prime mover output torque curves A0 and A2 in Fig. 6.3(b) highlights the effective control applied to the prime mover when under co-ordinate control showing the rapid reduction in output during the fault, followed by a fast recovery as soon as the fault is cleared. The co-ordinate control regains the steady state power level within two seconds of fault clearance, which is approximately half the time required by the standard system.

During the fault, all excitation controllers are swamped by the terminal voltage error signal, and for any given system, the responses must be the same. It is only after removal of

Control Number	Fault Duration	P.I.	$p^2\delta$ Feedback Gain		Valve Rate Limits pu/s	Ts
			Exciter	Governor		
A0	220ms	20.3	0.0	0.0	+4.0 -6.6	2.0
A1	220ms	32.44	0.0	-	- -	2.0
A2	220ms	2.03	0.02	0.05	+4.0 -6.6	2.0
A2(a)	220ms	2.03	0.02	0.05	+4.0 -6.6	2.0
A2(b)	220ms	3.11	0.02	0.05	+4.0 -6.6	0.5
B0	140ms	4.86	0.0	0.0	+4.0 -6.6	2.0
B1	140ms	0.749	0.02	0.05	+4.0 -6.6	2.0
B2	140ms	0.518	0.02	0.05	+4.0 -6.6	0.5
C0	220ms	20.3	0.0	0.0	+2.2 -3.3	2.0
C1	220ms	2.61	0.0133	0.037	+2.2 -3.3	2.0
C2	220ms	2.8	0.02	0.05	+2.2 -3.3	2.0

Table 6.1

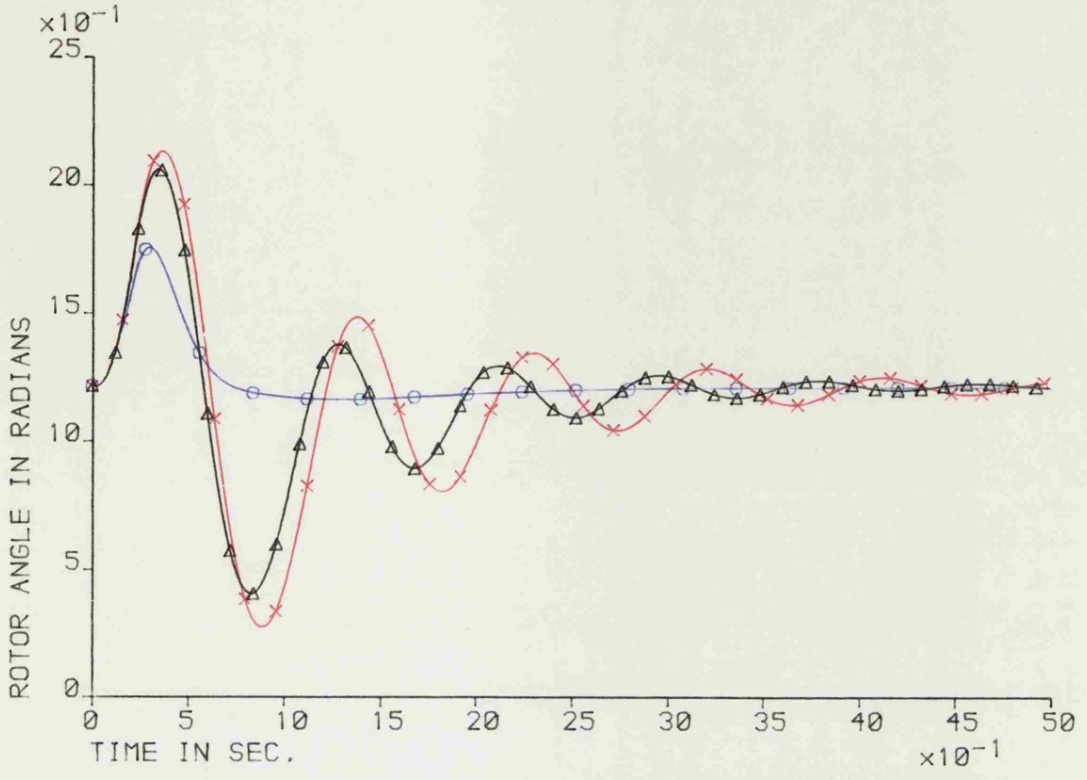

Fig. 6.3(a) Theoretical Load Angle Responses

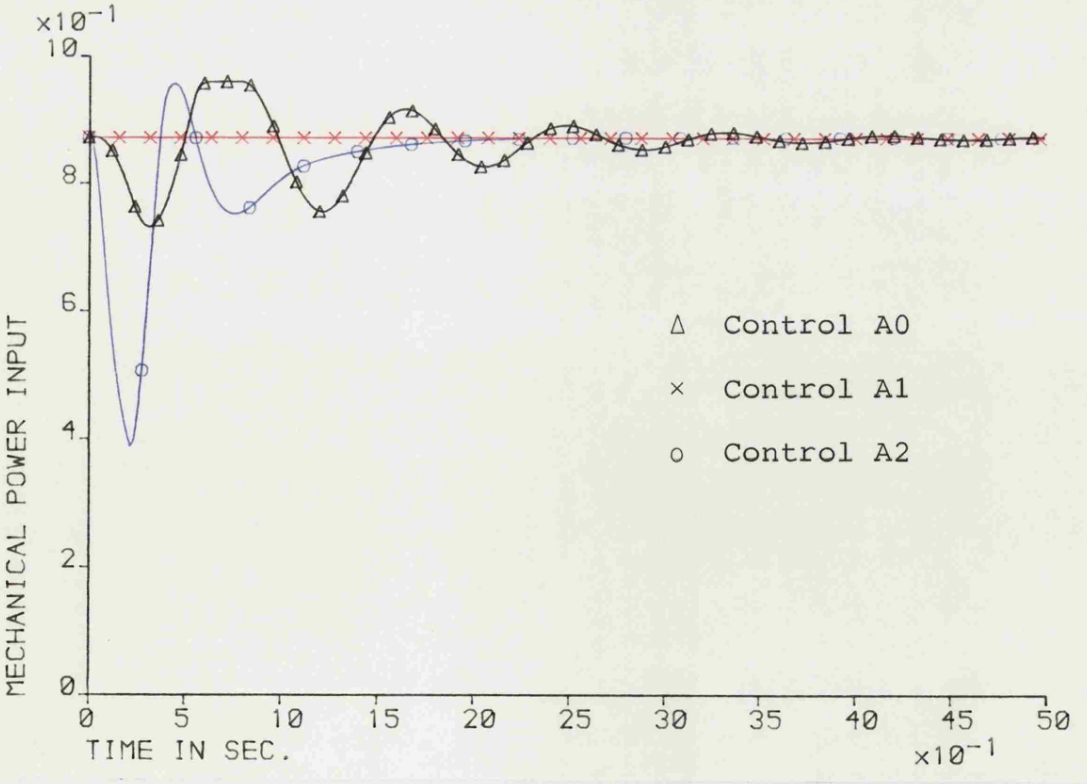

Fig. 6.3(b) Theoretical Mechanical Input Power Responses

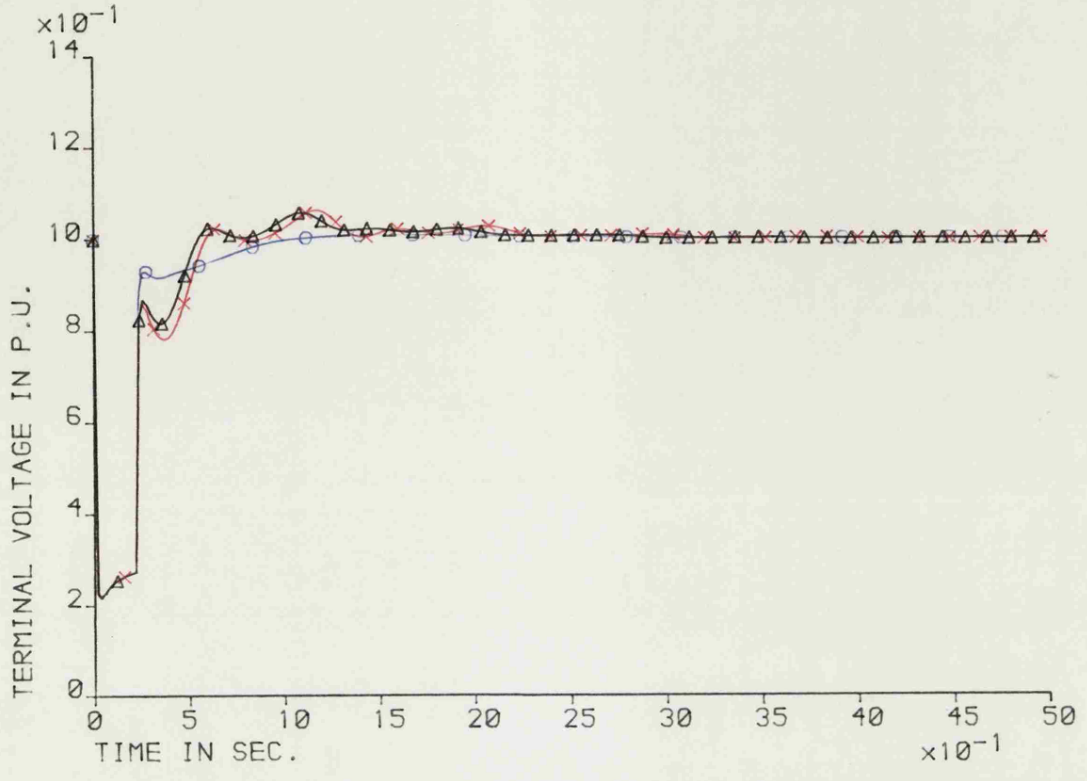

Fig. 6.3(c) Theoretical Terminal Voltage Responses

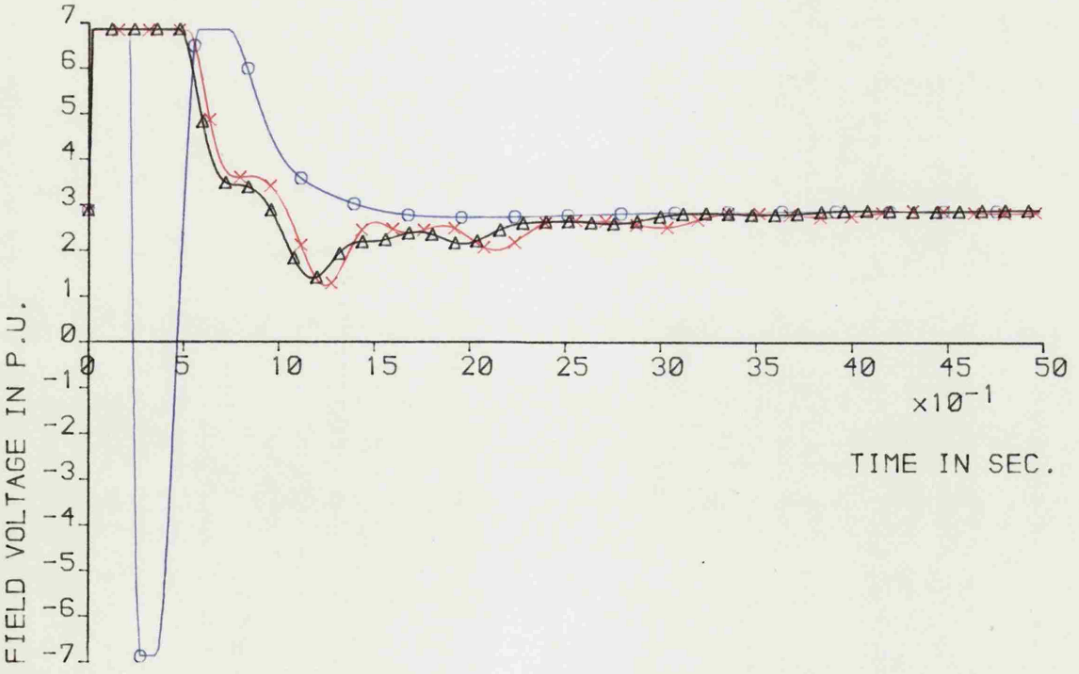

Fig. 6.3(d) Theoretical Field Voltage Responses

the fault that effective controls can be applied to the excitation system to improve system response. Fig. 6.3(c) and 6.3(d) give terminal voltage and main exciter field voltage responses for the controls A0, A1 and A2. It can be seen that the field voltage remains on the upper limit for both cases where there is no additional state feedback into the exciter. This produces the overshoot in terminal voltage. With the co-ordinate control the initial terminal voltage recovery is faster up to approximately 90% of the original value then reaches steady state slowly without oscillation, it attains the steady state value before either of the other controls.

6.4.2 Responses for Different System and Fault Duration

Fig. 6.4 gives a comparative set of responses for the standard system A0, the optimized co-ordinate control A2(a) applied to the standard system and the same control law A2(b) applied to the system with the automatic voltage regulator stabilizing feedback time constant changed from 2.0s to 0.5s. Even though control A2(b) uses the same gains as A2(a) and has not been optimized for the different stabilizing time constant, the results are still good. The performance index for the optimized system is 2.03, for the altered system with non optimized gains the performance index has risen to 3.11 but the value for the standard system is 20.3. The undershoot in the load angle response is within quite acceptable bounds and the terminal voltage response is possibly a little better.

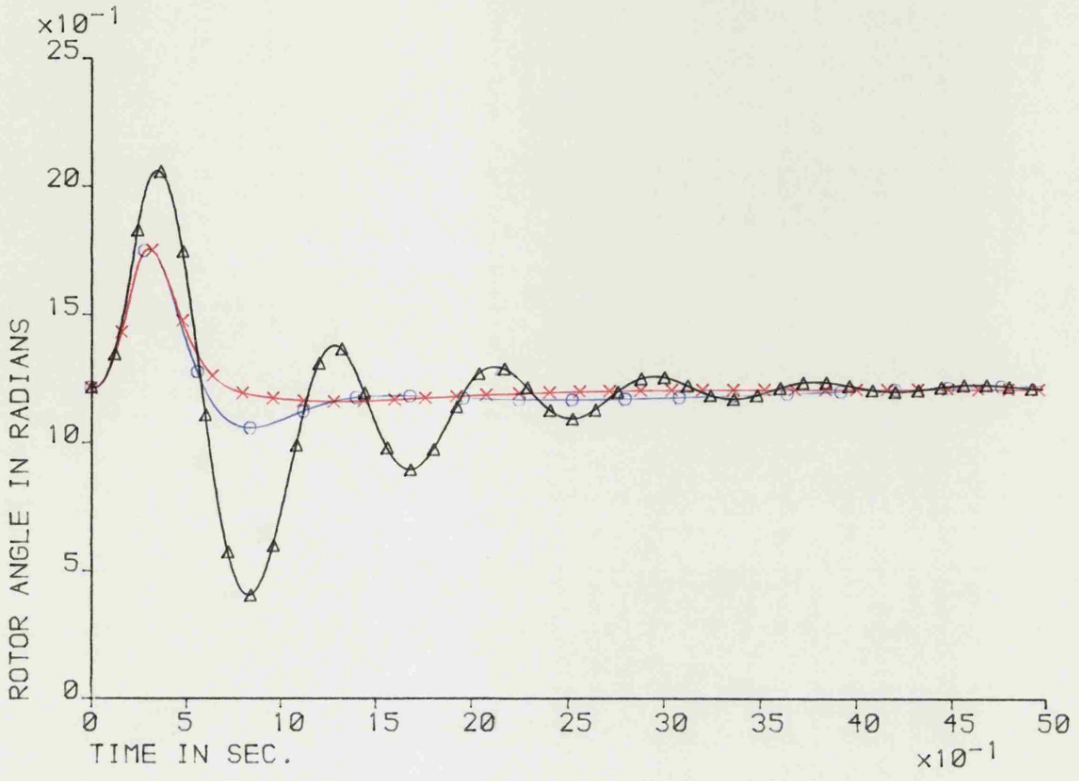

Fig. 6.4(a) Theoretical Load Angle Responses

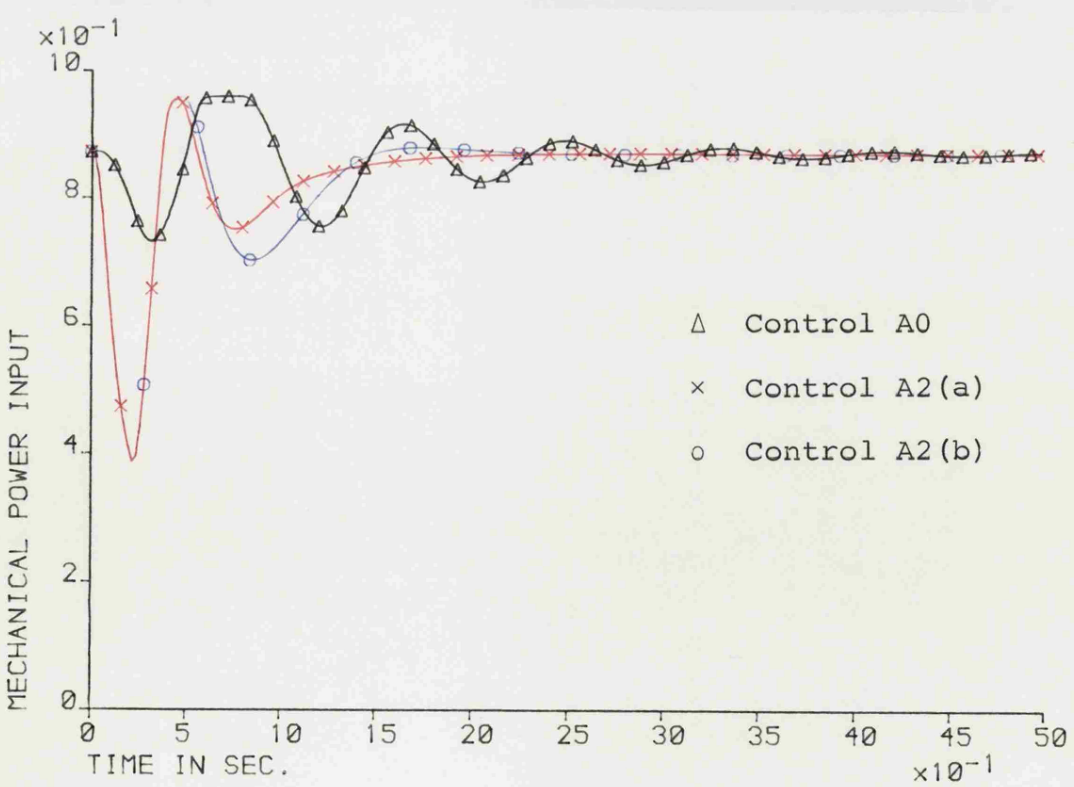

Fig. 6.4(b) Theoretical Mechanical Input Power Responses

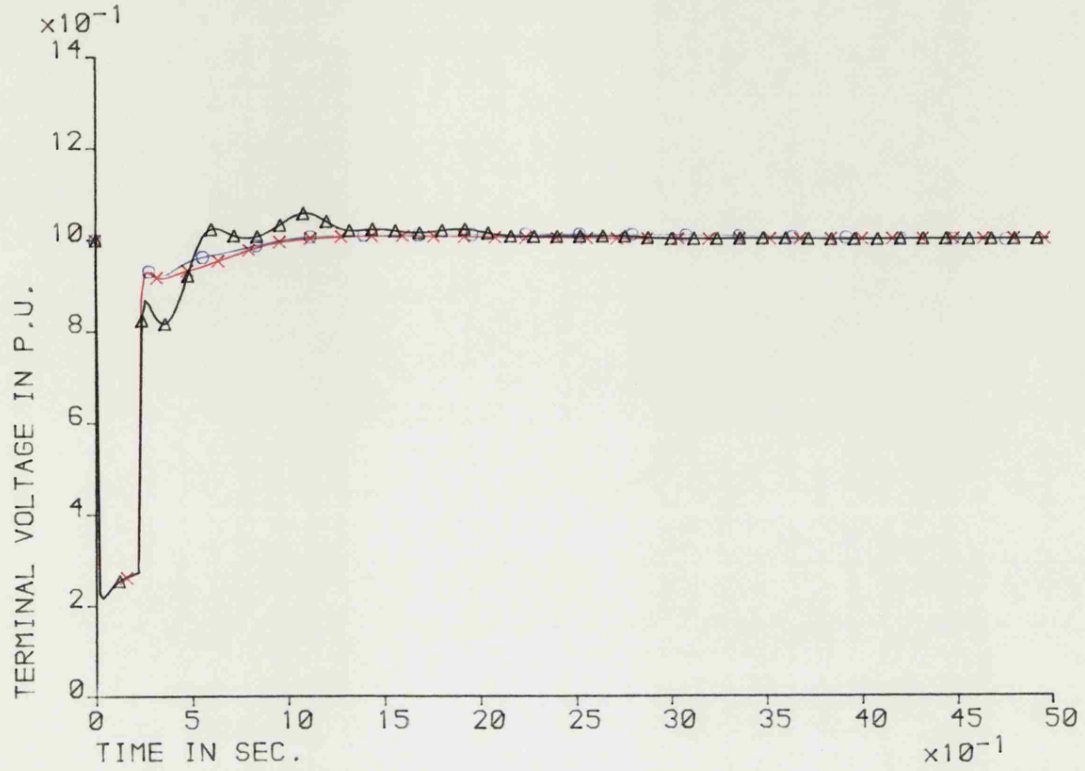

Fig. 6.4(c) Theoretical Terminal Voltage Responses

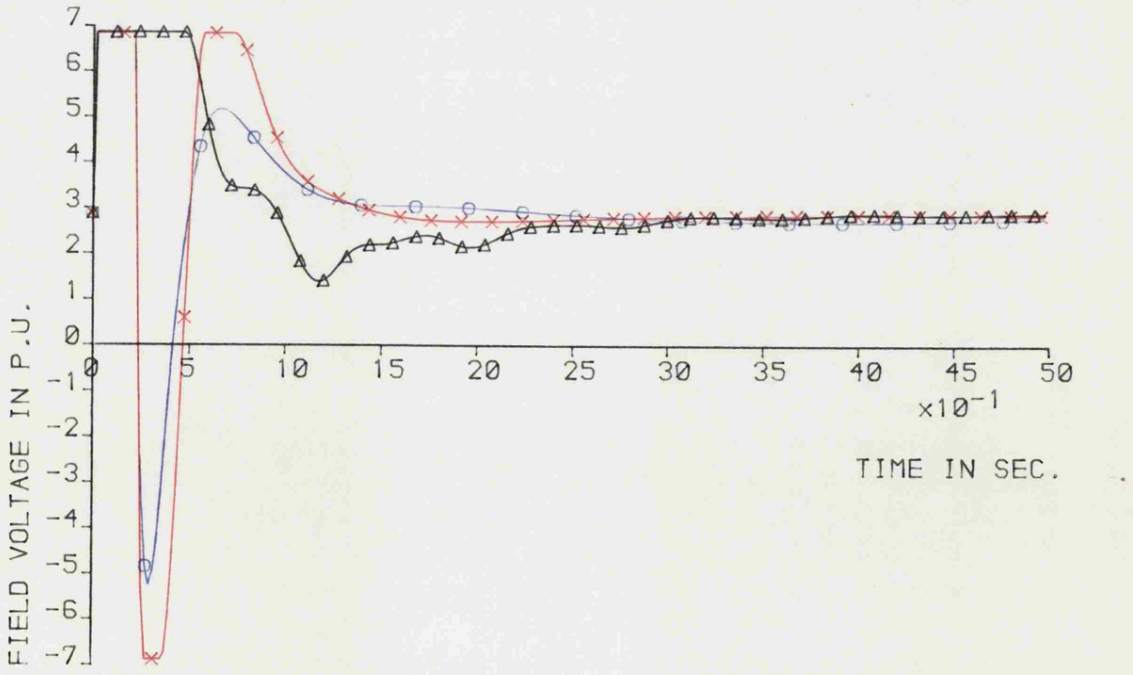

Fig. 6.4(d) Theoretical Field Voltage Responses

The co-ordinate control law of A2, which was optimized for a 220ms fault duration, has been applied to a 140ms duration fault on systems with automatic voltage regulator stabilizing time constants of 2.0s and 0.5s. These curves are labelled B1 and B2 respectively in Fig. 6.5. The standard curve in this case B0, is for a system comprising a fast governor and automatic voltage regulator with 2.0s stabilizing time constant. The performance index for the standard case is 4.86. The interesting feature of this set of curves is that the co-ordinate control applied to the system with the altered AVR stabilizer, curve B2, has a good load angle response, with a performance index of 0.518. The load angle response for the co-ordinate control B1 applied to the system with the original AVR stabilizer is not so good, yielding a performance index of 0.749. It is, however, significantly superior to the standard response. The prime mover torque curves show that the output power has stabilized within approximately 0.75s for control B1 and 1.5s for control B2. The elevated load angle for B1 is associated with the slightly lower terminal voltage until steady conditions are again established.

This suggests that the terminal voltage response and hence the load angle could be improved by reoptimization for the correct fault duration. Comparison of the main exciter field voltage curves indicate that a lowering of the feedback gain into the exciter would be advantageous.

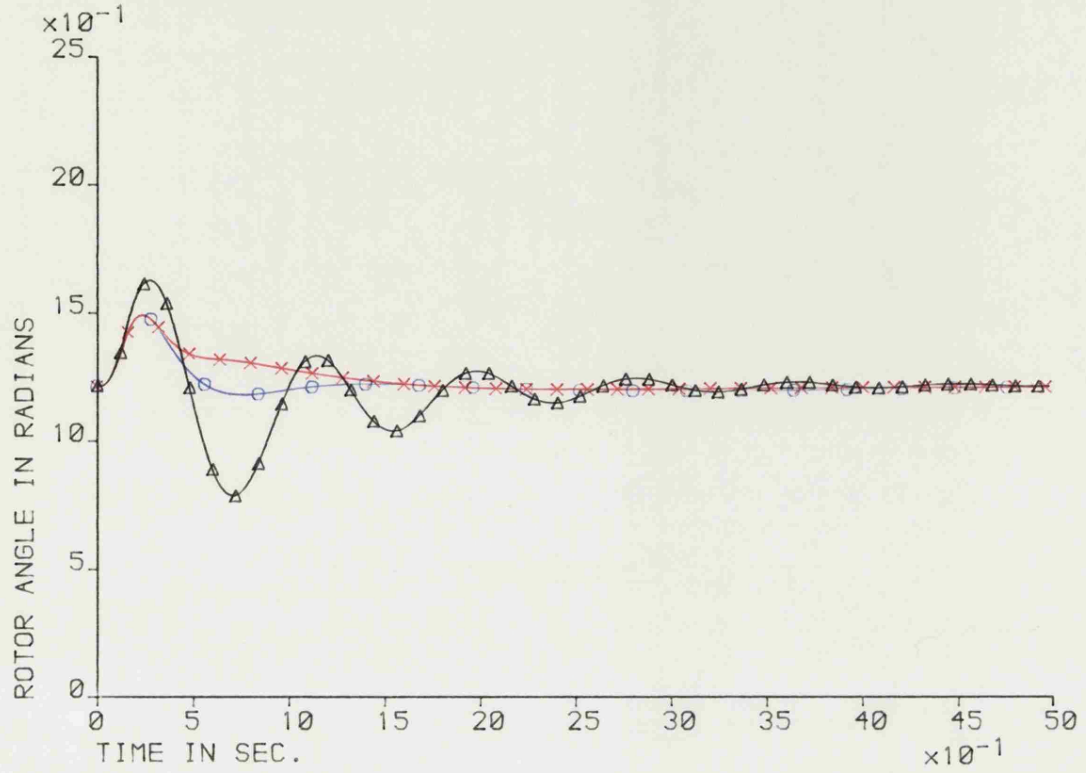

Fig. 6.5(a) Theoretical Load Angle Responses

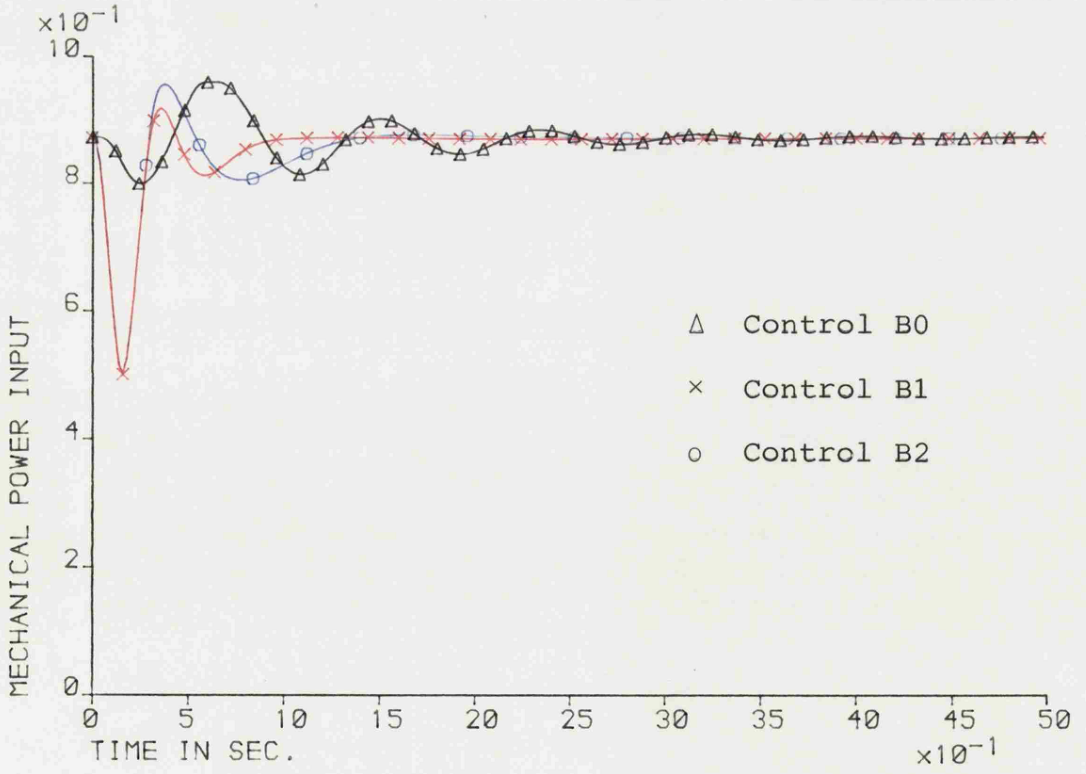

Fig. 6.5(b) Theoretical Mechanical Input Power Responses

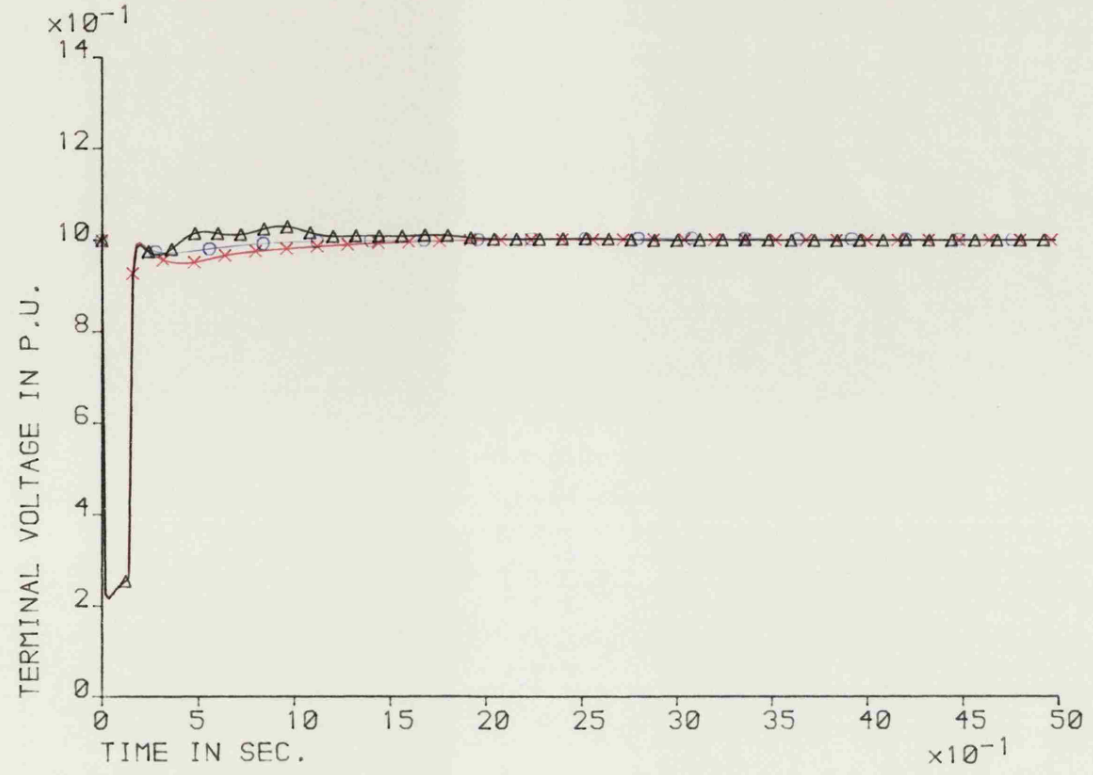

Fig. 6.5(c) Theoretical Terminal Voltage Responses

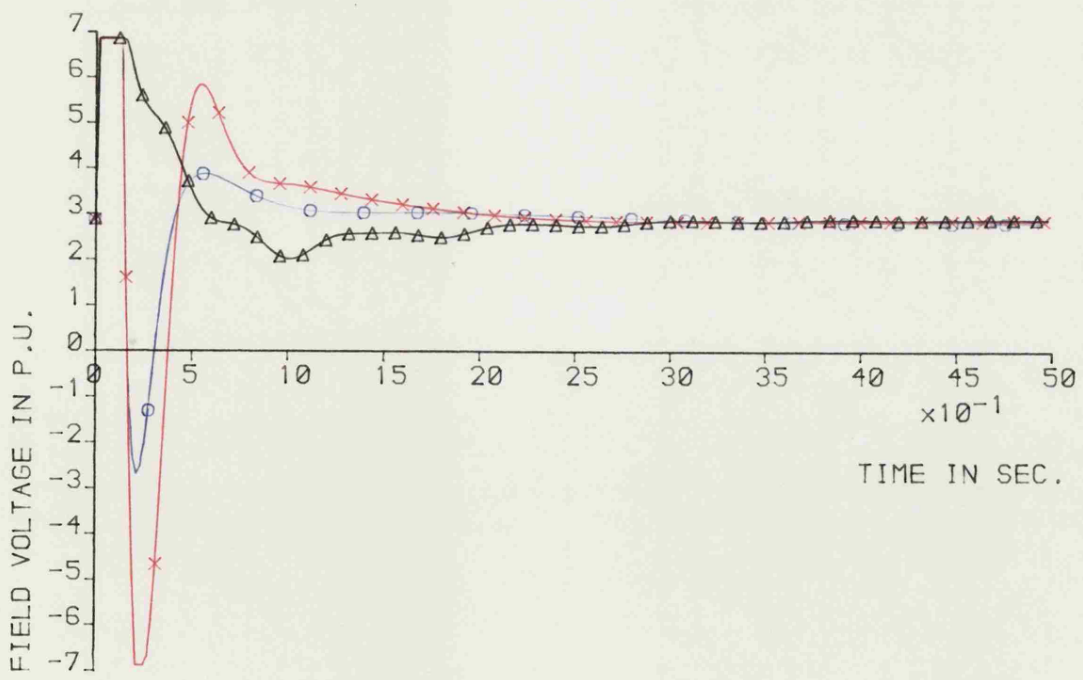

Fig. 6.5(d) Theoretical Field Voltage Responses

6.4.3 Effect of Governor Valve Slew Rate

Previous results have been obtained using governor valve velocity limits corresponding to +4.0 and -6.6pu per second[40]. These limits were arbitrarily reset to half the initial values and the system gains were reoptimized. The reoptimization resulted in a lowering of both the governor and exciter feedback gains and the corresponding curves are given in Fig. 6.6. The base case C0 has an identical performance index to that of the base case A0, which has the original higher velocity limits, confirming that without additional feedback signals, the full potential of the EH governor is not necessarily realized. The terminal voltage response curves for the co-ordinate controls are practically identical and the comments made for curves A0 and A2 discussed previously apply. Load angle curve C1 using the reoptimized gains shows a slight improvement over curve C2 which uses the original gains optimized for the faster valve systems. Both load angle curves undershoot and the reoptimized curve is better in this respect because the turbine output power has a smaller deviation from the steady state value. Both controls produce a fairly steady reduction in mechanical power and, when the fault is removed, output power is restored as fast as the rate limit will allow the valve to open. The slower response of the turbine governor system to the control signal aggravates the load angle responses. In the first instance, due to the lower peak rate at which the mechanical power can be reduced during the fault and secondly by the delay inherent in the limited valve opening rate in re-establishing full output power.

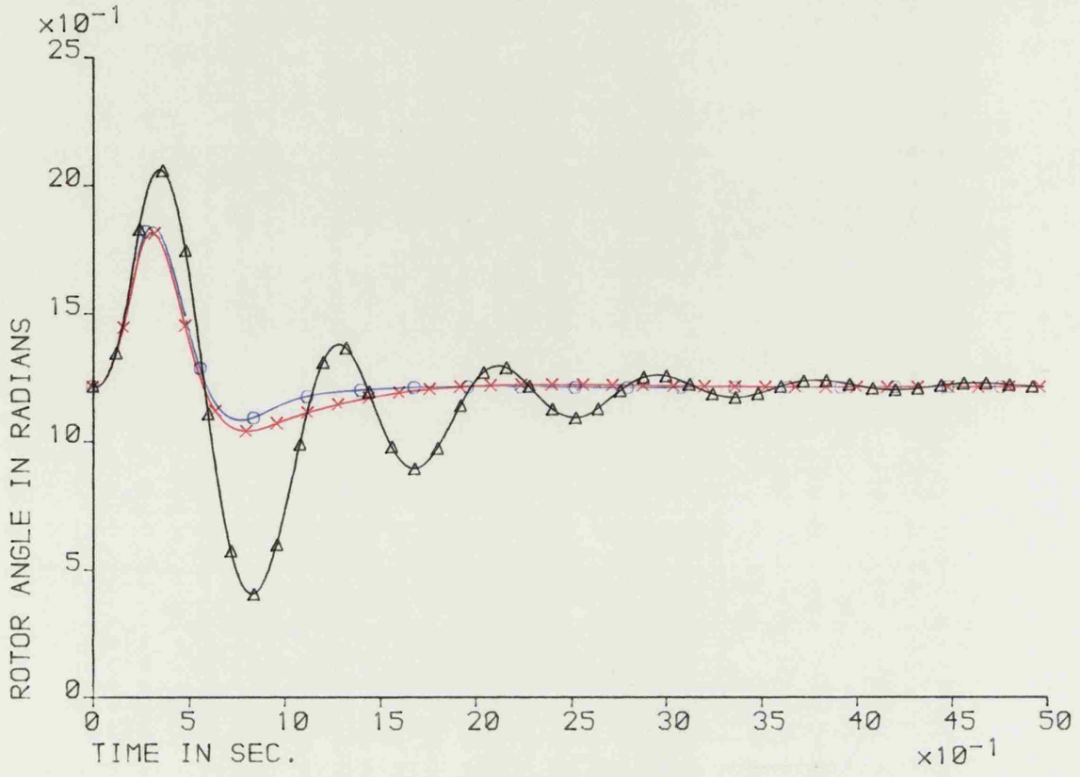

Fig. 6.6(a) Theoretical Load Angle Responses

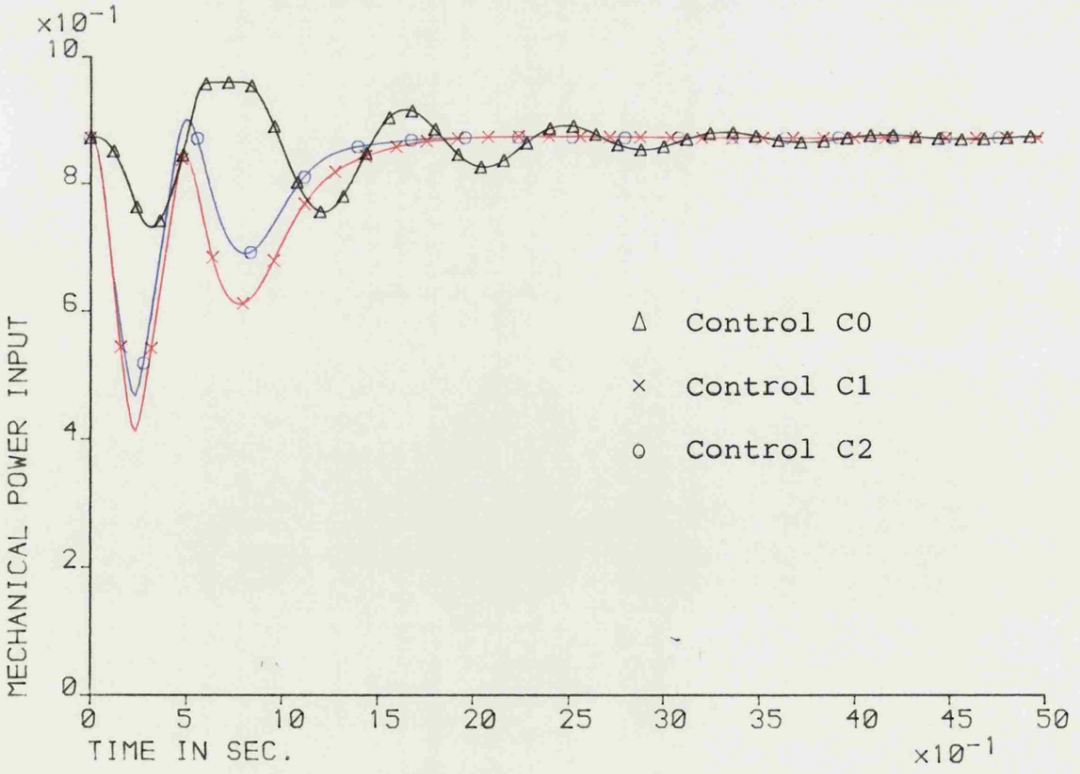

Fig. 6.6(b) Theoretical Mechanical Input Power Responses

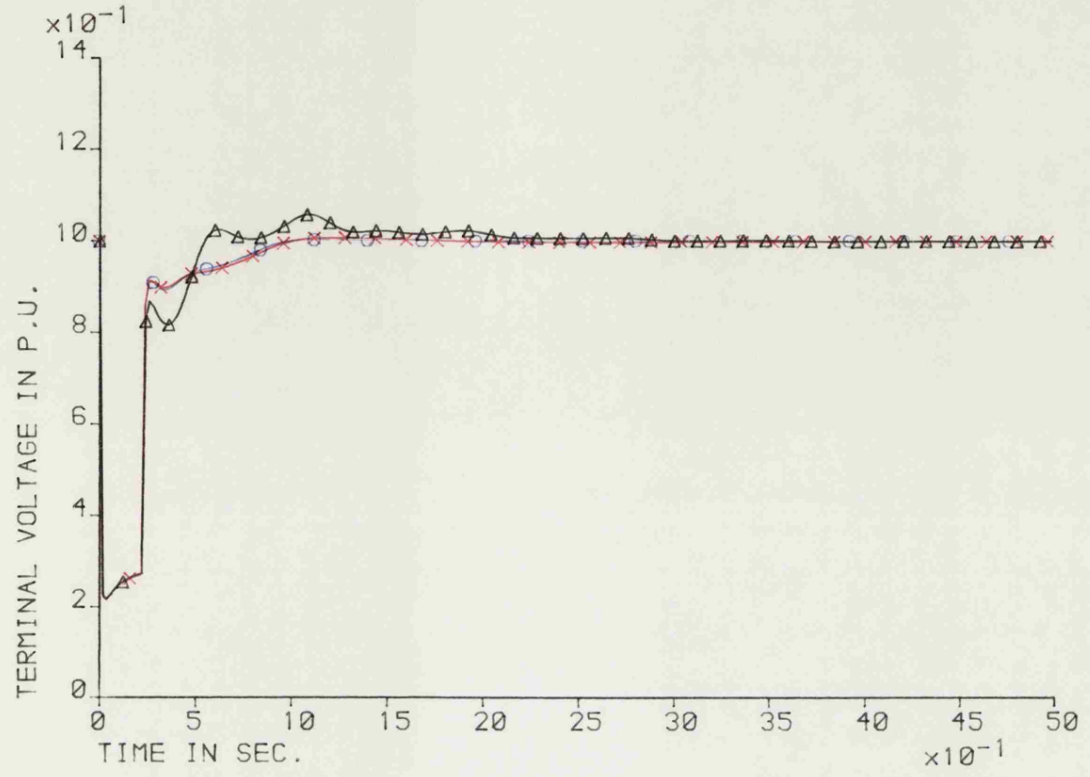

Fig. 6.6(c) Theoretical Terminal Voltage Responses

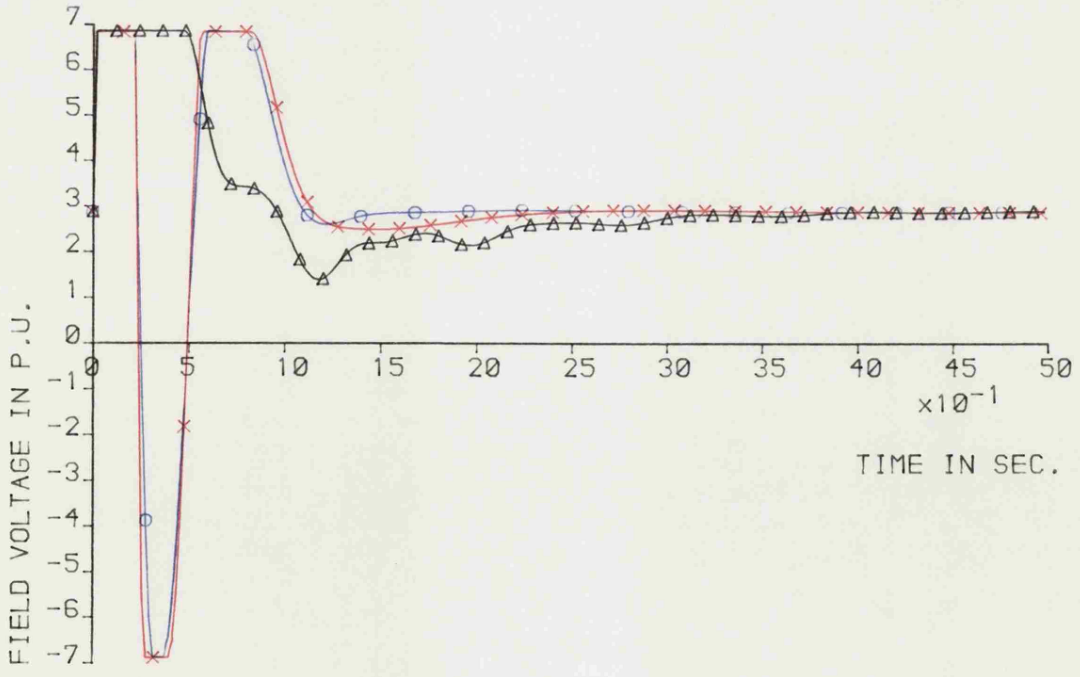

Fig. 6.6(d) Theoretical Field Voltage Responses

6.5 General Discussion of Theoretical Co-ordinate Control Results

The responses given have shown that there is a significant improvement to be made over the standard control system, by means of single variable co-ordinate control state feedback. The feedback gains optimized for one particular system and fault have been proven to remain beneficial, although not optimum, in the face of various changes to system and fault duration.

The responses obtained with the lower rate limits on the governor valves have reinforced two points. First, that a simple control may not necessarily make full use of the available hardware potential. The second is that physical limitations on the hardware will always dictate the best response obtainable; the control strategy can only work within these limitations to provide the best response, rather than the desired response.

CHAPTER 7 SINGLE MACHINE CO-ORDINATE CONTROL EXPERIMENTAL RESULTS

7.1 Introduction

The experimental results have been taken using the physical model systems described in Chapter 3. The governor turbine simulation developed in Chapter 2 is implemented in software running in the TMS 9900 microprocessor with the computed prime mover torque used as a demand input to the prime mover torque controller. The overall software environment is described in Chapter 5. The results have been taken on two machine sets. The results for machine set No.1 are discussed in detail. The results for the second machine are similar in overall form and so the discussion is restricted to significant differences between them and those of the first machine. The controls applied correspond to those of Table 6.1 on page 123.

7.2 Machine No.1 220ms Tests

The 220ms fault duration results are given in Fig. 7.1. The load angle responses, Fig. 7.1(a) follow the trend predicted by the theoretical studies in which the first swing peak is reduced from that of the AVR and constant steam flow case by the inclusion of a fast governor. The addition of co-ordinate control then further reduces the first peak and also damps out the rotor oscillations quickly. After the second load angle peak, the rotor oscillations for the constant torque system are smaller than the governed system, a trend which also follows the theoretical prediction.

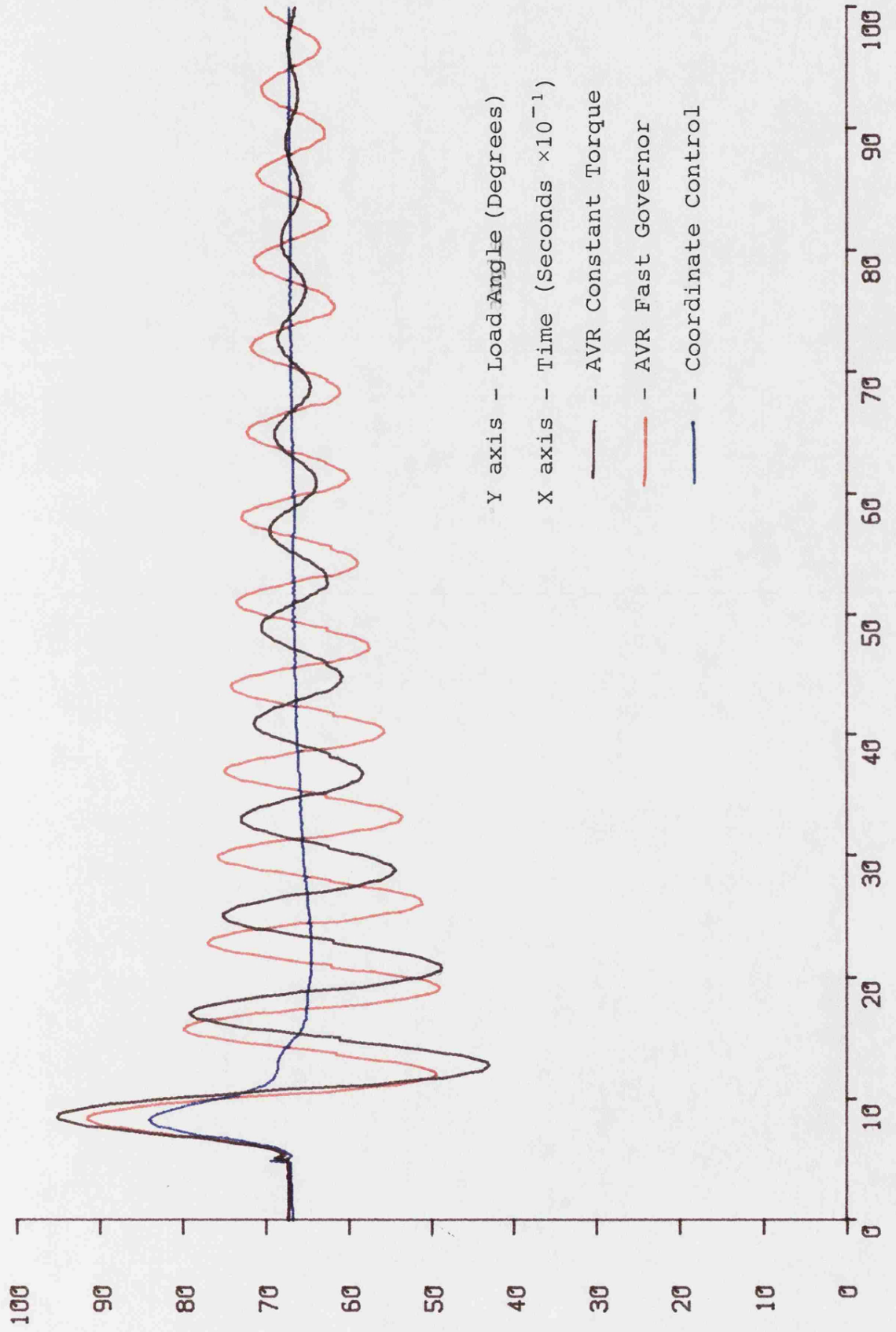

Fig. 7.1(a) Machine No.1 220ms Fault Load Angle

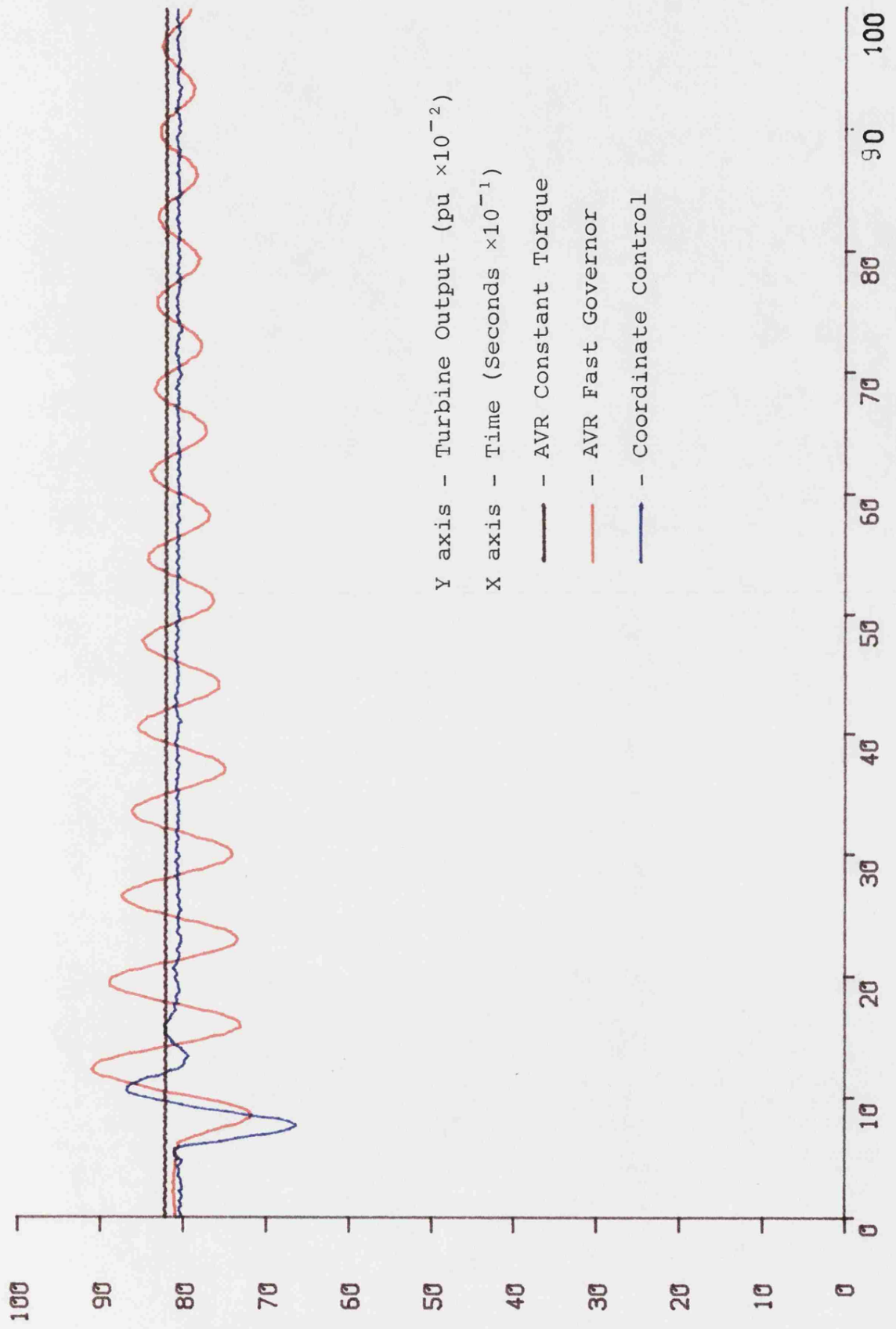

Fig. 7.1(b) Machine No.1 220ms Fault Turbine Output

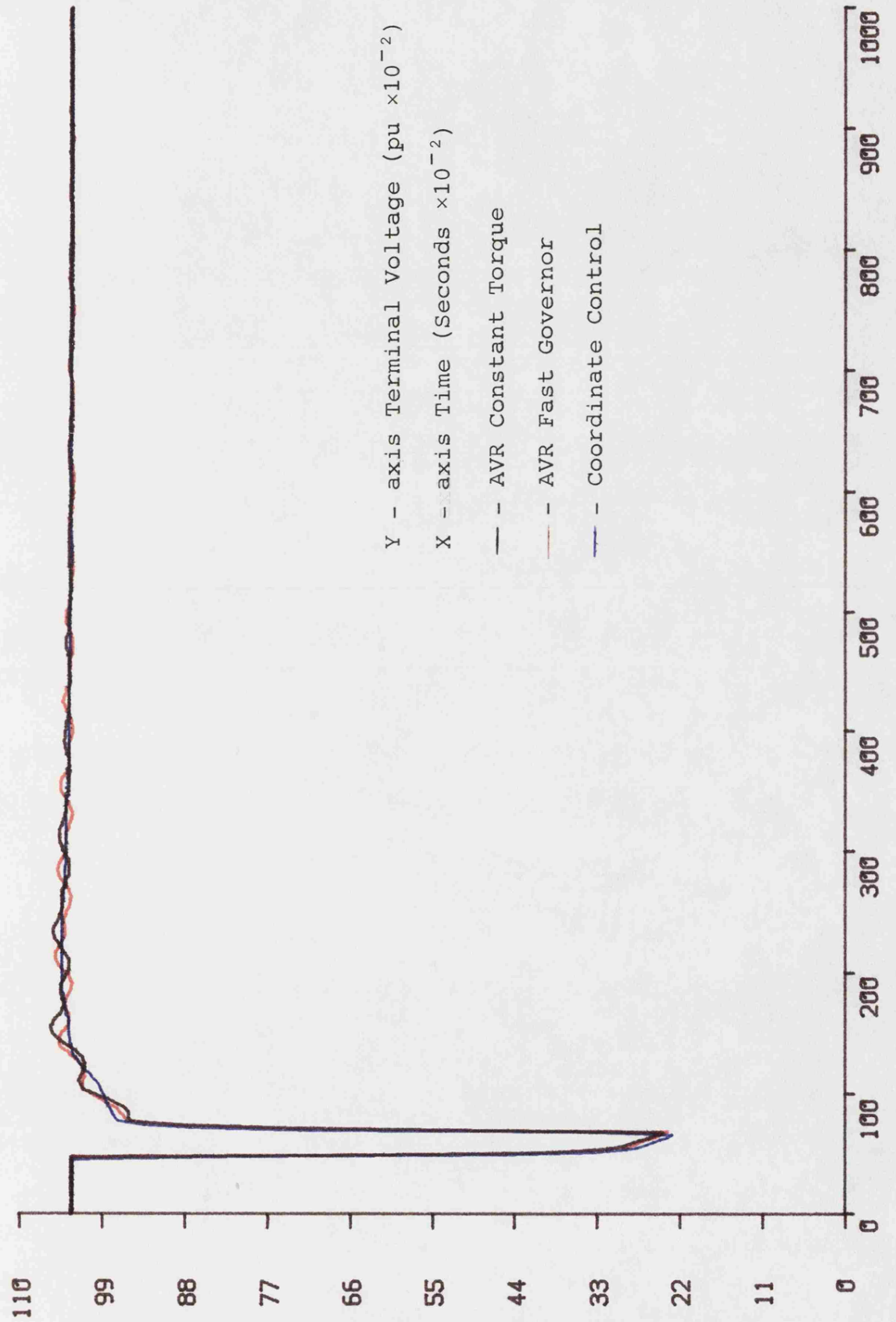

Fig. 7.1(c) Machine No.1 220ms Fault Terminal Voltage

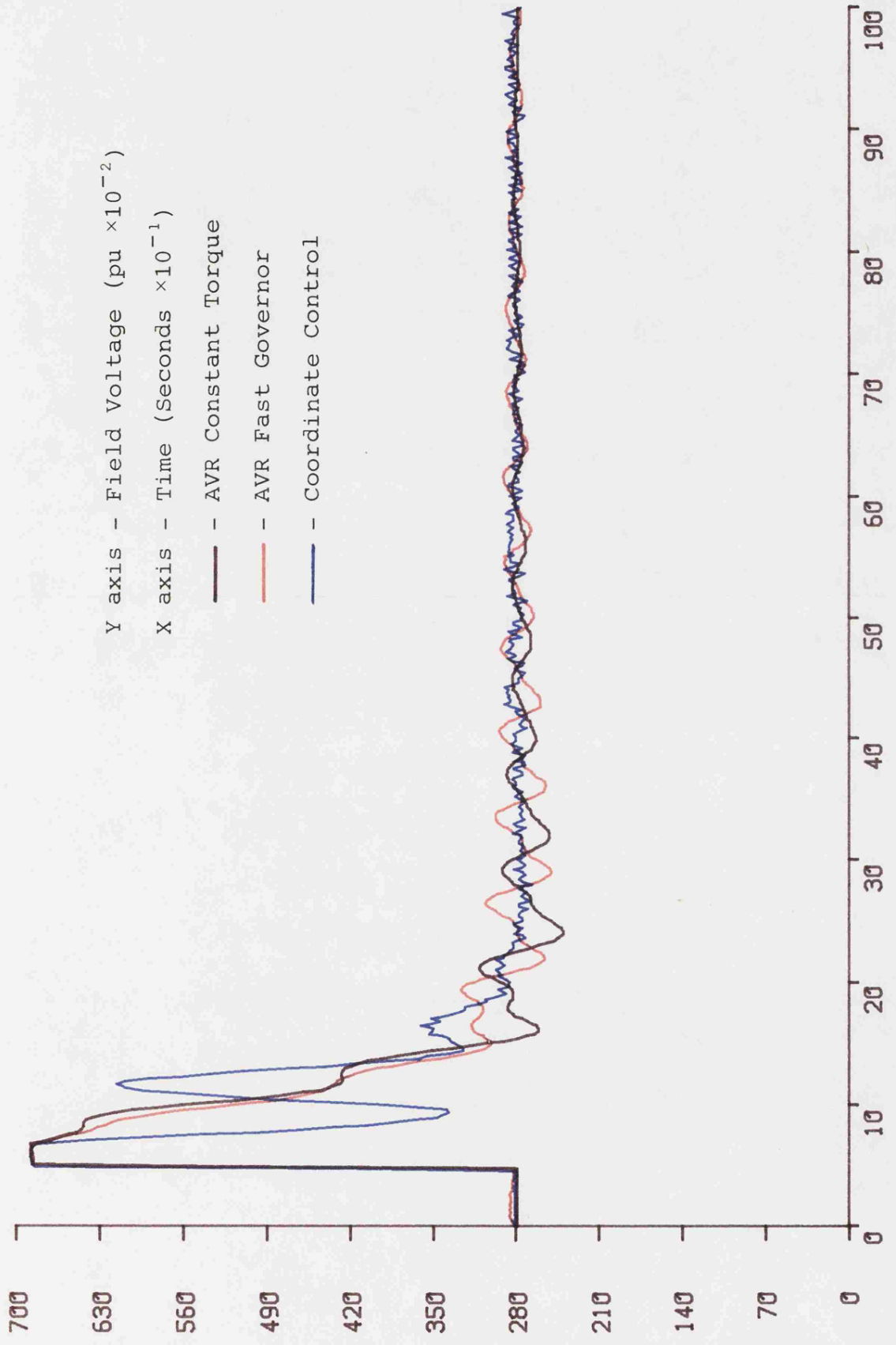

Fig. 7.1(d) Machine No.1 220ms Fault Field Voltage

The turbine output curves of Fig. 7.1(b) confirm the superior action of the co-ordinate control over that of the simple fast governor system in reducing the effect of the transient and bringing the output torque back to the steady state condition. Effectively the steady state is achieved within two seconds of fault clearance, when the additional feedback has fulfilled its role and may be removed. The additional feedback is retained in the experimental system for 10 seconds to show up any operational difficulties which may be apparent using the feedback system. Generally, it can be seen that even in the so called steady state there are numerous disturbances which effect the turbine output. These disturbances are however of small magnitude and high enough frequency not to significantly effect the machines mean operating point.

For the theoretical studies, the fixed mechanical loss torque due to losses in bearings etc. is not represented as a torque component since its value is not easily determined and under the assumption of only small speed changes it will remain virtually constant. However, in the micromachine system, these losses are present and so torque curves all have an effective positive offset compared with the theoretical plots. No attempt has been made to remove this offset as it is a valid contribution to torque in the micromachine system.

Moving on to the terminal voltage responses Fig. 7.1(c) and main exciter field voltage Fig. 7.1(d) it is interesting that all three terminal voltage responses are essentially similar and all exhibit a slight overshoot, the co-ordinate

control giving a quite acceptable recovery. The main exciter field voltage response curves show that the main control effort is over within two seconds and to avoid unnecessary noise being injected into the excitation system the additional control can be removed after that interval. The field voltage response for the co-ordinate control shows up the quantization in the acceleration signal used. The high frequency components do not have a serious effect on the system in general, because the long time constant of the main field winding effectively removes them. The co-ordinate control action on the field voltage follows the form of the theoretical studies but does not attain the negative limit or the second positive limit. To the best knowledge of the author, negative field forcing has never been attained in practice, despite careful attention to the setting of all gains in the system.

7.3 Machine No.1 140ms Tests

The curves of Fig. 7.2 give the responses for an automatic voltage regulator with constant torque system, a system comprising an automatic voltage regulator with a fast governor and an automatic voltage regulator with fast governor and co-ordinate control. The co-ordinate control used in the one optimized for a 220ms fault duration. Again, the load angle responses are as expected, with regard to first swing peak values. Also, the subsequent damping behaviour follows the pattern established in the 220ms results and theoretical studies. The form of the co-ordinate control response follows

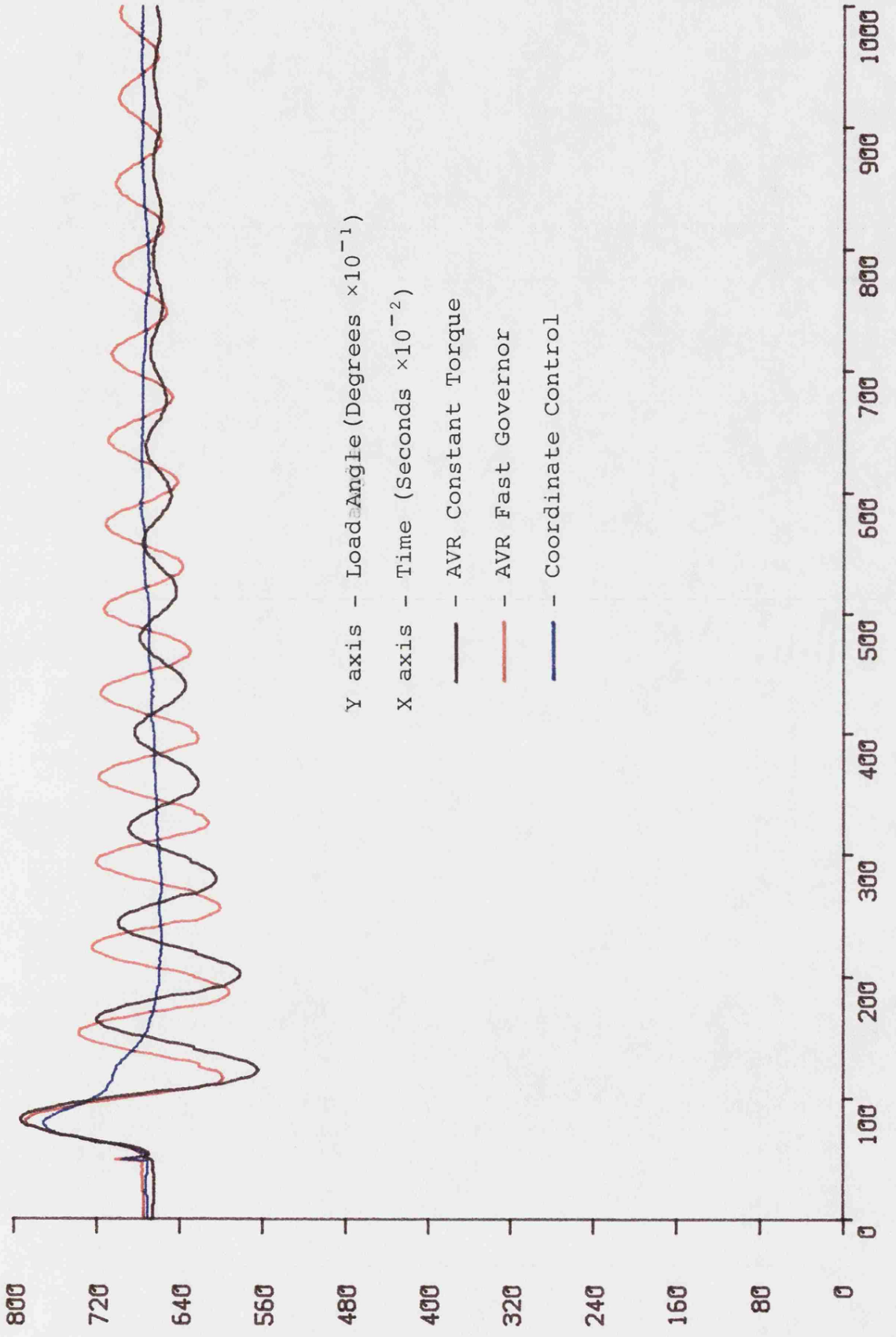

Fig. 7.2(a) Machine No.1 140ms Fault Load Angle

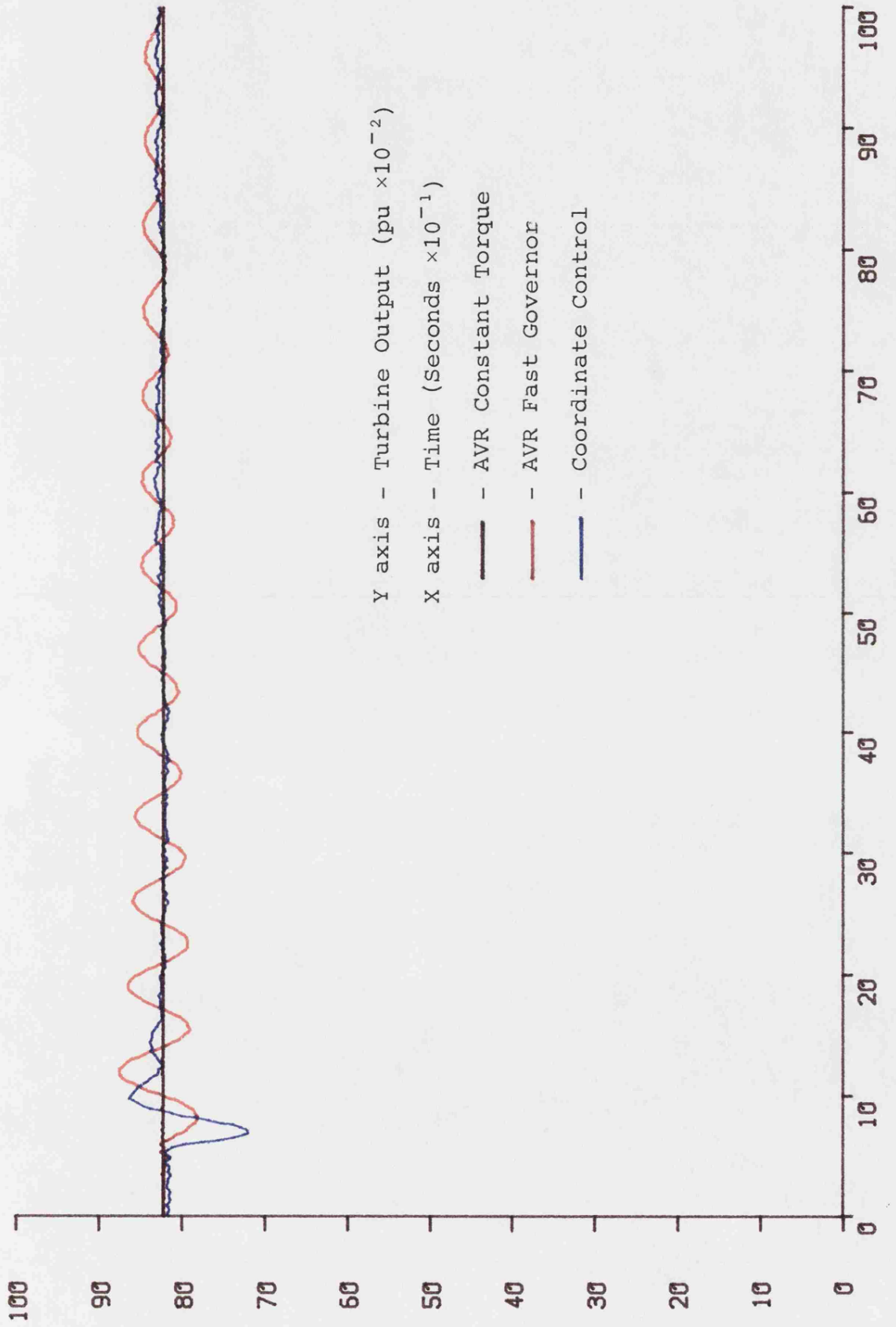

Fig. 7.2(b) Machine No.1 140ms Fault Turbine Output

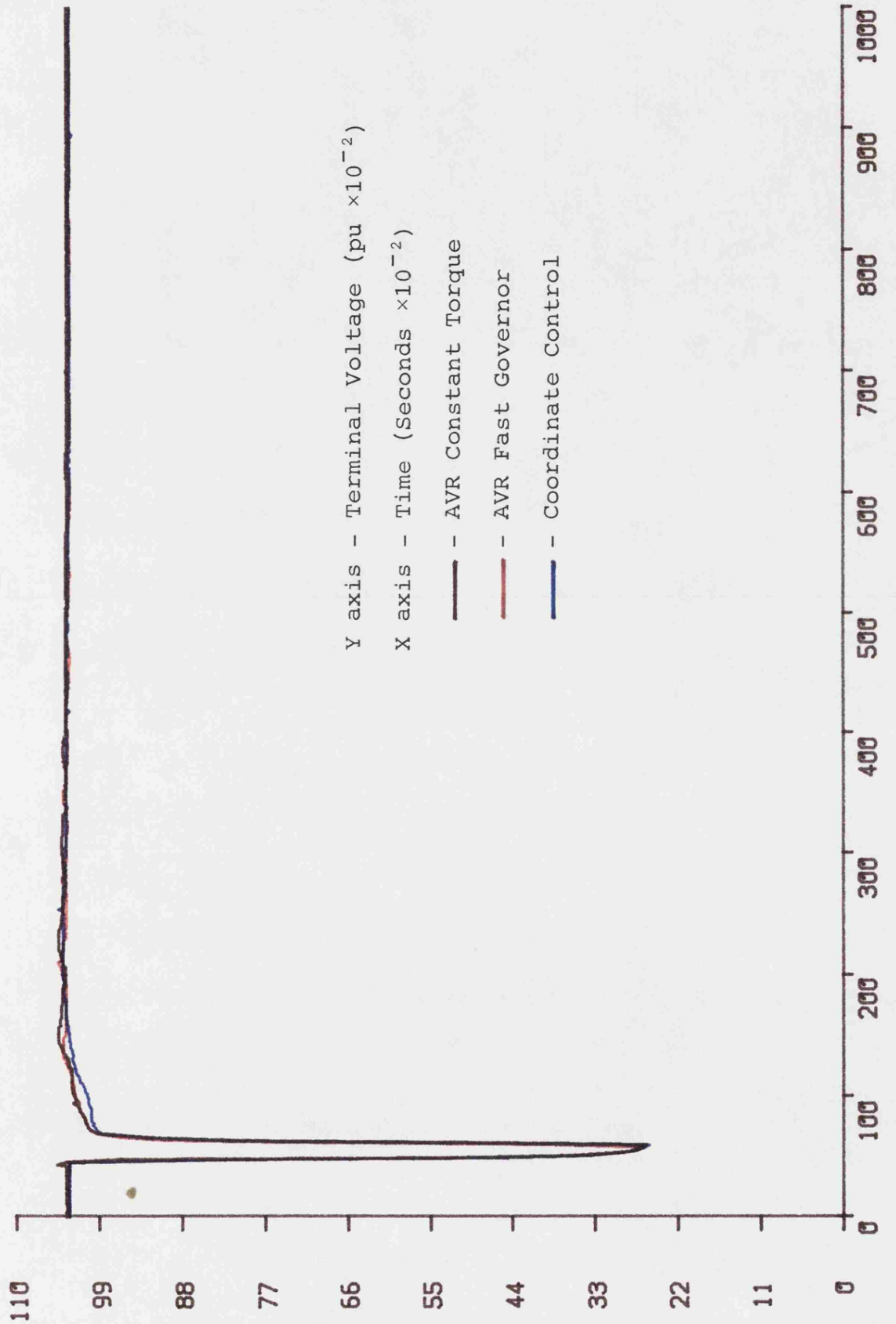

Fig. 7.2(c) Machine No.1 140ms Fault Terminal Voltage

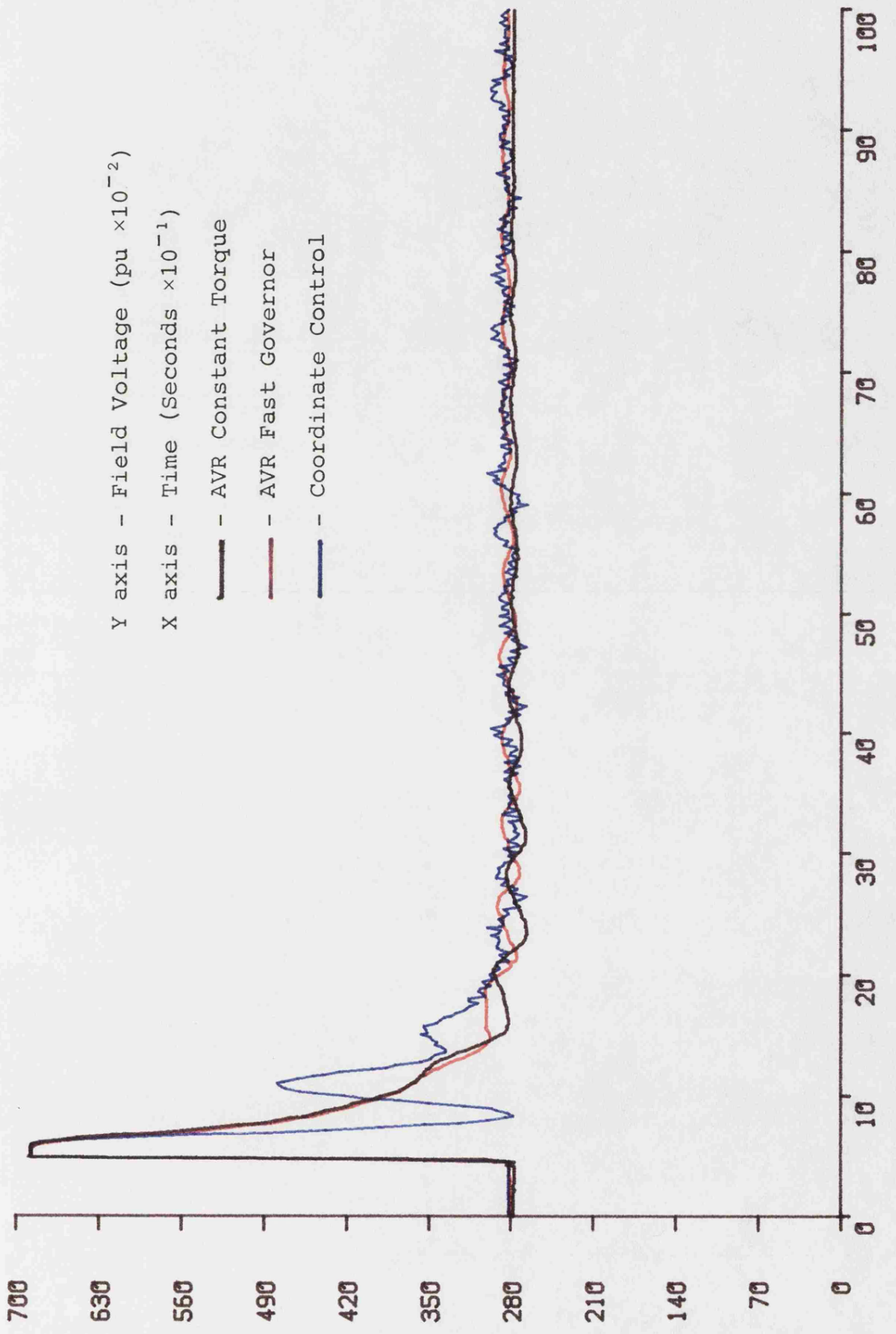

Fig. 7.2(d) Machine No.1 140ms Fault Field Voltage

the trend predicted by the equivalent theoretical curve. That is, the load angle returns approximately half way from the first swing peak and then more slowly ramps down to the initial value. In the experimental curve, there is a slight undershoot followed by a further slow ramp back to the steady state level. The undershoot and slow ramp back was also a feature of the 220ms experimental curve.

It is apparent from the terminal voltage recovery curves of Fig. 7.2(c) that, for both cases where steam flow control is employed as well as automatic voltage regulator action, the terminal voltage recovery is faster than when the automatic voltage regulator is acting alone.

The main exciter field voltage response curves of Fig. 7.2(b) and the turbine output curves of Fig. 7.2(d) follow the same trends as discussed for the equivalent 220ms fault duration curves.

7.4 Discussion of Machine No.1 Results

The foregoing curves have shown that a co-ordinate control optimized for one fault duration and operating condition can substantially improve the system response for a fault of significantly different duration. The correlation between the theoretical results of Chapter 6 and the experimental curves is sufficient to give confidence to the application of this type of control.

The load angle response curves occasionally contain a glitch at the instant of fault inception. The precise origin is not fully understood but the most likely cause is some form of distortion of the infinite bus voltage signal, as received by the transformer used in the load angle transducer. The problem, when it does occur, only lasts for a very short time and does not affect subsequent readings. Since the signal is used purely for instrumentation, and the load angle information at that particular instant is not critical, no attempt has been made to remove it.

7.5 Machine No.2 Tests

Figs. 7.3 and 7.4 show the response curves for machine No.2, for the equivalent tests presented in Figs. 7.1 and 7.2 for machine No.1. For the load angle curves, the first swing trend is as before, with the expected reductions in peak value from the constant torque case, for fast governed and co-ordinate control cases. The absolute values for the peaks are higher for machine No.2. The increased load angle peak together with the terminal voltage and field voltage response curves indicate that machine No.2 has a smaller resistive element in the fault impedance. The lower terminal voltage during the fault and subsequent recovery, gives a large error signal to the AVR, which tends to maintain the field voltage high for longer than is the case for machine No.1. This feature tends to swamp the additional feedback signal into the AVR for longer than both machine No.1 tests and theoretical studies. Subsequent oscillations on the load angle follow

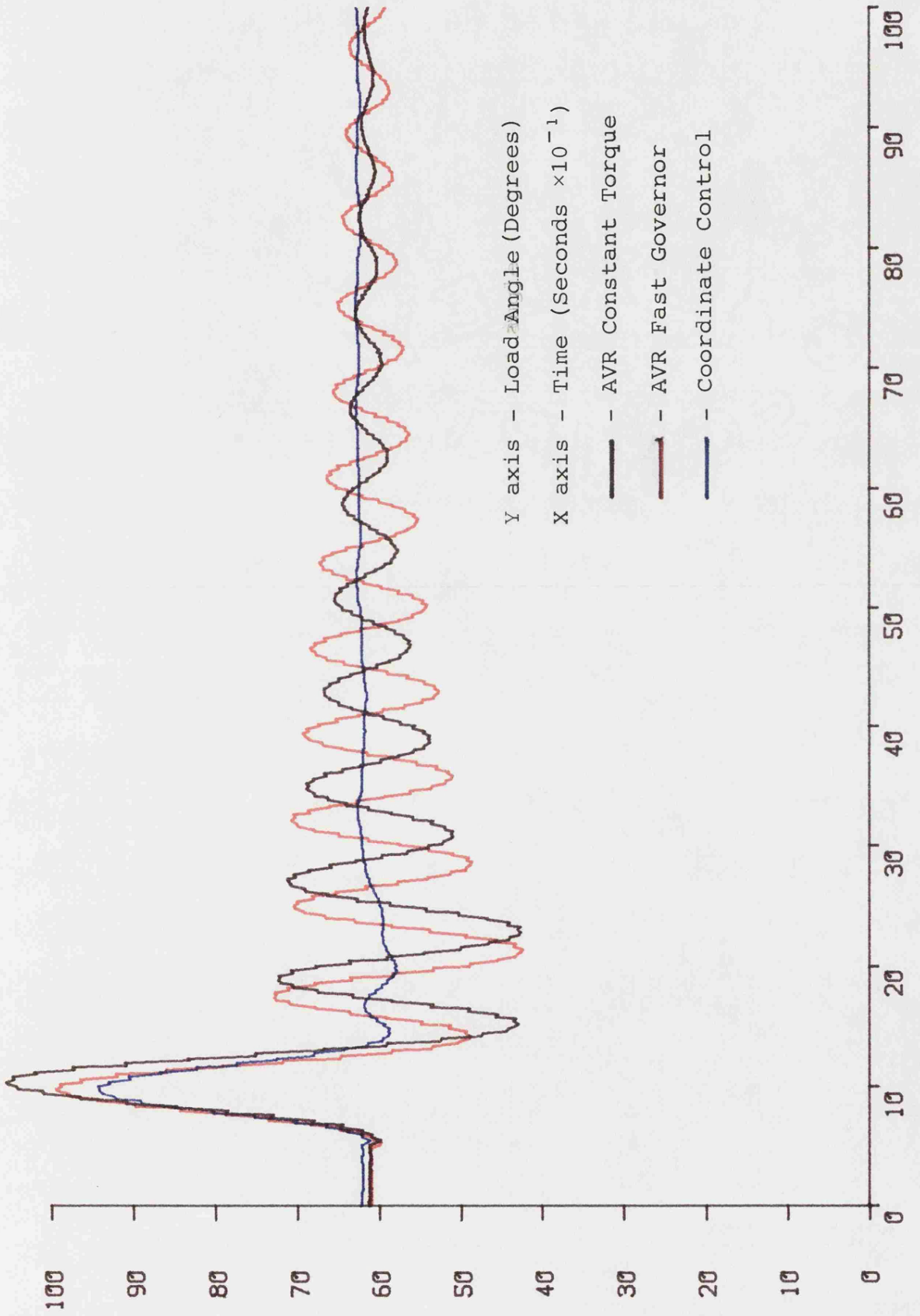

Fig. 7.3(a) Machine No.2 220ms Fault Load Angle

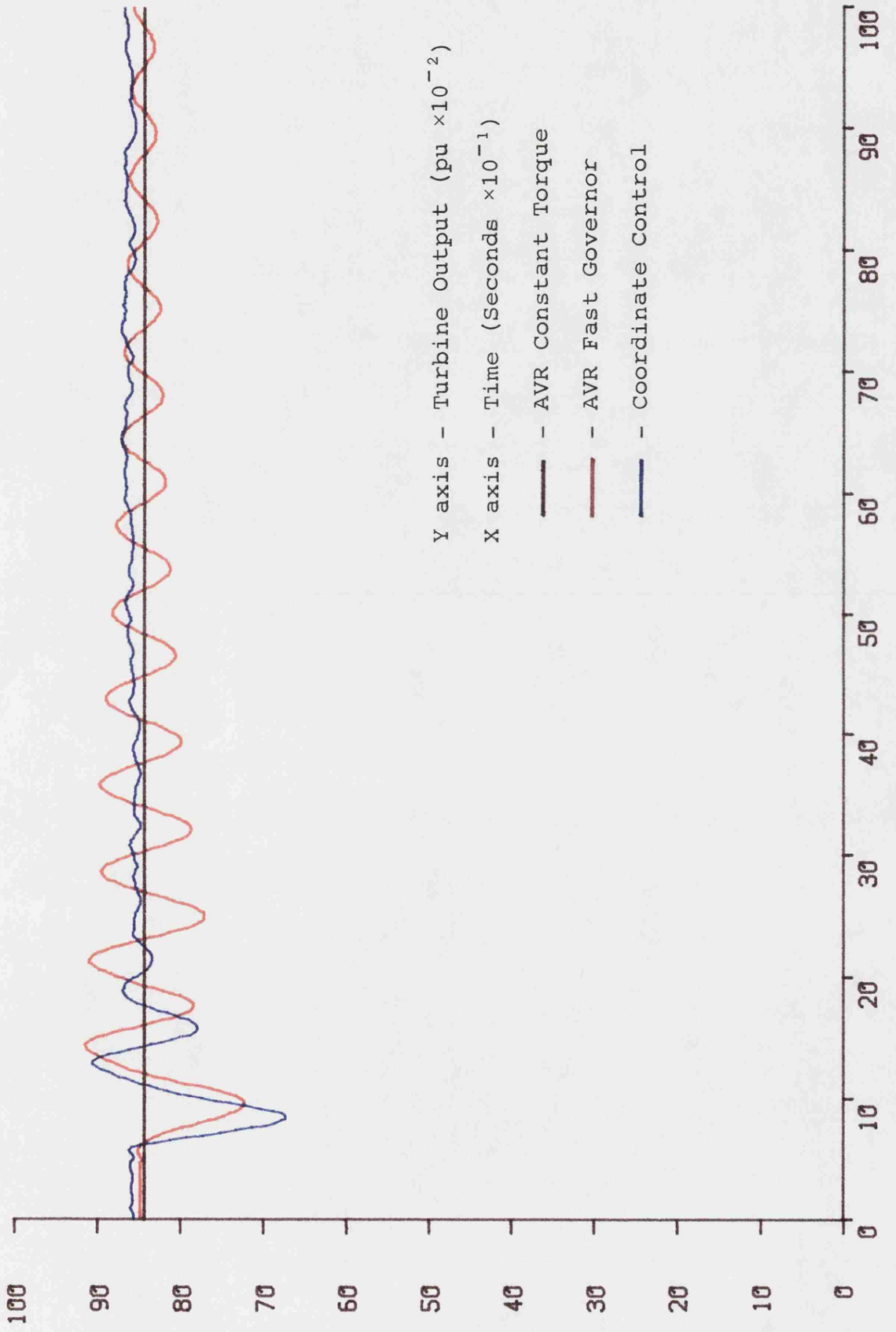

Fig. 7.3(b) Machine No.2 220ms Fault Turbine Output

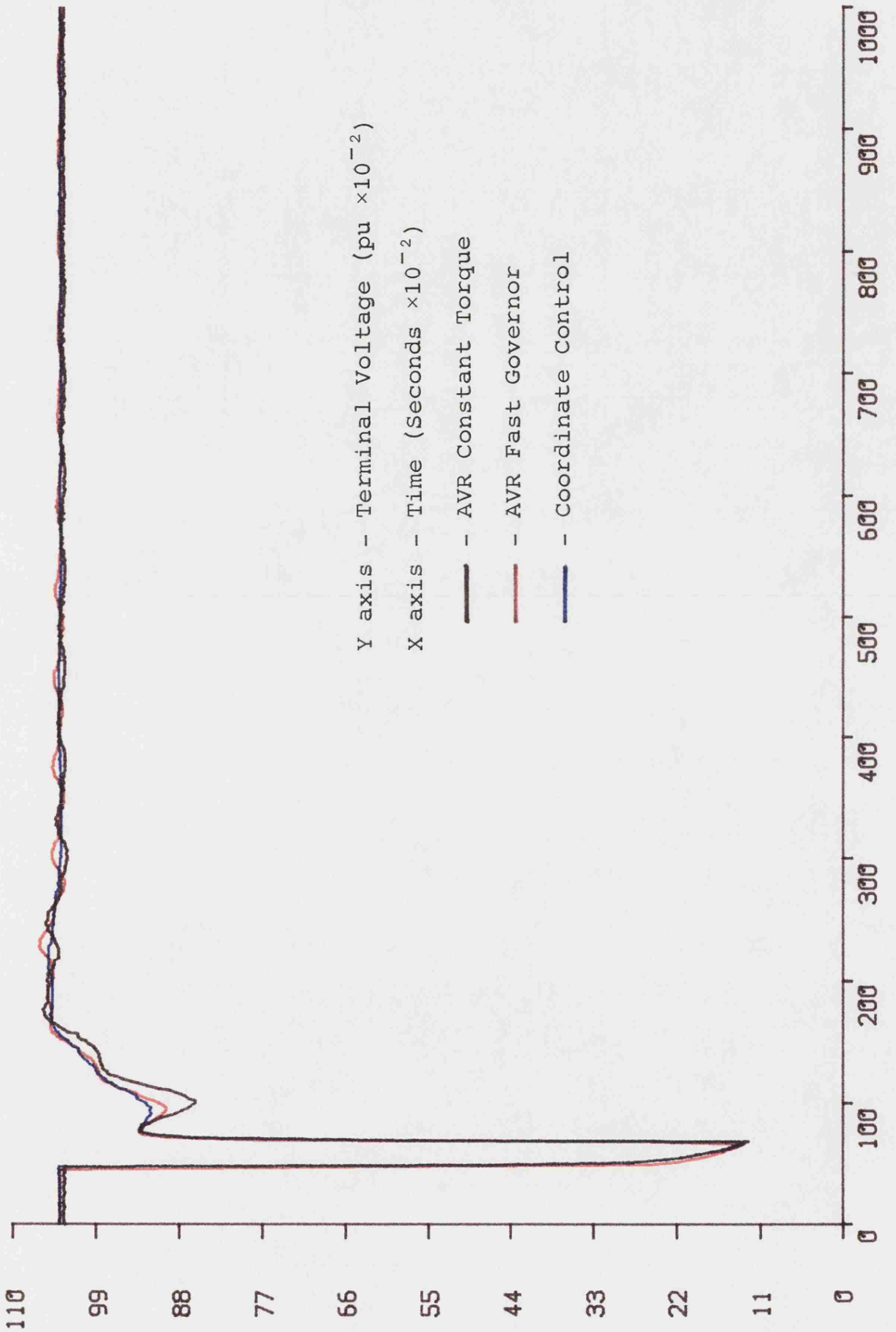

Fig. 7.3(c) Machine No.2 220ms Fault Terminal Voltage

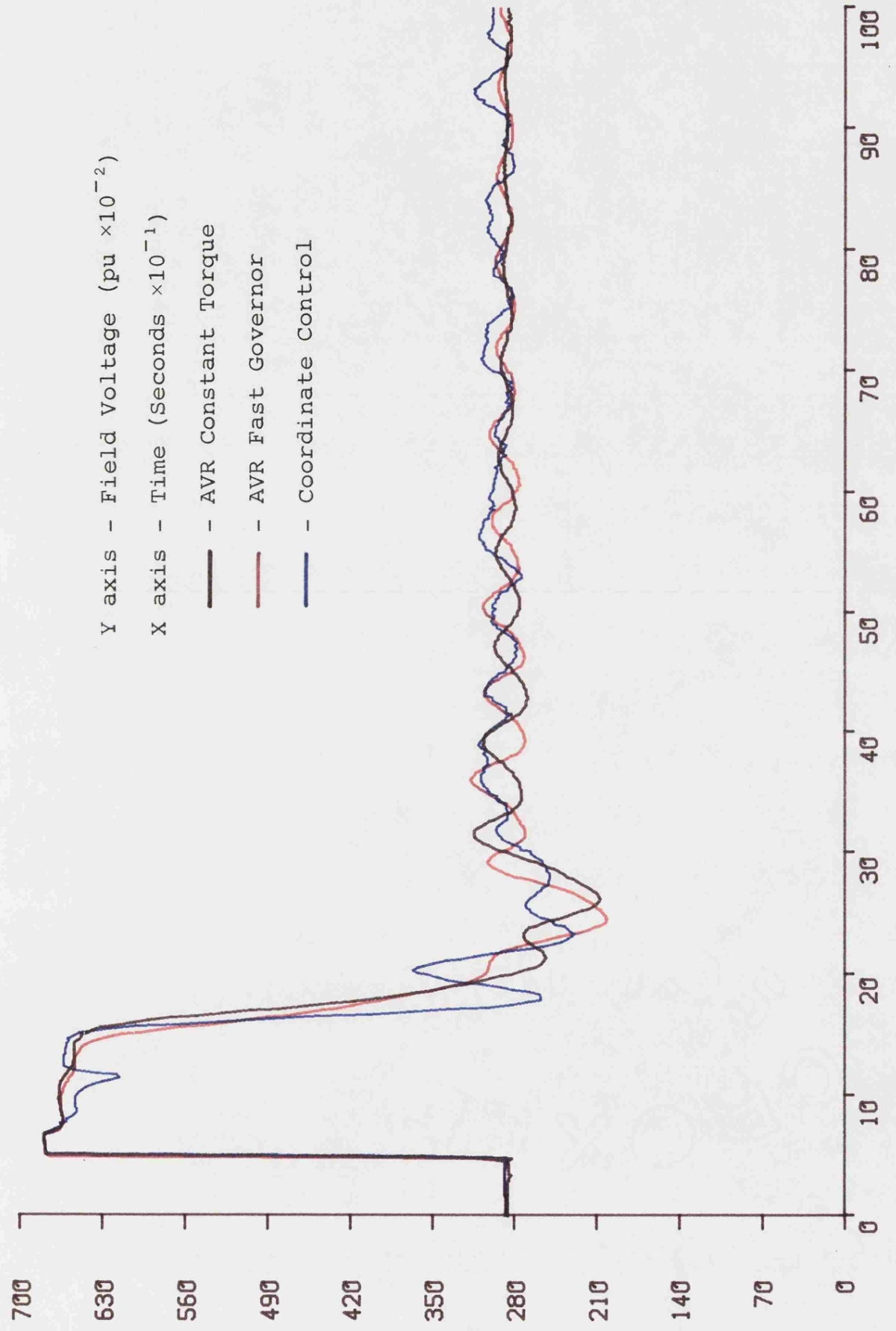

Fig. 7.3(d) Machine No.2 220ms Fault Field Voltage

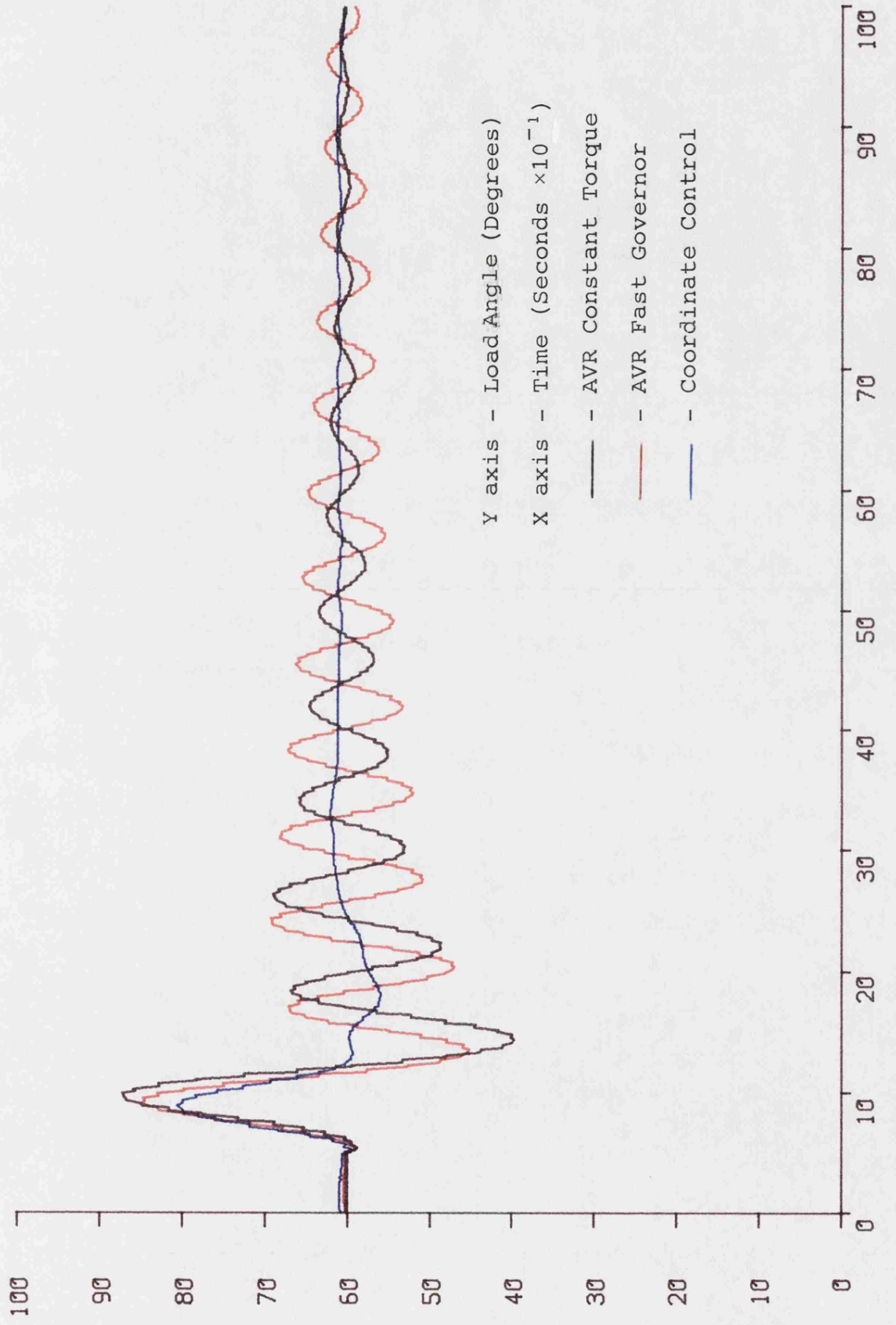

Fig. 7.4(a) Machine No.2 140ms Fault Load Angle

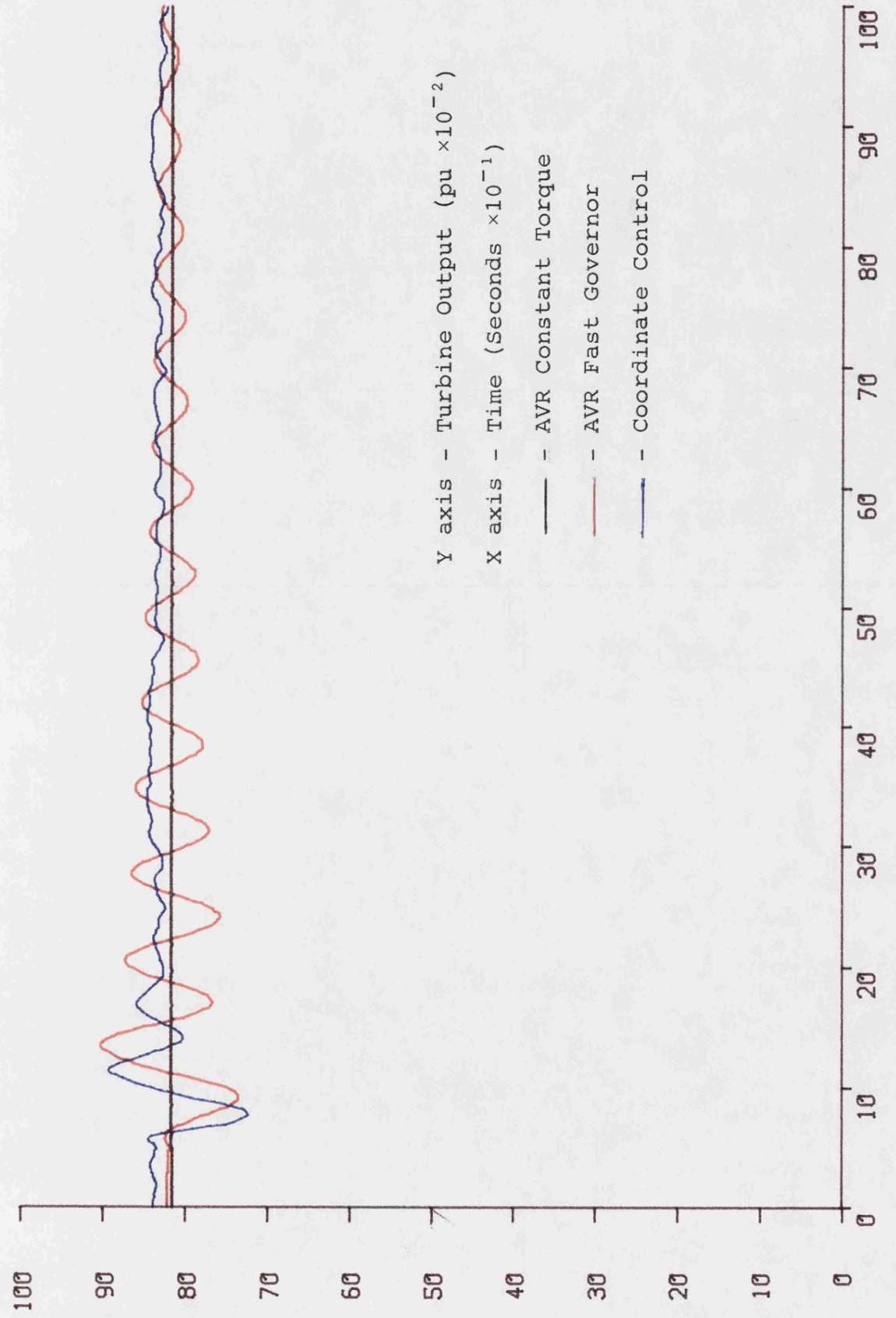

Fig. 7.4(b) Machine No.2 140ms Fault Turbine Output

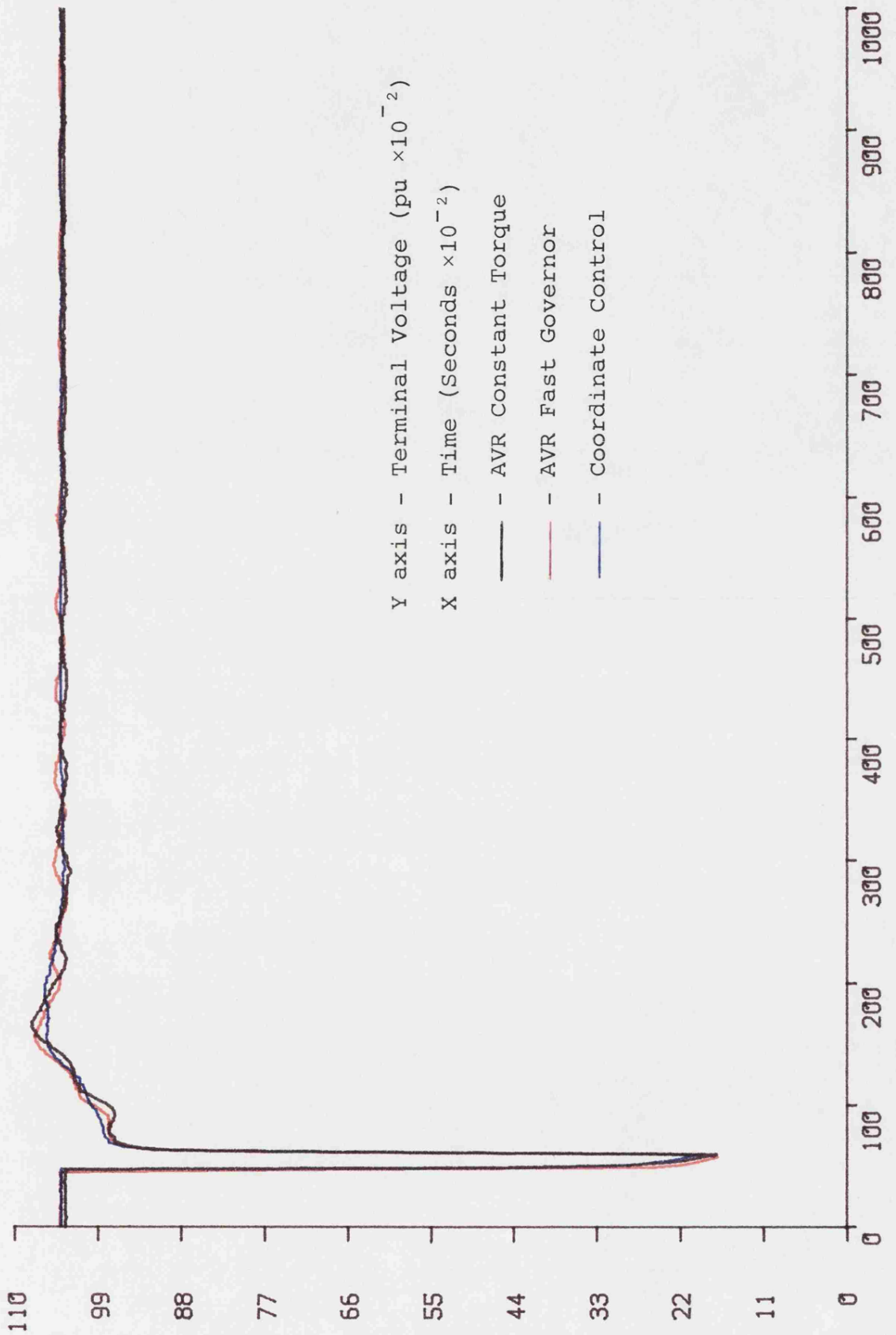

Fig. 7.4(c) Machine No.2 140ms Fault Terminal Voltage

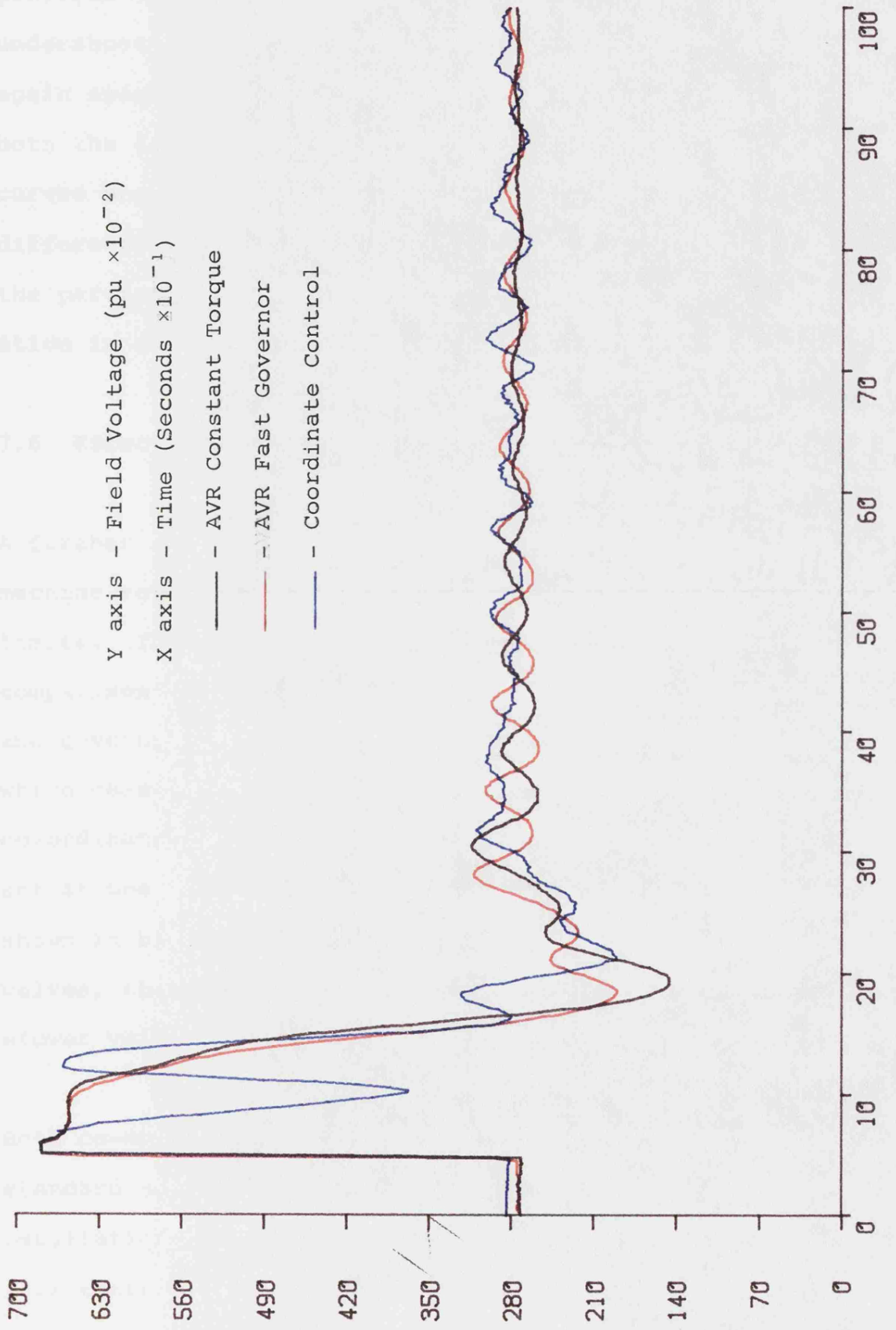

Fig. 7.4(d) Machine No.2 140ms Fault Field Voltage

previous trends, however, the co-ordinate controls give more undershoot than is present on the other machine, which is again associated with the prolonged field forcing. However, both the load angle and terminal voltage transient response curves show the expected form, in spite of the apparent difference in plant parameters. This fact confirms that, in the particular case of a single machine system, the optimization is quite insensitive to plant parameter changes.

7.6 Effect of Reduction in Valve Rate Limit on Performance

A further set of experimental results were obtained on machine set No.1 to check the effect of lower valve velocity limits. The response curves are given in Fig. 7.5. For comparison the standard system of automatic voltage regulator and governor is used. First with no additional controls, in which case neither valve velocity limit applies, and then co-ordinate controls are applied with the valve rate limits set at one half the original values. One co-ordinate control shown in blue, is that optimized for a 220ms fault and fast valves, the other control uses the gains reoptimized for the slower valves, controls C2 and C1 of Chapter 6 respectively.

Both co-ordinate controls are significantly better than the standard case, particularly in the damping of subsequent oscillation. The first rotor swing of control C2, the higher gain control, is slightly less than the reoptimized control C1. However, in most other respects, the controls behave similarly. The effect of the higher gain is also evident

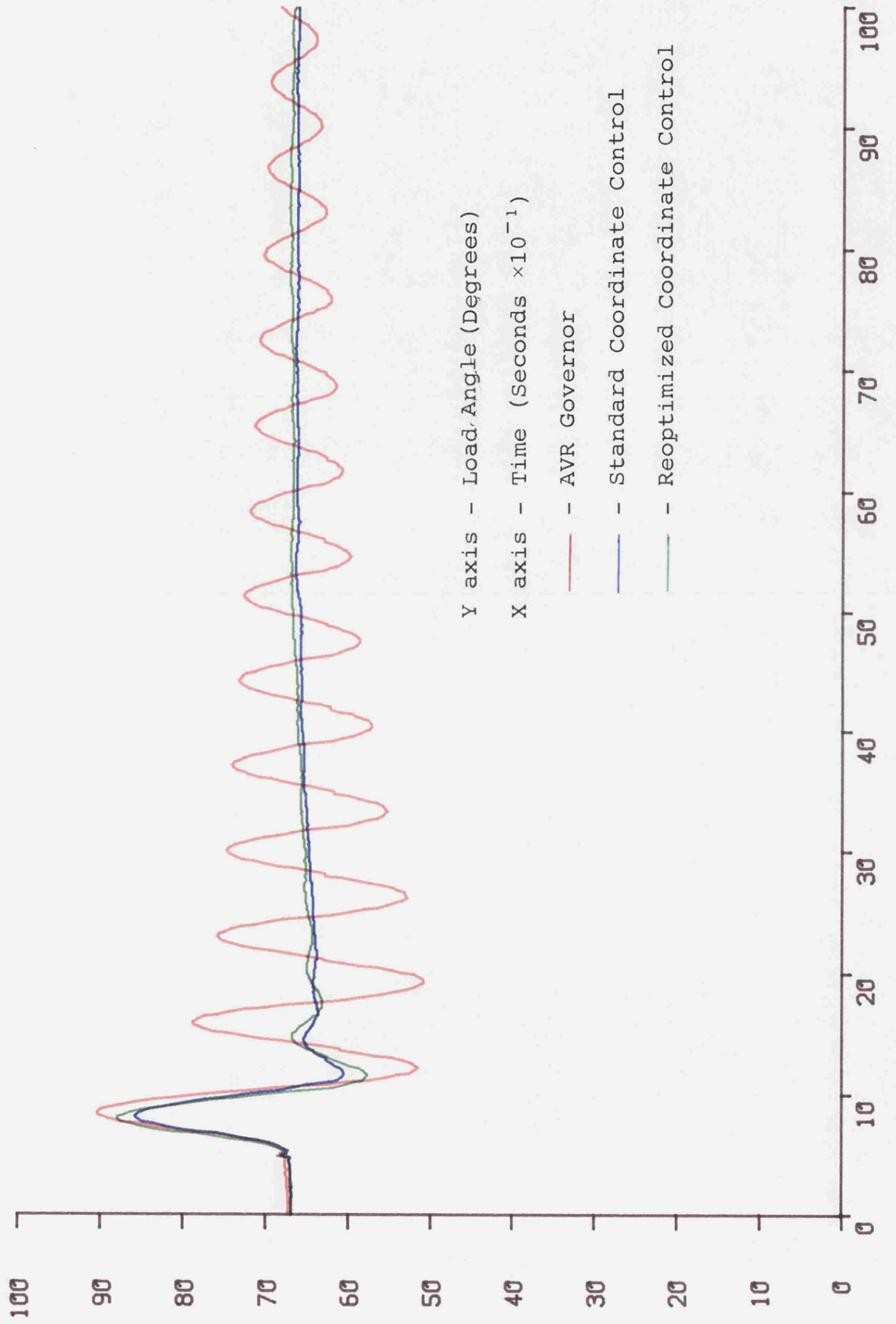

Fig. 7.5(a) Machine No.1 220ms Fault (Slow Governor)
Load Angle

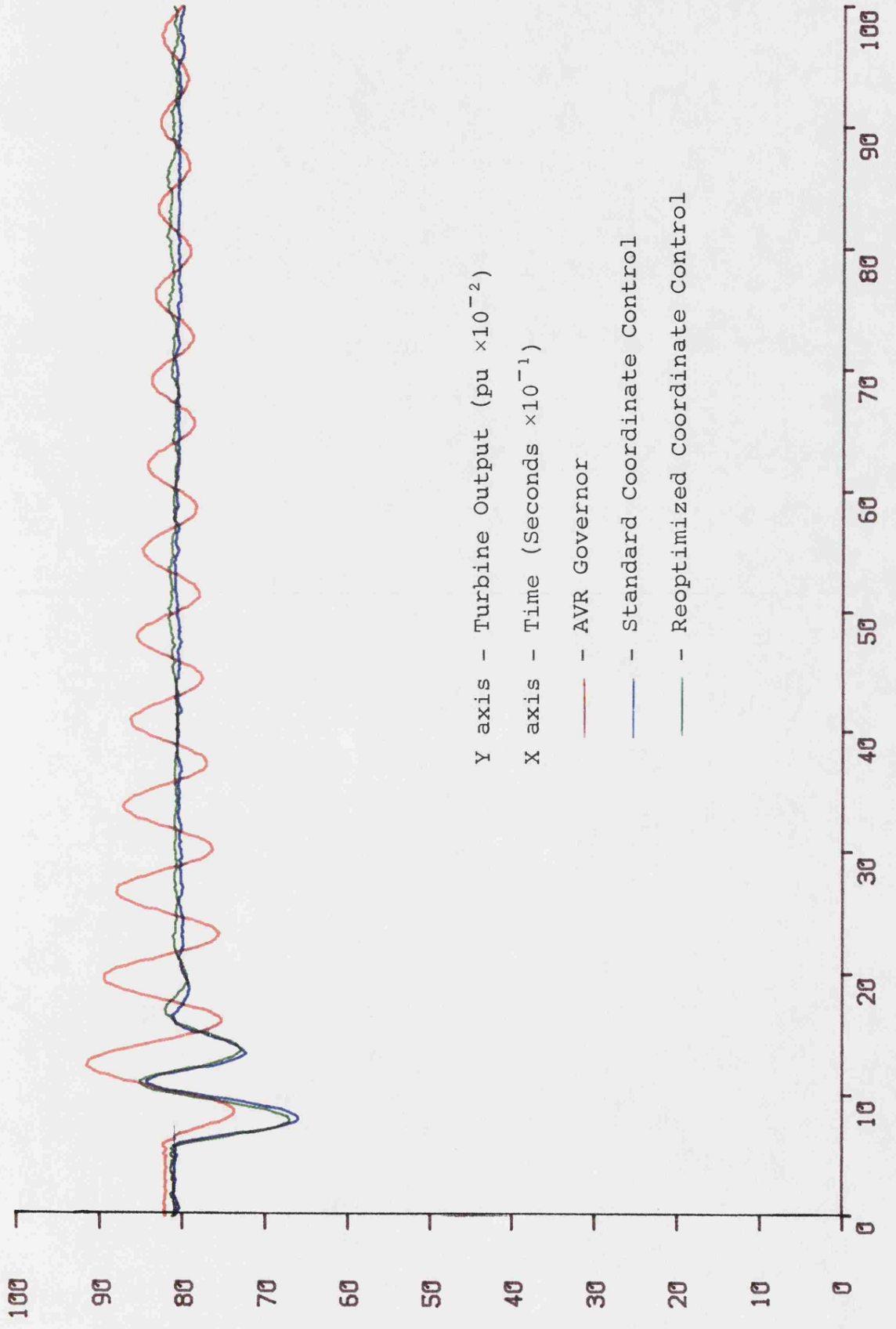

Fig. 7.5(b) Machine No.1 220ms Fault (Slow Governor)
Turbine Output

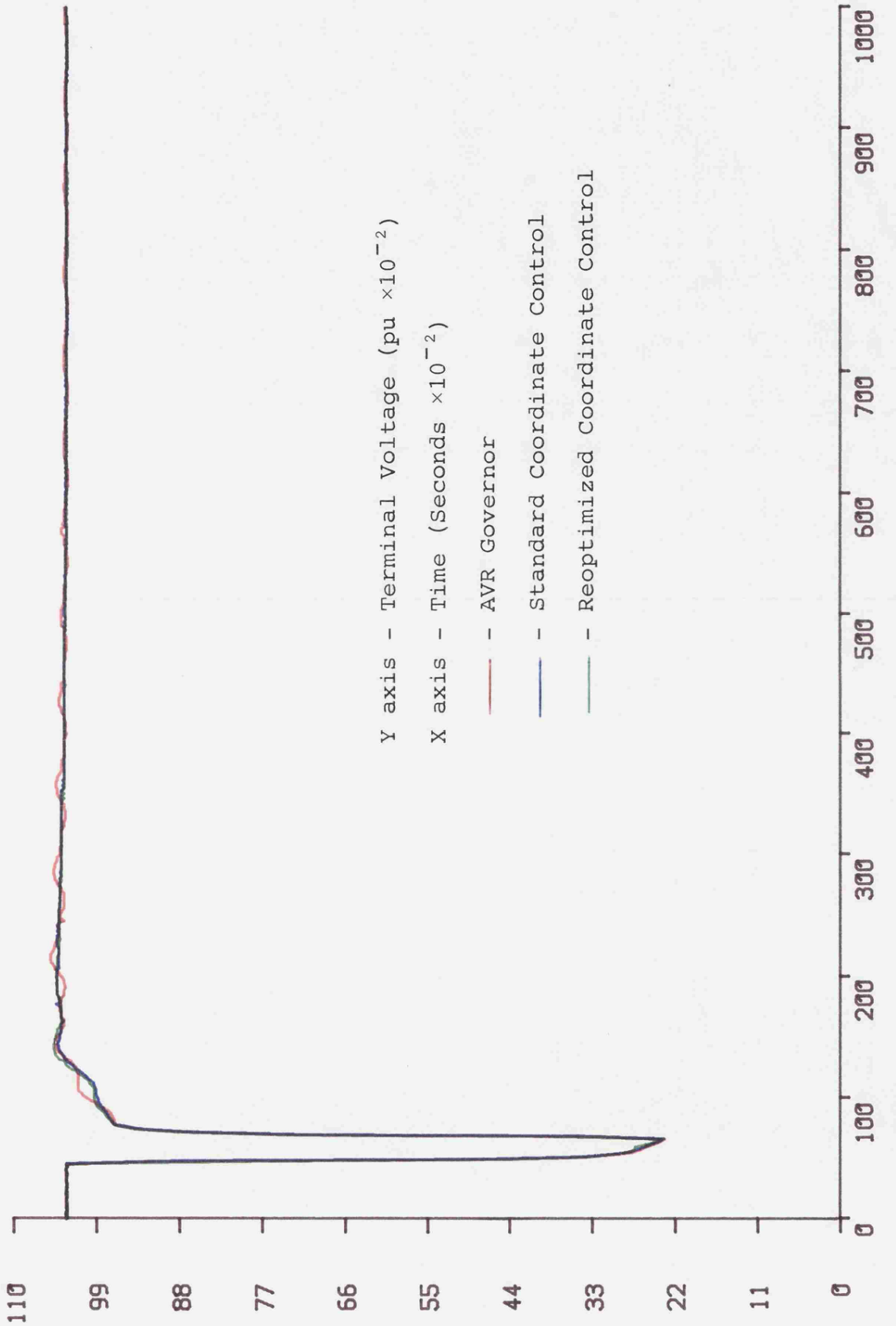

Fig. 7.5 Machine No.1 220ms Fault (Slow Governor)
(c) Terminal Voltage

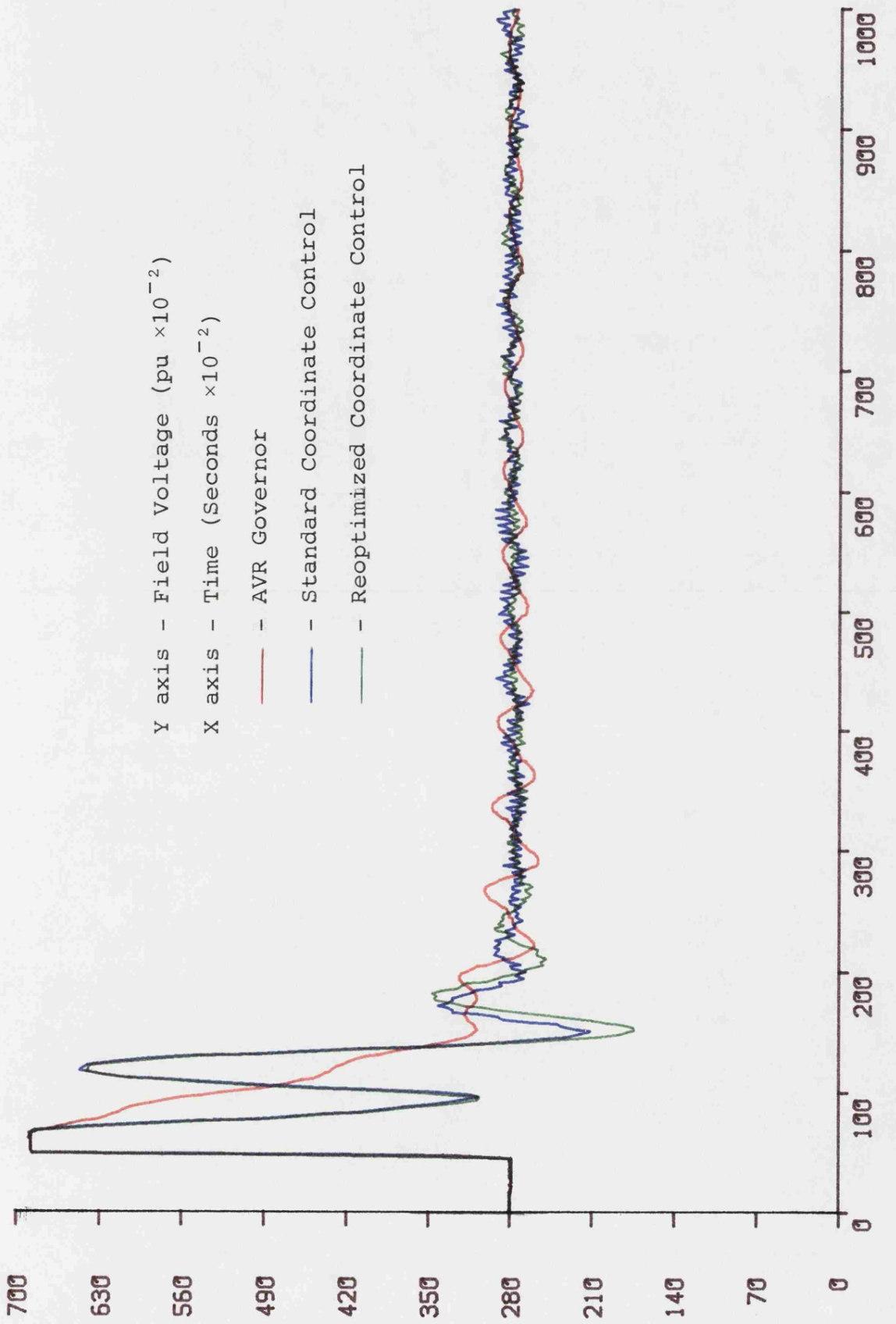

Fig. 7.5(d) Machine No.1 220ms Fault (Slow Governor)
Field Voltage

in the main exciter field voltage response curve of Fig. 7.5 (d). The terminal voltage responses for the co-ordinate controls are practically identical. It can be concluded that, despite halving the valve velocity rates, the original co-ordinate control, as well as the reoptimized control, have improved the system response compared with the conventional controller.

CHAPTER 8 MULTI-MACHINE THEORETICAL STUDY

8.1 Introduction

This study investigates, for a two machine, infinite bus system, the use of additional feedback signals for the purpose of transient response improvement. In the literature, for the control of multi-machine systems a common approach is to use the inverse Nyquist technique[27,49]. Optimal control theory has also been applied[60]. Excitation system interaction has also been studied using small perturbations and eigen value analysis[61]. All these approaches depend on a linearized system model. The general consensus is that, if one machine in a multi-machine system is fitted with controllers designed for a single machine, infinite bus system, the resulting response of the overall system may not be improved due to dynamic interaction between machines. To obtain the best response for the overall system, and reduced interaction between machines, each machine should be controlled by a multi-variable controller using signals derived from the dynamics of all the other machines in the system. This type of control, although theoretically possible, does suffer from the same problems experienced in optimal control of a single machine. That is, it may not be convenient or even possible to provide all the required information. Even if all the plant considered is on the same site, it is unlikely that such a control system could be implemented. Rather, a control strategy employing only measurable signals local to the controlled machine would be used.

The design requirement is to obtain a control strategy which will improve the overall system response rather than provide spectacular improvement in one machine at the expense of others. Naturally the physical limitations of the plant must be taken into account when the control system is designed.

8.2 The Multi-machine System

To afford comparison of the theoretical work with experimental studies, the scope of the study is confined to systems that are not only of practical interest, but also capable of physical implementation on the micromachine system. Such a system comprises two machines of identical inertia and similar electrical parameters, but have different governor-turbine systems. This may be practically thought of as a new plant with a modern fast acting governor-turbine, built in close proximity to an older power station of similar electrical output, but employing slower governing gear. Alternatively the arrangement could be considered as refitting a unit within an existing power station site with faster steam flow control. In view of the relative ease of upgrading an automatic voltage regulator system (subject to ceiling voltage limitation), it is not unreasonable to assume that the AVR characteristics would be the same for both machines. The resulting system is shown in simplified form in Fig. 8.1 where each machine takes the form detailed in Fig. 6.1 for a single machine. The disturbance applied to the system is a symmetrical 3-phase fault of 140ms duration, applied at the common bus linking the high voltage side of the generator transformers. The pre- and post-fault impedances are equal.

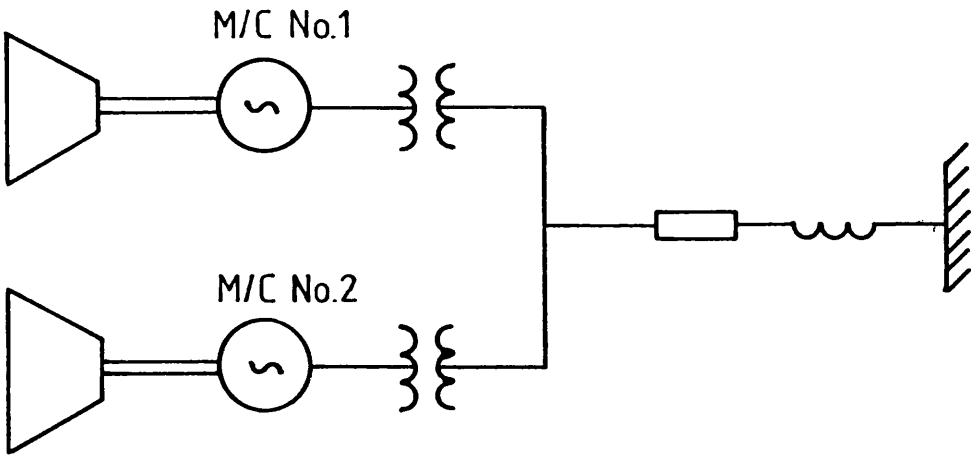

Fig. 8.1 Multi-Machine System Configuration

The generator models used are those developed in Chapter 2. Each generator is represented by a fifth order model. The AVR and governor-turbine representations are the second order models developed in Chapter 2, and used in Chapter 6, for the single machine co-ordinate control study. The fast governor-turbine uses the same parameters as in the single machine study and the slow governor-turbine has an identical form but with arbitrarily slower parameters :- t_a= 0.2s t_b= 0.5s and valve limits V_p= 0.935pu, V_c= 2.0pu per second and V_o= 1.0pu per second.

There are four possible inputs on the system where additional controls may be applied, corresponding to the T_i and V_i inputs of Fig. 6.1 for each machine. The V_i input is before the main exciter gain and as such is subject to its dynamics and is representative of a real system. The additional feedback

control is limited to rotor acceleration and may be applied at either, neither, or both control inputs of each machine.

No attempt has been made to provide signals corresponding to the rotor acceleration of one machine as a control input to the other machine. There are two reasons for this. Primarily, it may not be practical to implement such a scheme and also, eliminating the additional degrees of freedom reduces the computational burden significantly.

8.3 Two Machine Optimization

The two machine optimization program is based on a multi-machine simulation package developed by Davis[62], employing a fourth order Runge Kutta integration technique. The initial conditions are obtained from a load flow calculation based on a NAG library Quasi-Newton minimization routine rather than the more common Newton-Raphson approach[63]. The optimization program uses a NAG library routine based on the simplex method for function minimization[64]. The minimization routine requires only function values at each point and was chosen primarily for its ease of application rather than computational efficiency.

In general, a performance index surface has a number of local minima and, the one reached by a minimization algorithm depends on the starting point and acceptance criteria supplied to the routine. It is therefore necessary to perform a series of optimization runs starting at different estimates of the

minimum location. Once a set of minima are available, corresponding time responses are obtained which are then subjectively analysed. It may well be, that the time response for the smallest PI value of a set of local minima is not the best response from the engineering point of view. Also, the objective function may not be weighting certain aspects of the system performance sufficiently to arrive at the desired response. The design process thus becomes an iterative procedure, in which the objective function is modified until it provides an acceptable measure of the desired response. The initial multi-machine optimization used an objective function derived directly from the single machine studies as below

$$I = \int_0^t (\Delta V_{t1}^2 + \Delta V_{t2}^2) A1 + (1+A2\,t)(\Delta\delta_1^2 + \Delta\delta_2^2)\ dt \quad 8.1$$

When A1 and A2 were of equal and small magnitude, there was a tendency to improve the load angle response of the machine fitted with the fast governor, at the expense of a deterioration in load angle response of the machine with slower steam control. With equal weighting, for load angle deviation on both machines, a minimum could be found, such that the improvement in response of the fast machine was sufficient to compensate for the adverse effect on the slow machine. To avoid this problem, a greater weighting would be necessary on the load angle deviation of the machine with slower steam flow control. A new formulation for the objective function equation 8.2 was used in which machine No.2, is assumed to have the slower steam flow control.

$$I = \int_{o}^{T} (\Delta V_{t1}^{2} + \Delta V_{t2}^{2}) A1 + (1 + A2t) \Delta\delta_{1}^{2} +$$

$$\max \left[(1 + A2t) \Delta\delta_{2}^{2}; A3\Delta\delta_{2}^{2} \right] dt \qquad 8.2$$

This formulation allows for increasing the influence of the slow machine load angle in the early stages by raising the value A3. After the point at which (1 + A2t) is equal to A3 the load angle weighting becomes the same for both machines. With the objective function equation 8.2, it is possible to obtain minima which provide satisfactory load angle responses for both machines.

8.4 Optimization Results

When applying the final form of the objective function, equation 8.2, it is possible to obtain different values of feedback gains, depending on the precise choice of constants A1, A2 and A3. However, for all values of A1, A2 and A3, that produced acceptable time responses, the feedback gains would always fall in similar regions which depend on starting point provided to the optimization routine. If the optimization is started with an estimate of zero for all feedback gains to produce the minimum value of PI, then a low gain set is obtained. When the initial estimate is set at 0.1 say, for each feedback parameter, then the corresponding local minimum obtained is in that region and is referred to as a high gain

set. With limited time and resources, it is not possible to check all starting points for multiple local minima. However in the optimization runs performed, with all reasonable objective function formulations and starting points, the same regions of gains were found.

From the numerous optimization runs performed only a set of representative results will be presented. Table 8.1 summarizes the four feedback strategies considered, which range from single variable additional feedback into the governor of the machine fitted with fast steam flow control, to co-ordinate control of excitation and governing for the fast machine, and then co-ordinate control of the fast machine together with additional feedback into the AVR of the machine fitted with slower acting steam flow control. Since the formulation of the objective function was not always the same, the actual values for each performance index, are not quoted.

For clarity of presentation, the response curves will be colour coded. Curves for machine No.1, fitted with a fast AVR and slow governor-turbine system will be in blue for the base condition of M0, corresponding to no additional feedback, and green when additional controls are implemented on either machine. Curves for machine No.2, fitted with a fast AVR and fast governor-turbine are black for no additional controls (M0) and red when additional controls are applied.

Response curves for the base case (M0), where no additional controls are applied are given in Fig. 8.2. As would be

Acceleration Feedback Gains					
Control Number	Machine No. 1.		Machine No. 2.		Comment
	AVR	GOV	AVR	GOV	
M0	0.0	0.0	0.0	0.0	Base Case
M1	0.0	0.0	0.125	0.019	
M2	0.0	0.0	0.0	0.019	
M3	0.007	0.0	0.0039	0.0135	Low Gain Set
M4	0.168	0.0	0.053	0.148	High Gain Set

Table 8.1 Multi-machine Acceleration Feedback Gains

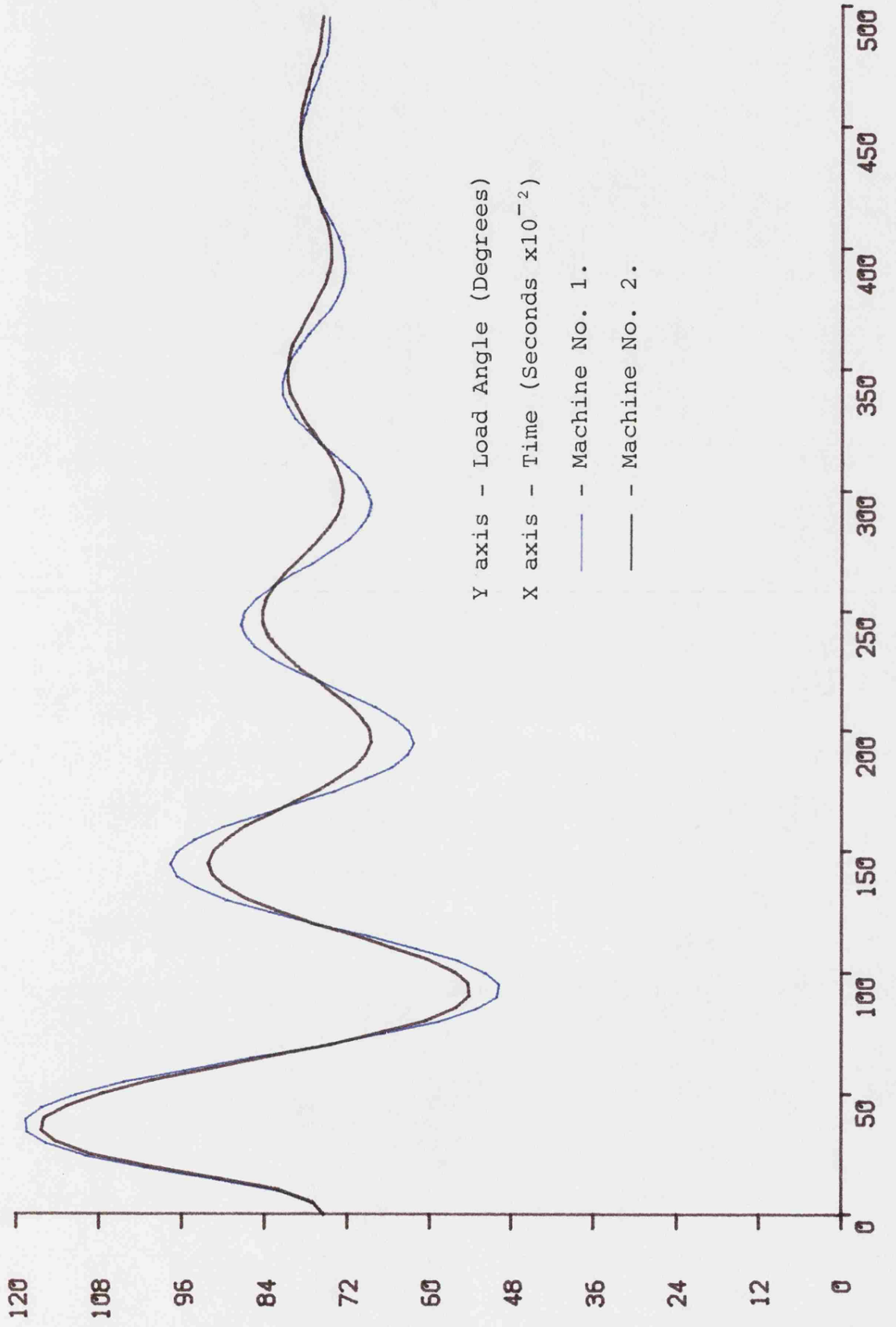

Fig. 8.2(a) Control M0 (Base Case) Load Angle

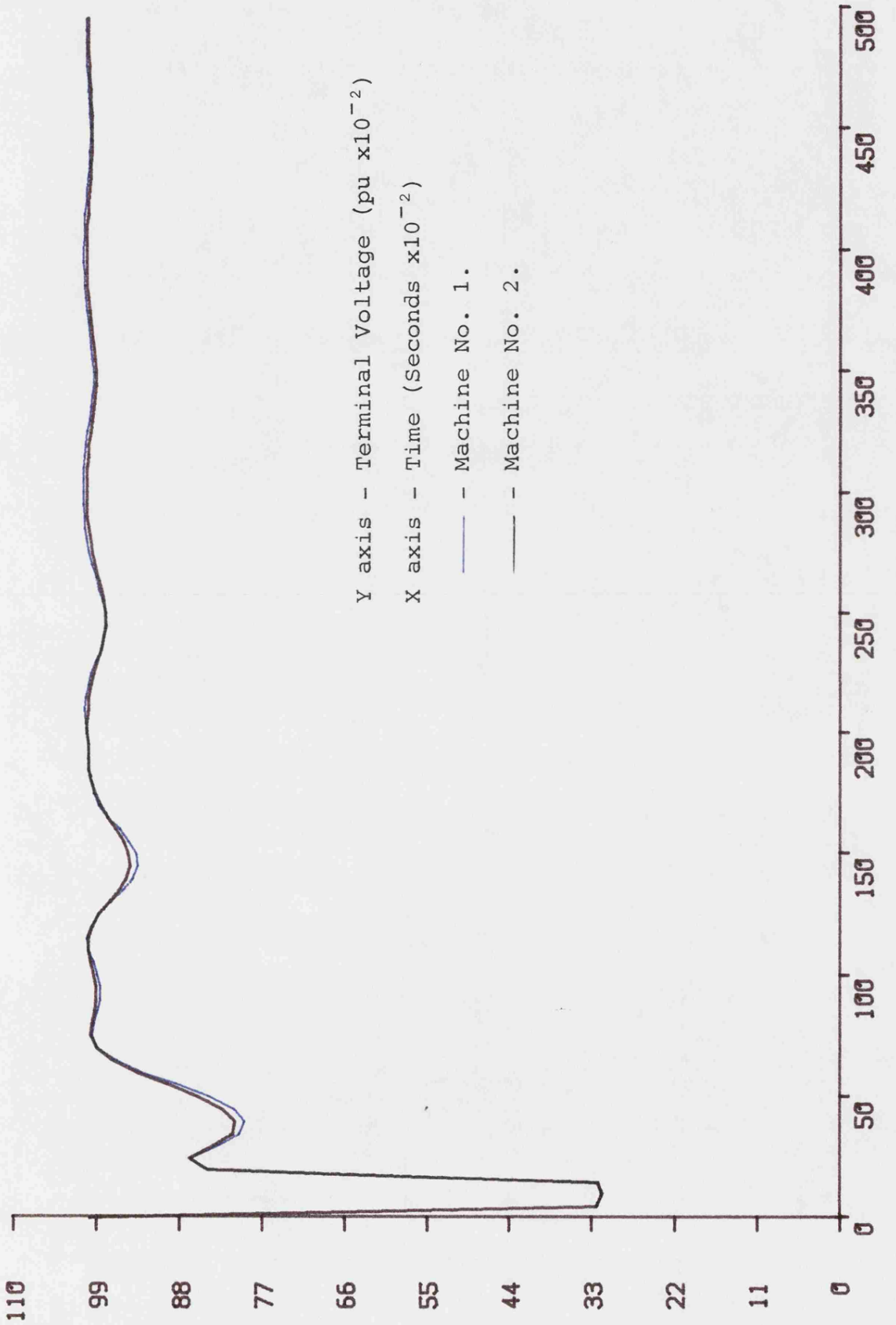

Fig. 8.2(b) Control M0 (Base Case) Terminal Voltage

expected, the load angle response Fig. 8.2(a) shows a lower first peak and smaller subsequent oscillations for the machine fitted with the fast governor-turbine. From the second swing onward, the fast governed machine appears to have a slightly longer period of oscillation, but the machines tend to swing together as they pull back into steady state operation. The terminal voltage responses given in Fig. 8.2(b) are similar, with the fast governed machine tending to have a slightly better response. The only points where significant differences can be seen between the machines, coincide with local maxima of the corresponding load angle curves. The curves of Fig. 8.2 will be used as a datum for comparison with responses obtained when additional controls are applied. For convenience the base case curves will be included in the plots for all subsequent controls. The control law M1 applies co-ordinate control to both control inputs of machine No.2, which is fitted with fast steam flow control as well as a fast acting AVR. In this case, machine No.1, which has a slow governor-turbine and fast AVR, is left with conventional control. The first swing in load angle for machine No.2, given in Fig.8.3(c) is significantly reduced and subsequent oscillations are very damped, following a fairly slow return from the first swing. The effect of applying control on machine No.2, is to also reduce the first swing in load angle for machine No.1, with attendent reductions in the amplitude of subsequent swings. The terminal voltage response curves of Fig. 8.3(b) show the effect of acceleration feedback into the AVR of machine No.2. In the early stages of the recovery after the fault is removed, the response of the controlled machine is more

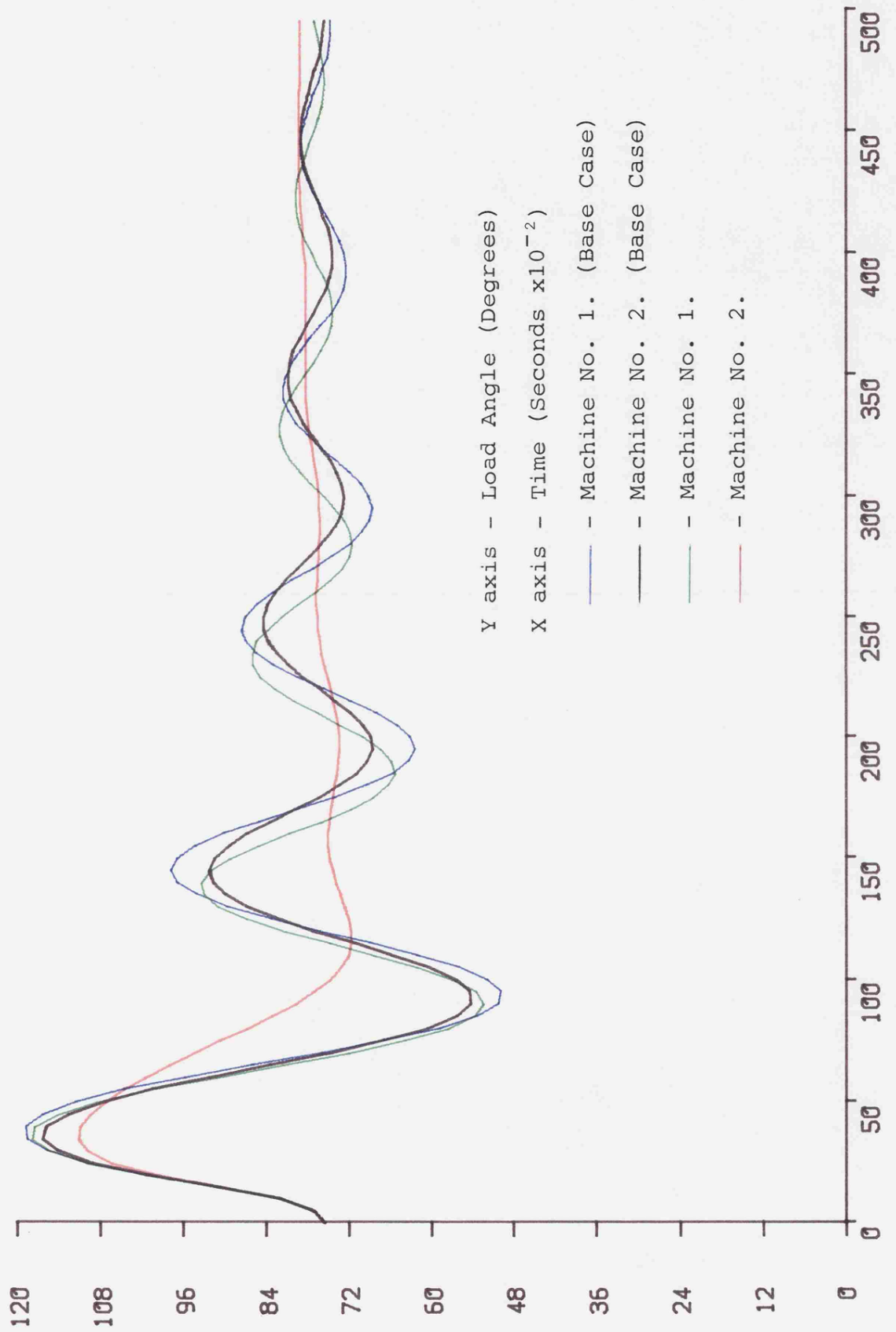

Fig. 8.3(a) Control M1 Load Angle

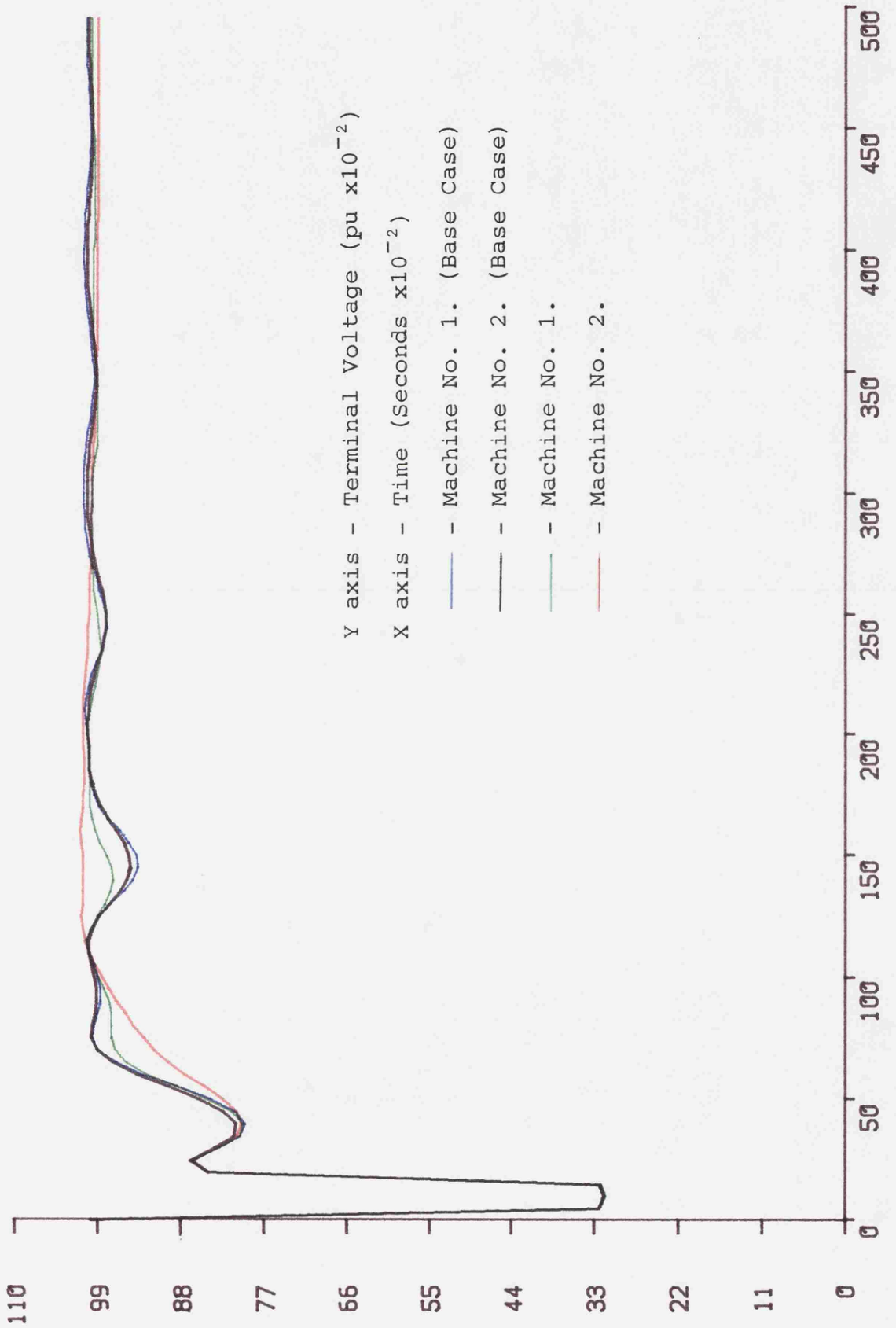

Fig. 8.3(b) Control M1 Terminal Voltage

sluggish than the base case, but once the normal operating level is attained there are no longer the dips previously associated with the maxima of the uncontrolled load angle response. Machine No.1, has a similar trend in that initial recovery is slowed down, but subsequently the depressions are less severe. The latter stages of the load angle and terminal voltage responses for the controlled machine indicate a low amplitude, very low frequency, oscillation as the set returns to steady state conditions. This phenomenon will be discussed in more detail later.

A set of responses for single variable feedback into only the governor of machine No.2, (Control M2), are given in Fig. 8.4. The feedback gain was arrived at using a standard performance index and a guided linear search technique. The load angle responses, Fig. 8.4(a) show that the additional control has been effective in reducing the first swing of the controlled machine, and has also reduced the amplitude of subsequent oscillations. Effects on the load angle response of the other machine are slight; subsequent damping is slightly improved and the first swing is only marginally effected. An interesting feature of this control is that both machines have an improved initial recovery in terminal voltage, but before steady state is reached both machines exhibit a marginal depression in terminal voltage. These effects being most noticable on the controlled machine. If the depression in terminal voltage were offset against the initial improvements in response attained with this control, the overall benefit to the system is small in terms of voltage recovery. However,

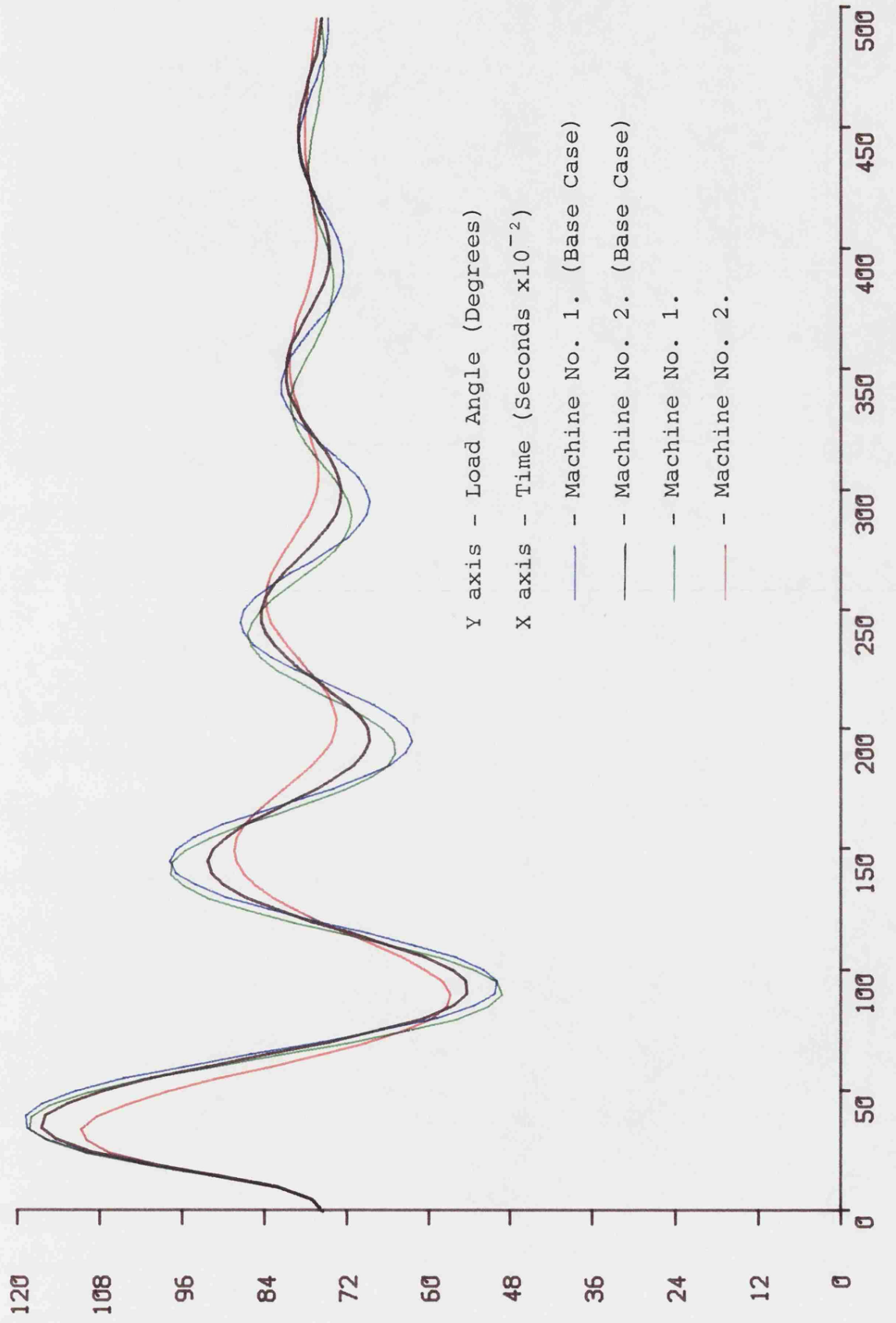

Fig. 8.4(a) Control M2 Load Angle

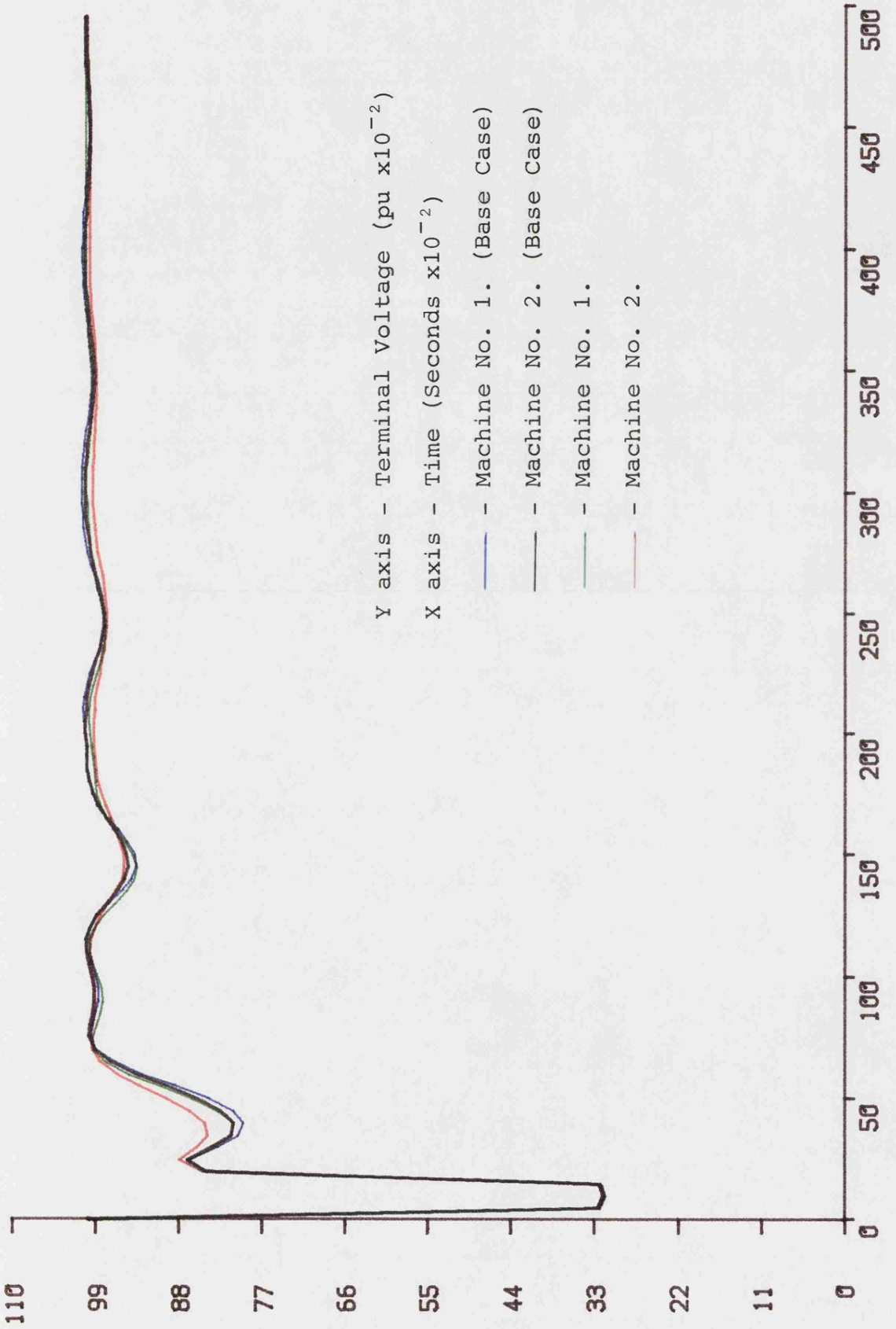

Fig. 8.4(b) Control M2 Terminal Voltage

the overall load angle responses are clearly improved.

The final pair of control strategies considered apply controls to all fast acting controllers on the system, that is, co-ordinate excitation and governing control of the fast governed machine (No.2) and also control into the fast acting AVR fitted to the machine with a slow governor-turbine representation (machine No.1). As stated previously in the optimization process, local minima were found that correspond to either high or low gains for the additional control signals. Responses for a low gain set are given in Fig. 8.5 and those for the high gain set are given in Fig. 8.6.

Taking the load angle responses Fig. 8.5(a) for the low gain control of M3, the control has reduced both the first swing and subsequent oscillations of machine No.2. The first peak of machine No.1, load angle is not effected but the whole of the subsequent oscillations are marginally reduced in amplitude and slightly elevated. The elevation is consistent with the depressed terminal voltage recovery in Fig. 8.5(b). Both machines exhibit an improvement in the early part of the terminal voltage recovery.

The responses for the high gain control M4, given in Fig. 8.6 clearly show both the advantages and possible disadvantages of this form of control in multi-machine systems. After the return from the first peak in load angle, both machines are heavily damped, both in terms of load angle and terminal voltage response. The effect of acceleration feedback is

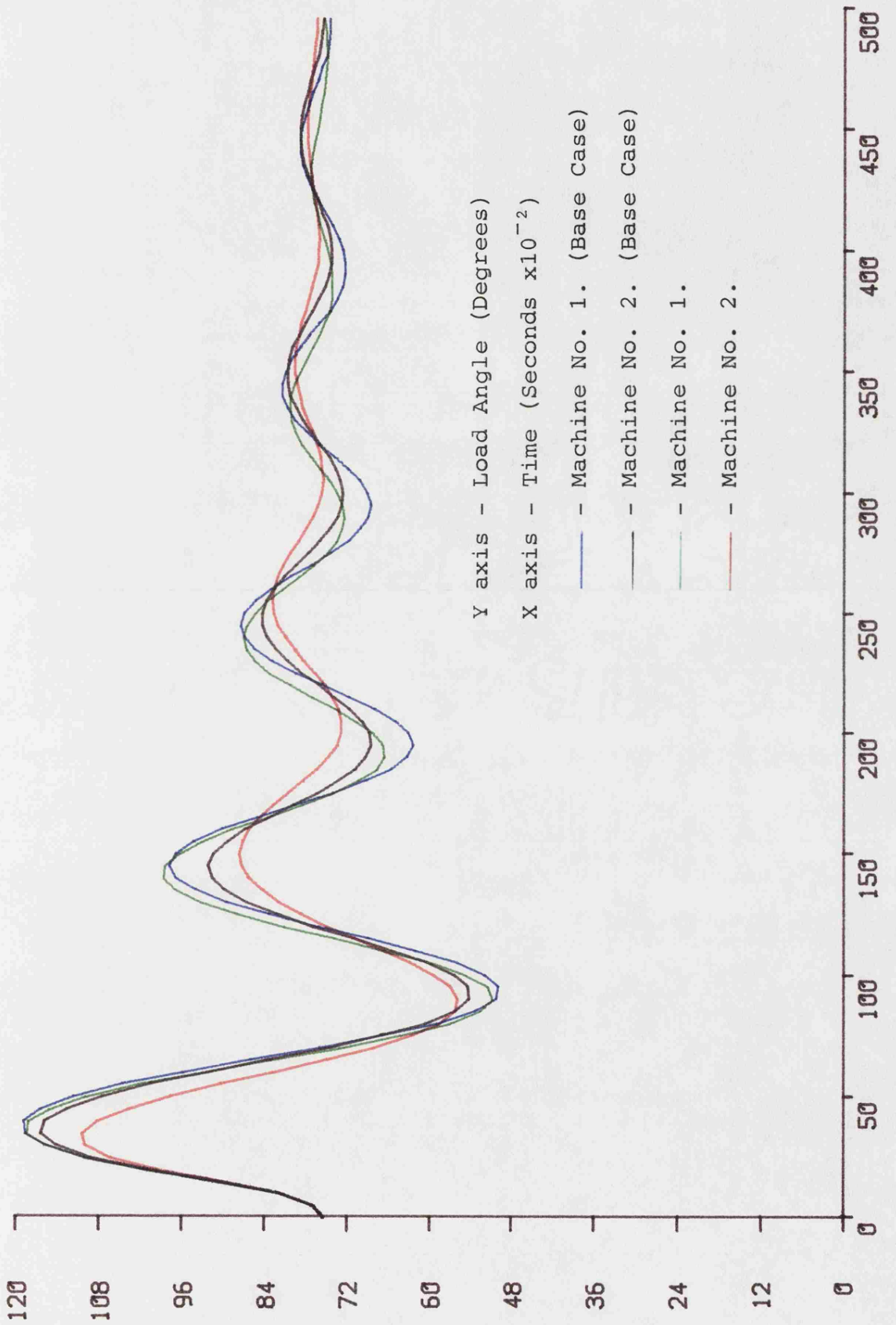

Fig. 8.5(a) Control M3 Load Angle

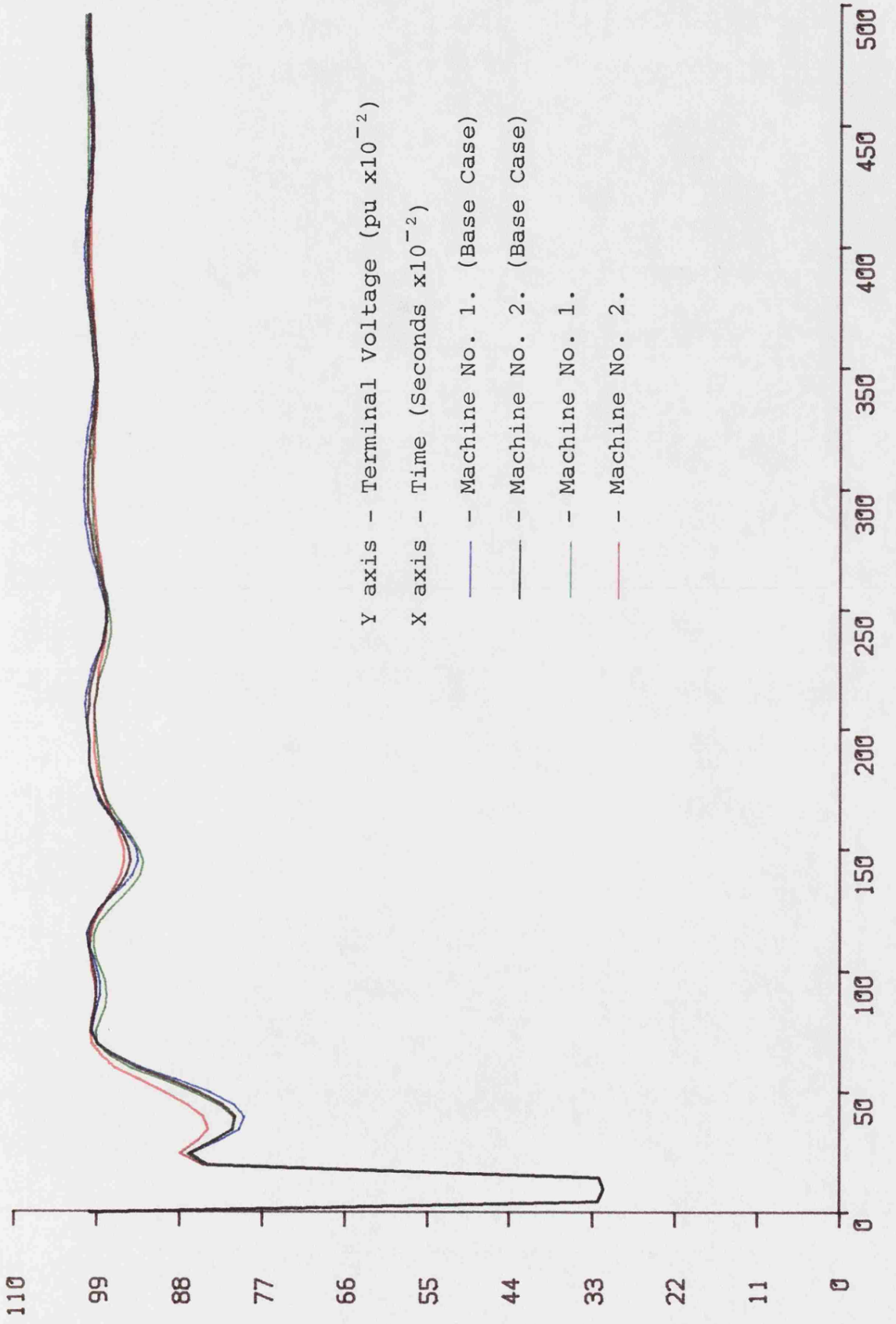

Fig. 8.5(b) Control M3 Terminal Voltage

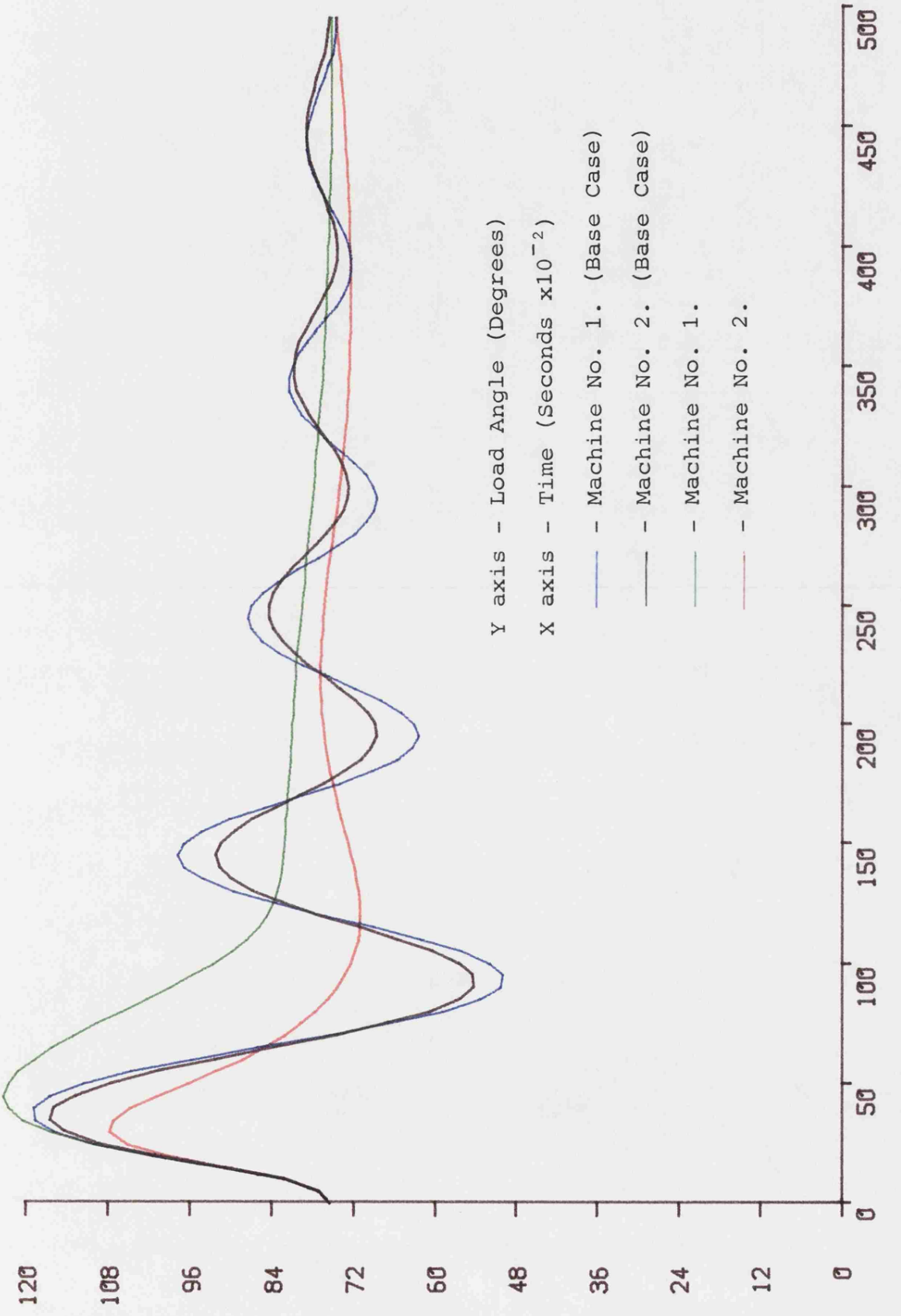

Fig. 8.6(a) Control M4 Load Angle

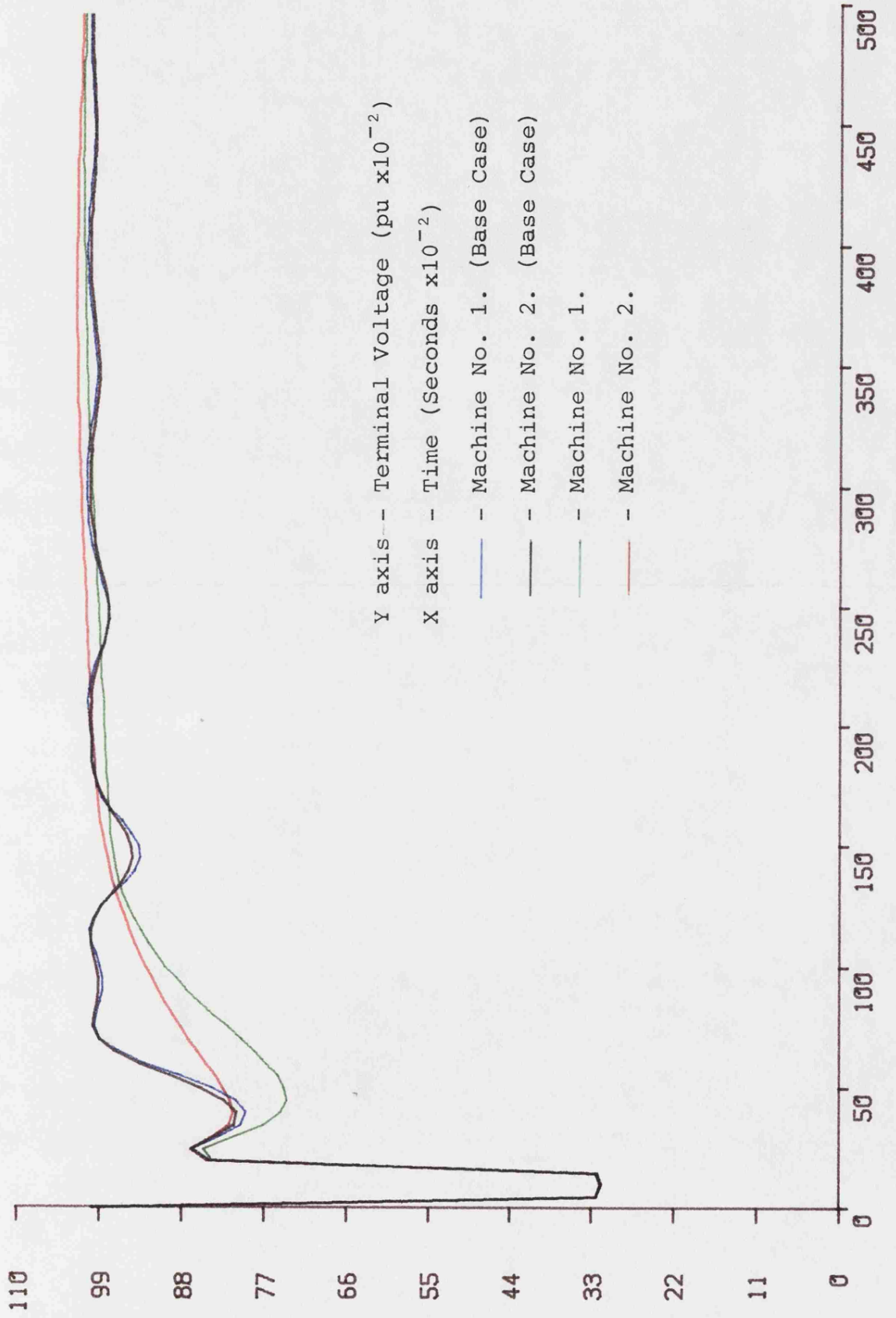

Fig. 8.6(b) Control M4 Terminal Voltage

clearly to cause an apparent increase in inertia for both machines. For machine No.2, the first swing load angle response is totally satisfactory, giving a much reduced peak value and fast return to the region of the normal operating point. However, the other machine suffers from an increase in first swing peak. This illustrates an important feature of a multi-machine system which is in contrast to the single machine infinite bus system often used in theoretical studies. In the single machine system the infinite bus, by definition, can deliver or absorb any level of power required as a result of a control scheme. It is a much different situation when two or more machines are interconnected. Controls applied to a machine with fast acting control gear can produce power flows which aggravate the position of plant less able to respond.

The high gain set has produced a good load angle response for the machine with co-ordinate control, at the expense of a sluggish terminal voltage response. The responses of the other machine are less desirable. Feedback of acceleration into the AVR with a high gain, combined with the interaction with the other machine has caused an initially higher peak in load angle. The high gain of the feedback into the AVR causes a very sluggish return to steady state of terminal voltage, with a correspondingly sluggish return of load angle. This tendency to maintain a fixed load angle is very desirable when starting from the normal operating point, but is not quite so useful when the effective starting point is much elevated, as in this case.

The slowly changing responses when nearing steady state, associated with high feedback gains for control M1 and M4 do not permit confirmation that a stable return to steady state is obtained when the simulation is performed over only 5s. Representative simulation runs over extended periods, indicate, that the systems do in fact settle.

The theoretical results obtained have shown that it is possible to improve the overall system response by feedback of the single variable, acceleration. It has also been shown that where as the effect of this variable is desirable in stabilizing the system, it may not be prudent to feedback this state with a fixed, high gain at all times. It is anticipated that the use of control schemes with variable gains could well improve on the overall system responses and as such should be investigated in further studies.

CHAPTER 9 MULTI-MACHINE STUDY EXPERIMENTAL RESULTS.

9.1 Introduction

There are several factors which limit the number of laboratory size micromachine systems available for use. The first of these is the combined contributions of the space occupied by such a system and the high capital cost of such an installation. A second and more academic reason is the fact that many real systems can be modelled in terms of a two machine system, with the main part of the system modelled by one machine and the appropriate equivalent transmission network with the second machine modelling that part of the system close to the disturbance whose effect is under investigation. It should also be remembered that although the micro-alternators themselves will have, within design limits, approximately the same per unit parameters, the complete system does involve the use of a time constant regulator, turbine governor, and AVR simulation, various system transducers and transformer modelling. There are, therefore, several degrees of freedom introduced when a micromachine laboratory model is built and the differences in each of these component systems can add up to make even the two turbine, generator, transformer models of the most simple multi-machine laboratory system somewhat different.

These factors, together with the inherent difficulty in accurately measuring the parameters of a micro-alternator, lead to the conclusion that the two component micromachine systems are not likely to have the same parameters. This

result has been confirmed for the laboratory system at the University of Bath by performing theoretically equivalent single machine tests on each of the two micromachines available. Machine 1 has been shown to exhibit transient response characteristics, which indicate that the combined alternator, transformer impedance is higher than that of Machine 2.

However, it has often been suggested in the past[18] that micro-machine studies should only be used to confirm the trends in improvement of performance predicted by theoretical studies. An absolute comparison of theoretical and experimental results is not valid under the constraint of the uncertainty of the knowledge of the micromachine parameters used in the theoretical studies. This approach has been used in the experimental investigation of the multi-machine study.

9.2 System Configuration

Both micromachine systems have been constructed to the same power system specification. The second installation was completed some time after the first and there is some difference in the rotor construction of the two micro-alternators. Each micromachine has a linear power transistor time constant regulator circuit, with a power transistor chopper controlling the armature current of the d.c. motor. Turbine, governor modelling is incorporated in the previously described TMS 9900 microprocessor system. The acceleration transducers used are somewhat different with the second device being of a more easily manufactured design than the first. The two transmission

networks were designed to be identical but, because of the configuration used, the impedance to the fault at the high voltage terminals of the generator transformer of the two micromachine systems is somewhat different.

The experimental configuration used in this study is described by Fig. 9.1 and corresponds to a two machine power system model with somewhat different machine parameters. It allows for the introduction of different AVR characteristics, different turbine parameters and, of most significance, different governor characteristics. It allows feedback of rotor acceleration as a control input to both the governing and excitation systems of both micromachines. One machine, No.1, is fitted with the standard fast AVR system described in section 2.3.3 and incorporates a slow governing system of the form described in Fig. 2.6 with the valve position limits at 0 and 0.935pu, the valve opening rate limit is set at 1.0pu per second and the closing rate limit is 2.0pu per second. The other machine No.2, also uses the standard fast AVR but uses a fast governing system, the form of the model is again given in Fig. 2.6 but the parameter values now reflect the faster system. The valve position limits are again set at 0 and 0.935pu but the opening rate is now 4.0pu per second and the closing rate is now 6.6pu per second.

Data acquisition from the two machines is performed by the TMS 9900 microprocessor systems, from the standard transducers previously described. Each machine set being supervised by software running under the RSX11M multi-user operating system

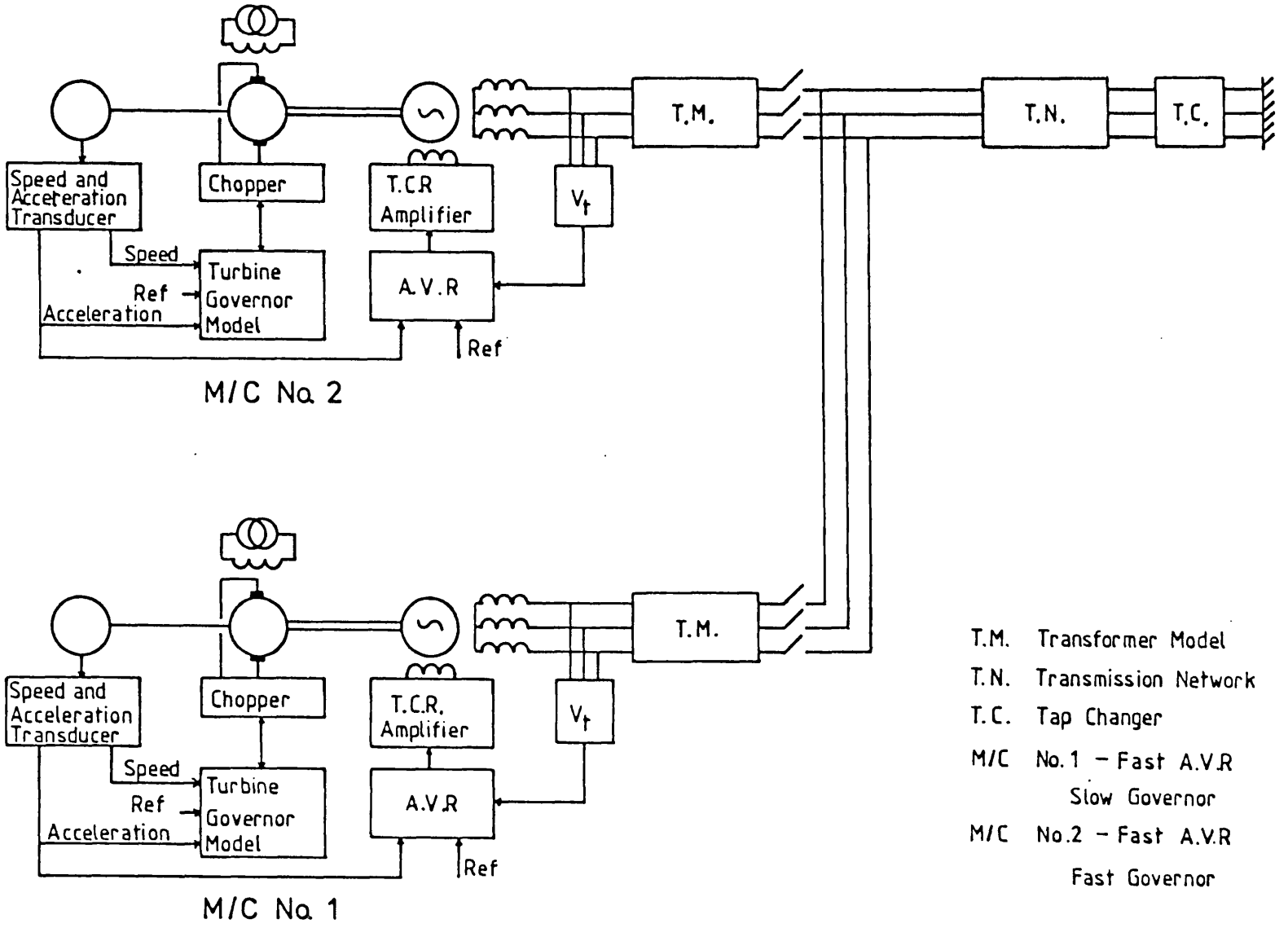

Fig. 9.1 The Experimental System Configuration

in the PDP 11/34 minicomputer.

9.3 Experimental Results

In order to clarify the presentation of results for the two machine system, which involves a comparison of the responses obtained with and without extra acceleration feedback into either or both of the governing and excitation systems of the two machines, the transient response curves for rotor angle and terminal voltage have been plotted in four different colours. Those for machine No.1, without extra feedback are plotted in blue, those with extra feedback are plotted in green. The corresponding curves for machine no.2, without extra feedback are plotted in black and those with extra feedback are plotted in red.

Each experimental investigation was performed for a symmetrical 3-phase short circuit at the commoned high voltage terminals of the generator transformers in Fig. 9.1. The fault duration was 140ms in all cases with the pre- and post-fault impedances equal. Both machines were operating at full load, with unity powerfactor at the infinite busbar. If the two micromachine sets had been identical, this would have resulted in a terminal voltage of 1.0pu on a combined system basis for both machines and the same operating load angle. The parameter differences between the two machines did not allow this condition to be achieved and, because of the location of the tap-changing transformer at the busbar of the model power system, it was decided to set the operating load angles to be equal. This resulted in

the initial terminal voltages of the two machines being unequal.

Table 9.1 summarizes the range of experimental results described in this section. Control M0 is the base case with no extra feedback of rotor acceleration to either machine. The use of rotor acceleration feedback into the governing system is associated with a fast governing system and, since machine No.1, is fitted with a conventional slow governor Table 9.1 shows that rotor acceleration feedback is never applied to the governor of machine No.1.

Acceleration Feedback Gains				
Control Number	Machine No. 1.		Machine No. 2.	
	AVR	GOV	AVR	GOV
M0	0.0	0.0	0.0	0.0
M1	0.0	0.0	0.125	0.019
M2	0.0	0.0	0.0	0.0128
M3	0.007	0.0	0.0039	0.0135
M4	0.168	0.0	0.053	0.148

Table 9.1 Multi-machine Acceleration Feedback Gains

Control M1 is the result of an optimization study with feedback into both governing and excitation systems of machine No.2. Control M2 corresponds to extra feedback into only the governing system of machine No.2. Controls M3 and M4 incorporate extra feedback into both machines and illustrate the different values of feedback constant associated with

two searches in different parameter spaces of the optimization studies, corresponding to a high and a low set of feedback gains. Fig. 9.2 shows the terminal voltage and load angle responses of both machines without extra feedback (Control M0) and represents the base case which all other experimental results will use as a reference point. A comparison of these results with the corresponding theoretical results of Chapter 8 (Fig. 8.2) illustrates some of the problems associated with micromachine experimental studies. The experimental load angle responses follow the same trend in decay after the first peak as the theoretical results but the experimentally obtained peaks in first swing are in direct contradiction to the theoretical values. Both experimental curves show that the first peak is lower than that predicted and that the first peak for machine No.1, fitted with a slow governor is lower than that for machine No.2, fitted with a fast governor. These apparent contradictions can be partially accounted for by the previously established fact that the resistance internal to the fault is higher on the real system than that assumed in the theoretical studies. The amount of energy available for acceleration during fault conditions is, therefore, less in practice than the theoretical value thereby reducing the peak in the first rotor swing. However, the presence of the fast governor on machine No.1, should reduce its peak rotor angle swing below that of machine No.1, fitted with a slow governor. This conclusion is not met in practice and a further investigation of this result is required. It has been established that, within the limits of experimental setting up accuracies, the governor and AVR models are

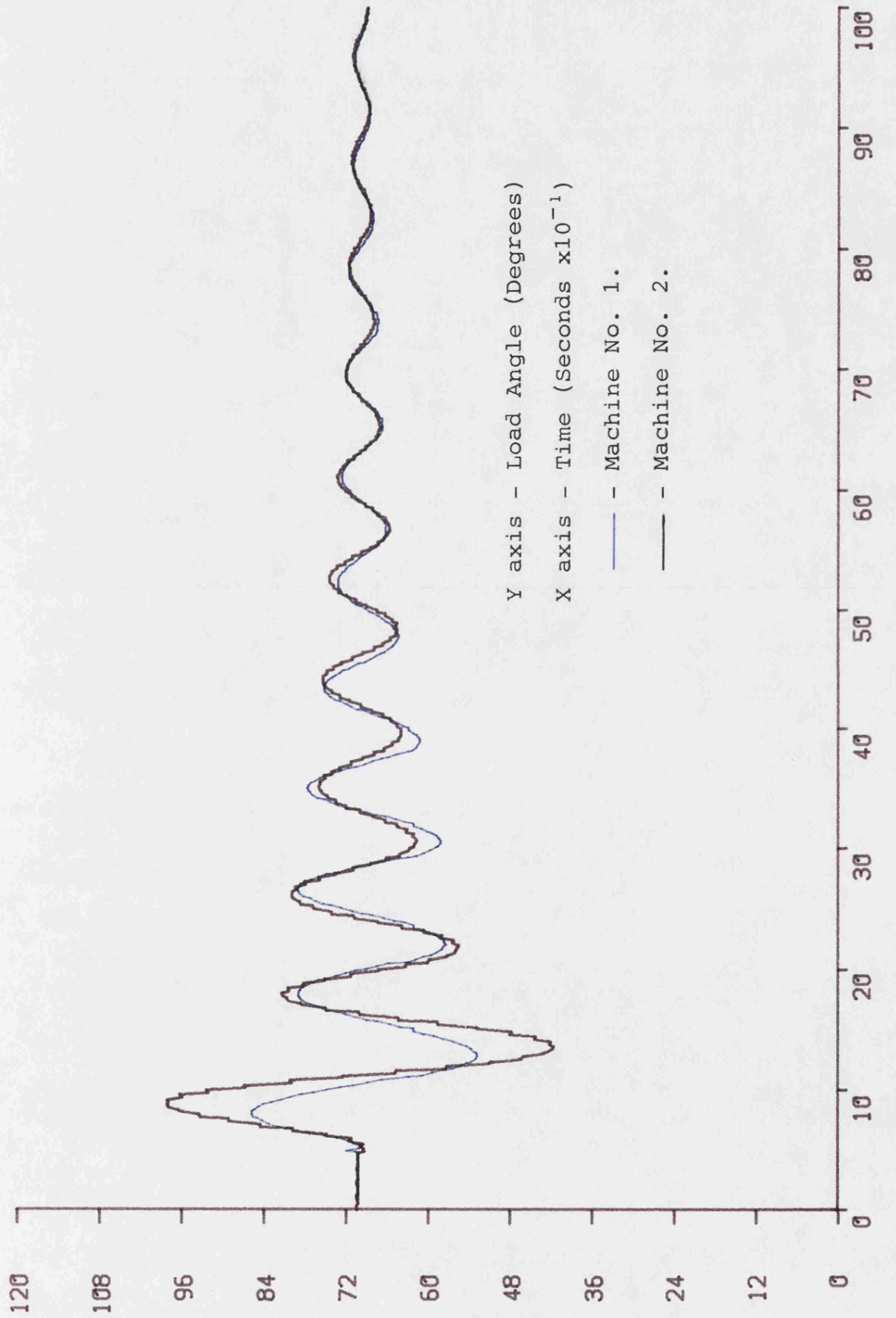

Fig. 9.2(a) Control M0 (Base Case) Load Angle

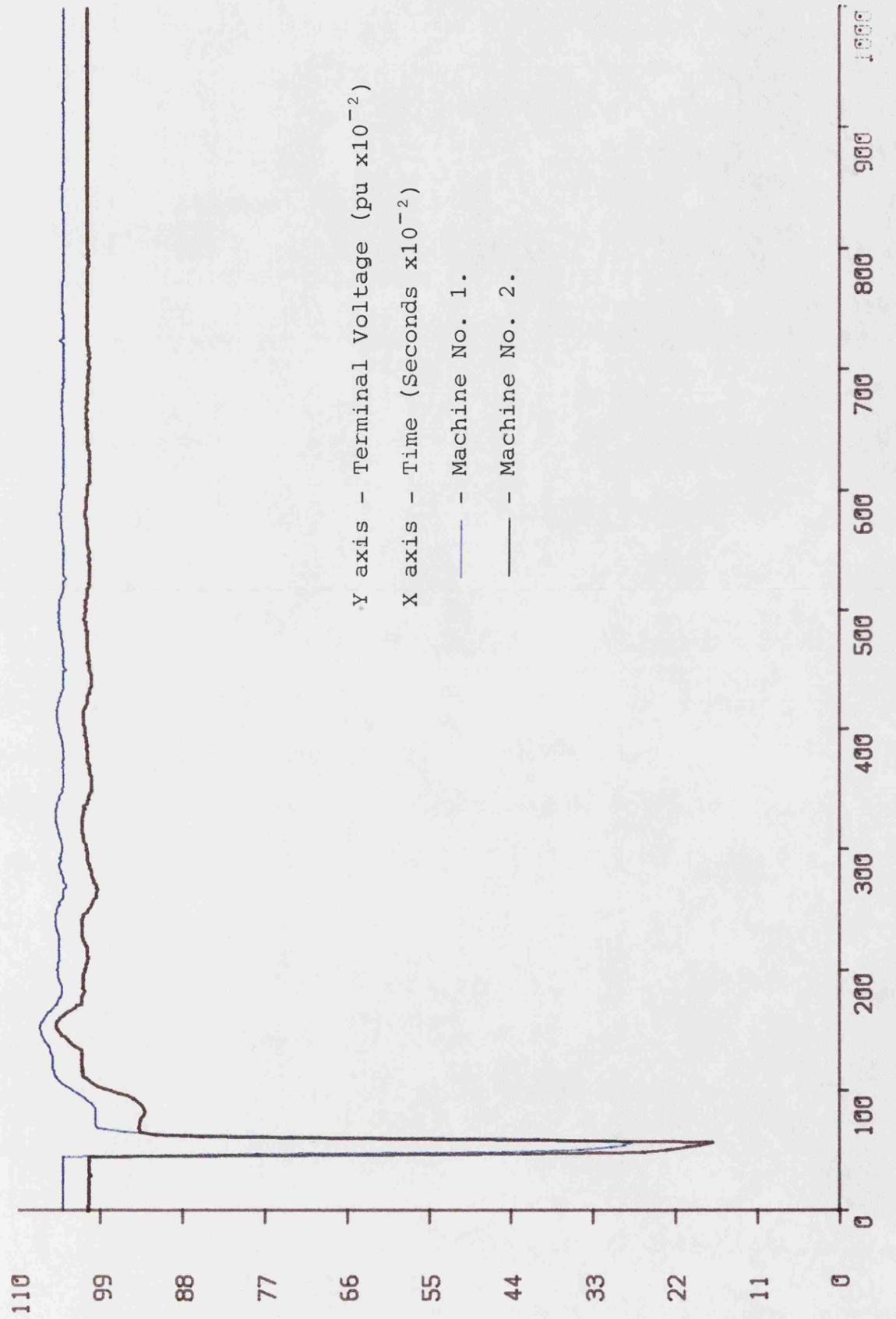

Fig. 9.2(b) Control M0 (Base Case) Terminal Voltage

satisfactory. When however, machines No.1 and No.2 were operated individually as single machine systems the results clearly showed the same significant difference in the first peak of the rotor angle response following the application of the standard fault. It can thus be stated that the individual machine transformer models forming the two machine system are not identical and that any experimental investigation of the results of optimizing the performance of a multi-machine system will only indicate trends in improving the system performance.

The first set of results corresponding to control M1 of Table 9.1, with extra feedback into both the governing and excitation systems of machine No.2 are given in Fig. 9.3. The transient load angle responses of Fig. 9.3 clearly show the significant improvement introduced into the response of machine No. 2, by extra feedback, both in terms of a reduction in first peak and an improvement in subsequent damping. The angle response of machine No.1, shows little change. The corresponding terminal voltage response curves of Fig. 9.3(b) show the expected difference in the initial values with a small improvement of the transient response of machine No.2, but little difference in that of machine No.1. The corresponding theoretical results obtained under the assumption that both micromachine systems are identical has been given previously in Fig. 8.3 and a comparison of these two sets of results confirm that the trends in improvement predicted in theory do exist in practice.

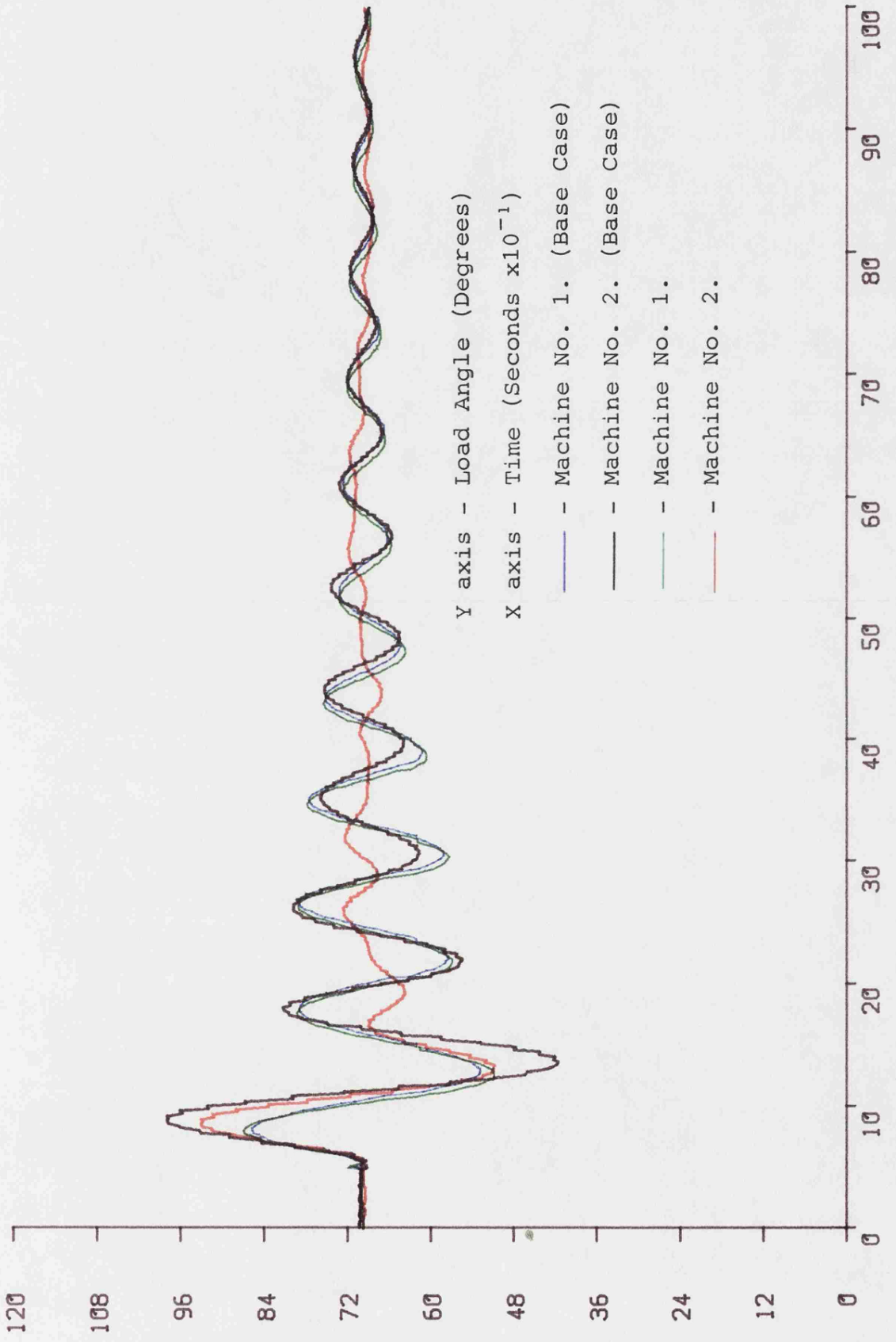

Fig. 9.3(a) Control M1 Load Angle

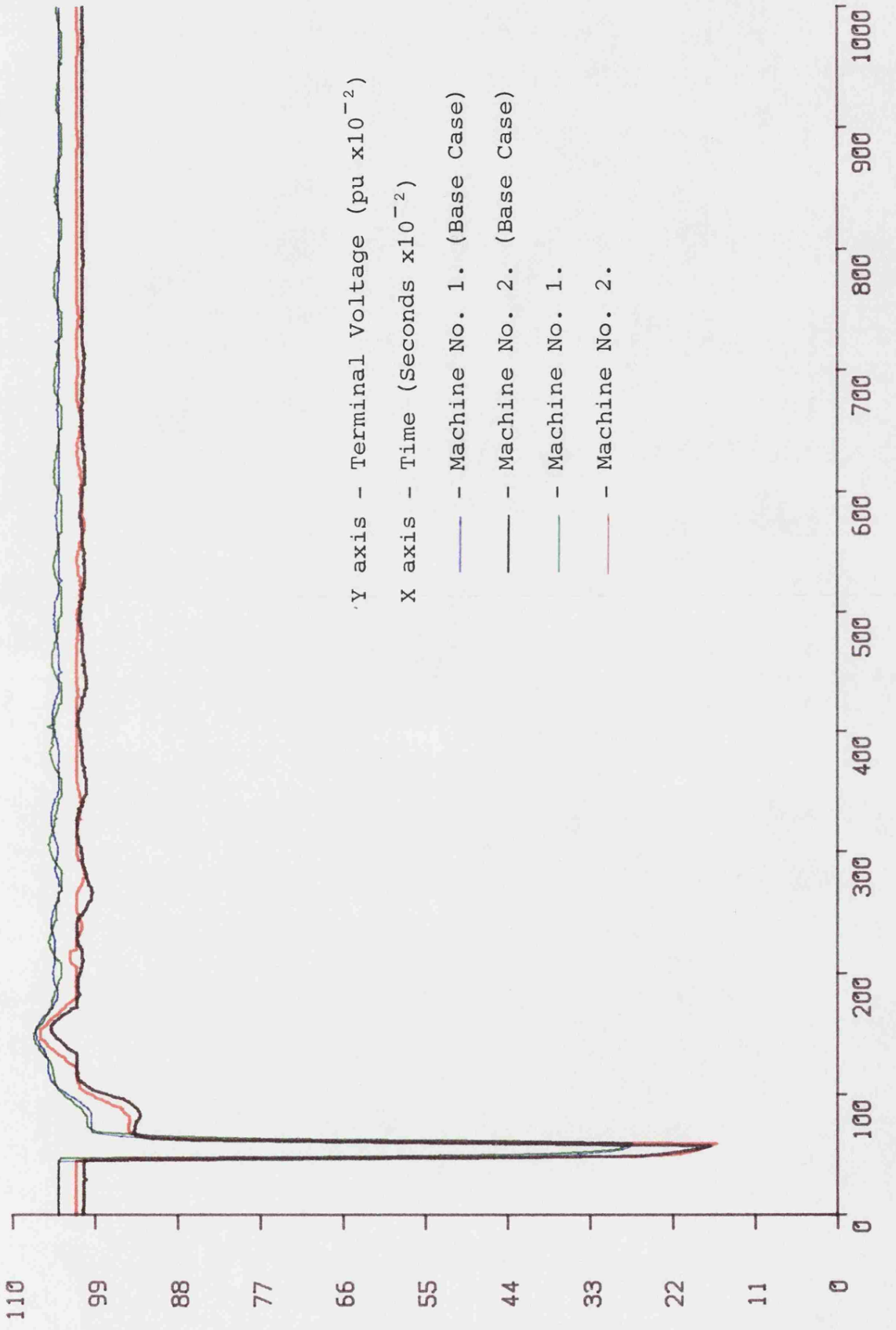

Fig. 9.3(b) Control M1 Terminal Voltage

Control M2 corresponds to the use of acceleration into only the governing system of machine No.2. The output transient response curves are given in Fig. 9.4. It was predicted that the use of this form of control should result in a reduction in the first peak in rotor angle swing for machine No.2, with little effect on its subsequent damping and little effect on the whole transient load angle response of machine No.1. This result is confirmed by the experimental rotor angle responses shown in Fig. 9.4(a) which, on the whole, clearly follow the trend shown in the corresponding theoretical responses of Fig. 8.4. The terminal voltage response curves obtained on the micromachine are shown in Fig. 9.4(b) which show the expected improvement for machine No.2, with little change for machine No.1, predicted by the theoretical study and shown in Fig. 8.4(b).

The final case investigated was that of co-ordinate excitation control and governing of machine No.2, with excitation control of machine No.1. This corresponds to feedback of acceleration into both inputs of machine No.2, and into the excitation system of machine No.1. It requires a theoretical optimization study with three feedback variables and the values obtained for these feedback constants depend on the starting point of the optimization study. It was shown in Chapter 8. that it is possible to obtain different feedback constants using different formulations for the objective function. However, each tend to give similar results with gains falling into two distinct ranges (a set of low

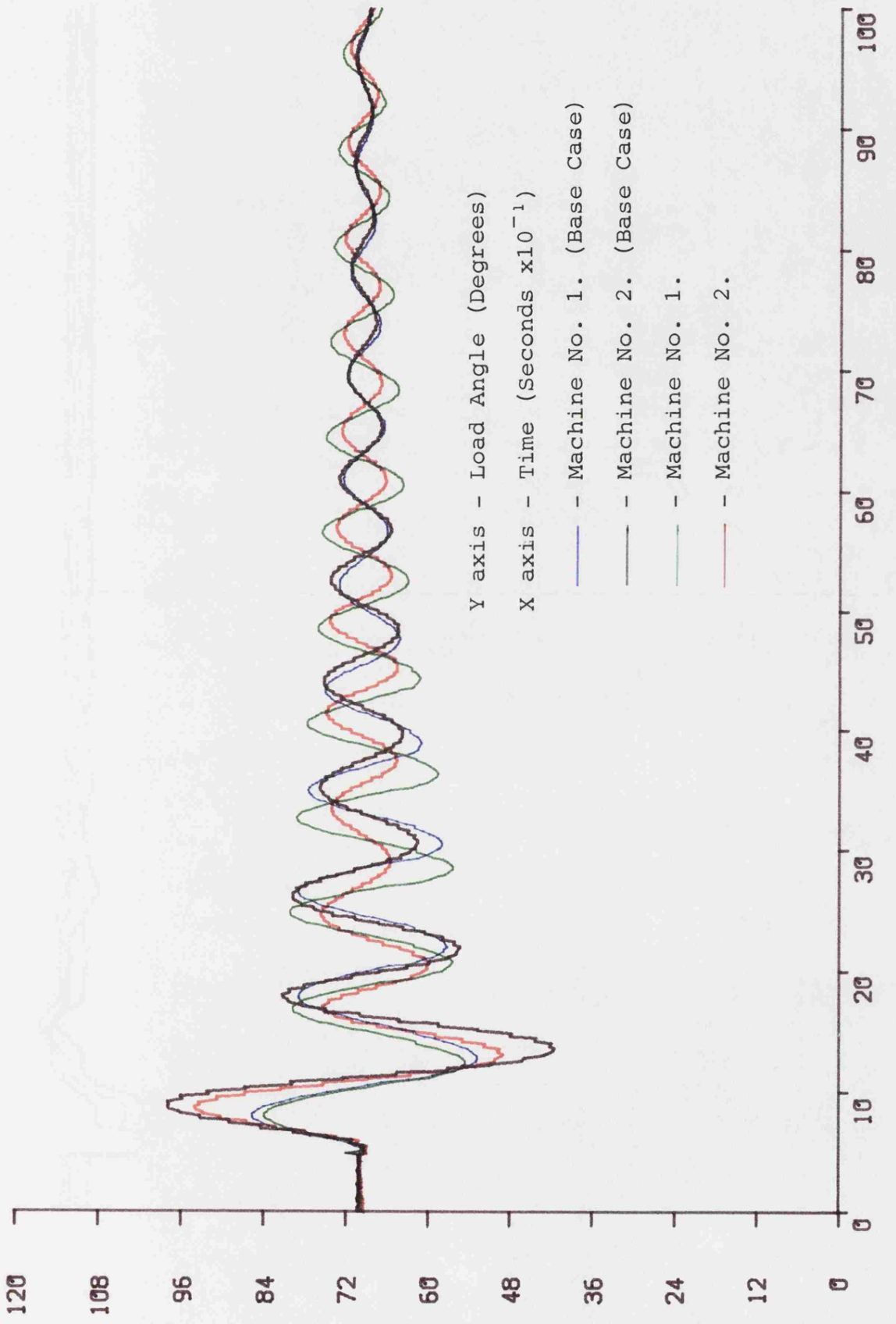

Fig. 9.4(a) Control M2 Load Angle

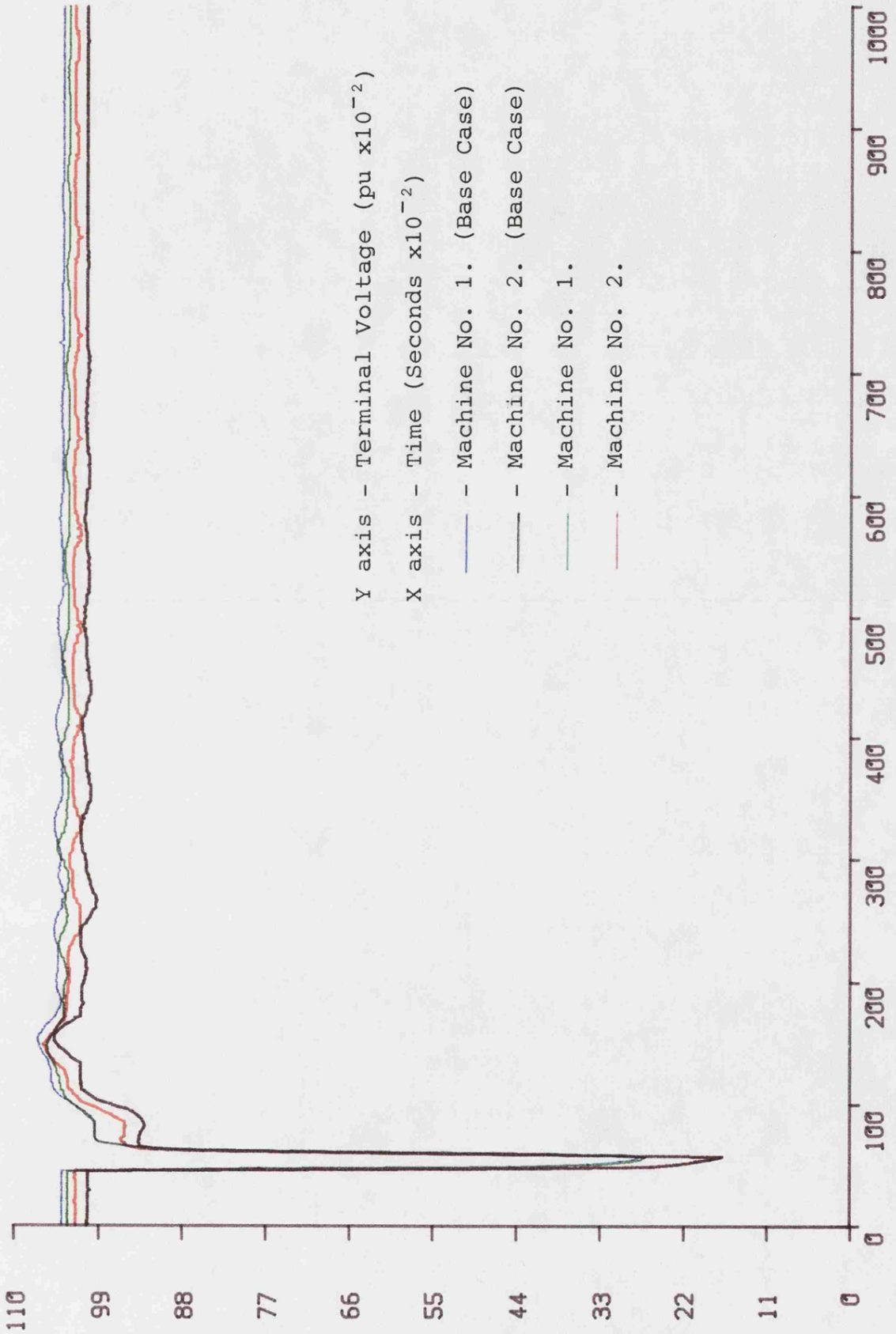

Fig. 9.4(b) Control M2 Terminal Voltage

values or a set of high values). The laboratory investigation has been limited to one set of results in each range given as control M3 in Table 9.1 for the low values of feedback constants and control M4 for high values of the feedback constants.

The results of the experimental investigation with full co-ordinate control corresponding to the low feedback gains of control M3 are given in Fig. 9.5. The load angle curves of Fig. 9.5(a) show the expected reduction in the first peak for machine No.2, with marginal changes in its subsequent damping. The corresponding curve for machine No.1, shows little change in the first peak with some loss of subsequent damping. The terminal voltage responses of Fig. 9.5(b) show an improvement for machine No.2, with little change for machine No.1. These results generally agree with the predicted results of Fig. 8.5 and confirm that the low value set of co-ordinate feedback gains do little to modify the power system performance.

Control M4 of Table 9.1 represents the case of a high gain, full co-ordinate control into all three fast acting controllers on the two machine system. The transient load angle responses of Fig. 9.6(a) clearly show a significant reduction in the first peak for machine No.2, (fitted with a fast acting governing system). Machine No.1, (fitted with the slow governor) shows practically no change in first peak. Both machines exhibit a pronounced improvement in load angle damping after the first peak and this improvement is associated

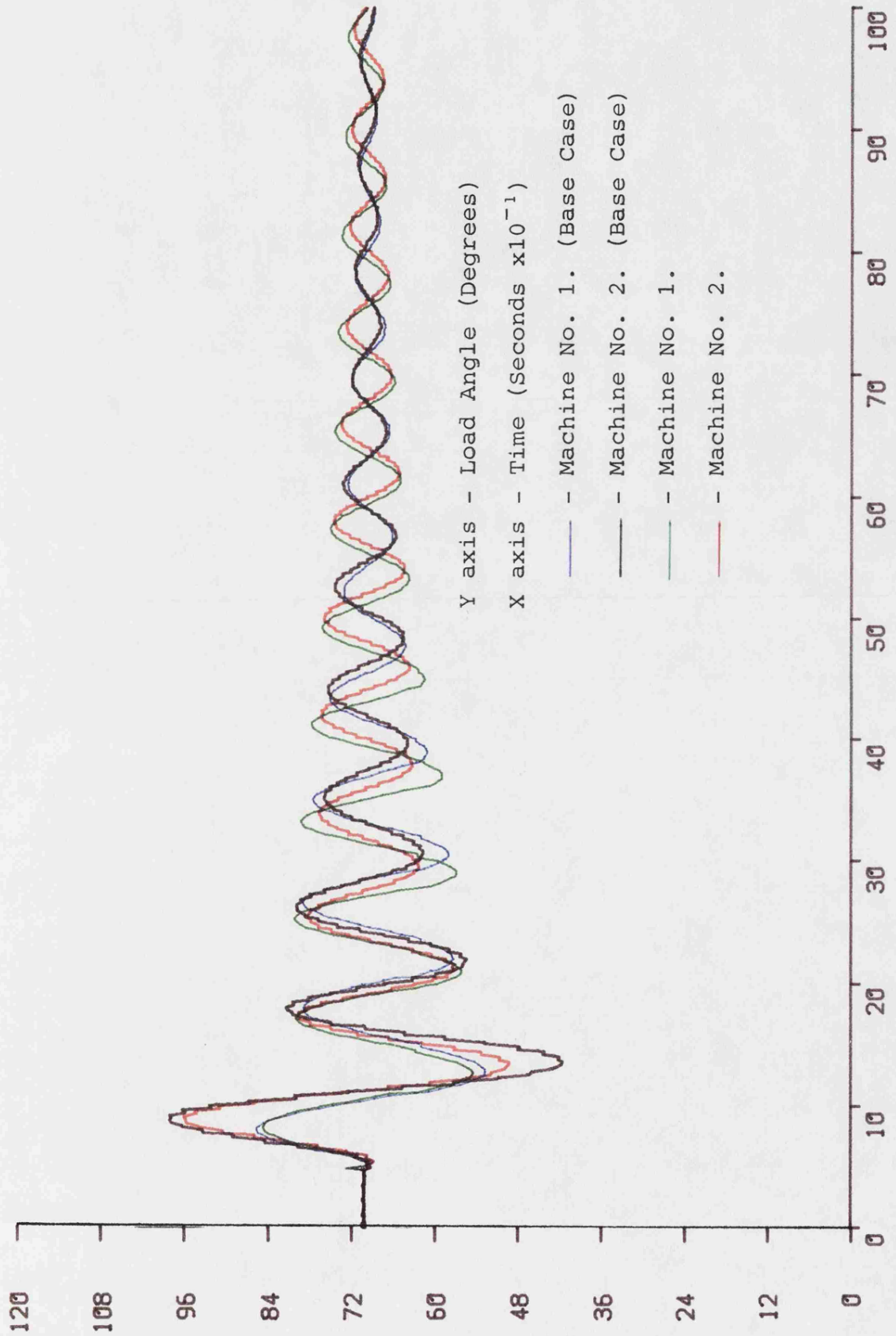

Fig. 9.5(a) Control M3 Load Angle

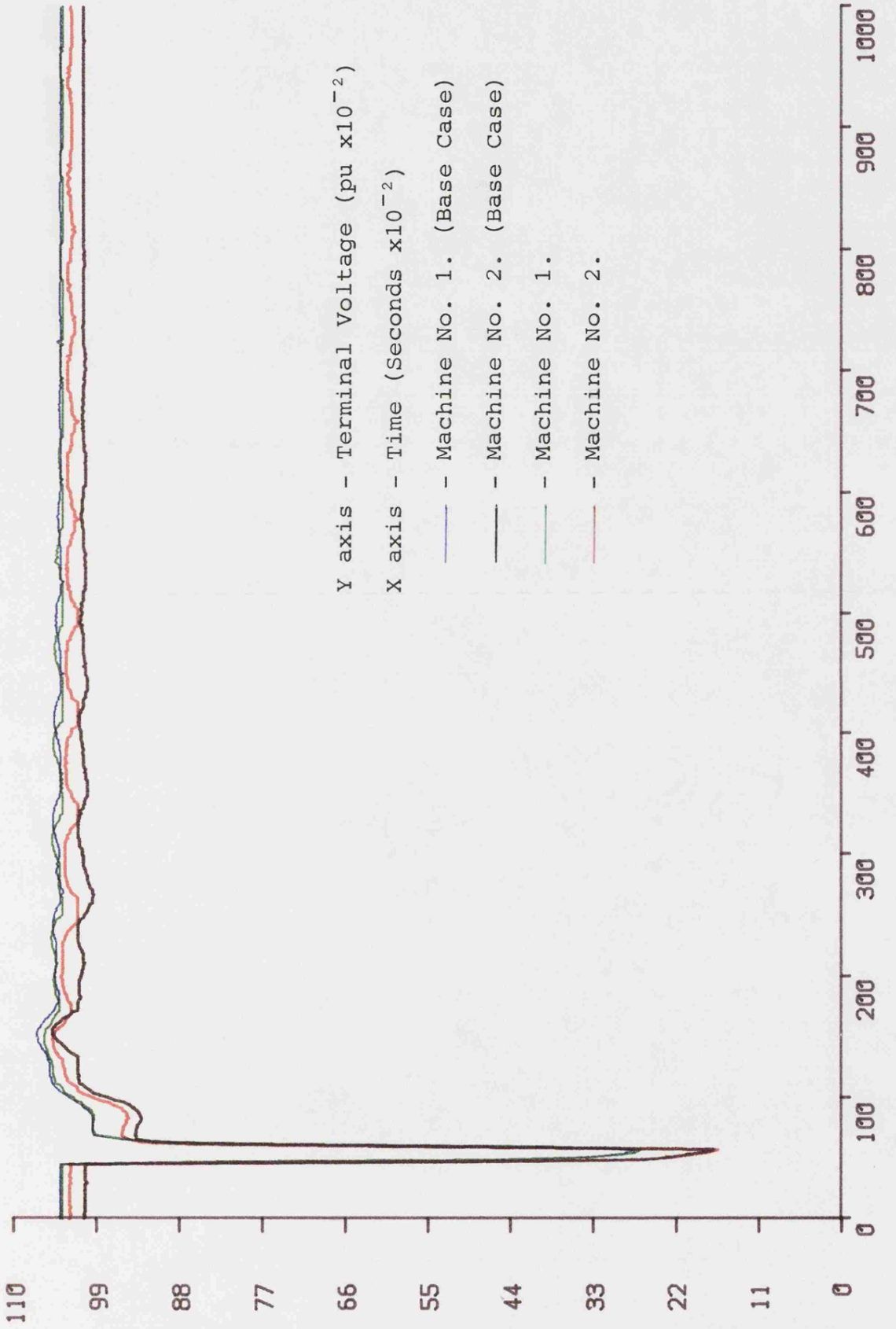

Fig. 9.5(b) Control M3 Terminal Voltage

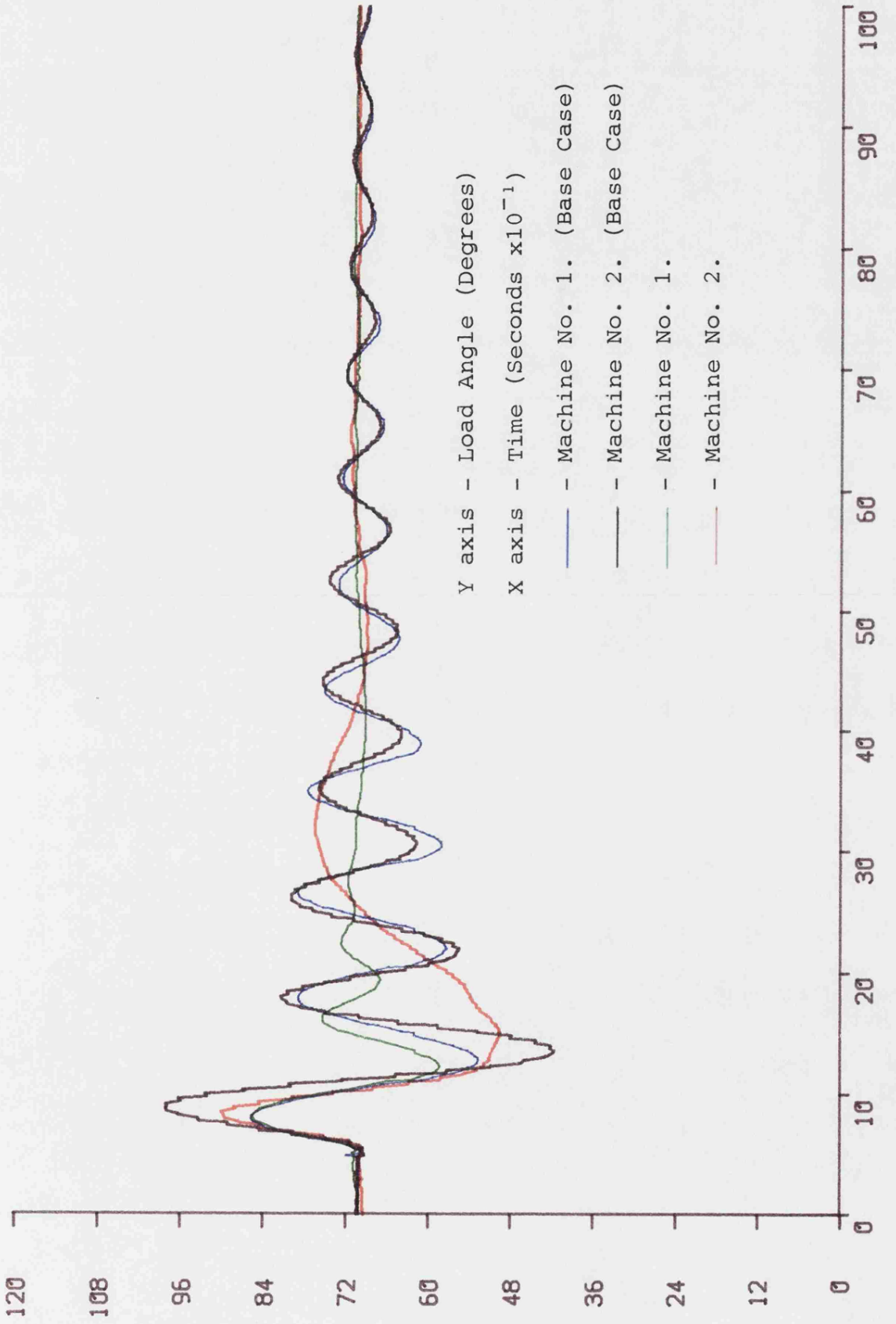

Fig. 9.6(a) Control M4 Load Angle

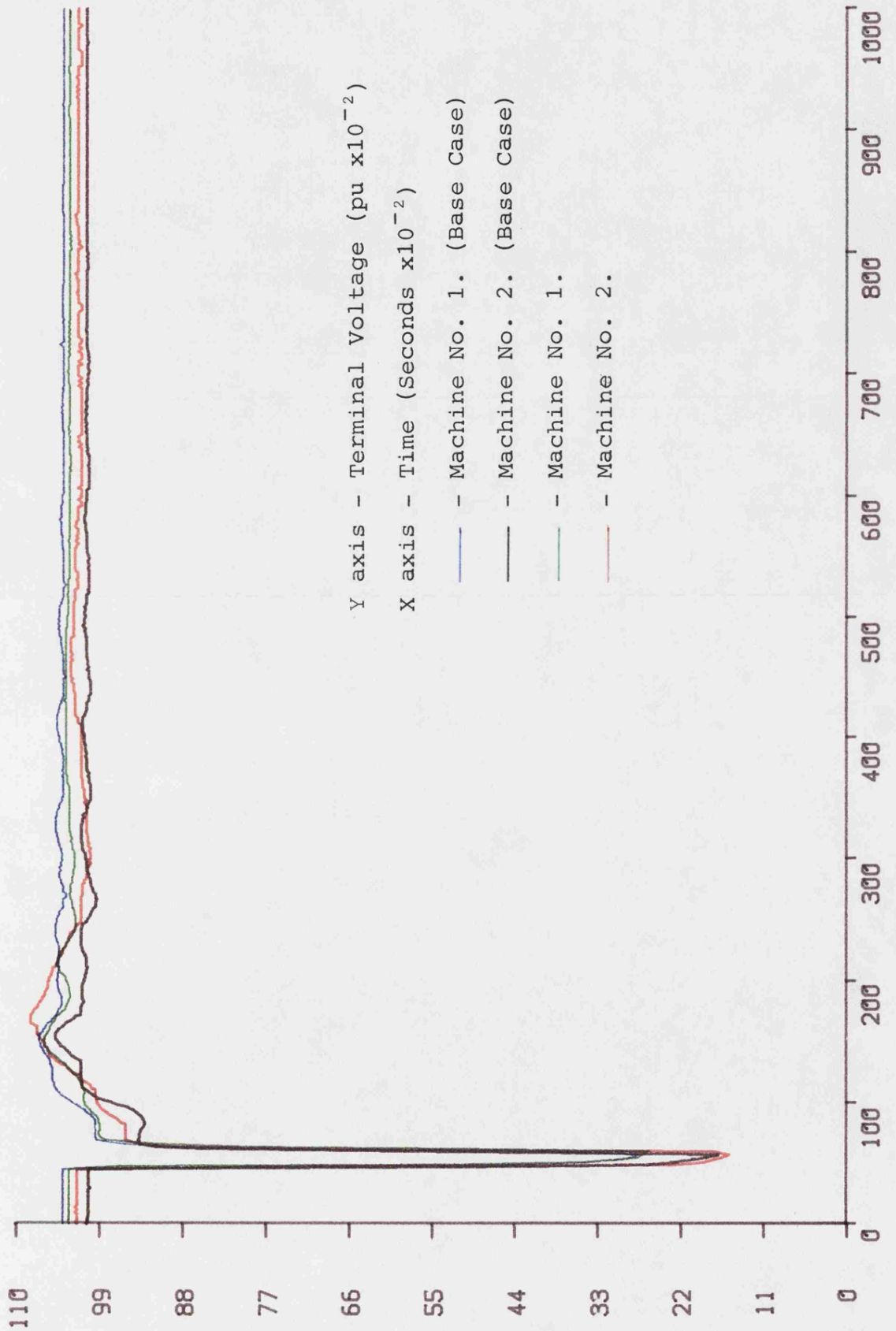

Fig. 9.6(b) Control M4 Terminal Voltage

with the extra feedback into their excitation systems. A comparison of these results with the corresponding theoretical results of Fig. 8.6 shows that the experimental investigation has confirmed the general trends in rotor angle responses predicted previously. In detail though, it is apparent that both machines experience more undershoot in the load angle recovery. The slow governed machine also shows a little more oscillation in the first part of the recovery than expected. When allowance is made for the initial offsets, the terminal voltage responses of Fig. 9.6(b), show the effect of increased damping in the system. The initial recovery follows the theoretical trend of a sluggish return to the nominal level as a result of the additional control. For machine No.2 there is a definite correlation between the low frequency oscillation in terminal voltage and load angle, before steady state is reached.

The fact that the component micromachine systems of the two machine configuration are not identical, forced a compromise in the setting up of initial operating conditions for the experimental results. Load angle was chosen to be the most important single variable and was fixed for each machine. In order to achieve this, the other machine variables were allowed to vary within acceptable bounds, which resulted in initial offsets in the terminal voltages. However, even though the theoretical results were based on a two machine system comprising electrically identical elements, which is evidently not the case for the micromachine system, there has been a general agreement in trends between the theoretical and practical results.

CHAPTER 10 CONCLUSIONS

10.1 General

Control strategies for the improvement of the transient response of turbo-generators have been obtained from theoretical studies of both single and multi-machine infinite busbar systems. The only additional state feedback used in these studies is that of rotor acceleration of the controlled machine. The method used to obtain the control strategy is to assume the form of the controller and then to obtain the required gain set by function minimization of a performance index which provides an arbitrary measure of the system performance. This approach has the major advantage over means by which so called optimal control may be derived in that the process may be restricted to use only those states available and, additionally it copes with nonlinearities in the system. The controls derived are necessarily suboptimal, in that not all the possible information is used. However they do benefit from being capable of practical implementation.

10.2 Theoretical Models

Models suitable for the representation of turbo-generator systems, under transient conditions are given,,with representations for the synchronous machine of seventh, fifth, and third order, together with suitable models for the generator transformer and transmission system. The two major control systems effecting the machine response are the automatic

voltage regulator and turbine governor system. These have been represented by models which retain their major non-linearities. In the case of the automatic voltage regulator, appropriate field voltage ceiling levels are enforced. The model used for the turbine governor has been obtained by reduction of a detailed nonlinear model. This representation is computational efficient, but retains the major nonlinear terms which are valve velocity and position limits.

10.3 Control Objectives

For the single machine, infinite bus system, theoretical controls have been derived for full co-ordinate control of excitation and governing using rotor acceleration as the single additional feedback signal. It has been shown to be possible to significantly reduce the first peak in rotor angle and achieve early damping out of rotor oscillations following a 3-phase short circuit fault.

With the multi-machine case, similar techniques have been applied to obtain controls for the same purpose. In this case, it is not so easy to obtain dramatic improvements in response, due to machine interaction. Nevertheless, controls have been derived which are beneficial to the overall system.

10.4 Micromachine Digital System

A microprocessor based system has been developed which is capable of performing three concurrent functions on the

micromachine laboratory rig. The first function is data collection from the various transducer, and, if necessary, this data is pre-processed before it is transmitted to the master computer for permanent storage. As part of the data collection system, a transducer has been developed which is capable of providing an estimate of rotor acceleration suitable for use in a control system. The second function is that of a real time simulation of the governor-turbine model, which takes input data from the system and computes the required turbine torque. The required torque signal is then used as a demand input to the armature current controller on the d.c. machine acting as a prime mover. Since the governor-turbine simulation is purely software, it is easily changed to reflect different machine parameter. The final major function of the digital processor system is to detect a system line fault, and then to computer and apply the control laws to both the excitation and governing systems.

With the exception of the initialization section all the digital processing is carried out under interrupt. This allows a fast response to the data communication and control requirements on a prioritized basis.

10.5 Single Machine Results

It has been shown that, for the single machine infinite bus system, the correlation between theoretically predicted responses and experimental micromachine results is good. In the single machine studies there is no need for absolute

identity between, say, the first swing peak in rotor angle, for the theoretical and practical results and, as long as the underlying trends are clearly the same, it can be concluded that verification of the applied controls has been obtained. When single machine results are taken from different machines, the absolute values of parameters are not the same, but the trends in improved response obtained by extra feedback are clearly similar. These results give confidence, in that the controls obtained on a theoretical model which is necessarily based on an inaccurate representation of the system, are proven to be useful on two physical systems, which are not identical. Since similar trends are experienced on all three systems, it is reasonable to assume that the controls obtained are insensitive to variations in plant parameters.

10.6 Multi-machine Results

The application of control laws derived from multi-machine theoretical studies, based on two electrically identical machines, to the micromachine system, highlights the differences between the two micromachine systems. When operating in the steady state, it was not possible to obtain identical initial conditions. For tests, the most meaningful results were obtained when the machine load angles were made equal, which necessitates slight differences in the other operating parameters. The inherent differences in response between the machines obtained when applying a standard 3-phase short circuit fault, must be taken into account when analysing the results obtained with additional controls applied. These

differences between the micromachines make direct comparison of theoretical and micromachine results less practical than for the single machine case. However, it is possible to see the obvious underlying trends.

10.7 Suggestions for Further Work

The multi-machine experimental results indicate that a detailed investigation should be carried out to determine the actual parameters of the micromachine systems. Theoretical studies can then be based on these parameters and a greater correlation could then be expected. The multi-machine theoretical results have shown that feedback of acceleration with a constant gain is not necessarily the best approach. More intelligent controllers with a variable structure could well be employed to obtain improved responses. The microprocessor based data acquisition system, using the cupped disc speed transducer is capable of providing rotor angle, rotor transient velocity and acceleration, which would be major inputs to such a controller.

APPENDIX A1 REDUCTION OF NONLINEAR GOVERNOR TURBINE MODEL

In the block diagram of Fig. 2.4 all the nonlinear elements are neglected, hence the HP valve position loop may be redrawn as

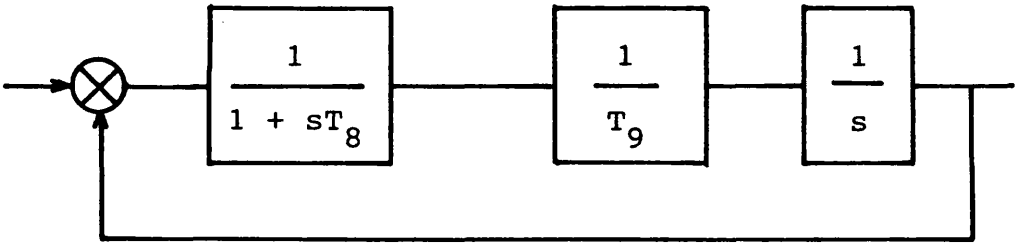

Which has an equivalent form.

$$\frac{1}{1 + T_9 s + T_8 T_9 s^2}$$

Including the governor network and turbine elements the transfer function from input to HP torque component is,

$$\frac{1 + sT_3}{1 + sT_4} \quad \frac{1}{1 + T_9 s + T_8 T_9 s^2} \quad \frac{1}{1 + T_{HP}} \quad FHP$$

Following the original reference the low pressure torque component is assumed to be zero. Additionally under the assumption that the reheater is an infinite steam source there is no interaction between the high pressure torque component and the intermediate pressure torque component.

The transfer function relating IP torque to the input is of a similar form to the HP torque component.

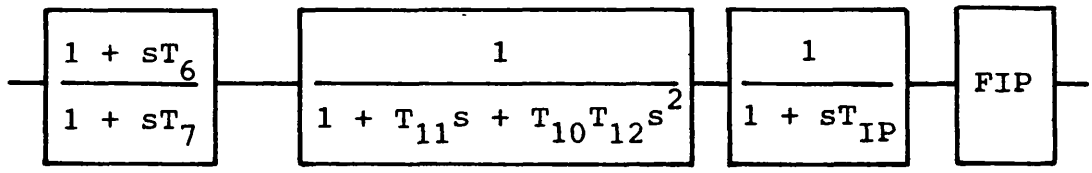

The HP and IP torque components may then be added,

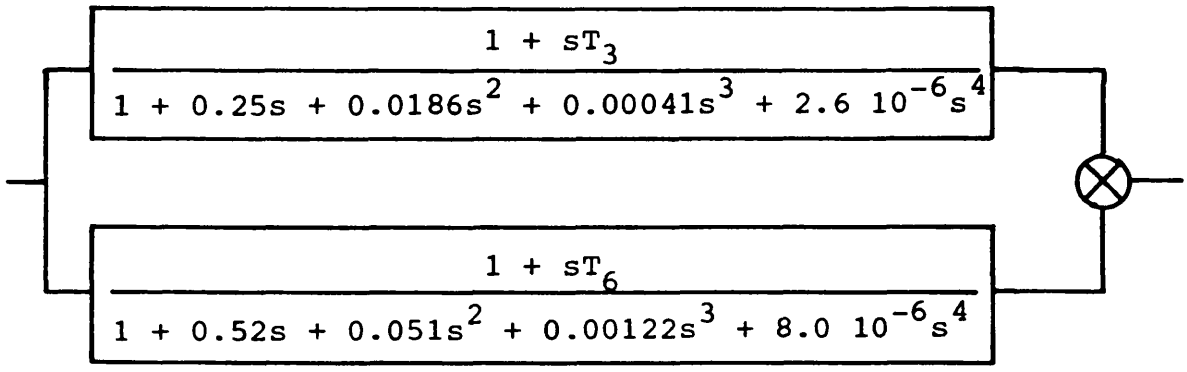

combining these into a single transfer function.

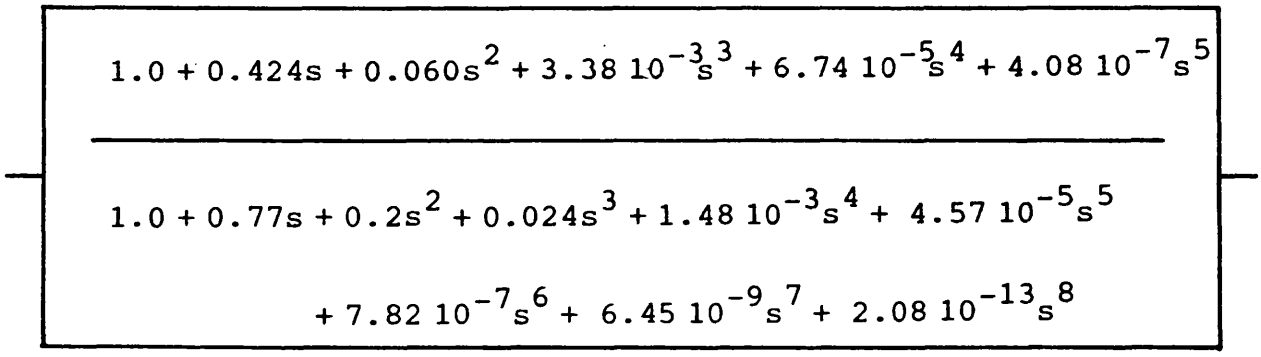

$T_3 = T_6 = T_9 = T_{11} = 0.1s$

$T_4 = T_7 = 0.02s$

$T_8 = T_{10} = 0.01s$

$T_{HP} = 0.13s \quad T_{IP} = 0.4s \quad T_{LP} = 0.02s$

$T_{RH} = 7.0s$

$K1 = K2 = 0.005pu$

$F_{HP} = 0.275pu \quad F_{IP} = 0.725pu \quad F_{LP} = 0.0pu$

$VO1 = VO2 = 4.0pus^{-1} \qquad VC1 = VC2 = 6.6pus^{-1}$

Table A1.1 Parameter Values for Detailed Governor Turbine Model

APPENDIX A2 PRIME MOVER TORQUE CONTROL

The prime mover is a separately excited d.c. machine with constant field current. The output torque is therefore proportional to the armature current. If the mean armature current follows control demands quickly, and variations about the mean level are of sufficiently high frequency to be smoothed by the inertia of the machine, then the prime mover torque control can be assumed to be a unity gain converter between software demanded torque and torque applied to the rotating system. The essential elements of the system are given in Fig. A2.1.

The slit width control circuits are housed in the main instrumentation rack adjacent to the digital system. Only two signals are passed between the slit width control electronics and the power unit, a shunt feedback signal which monitors the load current, and a drive control which is an optically isolated binary signal. Switching of the main power transistor is handled by the base drive control board, which floats at the potential of the emitter of the main power transistor. Fast turn on of the main power transistor is achieved by a low impedance source. An active current sink arrangement reduces turn off times to minimize transient power dissipation. The binary on-off signal from the slit width control electronics is used in conjunction with signals from the protection circuits to switch base drive to the main power device. The protection circuits handle minimum on and off times necessary for recovery of snubber networks, as well

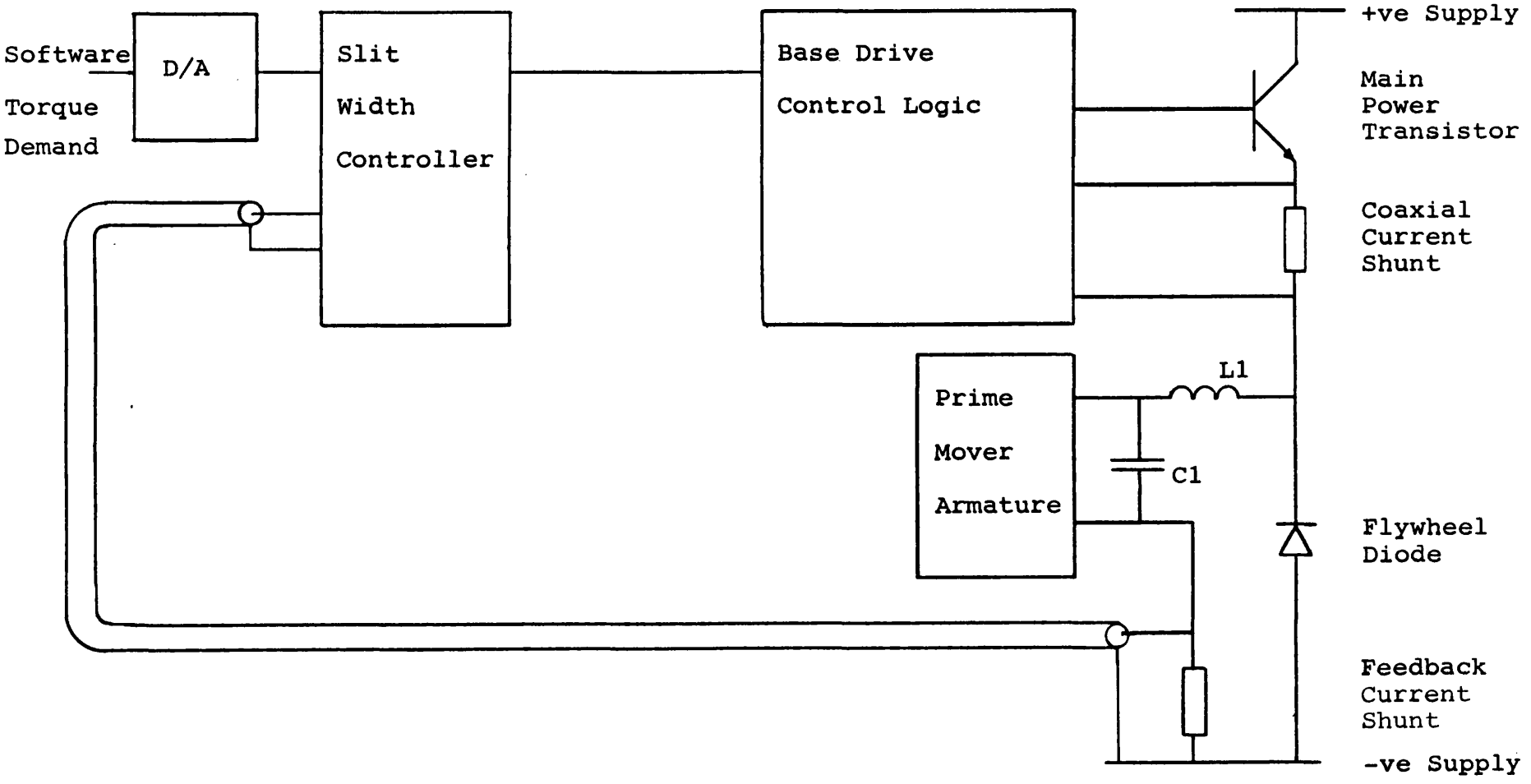

Fig. A.2.1 Prime Mover Armature Current Control

as overcurrent conditions sensed by the coaxial current shunt.

The switching arrangement can be seen to apply the d.c. supply voltage across the load circuit when the power transistor is on. When the power transistor is off, the inductance of the load maintains current flow through the flywheel diode. Fig. A2.2 represents the load current waveform for a step input, assuming a simple R - L load and a perfect switching source. The current rises on an exponential defined by the load time constant τ, until the upperbound of the slit width is reached. At this point the switch is opened and current continues to flow, but now through the flywheel diode, decaying on the same exponential.

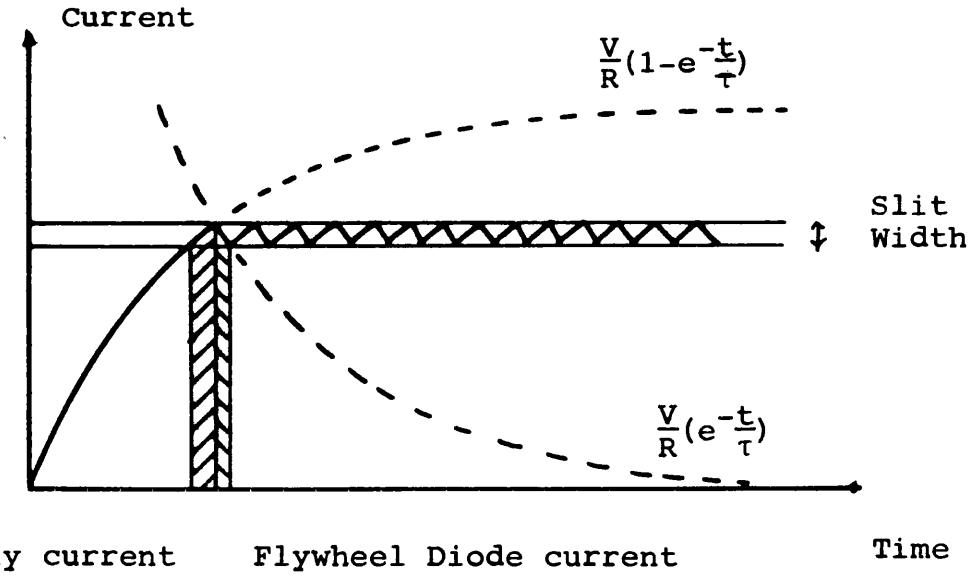

Fig. A.2.2 Step Input Current Waveform

The current control system can function satisfactorily without components L1 and C1 of Fig. A2.1 in circuit, using only the

armature winding inductance to control the rate of change of armature current. In practice two disadvantages were apparent in this mode of operation, associated with the rapid rates of change of current in the armature circuit. Electrical noise spikes were generated which effected some of the low level electronics in the vicinity. Also the d.c. machine windings were subjected to rapid changes in applied forces which produced unnecessary stress. With L1 and C1 in circuit the power transistor effectively sees only the inductance L1. The capacitor C1 does not effect the d.c. component of armature current, but suppresses transients, which would normally travel down and radiate from the armature leads. Thus, both the problems above are alleviated. The smoothing effect on the armature current also has the advantage that the effective armature current is actually smoother than would be indicated by measurements from the current shunt.

APPENDIX A3 PDP 11 - TMS 9900 DIGITAL INTERFACE AND DATA TRANSFER UNIT

A3.1.1 Digital Interface Card PDP 11 Programmers View

The interface card (I/F) provides a means of controlling the TMS 9900 microprocessor and its control busses for the purposes of program loading by Direct Memory Access (DMA) and for software debugging. All data to and from the PDP 11 is transferred over a parallel data link. The link comprises twenty twisted pair current loops in each direction. The Digital Equipment Corporation DR11-C[46] is used as an interface between the external parallel data lines and the PDP 11 Unibus[48]. The DR11-C is a memory mapped set of three registers, a control and status register DRCSR, an input register DRIBR and an output register DROBR.

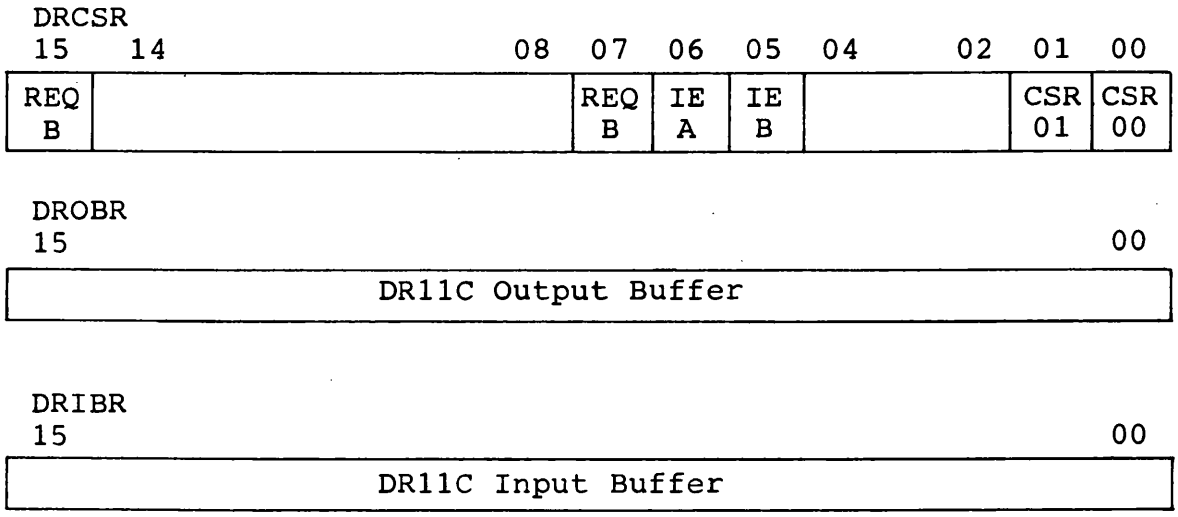

Fig. A3.1 DR11C Registers

Multiplexing of the DR11C data at the microprocessor end is performed under the control of the DR11C control and status register bits CSR00 and CSR01, in accordnce with Table A3.1.

CSR01	CSR00	Data Mode
0	0	DTU Data
0	1	Not Used
1	0	I/F Data
1	1	I/F CSR Data

Table A3.1 DR11C Data Modes

When in the I/F CSR data mode, the DR11C output data is directed to the interface control and status register (IFCSR) and input to the DR11C is obtained from the IFCSR.

Table A3.2 below gives the IFCSR bit functions, it should be noted at this point that the PDP11 bit labling takes the form MSB = bit 15 and LSB = bit 00 while the Texas TMS 9900 system uses the opposite convention. Since the IFCSR is only accessible from the PDP 11 the former system is used in the table.

Bit No.	Signal	Function
00 (LSB)	RESET	When set, forces the TMS 9900 system RESET line low. (read/write)
01	LOAD	When set, forces the TMS 9900 system LOAD line low. (read/write)
02	HOLDREQ	When set, forces the TMS 9900 system HOLD line low. (read/write)

Bit No.	Signal	Function
03	IFCSRA	Controls interface access in I/F CSR data mode. 1 = Access to TMS Address Bus 0 = Access to TMS Data Bus
04 05	DATLD0 DATLD1	These control the destination of DR11C data when in I/F data mode. DATLD1,DATLD0 0 0 Load data bus register 0 1 Load data bus register and initiate memory write cycle. 1 0 Load address register 1 1 Load interrupt priority register.
06	BPEN	Enables the software breakpoint routine to trigger an interface forced wait on the TMS 9900 cpu.
07	WT	Force a processor wait state on the next instruction acquisition cycle.
08	SST	Single step trap, when set the I/F disables the normal memory during instruction acquisition and jams on to the data bus the contents of the data bus buffer register.
09	PR	Proceed from wait state, an evanescent signal which should never be read as true.
10	TMSINT	When set an interrupt at the priority held in the interrupt priority register

Bit No.	Signal	Function
10	TMSINT	(continued) is forced on the TMS 9900. A low to high transistion of CRUO3 clears this bit and hence the interrupt
11	WAIT	A read only bit which indicates when the TMS 9900 is in an interface forced wait.
12	HLDACK	A read only bit indicating that the TMS 9900 is in a interface forced HOLD.
13	CRUO3	Monitors CRU output bit 3.
14	CRUO5	" " " " 5.
15	CRUO6	" " " " 6.

Table A3.2 IFCSR Bit Functions

A3.2 Digital Interface Hardware Description

For clarity, the circuit diagram of the digital interface has been split into two parts. The control and status register together with all control logic is presented in Fig. A3.2(a), the address and data paths are given in Fig. A3.2(b). In this and subsequent descriptions which refer to hardware, the following convention will be used. A strobe signal, generated by control logic to clock information etc. will be labelled Cn, where n is the control number. In the circuit diagrams these signals are contained in standard off page symbols if they are not linked directly to all points where they are used. When referring to a gate the chip position and relevant pins are used to define it, for example E6.11,12,13 is chip number 6 in column E of the circuit board. If the output of a gate or latch is referred to, then only

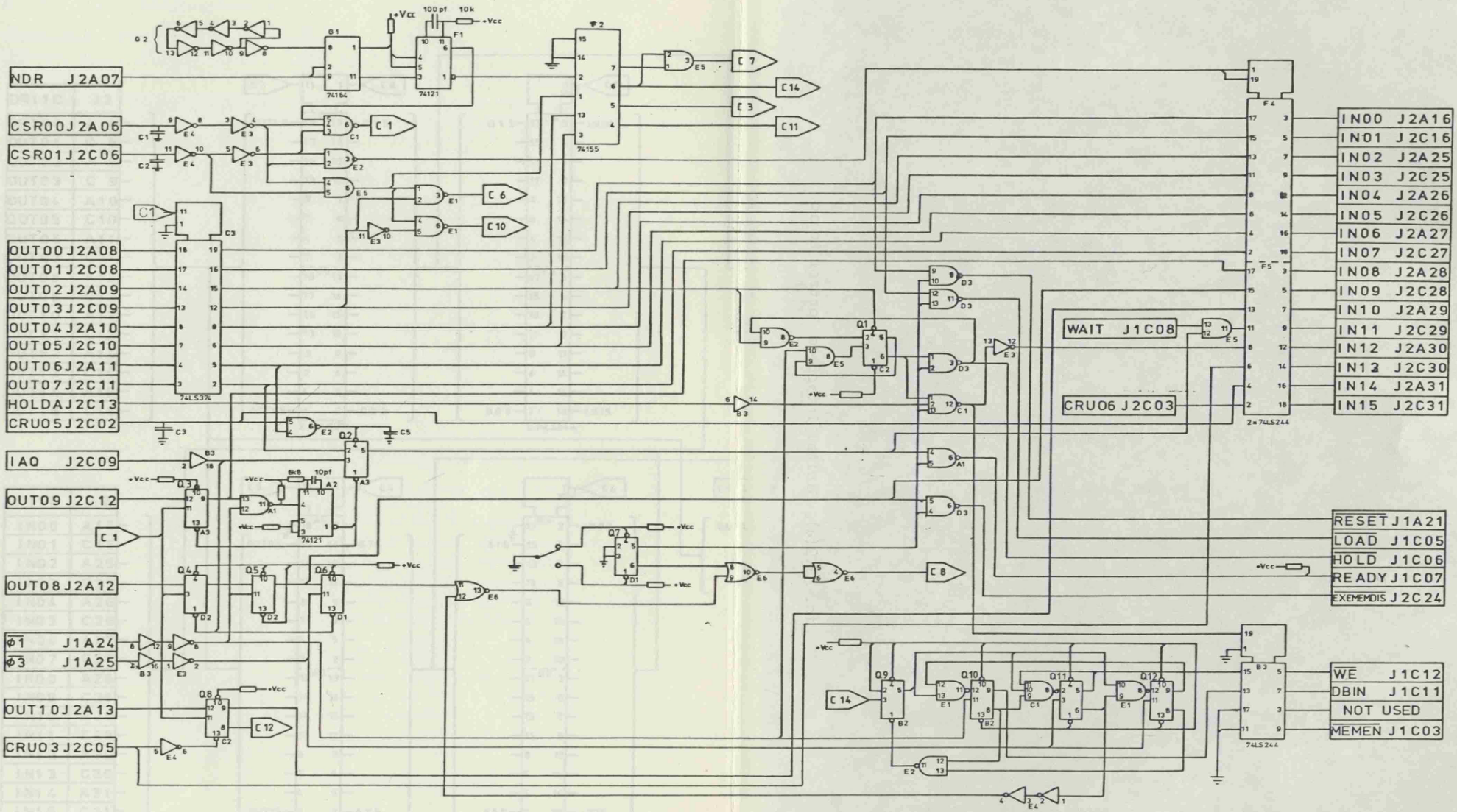

Fig. A3.2(a) Digital Interface Control Logic

Fig. A3.2(a) Digital Interface Control Logic

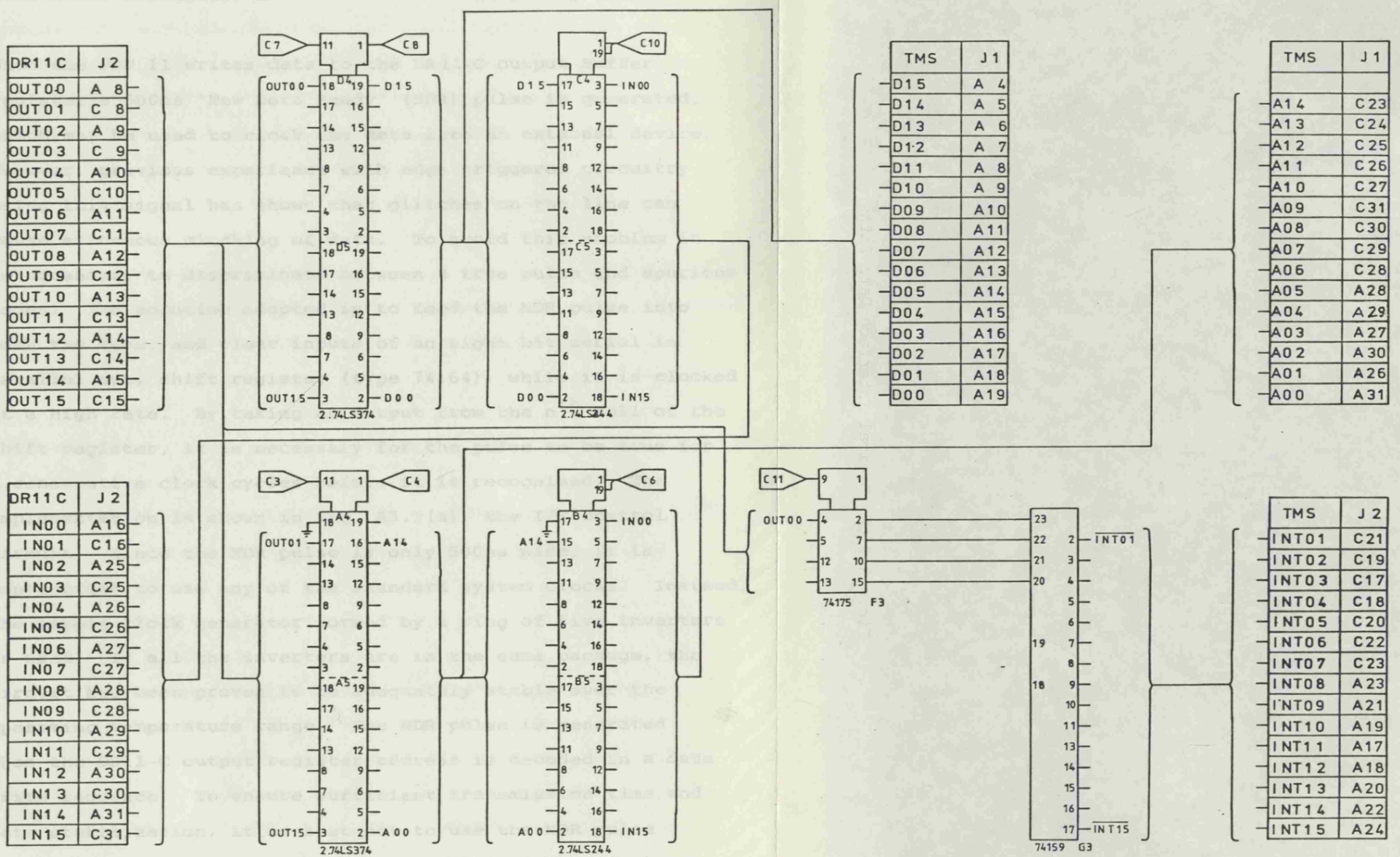

Fig. A3.2(b) Digital Interface Data Paths

Fig. A3.2(b) Digital Interface Data Paths

the chip number and relevant output pin will be used, eg. E6,13. For convenience flip flops are generally given an additional identifier Qn where n is the flip flop number.

When the PDP 11 writes data to the DR11-C output Buffer register a 500ns 'New Data Ready' (NDR) pulse is generated, which may be used to clock the data into an external device. However, previous experience with edge triggered circuitry using this signal has shown that glitches on the line can cause erroneous clocking of data. To avoid this problem it is necessary to discriminate between a true pulse and spurious edges. The solution adopted is to feed the NDR pulse into both the data, and clear inputs of an eight bit serial in parallel out, shift register (type 74164), while it is clocked at a high rate. By taking an output from the n^{th} cell of the shift register, it is necessary for the pulse to be true for n consecutive clock cycles before it is recognised. The implementation is shown in Fig. A3.2(a), the I/F control circuit. Since the NDR pulse is only 500ns wide, it is impractical to use any of the standard system clocks. Instead, the simple clock generator formed by a ring of five inverters is used. If all the inverters are in the same package, the circuit has been proven to be adequately stable over the operating temperature range. The NDR pulse is generated when the DR11-C output register address is decoded in a data write sequence. To ensure sufficient transmission time and data stabilization, it is best not to use the NDR pulse directly to clock data. Instead the falling edge of the deglitched NDR pulse is used to trigger a monostable (F1)

and the data is then clocked as the monostable returns to its stable state, thus providing sufficient settling time. When the DRC11-C CSR00 and CSR01 bits are both set true, NDR causes control C1 to strobe date into the IFCSR. The first eight bits of the IFCSR are contained in latch C3 and perform the following functions. Note that the interface enable switch must be set before any control is exercised over the TMS 9900 system.

RESET (OUT00)

The TMS 9900 system RESET line is forced low by open collector NAND gate D3.8 when reset C3.19 and interface enable D1.5 are both true.

LOAD (OUT01)

The LOAD line is forced low by open collector NAND gate D3.11 when load C3.16 and interface enable D1.5 are true.

HOLDREQ (OUT02)

Hold request is clocked into the IFCSR and is available on C3.15, NAND gate E2.8,9,10 is used to prevent further propagation of a hold request until the TMS 9900 system hold request line is high, ie. until no other device is requesting use of the systems busses. If this condition is satisfied E2.8 is low and is clocked into flip flop Q1 (C2.1-6) by the clock generated from Q1 and ¢1 in AND gate E5.8,9,10.

Once Q1 has changed state further clocking is inhibited, Q1 goes high and is combined with interface enable in open collector NAND gate D3.1,2,3 to pull the system HOLD line low. At the next non memory access cycle, the TMS 9900 enters a hold state and publishes HOLDA (active high), indicating that the cpu has relinquished control of the address, data and control busses. HOLDA is gated in NAND gate C1.1,2,13,12 to enable interface control of the system busses only when the cpu is in a hold state, the interface is enabled and the interface had requested the hold. The active low output of C1.12 is used to enable the interface address bus buffers A4,A5 and the control bus buffer B3.

IFCSRA (OUT03)

AND gate E5.4,5,6 is used to determine when the system is in I/F data mode, the active high output E5.6 is used as an enable input to NAND gates E1.1,2,3 and E1.4,5,6 which are fed with IFCSRA and IFCSRA respectively. The NAND gates are used to enable the tristate outputs of either the address bus reader or data bus reader to control the input data to the DR11-C.

DATLD (OUT04) DATLD1 (OUT05)

These bits are used by the 3 to 8 line decoder F2, to steer input data from the DR11-C when in the I/F data mode. Loading the interrupt priority register F3 and address bus register D4,D5 are simple clocking functions. The data bus

buffer register is loaded as a result of either a simple load operation or a load data bus register and start memory write sequence. AND gate E5.1,2,3 is used to generate the clock pulse for the buffer register. F2.6 is also used to clock Q9 (B2.1,6) and initiate the memory write sequence. The memory write timing diagram is shown in Fig. A3.3. There is no facility provided for extending the write cycle since it is not anticipated that slower memory will be used on the system.

BPEN (OUT06)

Software breakpoint enable BPEN is used in NAND gate E2.4,5,6 to gate the cpu card output signal CRUO5. When enabled CRUO5 presets flip flop Q2 (A3.1-6), Q2 is then gated with interface enable in NAND gate A1.4,5,6 to bring the READY line low. With the READY line low the cpu will enter a wait state on the next memory access. Q2 and the ensuing WAIT are ANDed by E4.11,12,13 and made available to the PDP 11 via the IFCSR. By this means a software breakpoint facility is produced. The final AND operation is required to prevent spurious PDP 11 action by reading a WAIT indication caused by cpu access to slow memory. Capacitors C3 and C5 are necessary to prevent operation of the circuit due to spikes on the CRUO5 line.

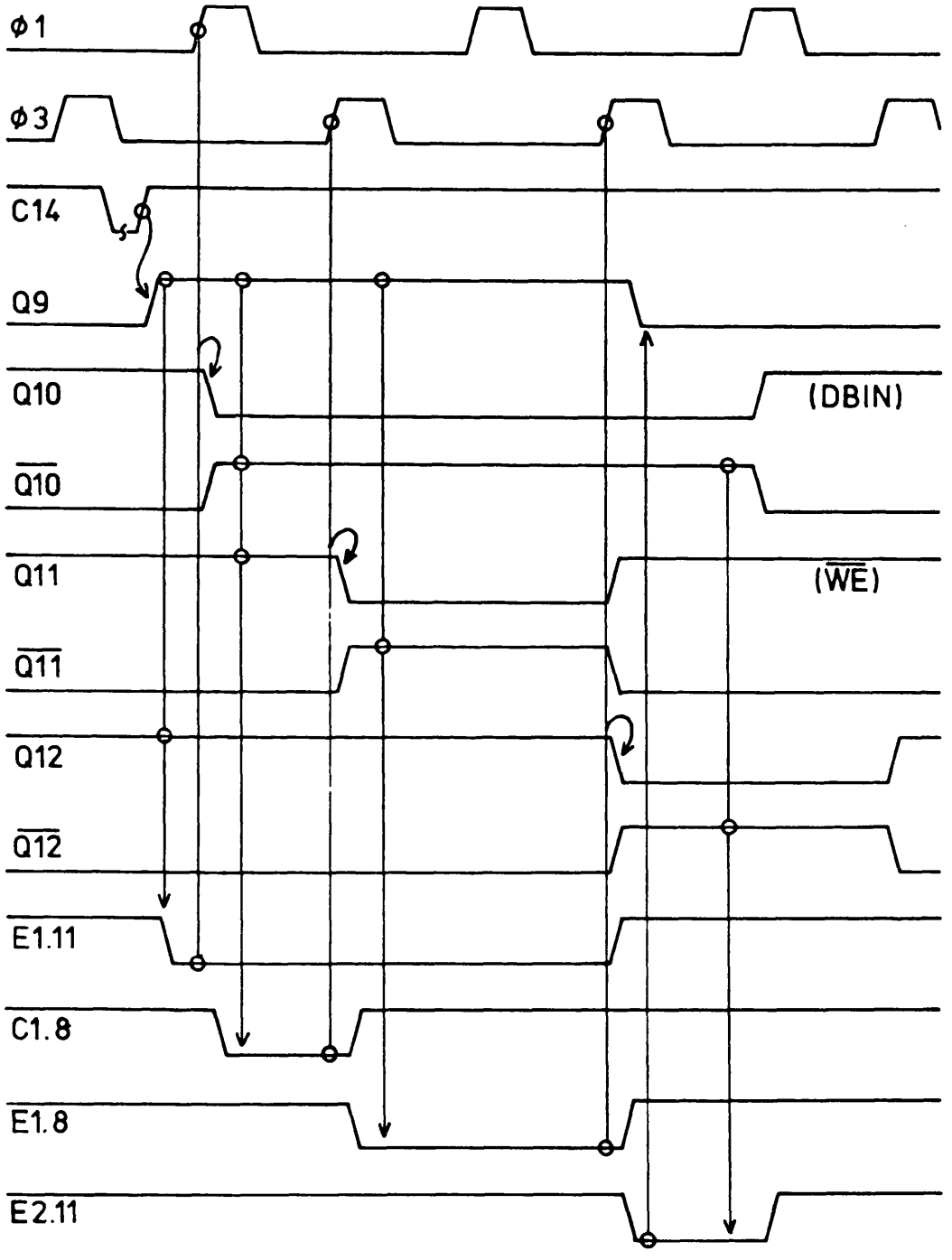

Fig. A3.3 Memory Write Timing Diagram

WT (OUT07)

WT, held in IFCSR on C3.2 is used as data for the Q2 flip flop. When the TMS 9900 cpu fetches an instruction from memory, the IAQ line is asserted as well as the standard memory control signals. IAQ is buffered by B3.2,18 and is used as the clock for Q2. With Q2 set the TMS 9900 is forced into a wait state as described under BPEN.

SST (OUT08)

This function is used in conjunction with interface forced wait states on the TMS 9900 cpu during instruction acquisition cycles. SST is clocked by IFCSR clock into Q4 (D2.1-6) Q4 is used as data for Q5 (D2.8-13) and thus synchronizes the SST to the TMS 9900 clocks. Q5 is clocked by ϕ1 and is in turn used as data for Q6 (D1.8-13) which is clocked by ϕ3. The delay between Q5 and Q6 is required to allow time for EXMEMDIS generated by Q5 and interface enable in open collector NAND gate D3.4,5,6 to disable the normal memory, before the I/F data bus buffer register is enabled. The I/F data bus buffer register is enabled by Q6 gated with interface enable.

PR (OUT09)

The proceed from wait state, PR, is clocked by the IFCSR clock into Q3 (A3.8-13) NAND gate A1.11,12,13 gates Q3 with ϕ1 to produce the negative edge required to trigger mono stable

A2. The Q output of A2 is used to clear Q3 and Q2 flip flops. Thus the READY line is released synchronously with $\phi 1$, but gate delays on the I/F card and cpu card are such that no effect is seen by the cpu during the current $\phi 1$. The READY line is stable in time for the next $\phi 1$ sampling and as a result the processor terminates the wait state and reads in the instruction, which may be from main memory or, if a SST is in operation, the data will be read from the I/F data bus buffer.

TMSINT (OUT10)

TMSINT is clocked by the IFCSR clock into Q8 (C2.8-13), Q8 is used to enable G4, an open collector one of sixteen decoder. The decoder asserts an interrupt on the TMS 9900 cpu card interrupt bus, the priority being determined by the contents of F3. To comply with TMS 9900 system conventions it is a requirement of all interrupt service routines to perform some action which resets the hardware that initiated the interrupt. For interrupts asserted by the interface, this requirement is met by setting and clearing CRUO3 which is inverted by E4.5,6 and then used to clear Q8.

A3.3 Data Transfer Unit Programmers View

The data transfer unit (DTU) has been developed to allow fast data communication between the TMS 9900 microprocessor and the PDP 11 mini-computer. The DTU has been designed specifically for use with the Digital Equipment Corporations

DR11-C and transfers are made in a 16 bit parallel fashion. A full hand shake system is available for controlling the flow of data. Software for transfers may be either on a simple flag test of the hand shake bits or the full interrupt structure may be used.

Separate interrupts with software programmable priority are available for input and output transactions. The possible priority levels range from the highest at level 1 to the lowest at level 15. This range gives flexibility to the software. There is no hardware restrictions on setting both interrupts to the same level, but, in this case, it is necessary to determine by software which of an input or output function is required. The layout of the control and status register DTUCSR has been carefully chosen to allow rapid determination of the presence of internal request flags. By placing the flags at the most significant bits of the bytes in the DTUCSR, a simple move instruction will set the processor condition code for a negative value if the flag is set. Thus a simple conditional jump following the move can be used to direct further processing.

All DTU registers are memory mapped 16 bit words, to allow parallel operations using the full range of TMS 9900 instructions. The mapping is given below in table A3.3.

Lable	Address	Function
DTUCSR	171770	DTU Control and Status Register
DTUOBR	171772	DTU Output data Buffer Register
DTUIBR	171774	DTU Input data Buffer Register

Table A3.3 DTU Registers

DTUCSR Bit Functions

00	01	02	03	04	05	06	07	08	09	10	11	12	13	14	15
β	INIT	REQ A	IE β	β0	β1	β2	β3	α		REQ B	IE α	α0	α1	α2	α3
MSB															LSB

Bit No.	Label	Function
00 (MSB)	β	Interrupt request β. Set when the input buffer register is loaded with new data from the PDP 11 and reset by either reading the input buffer register or by INIT. (read only)
01	INIT	Initialization bit, a low to high transition of this bit is used to clear all request flags. INIT is also reset as part of the same operation and should never be read as true. (read/write)
02	REQ A	Monitors the Request A input to the DR11-C (read only)
03	IE β	Request β interrupt enable (read/write)
04-07	β0-β3	Request β interrupt priority (read/write)
08	α	Interrupt request α. Set when the PDP 11 reads the data present on DTUOBR and reset by either writing new data to the output data buffer register or by INIT. (read only)
09	-	Not used.
10	REQ B	Monitors the Request B input to the DR11-C (read only)
11	IE α	Request α interrupt enable. (read/write)
12-15	α0-α3	Request α interrupt priority. (read/write)

Table A3.4 DTUCSR Bit Functions

A3.3.1 Operation of DTUCSR Flags

The DTU contains two pairs of flags which are used in data transfer operations. Request A (REQA) and Request B (REQB) provide interrupt requests inputs to the PDP 11 DR11-C. Request α (REQα) and Request β (REQβ) are used as interrupt request flags for the TMS 9900 DTU. Data transfers are performed using these flags for handshaking purposes. In the description of a typical transfer process the following assumptions are made for clarity.

i) Both the PDP 11 and TMS 9900 are engaged solely with the data transfer.
ii) Both processors use a simple flag test routine.
iii All flags in the DTUCSR are initially clear.
iv) The DR11-C control and status register bits CSR00 and CSR01 are clear enabling data transfer mode.

The sequence of events for transfers from the TMS 9900 to the PDP 11 is depicted in Fig. A3.4. The TMS 9900 writes data to the DTU output buffer register DTUOBR and the DTU hardware automatically sets Request B at time T1. When the PDP 11 reads a true value for REQB, it indicates that valid data is available to the DR11-C input Register DRIBR from the DTU output register. When the PDP 11 reads the DR11-C DRIBR at T2 a 500ns Data Transmitted pulse DTMD is generated. The DTU uses DTMD to reset REQB and set REQ . When the TMS 9900 next samples REQ it will be set, indicating that the PDP 11 has accepted the last data. The TMS 9900 is now free to load

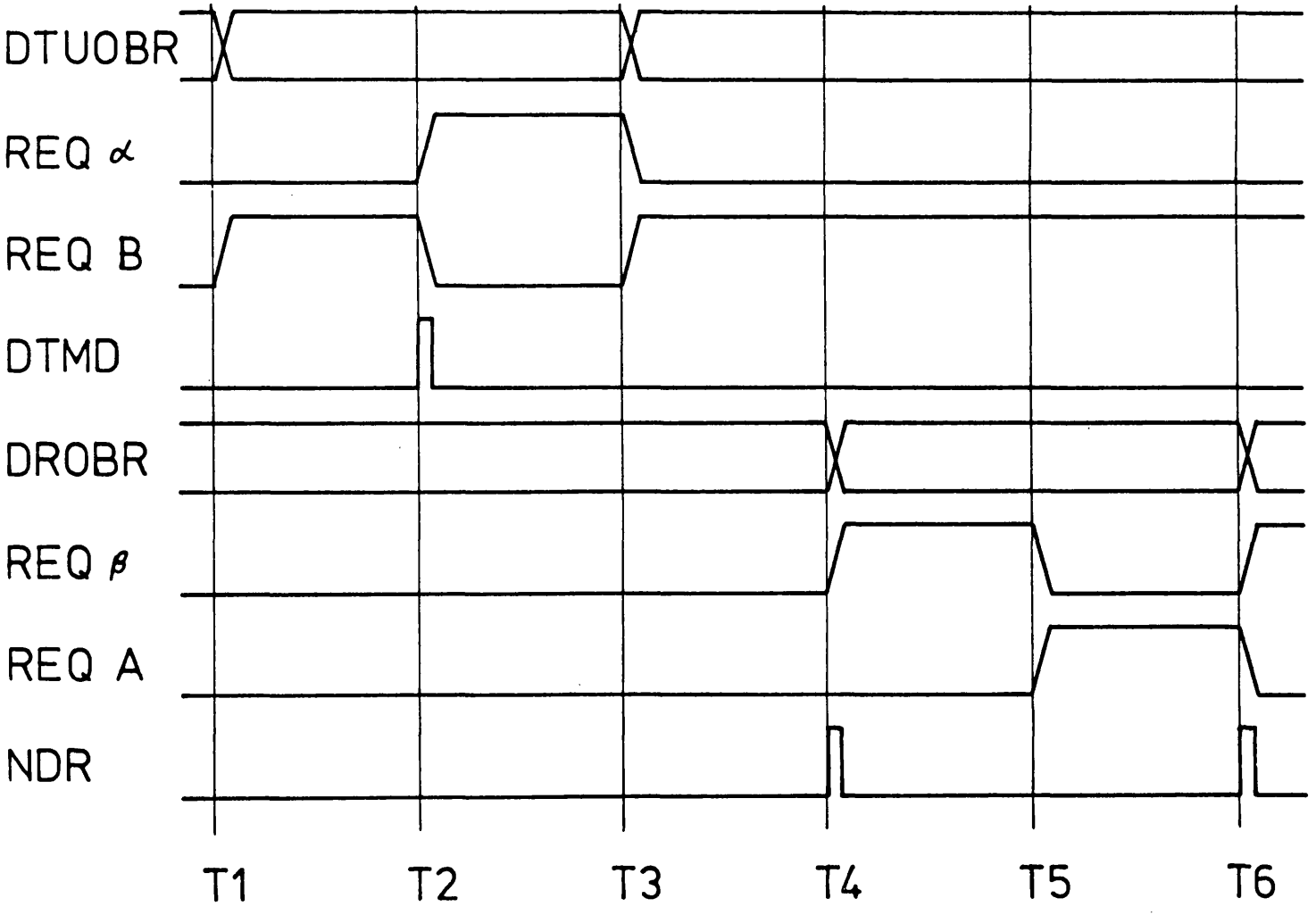

Fig. A3.4 Operation of Data Transfer Unit Flags

DTUOBR which it does at T3. The DTU hardware resets REQα and sets REQB when DTUOBR is decoded so that the condition of flags immediately after T3 is identical with the condition just after T1. It can be seen that the transfer of data can continue in this fashion until all data is sent.

Communication in the other direction, from the PDP 11 to the TMS 9900 follows a similar pattern, as shown in Fig. A3.4. When the PDP 11 addresses the DR11-C output register DROBR and moves data to it a 500ns New Data ready pulse (NDR) is transmitted. NDR is used by the DTU to set REQβ, clear REQA and latch data into the DTU input buffer register DTUIBR, as at time T4. The REQβ flag indicates to the TMS 9900 that new data is available in DTUIBR. This data is read at time T5. When DTUIBR is read by the TMS 9900 the DTU hardware resets REQβ and sets REQA.

With Request A set the PDP 11 can now output new data which is accompanied by the NDR pulse at time T6. Again NDR is used to latch the new data, clear REQA and set REQβ, which brings the flip flop conditions back to those effective immediately after T4. Clearly, data transfers in one direction have no effect on transfers in the other direction as far as the hardware is concerned, and so may be treated by the software as independent processes.

The positive action of the handshake bits enables data transfers to take place at any rate without fear of data loss. The handshake feature is particularly important if either

or both machines are engaged in other activities concurrent with the transfer operation. This is of importance if optimum use is to be made of each processor. If the full potential of each processor is to be realized it is necessary to employ an interrupt based approach to the data transfer system. In this way each machine can be nominally performing a low priority process, but this process is dropped whenever a higher priority function is required, in this case the interrupt service routine.

A3.4 Data Transfer Unit Hardware

The circuit diagram for the DTU is given in Fig. A3.5. The data transfer unit registers are memory mapped to the locations given above. The address lines A0 - A12 together with the memory enable control line MEMEN are decoded with NAND gates B1 and B2 to provide a block decode signal which enables the one of sixteen decoder A2. A2 uses the least significant address bits A13 and A14 with the memory control lines DBIN and WE to generate the appropriate read and write enable strobes. The output buffer write strobe C2 is also used to set REQB (D1.8) and reset REQα (D2.6). The input buffer read enable C4 is similarly used to set REQA (D1.6) and clear REQβ (D2.8). Because of the multiplexing of DR11-C Data in the TMS 9900 system, it is necessary to discriminate between DR11-C control pulses NDR and DTMT intended for use with the DTU and the same pulses intended for use with other devices. DR11-C control and states register bits CSR00 and CSR01 are used for this purpose and data transfer mode is enabled when

D3883/82
HAZELL PA
Bath

Fig. A3.5 Data Transfer Unit Ciruit Diagram

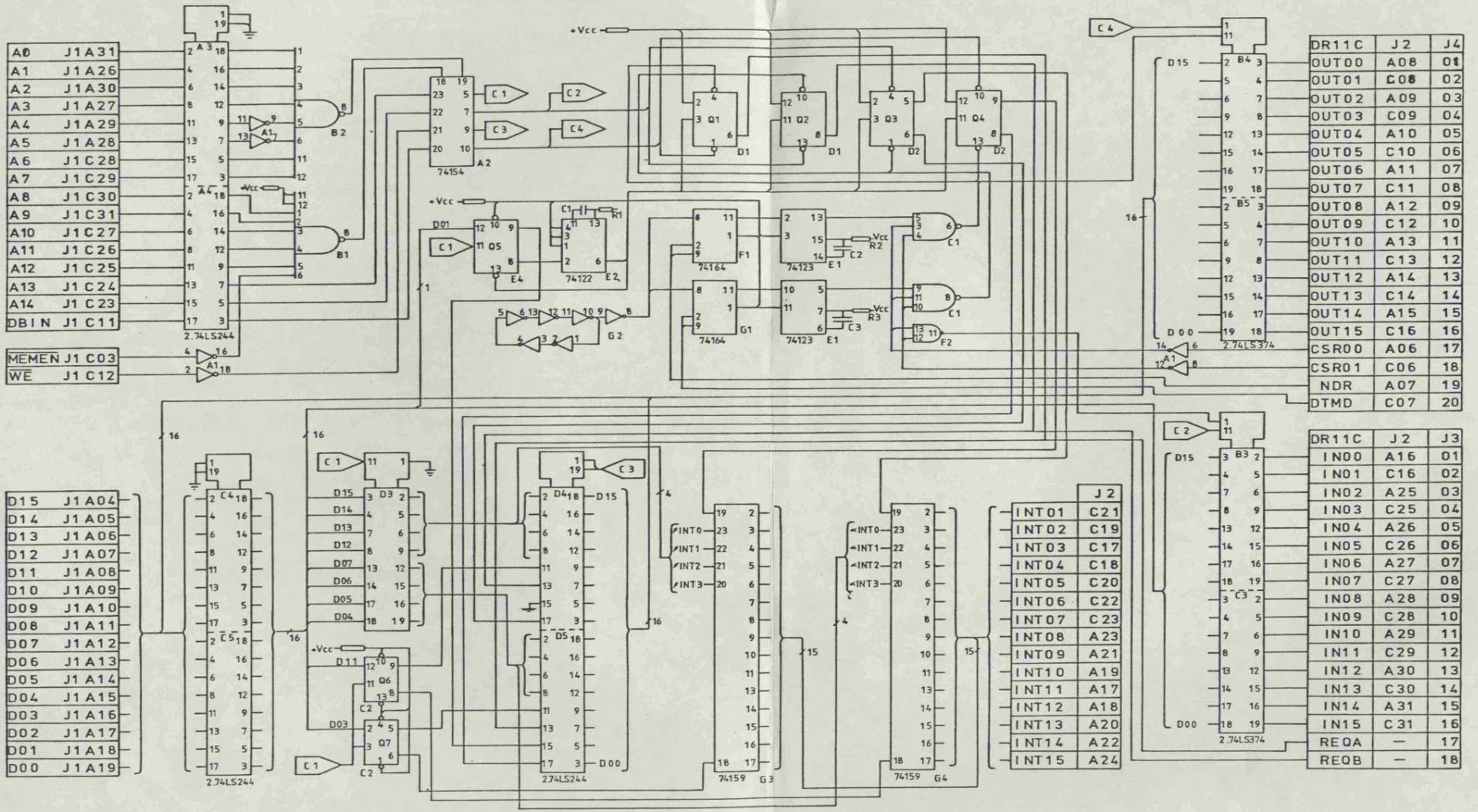

Fig. A3.5 Data Transfer Unit Ciruit Diagram

they are both clear.

The NDR and DTMD pulses are both filtered using the deglitch circuit described in the I/F section for NDR. The clean NDR pulse is gated with CSR00 and CSR01 in Nand gate C1.3-6 to clock DR11-C output data into DTUIBR (B4,B5), it is also used to clear REQA (D1.6) and set REQβ (D2.8). The clean DTMD pulse is similarly gated with CSR00 and CSR01 in NAND gate C1.8-11 to clear REQB (D1.8) and set REQα (D2.5).

The DTU control and status register bit functions are described in table A1.4. The bits used to monitor the request lines are read only. The INIT bit is read write and is used as one input to the reset monostable E2, the other input is the general system reset line. The reset function is performed by Q (E2.6) of the reset monostable. The low level of Q is used to clear INIT and the rising edge of Q is used to clock input data into the request flip flops. At this point it should be noted that the request lines are obtained from the Q outputs of the flip flops, so that clocking in true data resets the requests.

Interrupt control for α and β are similar, so only circuits for α are described. An open collector one of sixteen decoder, type 74159, is used to interface with the TMS 9900 system interrupt bus. The interrupt priority αo-α3 is latched in the control and status register (D3 and is then used as an address value for the decoder. Two active low enables are required before the decoder will assert a low level on the

selected interrupt line.

The first enable is derived from the Q output of the IEα flip flop (C2.9) of the control and status register. The other enable is available from α (D2.5) asserted when α is set. A visual indication of the α and β interrupt enables and all the Request bits is given by an LED display.

Interface Connection Schedule

Connector J1

Row A	Function	Row C	Function
1	0v	1	0v
2		2	
3		3	$\overline{\text{MEMEN}}$
4	D15 (LSB)	4	
5	D14	5	$\overline{\text{LOAD}}$
6	D13	6	$\overline{\text{HOLD}}$
7	D12	7	READY
8	D11	8	WAIT
9	D10	9	IAQ
10	D09	10	
11	D08	11	DBIN
12	D07	12	$\overline{\text{WE}}$
13	D06	13	HOLDA
14	D05	14	
15	D04	15	
16	D03	16	
17	D02	17	
18	D01	18	
19	D00	19	
20		20	
21	$\overline{\text{RESET}}$	21	
22	$\overline{\phi 2}$ Clock	22	
23	$\overline{\phi 4}$ "	23	A14 (LSB)
24	$\overline{\phi 1}$ "	24	A13
25	$\overline{\phi 3}$ "	25	A12
26	A01	26	A11
27	A03	27	A10
28	A05	28	A06
29	A04	29	A07
30	A02	30	A08
31	A00 (MBS)	31	A09
32	+5v	32	+5v

Interface Connection Schedule

Connector J2

Row A	Function	Row C	Function
1	0v	1	0v
2		2	CRUO 05
3		3	CRUO 06
4		4	
5		5	CRUO 03
6	DR11C CSR 00	6	DR11C CSR 01
7	" NDR	7	" DTMD
8	" OUT 00 (LSB)	8	" OUT 01
9	" OUT 02	9	" OUT 03
10	" OUT 04	10	" OUT 05
11	" OUT 06	11	" OUT 07
12	" OUT 08	12	" OUT 09
13	" OUT 10	13	" OUT 11
14	" OUT 12	14	" OUT 13
15	" OUT 14	15	" OUT 15 (MSB)
16	" IN 00 (LSB)	16	" IN 01
17	$\overline{\text{INT 11}}$	17	$\overline{\text{INT 3}}$
18	$\overline{\text{INT 12}}$	18	$\overline{\text{INT 4}}$
19	$\overline{\text{INT 10}}$	19	$\overline{\text{INT 2}}$
20	$\overline{\text{INT 13}}$	20	$\overline{\text{INT 5}}$
21	$\overline{\text{INT 09}}$	21	$\overline{\text{INT 1}}$
22	$\overline{\text{INT 14}}$	22	$\overline{\text{INT 6}}$
23	$\overline{\text{INT 08}}$	23	$\overline{\text{INT 7}}$
24	$\overline{\text{INT 15}}$	24	$\overline{\text{EXMEMDIS}}$
25	DR11C IN 02	25	DR11C IN 03
26	" IN 04	26	" IN 05
27	" IN 06	27	" IN 07
28	" IN 08	28	" IN 09
29	" IN 10	29	" IN 11
30	" IN 11	30	" IN 13
31	" IN 13	31	" IN 15 (MSB)
32	+5v	32	+5v

Data Transfer Unit Connection Schedule

Connector J1

Row A	Function	Row C	Function
1	0v	1	0v
2		2	
3		3	$\overline{\text{MEMEN}}$
4	D15 (LSB)	4	
5	D14	5	
6	D13	6	
7	D12	7	
8	D11	8	
9	D10	9	
10	D09	10	
11	D08	11	DBIN
12	D07	12	$\overline{\text{WE}}$
13	D06	13	
14	D05	14	
15	D04	15	
16	D03	16	
17	D02	17	
18	D01	18	
19	D00	19	
20		20	
21	$\overline{\text{RESET}}$	21	
22	$\overline{\phi 2}$ Clock	22	
23	$\overline{\phi 4}$ "	23	A14 (LSB)
24	$\overline{\phi 1}$ "	24	A13
25	$\overline{\phi 3}$ "	25	A12
26	A01	26	A11
27	A03	27	A10
28	A05	28	A06
29	A04	29	A07
30	A02	30	A08
31	A00 (MSB)	31	A09
32	+5v	32	+5v

Data Transfer Unit Connection Schedule

Connector J2

Row A	Function				Row C	Function			
1	0v				1	0v			
2					2				
3					3				
4					4				
5					5				
6	DR11C	CSR	00		6	DR11C	CSR	01	
7	"	NDR			7	"	DTMD		
8	"	OUT	00	(LSB)	8	"	OUT	01	
9	"	OUT	02		9	"	OUT	03	
10	"	OUT	04		10	"	OUT	05	
11	"	OUT	06		11	"	OUT	06	
12	"	OUT	08		12	"	OUT	09	
13	"	OUT	10		13	"	OUT	11	
14	"	OUT	12		14	"	OUT	13	
15	"	OUT	14		15	"	OUT	15	(MSB)
16	"	IN	00	(LSB)	16	"	IN	01	
17	$\overline{\text{INT 11}}$				17	$\overline{\text{INT 3}}$			
18	$\overline{\text{INT 12}}$				18	$\overline{\text{INT 4}}$			
19	$\overline{\text{INT 10}}$				19	$\overline{\text{INT 2}}$			
20	$\overline{\text{INT 13}}$				20	$\overline{\text{INT 5}}$			
21	$\overline{\text{INT 9}}$				21	$\overline{\text{INT 1}}$			
22	$\overline{\text{INT 14}}$				22	$\overline{\text{INT 6}}$			
23	$\overline{\text{INT 8}}$				23	$\overline{\text{INT 7}}$			
24	$\overline{\text{INT 15}}$				24				
25	DR11C	IN	02		25	DR11C	IN	03	
26	"	IN	04		26	"	IN	05	
27	"	IN	06		27	"	IN	07	
28	"	IN	08		28	"	IN	09	
29	"	IN	10		29	"	IN	11	
30	"	IN	12		30	"	IN	13	
31	"	IN	14		31	"	IN	15	(MSB)
32	+5v				32	+5v			

Data Transfer Unit Connection Schedule

Connectors J3 and J4

Signal No.	Pin No.	J3 Function	J4 Function	
1	1	DR11C IN 00	DR11C OUT 00	
2	3	" " 01	" " 01	
3	5	" " 02	" " 02	
4	7	" " 03	" " 03	
5	9	" " 04	" " 04	
6	11	" " 05	" " 05	
7	13	" " 06	" " 06	
8	15	" " 07	" " 07	
9	17	" " 08	" " 08	
10	19	" " 09	" " 09	
11	21	" " 10	" " 10	
12	23	" " 11	" " 11	
13	25	" " 12	" " 12	
14	27	" " 13	" " 13	
15	29	" " 14	" " 14	
16	31	" " 15	" " 15	(LSB)
17	33	" REQ B	" CSR 00	
18	35	" REQ A	" CSR 01	
19	37	Not Used	" NDR	
20	39	"	" DTMD	

N.B. All even numbered pins carry 0v screen

Differential Line Driver-Receiver Card Connection Schedule

Line Driver Connections

Signal No.	Connector J3	Connector J1	Dee Range (Male)	Connector J1	Dee Range (Male)
1	1	a30	39	c30	40
2	3	c29	37	a29	38
3	5	a28	35	c28	36
4	7	c27	33	a27	34
5	9	a26	31	c26	32
6	11	c25	29	a25	30
7	13	a24	27	c24	28
8	15	c23	25	a23	26
9	17	a22	23	c22	24
10	19	c21	21	a21	22
11	21	a14	19	c14	20
12	23	c13	17	a13	18
13	25	a12	15	c12	16
14	27	c11	13	a11	14
15	29	a10	11	c10	12
16	31	c09	9	a09	10
17	33	a08	7	c08	8
18	35	c07	5	a07	6
19	37	a06	3	c06	4
20	39	c05	1	a05	2

Differential Line Driver-Receiver Card Connection Schedule

Line Receiver Connections

Signal No.	Connector J4	Connector J2	Dee Range (Female)	Connector J2	Dee Range (Female)
1	1	c30	39	a30	40
2	3	c29	37	a29	38
3	5	c28	35	a28	36
4	7	c27	33	a27	34
5	9	c26	31	a26	32
6	11	c25	29	a25	30
7	13	c24	27	a24	28
8	15	c23	25	a23	26
9	17	c22	23	a22	24
10	19	c21	21	a21	22
11	21	c14	19	c14	20
12	23	c13	17	a13	18
13	25	c12	15	a12	16
14	27	c11	13	a11	14
15	29	c10	11	a10	12
16	31	c09	9	a09	10
17	33	c08	7	a08	8
18	35	c07	5	a07	6
19	37	c06	3	a06	4
20	39	c05	1	a05	2

APPENDIX A4 AUXILIARY HARDWARE

A4.1 Acceleration Transducer Hardware

The mechanical considerations and data utilization aspects of the cupped disc transducers have been considered in Chapter 4. This section is restricted to a description of the electronic hardware used in the machine period measurement system.

The circuits associated with the optical transmissive assembly used to detect the presence of a transducer slot are given in Fig. A4.1, for the single slot eight pickup system. The infra-red light emitting diode is fed from a 20mA constant current source. The output of the phototransistor is a low level current approximately proportional to the intensity of the infra-red light falling on it. The switching characteristic of the phototransistor is such that the turn off time is substantially longer than the turn on time. The detector circuit monitors the phototransistor output current, and when it is large enough to trigger the comparator circuit, the positive feedback arrangement ensures a fast switching with no jitter on the comparator output. As the phototransistor turns off, the hystersis inherent in the positive feedback circuit around the operational amplifier, used as the comparator, ensures that no spurious spikes are generated. The rising edge of the comparator output is used to trigger a monostable which provides a stop/start pulse of 500ns duration to the relevant period counter. To ensure noise free

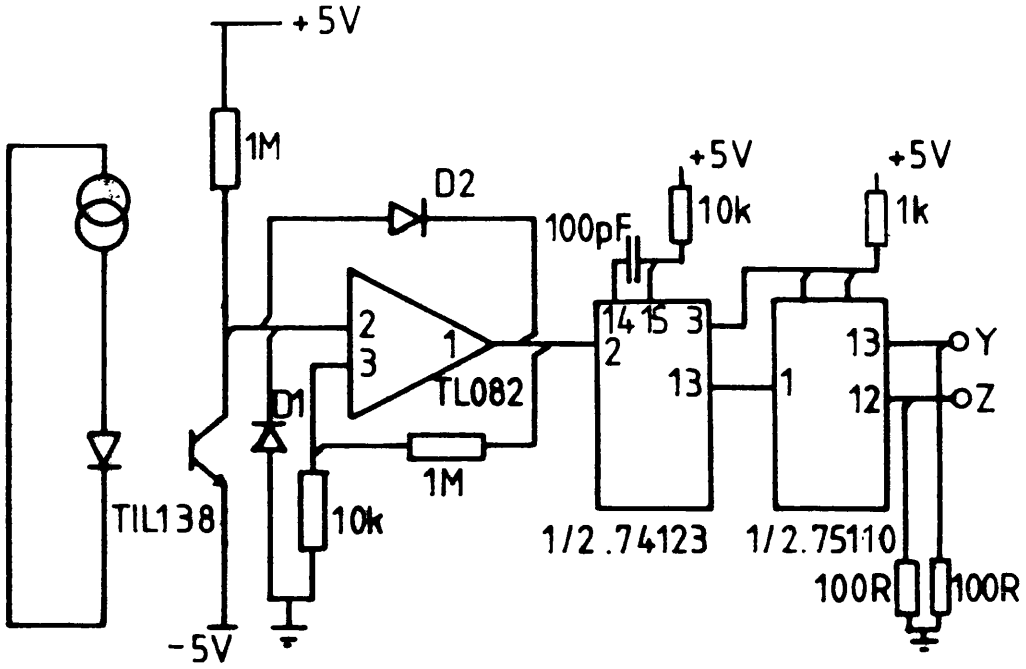

Fig. A4.1 Slot Detection Circuit

transmission of this pulse from the electronics mounted on the cupped disc transducer, to the counter circuits in the auxiliary rack, a twisted pair constant current loop driver, receiver system is used. The receiver circuit and back plane wiring are evident from the auxiliary rack circuit diagram of Fig. A4.2

For the eight slot single pickup system, the phototransistor current sensing comparator output, is fed to coding logic. This logic is then used to generate pulses in a form identical with those of the other transducer. Essentially, the longer pulse from the wide slot is used as an index to clear a counter system which is incremented after each pulse. At operational speeds the index slot forces the pulses to have a fixed relationship with the rotor of the machine.

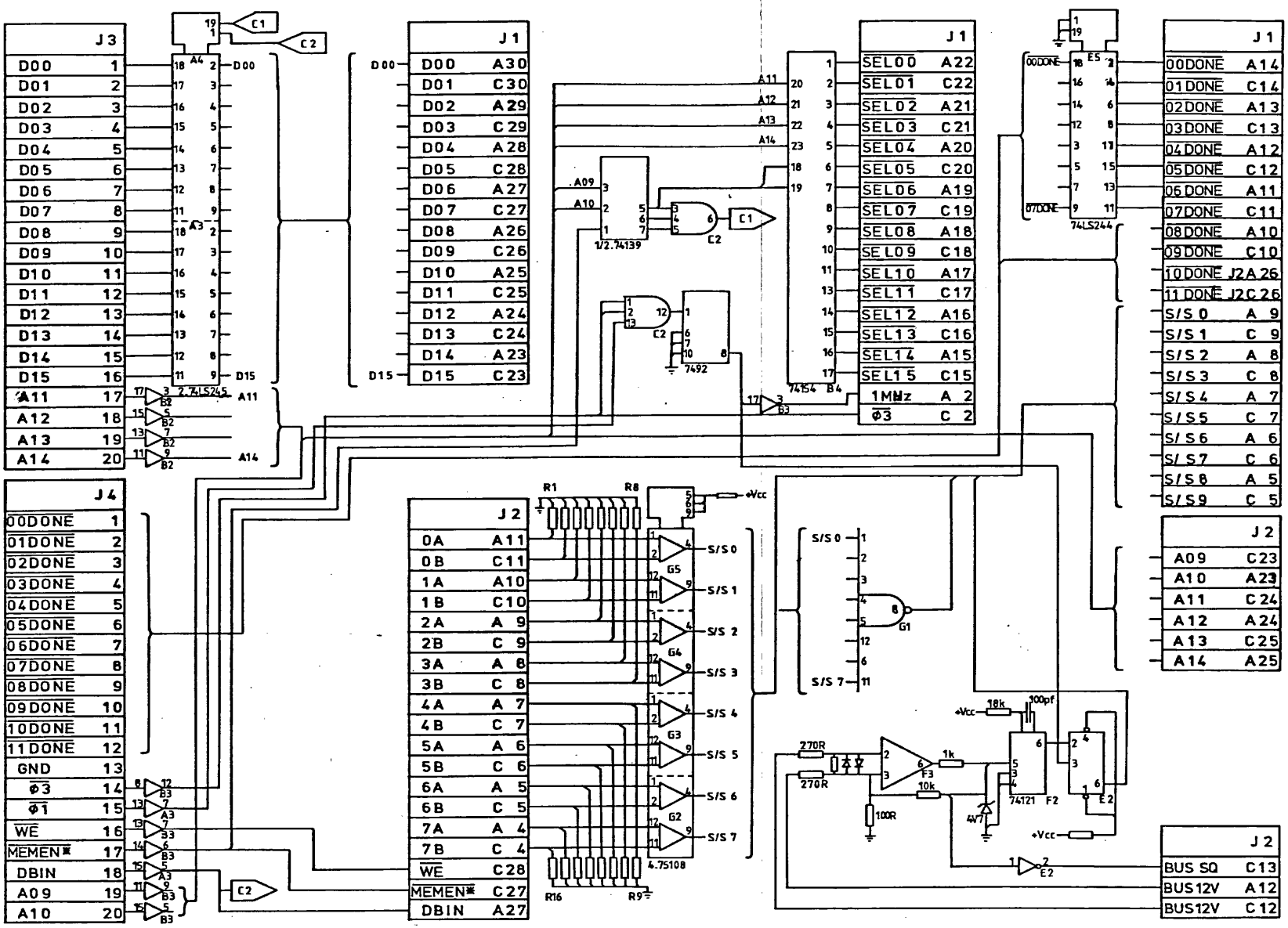

Fig. A4.2 Auxiliary Rack Buffer Card (Aux)

Fig. A4.2 Auxiliary Rack Buffer Card (Aux)

A typical machine period counter circuit is given in Fig. A4.3. The stop/start pulse of 500ns duration is used to initiate the sequence given in the timing diagram of Fig. A4.4. The stop/start pulse is asynchronous to the system clocks, so flip flop Q1 is used to catch and hold the stop/start command, which is then synchronized by flip flop Q2. While Q2 is active the counter clock is disabled, allowing sufficient time for the counter circuits to ripple through and present stable data at the buffer register data inputs. Flip flop Q3 is used to latch the count data in the buffer register and also to clear the counters. This technique is possible since the latches used have a zero hold time requirement, and the counter clear operation is not instanteous.

$\overline{Q3}$ is used to clear Q1, Q2 and preset Q4 which is used as a done flag for the particular counter unit. By convention the $\overline{Q4}$ output is used as the active output. Q4 remains set until the data is read from the period data buffer register.

A4.2 Acceleration Transducer Control and Status Register

When a period counter unit receives a stop/start pulse, the done flag is set to indicate that valid data is present in the counter data buffer register. The acceleration transducer control and status register (CSR) located on the auxiliary rack buffer card (TMS) Fig. A4.5, provides access to all the counter done bits, and controls system interrupts. When any unit is done the relevant bit is set in the low order byte of the CSR and the most significant bit (MSB) is also set.

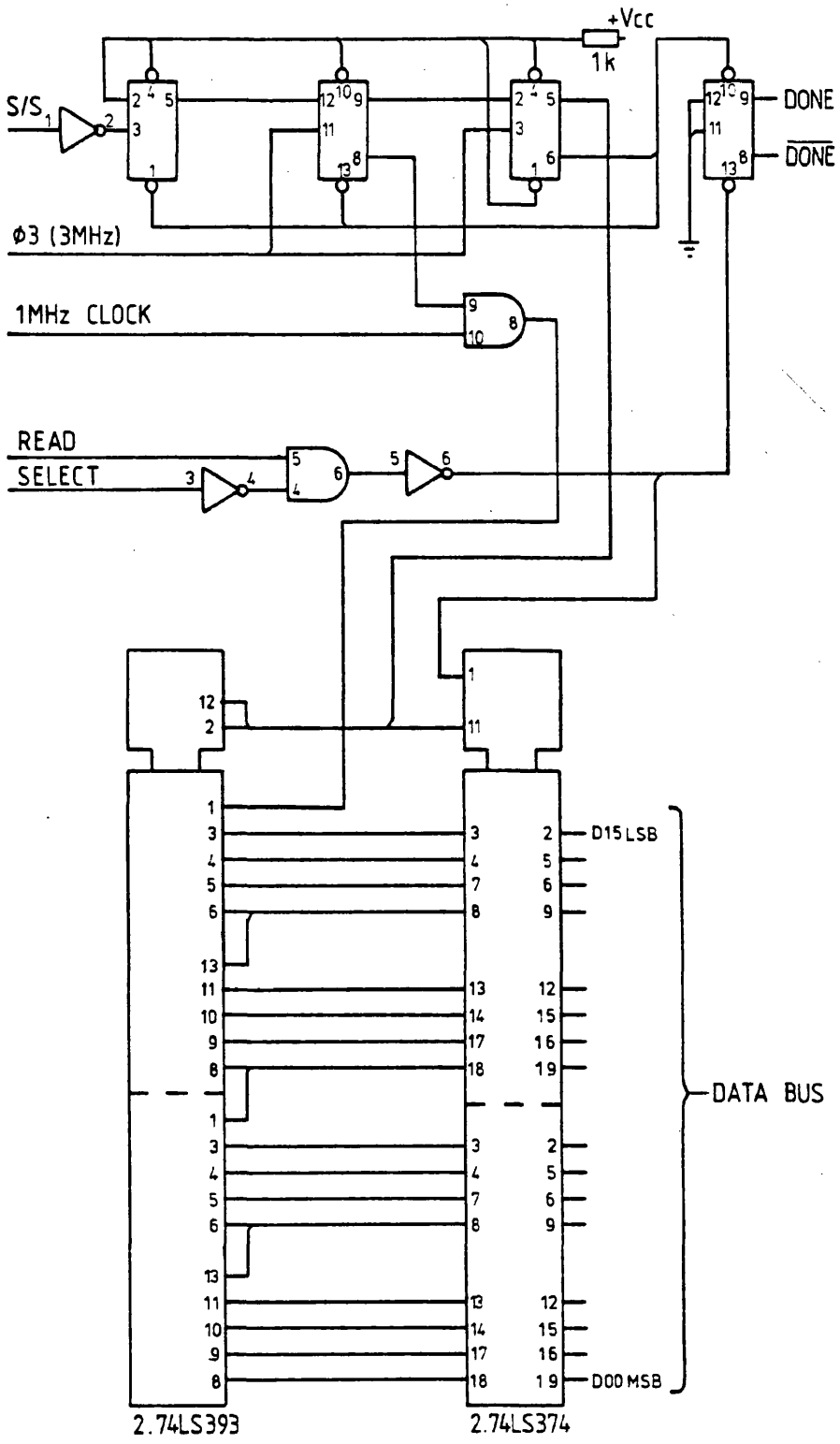

Fig. A4.3 Machine Period Counter Circuit

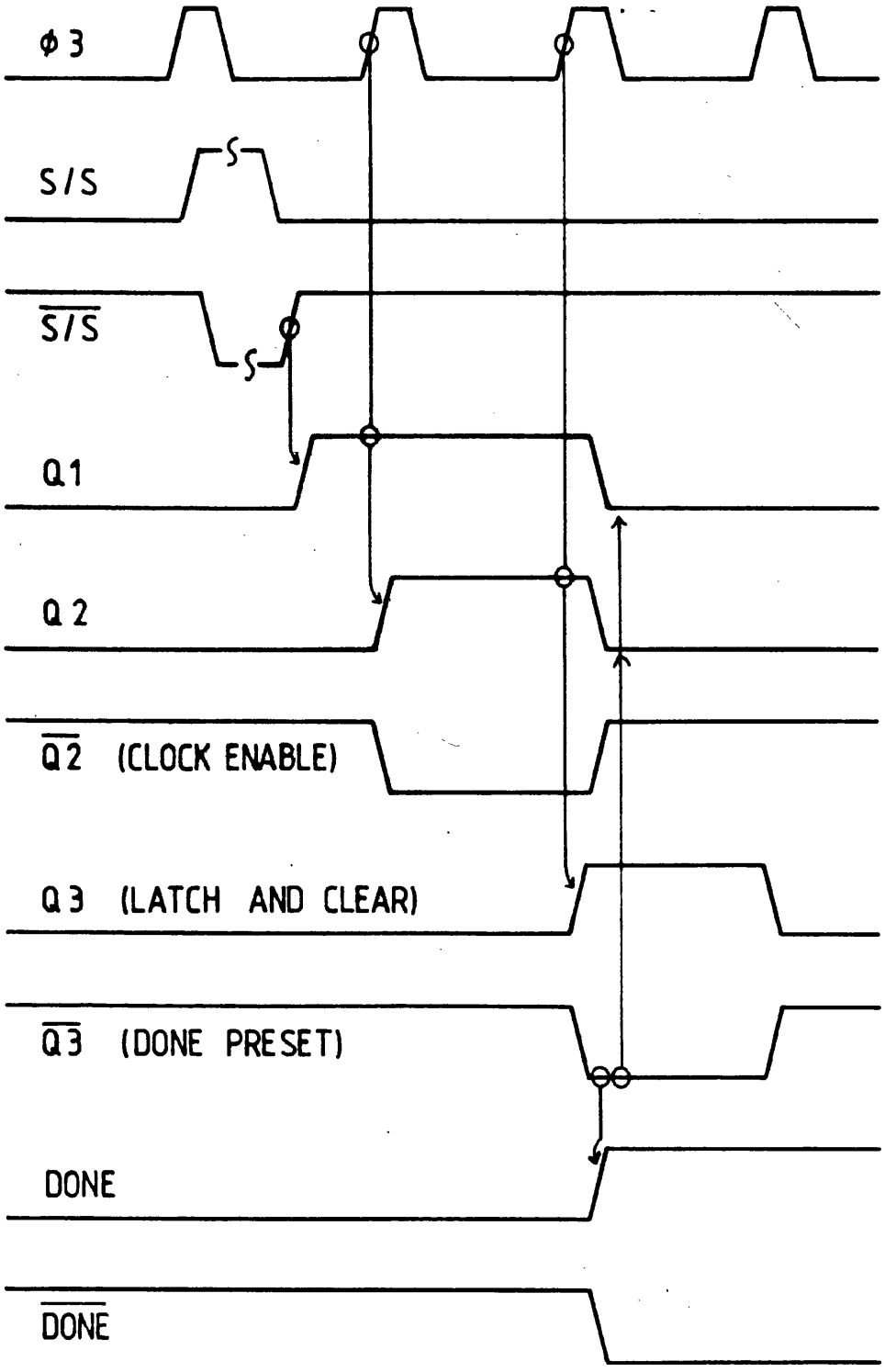

Fig. A4.4 Stop/Start Sequence Timing Diagram

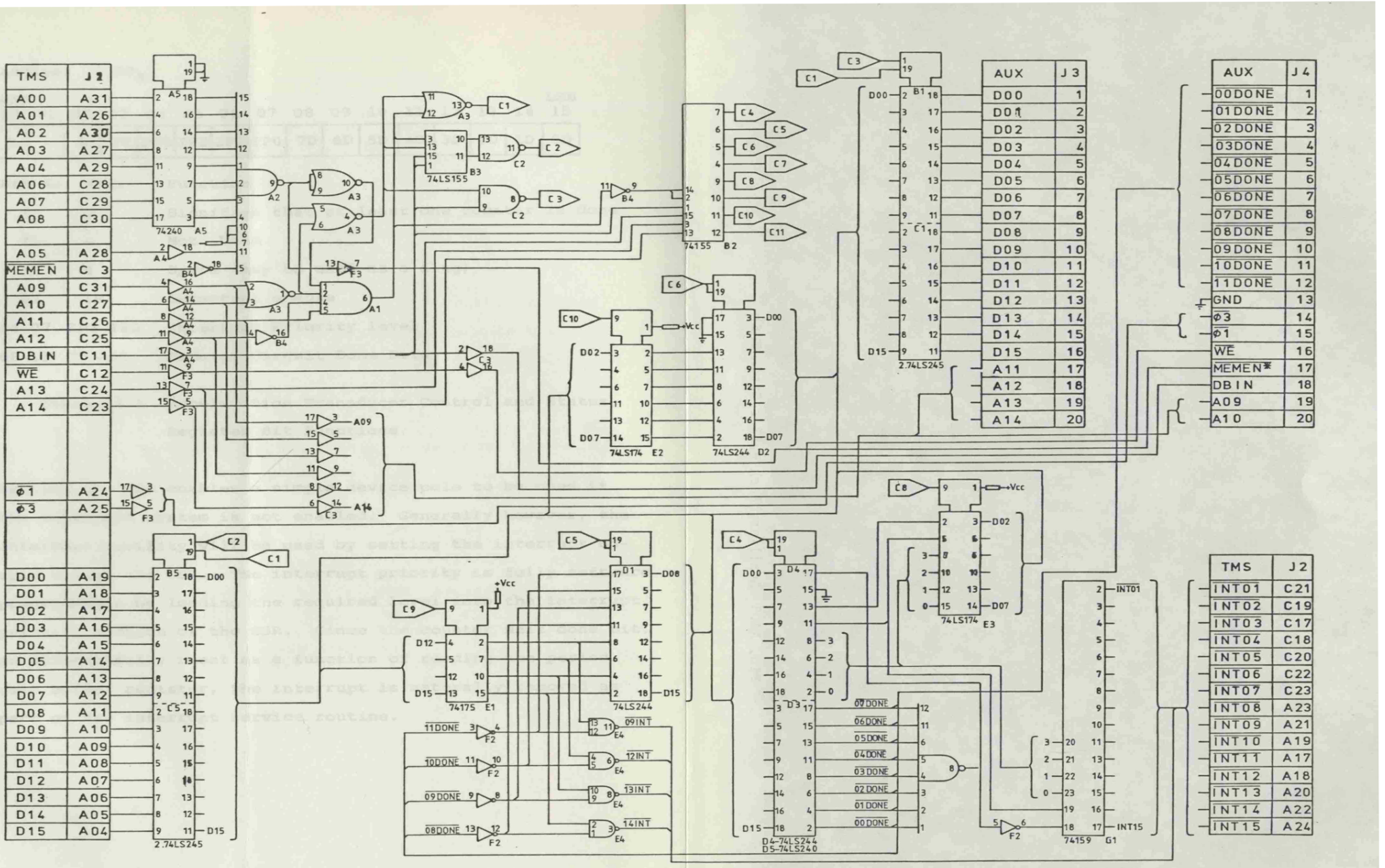

Fig. A4.5 Auxiliary Rack Buffer Card (TMS)

Fig. A4.5 Auxiliary Rack Buffer Card (TMS)

Address 2020_8

MSB 00	01	02	03	04	05	06	07	08	09	10	11	12	13	14	LSB 15
D	-	S	IE	IP3	IP2	IP1	IP0	7D	6D	5D	4D	3D	2D	1D	0D

Bit No.	Name	Function
00	D	Signifies that at least one counter is done
01	-	Not Used
02	S	Spare (may be used as a flag)
03	IE	Interrupt enable
04-07	IP3-IP0	Interrupt Priority level
08-15	7D - 0D	Counter Circuit Done Bits

Table A4.1 Acceleration Transducer Control and Status Register Bit Functions

Setting the MSB enables a simple device pole to be used if the interrupt system is not enabled. Generally however, the interrupt facility will be used by setting the interrupt enable bit in the CSR. The interrupt priority is fully software programmable by loading the required level into the interrupt priority section of the CSR. Since the counter unit done bit, is automatically reset as a function of reading the period data buffer register, the interrupt is naturally removed as part of the interrupt service routine.

A4.3 Miscellaneous Interrupt Control Register

Word Address 2022_8

Byte Address 2023_8

08	09	10	11	12	13	14	15
DONE11	DONE10	DONE09	DONE08	DONE11 IE	DONE10 IE	DONE09 IE	DONE08 IE

This is a single byte register, which monitors done flags 8 - 11, and can be used to enable interrupts when the done flags are active. Each interrupt priority is hardware link selectable and the present utilization is as below.

Done 9 ; Infinite bus period counter - interrupt level 13

Done 11 ; Terminal voltage low - interrupt level 9

The infinite bus interrupt request is reset by reading the period data in the same manner as for the machine period counter circuits. The terminal voltage low interrupt is cleared by setting bit 12 in the analogue to digital conversion control and status register.

A4.4 Analogue To Digital Conversion Control and Status Register

Address 2100_8

MSB		LSB
00		15

Bit No.	Name	Function
00	RID	Rig identification bit 0 - M/C No.1 1 - M/C No.2
01	-	Not Used
02	-	" "
03	AD4S	Analogue to digital converter No. 4 Status
04	-	Not Used
05	-	" "
06	-	" "
07	AD4C	Analogue to digital converter No. 4 Start Bit
08	VTL	Terminal voltage low indicator
09	AD3S	Analogue to digital converter No. 3 Status
10	AD2S	" " " " No. 2 Status
11	AD1S	" " " " No. 1 Status
12	VTLR	Terminal voltage low interrupt reset
13	AD3C	Analogue to digital converter No. 3 Start Bit
14	AD2C	" " " " No. 2 Start Bit
15	AD1C	" " " " No. 1 Start Bit

Table A4.2 Analogue to Digital Conversion CSR Bit Functions

This register is used to start and monitor the analogue to digital converters. Additionally it gives access to the terminal voltage low indicator. The indicator is clocked by a comparator which compares the terminal voltage with a

fixed level. The reset function for the indicator is obtained by setting Bit 12 of the control and status register. The most significant bit of the control and status register is used to guide rig dependent software, it monitors a hard wired level on the auxiliary rack backplane.

Address	Range	Function
2102	0-10V	Terminal voltage A/D
2104	±10V	Field voltage A/D
2106	±2.5V	Auxiliary A/D
2110	±10V	Vi-State feedback D/A
2112	0-5V	d.c. machine armature current A/D
2114	0-5V	d.c. machine armature current demand D/A

Table A4.3 A/D D/A Converter Memory Map

APPENDIX A5 CENTRAL PROCESSOR UNIT AND MEMORY

The TMS 9900 cpu is mounted on a Texas Instruments 'Micro 99' cpu card, which has an elementary 'Tibug' monitor, resident in read only memory. The 'Tibug' monitor can be used for program development using a local terminal. This feature is not used since the digital interface and PDP 11 based development system is more suitable for efficient generation and debugging of programs. The 'Micro 99' cpu card is used mainly to buffer the cpu from the system busses, and to provide the necessary clocks. The only features used on the card are the 256 words of random access memory and a number of dedicated CRU lines.

The control software requires only a modest amount of memory, which is supplied by an in-house 4k word static random access memory card. The memory may be mapped to any 4k word boundary by the use of the bank select links as below.

Address (Hex)	Links Required On J2 Backplane		
0000 - 1FFF	A16 - C16	A12 - C12	A14 - C14
2000 - 3FFF	A16 - C16	A12 - C12	A13 - C13
4000 - 5FFF	A16 - C16	A11 - C11	A14 - C14
6000 - 7FFF	A16 - C16	A11 - C11	A13 - C13
8000 - 9FFF	A15 - C15	A12 - C12	A14 - C14
A000 - BFFF	A15 - C15	A12 - C12	A13 - C13
C000 - DFFF	A15 - C15	A11 - C11	A14 - C14
E000 - FFFF	A15 - C15	A11 - C11	A13 - C13

CPU Card Connection Schedule

Connector J1

Row A	Function	Row C	Function
1	-5v	1	+12v
2	-12v	2	CRUOUT
3		3	$\overline{\text{MEMEN}}$
4	D15 (LSB)	4	CRUIN
5	D14	5	$\overline{\text{LOAD}}$
6	D13	6	$\overline{\text{HOLD}}$
7	D12	7	READY
8	D11	8	WAIT
9	D10	9	IAQ
10	D09	10	CRUCLK
11	D08	11	DBIN
12	D07	12	$\overline{\text{WE}}$
13	D06	13	HOLDA
14	D05	14	
15	D04	15	
16	D03	16	
17	D02	17	
18	D01	18	
19	D00	19	
20		20	
21	$\overline{\text{RESET}}$	21	
22	$\overline{\phi 2}$ Clock	22	
23	$\overline{\phi 4}$ "	23	A14 (LSB)
24	$\overline{\phi 1}$ "	24	A13
25	$\overline{\phi 3}$ "	25	A12
26	A01	26	A11
27	A03	27	A10
28	A05	28	A06
29	A04	29	A07
30	A02	30	A08
31	A00 (MSB)	31	A09
32	0v	32	+5v

CPU Card Connection Schedule

Connector J2

Row A	Function	Row C	Function
1	CRUI 00	1	CRUO 04
2	" 01	2	" 05
3	" 02	3	" 06
4	" 03	4	" 07
5	" 07	5	" 03
6	" 06	6	" 02
7	" 05	7	" 01
8	" 04	8	" 00
9	" 08	9	" 12
10	" 09	10	" 13
11	" 10	11	" 14
12	" 11	12	" 15
13	" 15	13	" 11
14	" 14	14	" 10
15	" 13	15	" 09
16	" 12	16	" 08
17	$\overline{\text{INT 11}}$	17	$\overline{\text{INT 03}}$
18	$\overline{\text{INT 12}}$	18	$\overline{\text{INT 04}}$
19	$\overline{\text{INT 10}}$	19	$\overline{\text{INT 02}}$
20	$\overline{\text{INT 13}}$	20	$\overline{\text{INT 05}}$
21	$\overline{\text{INT 09}}$	21	$\overline{\text{INT 01}}$
22	$\overline{\text{INT 14}}$	22	$\overline{\text{INT 06}}$
23	$\overline{\text{INT 08}}$	23	$\overline{\text{INT 07}}$
24	$\overline{\text{INT 15}}$	24	SRDI 0
25	RS232O 1	25	SRDI 1
26	RS232O 0	26	SRDI 1
27	RS232O 2	27	RS232O 3
28	RS232I 2	28	SRDI 0
29	RS232I 1	29	+12v
30	RS232I 3	30	-12v
31	RS232I 0	31	-5v
32	0v	32	+5v

Memory Card Connection Schedule

Connector J1

Row A	Function		Row C	Function
1	0v		1	0v
2			2	
3			3	$\overline{\text{MEMEN}}$
4	D15	(LSB)	4	
5	D14		5	
6	D13		6	
7	D12		7	
8	D11		8	
9	D10		9	
10	D09		10	
11	D08		11	DBIN
12	D07		12	$\overline{\text{WE}}$
13	D06		13	
14	D05		14	
15	D04		15	
16	D03		16	
17	D02		17	
18	D01		18	
19	D00	(MSB)	19	
20			20	
21			21	
22			22	
23			23	A14 (LSB)
24			24	A13
25			25	A12
26	A01		26	A11
27	A03		27	A10
28	A05		28	A06
29	A04		29	A07
30	A02		30	A08
31	A00	(MSB)	31	A09
32	+5v		32	+5v

Memory Card Connection Schedule

Connector J2

Row A	Function	Row C	Function
1	0v	1	0v
2		2	
3		3	
4		4	
5		5	
6		6	
7		7	
8		8	
9		9	
10		10	
11	MADSEL 1	11	MAD 1
12	MADSEL 1	12	MAD 1
13	MADSEL 2	13	MAD 2
14	MADSEL 2	14	MAD 2
15	MADSEL 0	15	MAD 0
16	MADSEL 0	16	MAD 0
17		17	
18		18	
19		19	
20		20	
21		21	
22		22	
23		23	
24		24	$\overline{\text{EXMEMDIS}}$
25		25	
26		26	
27		27	
28		28	
29		29	
30		30	
31		31	
32	+5v	32	+5v

REFERENCES

1 VICKERS, V.J. "Recent trends in turbogenerators", Proc. IEE, Vol. 121, No.11R, Nov 1974, pp. 1273-1306

2 HARLEY, R.G. and ADKINS, B. "Calculation of the angular back swing following a short circuit of a loaded alternator", ibid. 1970, 117, (2) pp. 377-386

3 WILSON, A.R., and PORAY, A.T.: "Comparison of methods improving the transient performance of power stations", System Technical Report No. PL-ST/3/73, CEGB

4 ELLIS, H.M, HARDY, J.E., BLYTH, A.L., and SKOOGLUND, J.W,: "Dynamic stability of the Peace River transmission system", Trans. IEEE, 1966, PAS-85, pp. 586-600

5 WATSON, W., and MANCHUR, G.: "Experience with supplementary damping signals for generator static excitation systems", ibid., 1973, PAS-92, pp. 199-204

6 BAYNE, J.P., LEE, D.C., and WATSON, W.: "A power system stabiliser for termal units based on derivation of accelerating power", ibid., 1977, PAS-96, pp. 1777-1783

7 DEMELLO, F.P., HANNETT, L.N., and UNDRILL, J.M.: "Practical approaches to supplementary stabilising from accelerating power", ibid., 1978, PAS-97, pp. 1515-1522

8 KEAY, F.W,, and SOUTH, W.H.: "Design of power system stabiliser sensing frequency deviation", ibid., 1971, PAS-90, pp. 707-713

9 HUMPHRIES, H.J., and FAIRNEY, W.: "Excitation rectifier schemes for large generators", Proc. IEE., 1972 Vol.119, No.6. pp. 661-671

10 IYER, S.N., and CORY, B.J.: "Optimisation of turbo-generator transient performance by differential dynamic programming", Trans., IEEE., 1971, PAS-90, pp. 2149-2157

11 IYER, S.N., and CORY, B.J.: "Optimal control of a turbo-generator including an Exciter and Governor", ibid, 1971, PAS-90, pp. 2142-2148

12 SULLIVAN, A.C., YEE, H., and EVANS, F.J.: "Improved transient performance of turboalternators using fast governing and excitation control" Presented at PICA 73 (ABS VII-B TPAS 74 Jan/Feb 7-8 (lAlO))

13 YU, Y.N., VONSURIYA, K., and WEDMAN, L.N.: "Application of an optimal control theory to a power system", IEEE., Trans., 1970, PAS-89, pp. 55-62

14 DANIELS, A.R., DAVIS, D.H., and PAL, M.K.: "Linear and nonlinear optimisation of power system performance", ibid., 1975, PAS-94, pp. 810-818

15 CHANA, G.S., DANIELS, A.R.: "Turboalternator excitation control incorporating nonlinear state feedback", Summary Proc. IEE., Vol.125, No.11, Nov. 1978

16 LEE, Y.B.: "Sensitivity and optimal control studies of power systems", Ph.D. Thesis, University of Bath, 1975

17 LU, H.: "Optimisation studies of a single-machine power system", Ph.D. Thesis, University of Bath, 1979

18 DANIELS, A.R., and LU, H.: "Nonlinear single-variable optimisation studies of a.c. turbogenerator performance", Proc. IEE, Vol.126, No.5, May 1979 pp. 403-410

19 DINELEY, J.L., and MIKHAIL, S.E.: "Effect of feedback signals in excitation and governor/turbine systems on transient and dynamic stability", IEEE PES Meeting Paper A 76,113-1, Jan. 1976

20 CANAY, M., and BLOCH, BADEN.: "Fast valving - a means of improving power system stability", Brown Boveri Rev. 1979 (6) pp. 401-407

21 NEWTON, M.E., and HOGG, B.W.: "Optimal control of a micro-alternator system", IEEE Trans., 1976, PAS-95, pp. 1822-1830

22 PULLMAN, R.T., and HOGG, B.W.: "Discrete state-space controller for a turbogenerator", Proc. IEE, Vol. 126, 1979, pp. 87-92

23 DANIELS, A.R., LEE, Y.B., and PAL, M.K.: "Nonlinear power-system optimisation using dynamic sensitivity analysis", ibid. Vol. 123, 1976, pp. 365-370

24 MOYA, O.E.O., and CORY, B.J.: "Online control of generator stability by minicomputer", ibid., Vol. 124, 1977, pp. 252-258

25 BURROWS, P.J., and DANIELS, A.R.: "Digital excitation control of a.c. turbogenerators using a dedicated microprocessor", ibid., Vol. 125, 1978, pp. 237-240

26 ASHSON S.I., and HOGG B.W.: "Application of multi-variable frequency response methods to control of turbogenerators", INT. J. Control, 1979, Vol. 30, No.4. pp. 533-548

27 BUMBY, J.R., and PREECE, C.: "Decoupling the transient dynamics of adjacent alternators", Trans. IEEE, 1975 PAS-94, pp. 1147-1156

28 BUMBY, J.R., and PREECE C.: "Influence of forcing limits on the control of transient interaction between adjacent alternators", IEEE, PES Winter Meeting and Tesla Symposium, New York, N.Y., Jan. 25-30 1976. Paper No. A 76 133-9

29 SPEEDY,C.B., Brown, R.F., and Goodwin, G.C.: "Control theory: Identification and optimal control", Oliver and Boyd, Edinburgh,1970

30 FRANK, P.M.: "Introduction to system sensitivity theory", Academic Press, New York, 1978

31 PARK, R.H.: "Two-reaction theory of synchronous machines; generalised methods of analysis", Part 1, IEEE Trans., 1929, 48, pp. 716-730; Part 2, 1933, 52, pp. 352-355

32 PARK, R.H.: "Definition of an ideal synchronous machine and formula for the armature flux linkages", General Electrical Review, 1928, 31, pp. 332

33 KIMBARK, E.W.: "Power system stability", Vol. 3, John Wiley, New York, 1956

34 SHACKSHAFT, G.: "General purpose turbo-alternator model", Proc. IEE, Vol. 110, 1963, pp. 707-713

35 PAL, M.K.: "Mathematical methods in power system stability studies", Ph.D. Thesis, University of Aston Birmingham, 1971

36 SULLIVAN, A.C., and YEE, H.: "Fast governing of turbo-generators during transients", Proc. IEE, Vol. 120, 1973, pp. 371-378

37 VENIKOV, V.A.: "Transient phenomena in electrical power systems", Pergamon, 1964

38 MEHTA, D.B., and ADKINS, B.: "Transient torque and load angle of a synchronous generator following several types of system disturbance", Proc. IEE, Vol. 107, 1960, pp. 61-74

39 MAXWELL, J.C.: "On governors", Proc. Roy. Soc. 1868, 16, pp. 207-283

40 HAM, P.A.P., JENKINS, K., and MIKHAIL, S.E.: "Performance and control capabilities of electro-hydraulic governing systems for steam turbine-generators", Reyrolle Parsons Review, Vol. 2, No.5, Summer 1976

41 CONCORDIA, C.: "Effect of steam-turbine reheat on speed-governor performance", Trans. ASME, April, 1959, pp. 201-207

42 Private communication from GEC Turbines Ltd., Stafford. England.

43 MARTIN, M.A.: "Micromachine studies of power systems", M.Sc. Thesis, University of Bath, 1973

44 HAMMONS, T.J., and PARSONS, A.J.: "Design of micro-alternator for power-system-stability investigations", Proc. IEE, Vol. 118, No.10. Oct. 1971

45 BURROWS, P.J.; "Direct digital method of a micromachine model power system", Ph.D. Thesis, University of Bath, 1977

46 DIGITAL EQUIPMENT CORPORATION: "PDP 11 peripherals handbook", 1978-79

47 TEXAS INSTRUMENTS: "9900 Family systems design and data book",

48 DIGITAL EQUIPMENT CORPORATION: "PDP 11 processor handbook", 1978-79

49 DINLEY, J.L., MORRIS, A.J., and PREECE, C.: "Optimised transient stability from excitation control of synchronous generators", IEEE Trans., 1968, PAS-87, pp. 1696-1705

50 RAINA V.M., ANDERSON, J.H, WILSON, W.J., and QUINTANA, V.H.; "Optimal output feedback control of power systems with high-speed excitation systems", Trans. IEEE, PAS-95, 1976, pp. 677-686

51 AANSTAD, O.J., and LOKAY, H.E.: "Fast valve control can improve turbine generator response to transient disturbances", Westinghouse Engineer, July, 1970

52 CUSHING, E.W., DRECHSLER, G.E., KILLGOAR, W.P., MARSHALL, H.G., and STEWART, H.R.: "Fast valving as an aid to power system transient stability and prompt resynchronisation and rapid reload after full load rejection", IEEE Trans. 1972, PAS-91, pp. 1624-1636

53 ANDERSON, J.H.: "The control of a synchronous machine using optimal control theory", Proc. IEEE, Vol. 59, No.1. Jan. 1971, pp. 25-35

54 DAVISON, E.J., and RAU, N.S.: "The optimal output feedback of a synchronous machine", IEEE Trans.,1971, PAS-90, pp. 2123 2134

55 ELEMETWALLY, M.M., RAO, N.D., and MALIK, O.P.: "Experimental results on the implementation of an optimal control for synchronous machines", IEEE Trans., 1975, PAS-94, pp. 1192-2000

56 ANDERSON, J.H., HUTCHISON, M.A., WILSON, W.J., ZOHDY, M.A., and APLEVICH, J.D.: "Microalternator experiments to verify the physical realisibility of simulated optimal controllers and associated sensitivity studies", Trans., IEEE, 1978, PAS-97, pp. 649-658

57 DHALIWAL, N.S., and WICHERT, H.E.: "Analysis of P.I.D. governors in multimachine system", ibid., 1978, PAS-97, pp. 456-463

58 DANIELS, A.R., LEE, Y.B., and PAL, M.K.: "Combined suboptimal excitation control and governing of a.c. turbogenerators using dynamic sensitivity analysis", Proc. IEE, 1977, 125, pp. 473-478

59 GILL, P.E., and MURRAY, W.: "Quasi-Newton methods for unconstrained optimisation", J. Inst. Maths. Appl., 1972, 9, pp. 91-108

60 YU, Y.N., and MOUSSA, H.A.M.: "Optimal stabilization of a multi-machine system", Trans., IEEE., 1972, PAS-91, pp. 1174-1182

61 BAKER, D.H., KRAUSE, P.C., and RUSCHE, P.A.: "An investigation of excitation system interaction", Trans., IEEE., 1975, PAS-94, pp. 705-715

62 DANIELS, A.R., and DAVIS, D.H.: "Suboptimal excitation control and governing of turboalternators", presented at - 12th UPEC, Brunel University, 20-22 April 1977

63 STOTT, B.: "Review of load-flow calculations methods", Proc. IEEE., 62, No.7. 1974

64 NELDER, J.A., and MEAD, R.: "A simplex method for function minimization", Computer J., 1965, Vol.7. pp. 308-313